

University of Warwick institutional repository: <http://go.warwick.ac.uk/wrap>

A Thesis Submitted for the Degree of PhD at the University of Warwick

<http://go.warwick.ac.uk/wrap/56133>

This thesis is made available online and is protected by original copyright.

Please scroll down to view the document itself.

Please refer to the repository record for this item for information to help you to cite it. Our policy information is available from the repository home page.

Library Declaration and Deposit Agreement

1. STUDENT DETAILS

Please complete the following:

Full name:

University ID number:

2. THESIS DEPOSIT

2.1 I understand that under my registration at the University, I am required to deposit my thesis with the University in BOTH hard copy and in digital format. The digital version should normally be saved as a single pdf file.

2.2 The hard copy will be housed in the University Library. The digital version will be deposited in the University's Institutional Repository (WRAP). Unless otherwise indicated (see 2.3 below) this will be made openly accessible on the Internet and will be supplied to the British Library to be made available online via its Electronic Theses Online Service (EThOS) service.

[At present, theses submitted for a Master's degree by Research (MA, MSc, LL.M, MS or MMedSci) are not being deposited in WRAP and not being made available via EthOS. This may change in future.]

2.3 In exceptional circumstances, the Chair of the Board of Graduate Studies may grant permission for an embargo to be placed on public access to the hard copy thesis for a limited period. It is also possible to apply separately for an embargo on the digital version. (Further information is available in the *Guide to Examinations for Higher Degrees by Research*.)

2.4 If you are depositing a thesis for a Master's degree by Research, please complete section (a) below. For all other research degrees, please complete both sections (a) and (b) below:

(a) Hard Copy

I hereby deposit a hard copy of my thesis in the University Library to be made publicly available to readers (please delete as appropriate) EITHER immediately OR after an embargo period of months/years as agreed by the Chair of the Board of Graduate Studies.

I agree that my thesis may be photocopied. YES / NO (Please delete as appropriate)

(b) Digital Copy

I hereby deposit a digital copy of my thesis to be held in WRAP and made available via EThOS.

Please choose one of the following options:

EITHER My thesis can be made publicly available online. YES / NO (Please delete as appropriate)

OR My thesis can be made publicly available only after (Please give date)
YES / NO (Please delete as appropriate)

OR My full thesis cannot be made publicly available online but I am submitting a separately identified additional, abridged version that can be made available online.
YES / NO (Please delete as appropriate)

OR My thesis cannot be made publicly available online. YES / NO (Please delete as appropriate)

3 GRANTING OF NON-EXCLUSIVE RIGHTS

Whether I deposit my Work personally or through an assistant or other agent, I agree to the following:

Rights granted to the University of Warwick and the British Library and the user of the thesis through this agreement are non-exclusive. I retain all rights in the thesis in its present version or future versions. I agree that the institutional repository administrators and the British Library or their agents may, without changing content, digitise and migrate the thesis to any medium or format for the purpose of future preservation and accessibility.

4 DECLARATIONS

(a) I DECLARE THAT:

- I am the author and owner of the copyright in the thesis and/or I have the authority of the authors and owners of the copyright in the thesis to make this agreement. Reproduction of any part of this thesis for teaching or in academic or other forms of publication is subject to the normal limitations on the use of copyrighted materials and to the proper and full acknowledgement of its source.
- The digital version of the thesis I am supplying is the same version as the final, hard-bound copy submitted in completion of my degree, once any minor corrections have been completed.
- I have exercised reasonable care to ensure that the thesis is original, and does not to the best of my knowledge break any UK law or other Intellectual Property Right, or contain any confidential material.
- I understand that, through the medium of the Internet, files will be available to automated agents, and may be searched and copied by, for example, text mining and plagiarism detection software.

(b) IF I HAVE AGREED (in Section 2 above) TO MAKE MY THESIS PUBLICLY AVAILABLE DIGITALLY, I ALSO DECLARE THAT:

- I grant the University of Warwick and the British Library a licence to make available on the Internet the thesis in digitised format through the Institutional Repository and through the British Library via the EThOS service.
- If my thesis does include any substantial subsidiary material owned by third-party copyright holders, I have sought and obtained permission to include it in any version of my thesis available in digital format and that this permission encompasses the rights that I have granted to the University of Warwick and to the British Library.

5. LEGAL INFRINGEMENTS

I understand that neither the University of Warwick nor the British Library have any obligation to take legal action on behalf of myself, or other rights holders, in the event of infringement of intellectual property rights, breach of contract or of any other right, in the thesis.

Please sign this agreement and return it to the Graduate School Office when you submit your thesis.

Student's signature: Date:

UNIVERSITY OF WARWICK

Injection Moulding Electroluminescent Devices

by

BETHANY JANE MIDDLETON

A THESIS SUBMITTED IN PARTIAL FULFILMENT OF THE REQUIREMENTS FOR THE

DEGREE OF

DOCTOR OF PHILOSOPHY IN ENGINEERING

UNIVERSITY OF WARWICK, WARWICK MANUFACTURING GROUP

NOVEMBER 2012

TABLE OF CONTENTS

LIST OF FIGURES	vii
LIST OF TABLES	xvi
LIST OF EQUATIONS	xxi
Acknowledgements.....	xxii
Abstract.....	xxiii
ABBREVIATIONS	xxiv
1 Introduction	1
2 <i>Smart</i> Material Systems	9
2.1 Definition of <i>Smart</i> Materials.....	9
2.2 Types of <i>Smart</i> Materials	10
3 Electroluminescent Systems	19
3.1 The Relevance of Electroluminescence.....	19
3.2 Types of EL Devices.....	21
3.2.1 Inorganic.....	23
3.2.2 Organic	24
3.3 Electroluminescent Emission Mechanisms	25
3.4 Uses and Applications	26
3.5 Benefits of Electroluminescence	26
3.5.1 Benefits of EL over other light sources	27
3.5.2 Benefits of LEDs in FPD Technology.....	27
3.5.3 Benefits of PLEDs over LEDs.....	27
3.6 Structure of EL Devices.....	28
3.6.1 Layer Structures	29
3.7 Device Layers.....	30
3.7.1 Transparent Electrode.....	30

3.7.2	Busbar	30
3.7.3	Light Emission Layer	30
3.7.4	Buffer Layers	31
3.7.5	Cathode	31
3.7.6	Transport Layers.....	31
3.8	Production Methods.....	32
3.8.1	Spin-Coating	32
3.8.2	Screen Printing	33
3.8.3	Inkjet Printing.....	33
3.8.4	Roll-to-roll	33
3.9	Recent Developments in Organic EL Devices	34
3.10	Summary	36
4	Plastic Materials	37
4.1	Thermoplastics	40
4.2	Cross-linked Plastics; Thermosets and Elastomers	41
4.3	Blends and Alloys.....	42
4.3.1	Multi-layer Plastics.....	43
4.4	Additives and Modifiers	45
4.5	Conductive Polymers.....	46
4.5.1	Types	46
4.5.2	Uses	49
4.5.3	Recent Developments.....	49
4.6	Plastic Behaviour and Properties	50
4.6.1	Amorphous.....	51
4.6.2	Crystalline and Semi-crystalline	51
4.6.3	Thermal Transitions	52

4.6.4	Structure and Properties.....	54
4.6.5	Testing and Equipment	56
4.7	Summary.....	57
5	Processing Plastics.....	59
5.1	Injection Moulding	60
5.1.1	Machine and Mould Tool	61
5.1.2	The Process	62
5.1.3	Tool Heating and Cooling.....	65
5.1.4	Variations on Injection Moulding.....	67
5.2	Spray Deposition	78
5.3	Summary.....	79
6	Thermal Modelling.....	80
6.1	Single Layer Thermal Model.....	80
6.1.1	The Problem	81
6.1.2	The Model	84
6.1.3	The Results	87
6.2	Multi-layer Thermal Model	91
6.2.1	The Problem	92
6.2.2	The Model	93
6.2.3	The Results	99
7	Scoping Experiments.....	105
7.1	Materials and Equipment.....	106
7.1.1	Materials	106
7.1.2	Equipment.....	108
7.2	Thick Layer Application Method.....	111
7.2.1	Equipment Selection	112

7.2.2	Masking Template Design	113
7.2.3	Structure Investigation.....	115
7.2.4	Suitability to Injection Moulding.....	118
7.2.5	Early Insert Moulding Trials	121
7.3	Airbrush Layer Application	124
7.3.1	Dilution.....	125
	2-(2-Butoxyethoxy)ethanol	127
	Methoxypropoxypropanol	127
7.3.2	Layer Build Up	130
7.4	Airbrush Produced Inserts.....	132
7.4.1	LDPE Film.....	133
7.4.2	PET Film	135
7.4.3	PTFE Coated Woven Sheet.....	136
7.4.4	PTFE Film	137
7.4.5	Summary	139
7.5	In-mould layer Application	140
7.5.1	Adhesion between Layer Materials and the Substrate	141
7.5.2	Changing the Injection Substrate Material	142
7.5.3	Mould Release.....	143
7.6	Findings from Scoping Experiments	145
7.6.1	Summary	146
8	Process Refinement Experiments	148
8.1	Overcoming Adhesion Problems	150
8.1.1	Using Different PEDOT:PSS Brands	151
8.1.2	Intermediate Bonding Layer	154
8.1.3	Adhesion Tests	157

8.1.4	Solution to Adhesion Problems.....	164
8.2	Improvements to PE Insert Production.....	167
8.3	Implementation of the Optimised Processes.....	170
8.3.1	In-Mould Layer Application.....	170
8.3.2	Insert Moulding.....	173
8.4	Post Mould Layer Application	176
8.5	Findings from Process Refinement Experiments	179
8.5.1	Summary	180
9	Characterisation Experiments.....	182
9.1	Device Characterisation.....	182
9.1.1	Illuminance.....	183
9.1.2	Layer Thickness	185
9.2	Degradation Investigation	190
10	Results.....	193
10.1	Device Characterisation.....	193
10.1.1	Illuminance.....	193
10.1.2	Layer Thickness	200
10.2	Degradation Test.....	212
11	Analysis.....	217
11.1	Device Characterisation.....	217
11.1.1	Illuminance.....	217
11.1.2	Layer Thickness	241
11.1.3	Comparing Layer Thickness with Illuminance.....	277
11.1.4	Error Analysis	279
11.2	Degradation Tests.....	281
11.2.1	Thick Film Devices	282

11.2.2	Airbrush Devices.....	284
11.2.3	Comparisons.....	286
12	Modelling a Real Device.....	288
13	Discussion.....	293
13.1	Methods for Injection Moulding 3D Organic EL Devices.....	293
13.2	Solutions to Current Problems	296
13.3	The Wider Impact of this Research.....	299
14	Conclusions	302
15	Further Work.....	307
15.1	Extension work related to this project	307
15.2	Developments to make the Process more Commercially Viable	310
15.3	Further projects	312
16	References.....	314

LIST OF FIGURES

Figure 1-1: An overview of project.	8
Figure 2-1: A diagram showing how electrochromic windows work.....	12
Figure 2-2: A diagram showing how common nematic liquid crystals can (within a multi-layer structure) transmit (left) or block (right) light; the electrode layers have been omitted for simplicity.....	15
Figure 2-3: A diagram showing the typical structure and mechanism of a PV cell.	16
Figure 3-1: An example of a multi-layer electroluminescent structure	21
Figure 3-2: A Venn diagram showing the categorisation of electroluminescent devices.....	22
Figure 3-3: OLED devices structures. (L to R); single layer, double layer ETL-emissive, double layer HTL-emissive and triple layer. The dotted red line indicates in which layer emission occurs.	29
Figure 4-1: A diagram to show both linear (A) and an example of branched (B) chain structures within a thermoplastic.....	40
Figure 4-2: A diagram representing partially crosslinked (A) and highly crosslinked (B) chain structures	41
Figure 4-3: A cross-section showing a typical multi-layer plastic structure incorporating recycled material, barrier properties and surface decoration.....	44
Figure 4-4: A representation of the molecular organisation of A, an amorphous plastic and B, a semi-crystalline plastic.....	51
Figure 4-5: A graph to show the change in volume as a function of temperature for A, an amorphous plastic; B, a semi-crystalline plastic and C, a crystalline material. Transitions labelled are T_g , glass transition temperature and T_M , melting point. The schematic below the graph indicates the change in the materials physical behaviour.	53
Figure 5-1: An injection moulding machine.....	61
Figure 5-2: The injection moulding process; a, injection and hold; b, screw back; c, unit retraction; d, open and eject.	63

Figure 5-3: The different stages of an injection mould cycle (the diagram is not to scale; the angle of each section does not represent the proportion of time in the cycle it merely shows the cycle sequence).	64
Figure 5-4: The over moulding process; A, an open mould; B, a preform is placed in the mould; C, the mould is closed; D, a different material is injection moulded; E, the ejected two material part.	68
Figure 5-5: The co-injection moulding process; the skin material is injected first followed by the core material to pack the moulding out.	71
Figure 5-6: Film insert moulding: A, the film substrate; B, the label is printed; C, the label is pre-moulded to the correct shape (this stage is not always required); D, the predecorated film; E, the film is placed in the mould cavity; F, the mould is closed; G, the part is moulded; H, the decorated product.	73
Figure 6-1: A representation of a single side painted sample injection moulded part. .	82
Figure 6-2: A diagram showing a cross-section of the thermoset-thermoplastic system in-mould.....	83
Figure 6-3: A graph showing ABS substrate temperature and the rate of energy transfer to the thermoset film over time.	88
Figure 6-4: A graph showing how the temperature profile across the depth of the thermoset film changes over time.	89
Figure 6-5: A graph comparing the film depth penetrations of heat exposure times using different substrates.	91
Figure 6-6: A diagram showing the multi-layer structure within the mould tool.	93
Figure 6-7: A diagram showing the layers and boundary abbreviations.	95
Figure 6-8: The substrate polymer temperature and the rate of heat transfer through the multi-layer EL system as a function of time.....	101
Figure 6-9: The temperature gradient across the dielectric layer at each of the selected times.	103
Figure 6-10: The complete temperature profile across the multi-layer EL system at selected times after injection.	104
Figure 7-1: The EL structure and operating conditions as recommended by H C Starck.....	106
Figure 7-2: The compressor, airbrush and jars used to apply the layer materials.	109

Figure 7-3: Sandretto Micro 30.....	109
Figure 7-4: The mould cavity.....	110
Figure 7-5: An example of a part moulded in the tool used in this project.....	110
Figure 7-6: The dimensions of the moulded parts made in this project; the removable sprue dimensions have not been included.....	111
Figure 7-7: The screen printing technique. From top to bottom: a) a mesh screen is placed on a substrate, b) areas of the screen may be masked off, c) a viscous liquid is applied on the mesh, d) the flexible scraper forces material through the mesh, e) across the whole frame.....	113
Figure 7-8: The suggested layer design; a) Clevios™ PEDOT:PSS, b) silver bus, c) phosphor, d) dielectric, e) Clevios™ PEDOT:PSS and f) silver.	114
Figure 7-9: The real layer by layer build up.	114
Figure 7-10: The simplified EL structure consisting of four layers.....	116
Figure 7-11: A four layer working EL device made on a PC substrate using a rigid scraper.....	117
Figure 7-12: A shaped EL device made using a rear electrode shaped like the WMG logo.....	118
Figure 7-13: A diagram showing the order that the layer materials are applied in-mould and appear on the final part.....	119
Figure 7-14: The in-mould layer application. Left to right; Clevios™, phosphor, dielectric and silver.	119
Figure 7-15: A moulded part with phosphor, dielectric and silver transferred onto it.	120
Figure 7-16: The illumination of the phosphor at the electrical contact point.	120
Figure 7-17: A working insert moulded EL device.	123
Figure 7-18: Dilution of Clevios with MEK, propanol and water and the resulting layers.	129
Figure 7-19: The molecular structure of ER1.	130
Figure 7-20: The poor coverage of materials when diluted with ER1 compared to the good coverage with MEK.	130
Figure 7-21: The adapted four layer structure; including a larger phosphor layer and a silver bus.....	131
Figure 7-22: A working EL device made using the airbrush application method.	132

Figure 7-23: An illuminated EL device manufactured using a LDPE insert; flow lines are visible.	133
Figure 7-24: A diagram showing how the insert pulled away from the part during ejection. The purple represents the EL layers on the pale blue LDPE with orange copper strips.....	134
Figure 7-25: A diagram showing the displacement of the copper connectors, separating them from the electrode layers.	134
Figure 7-26: The PET film and Clevios™ did not adhere to the part.....	136
Figure 7-27: An injection moulded EL device made using PTFE coated woven mat inserts.....	137
Figure 7-28: If sprayed at a close distance, Clevios™ did not coat the PTFE evenly.....	138
Figure 7-29: A more even coated PTFE insert, after insert moulding and illuminated.	138
Figure 7-30: EL layer materials on a plastic part made directly in-mould	141
Figure 7-31: The adhesion between layers is investigated. Silver layer only (left), the silver and dielectric layers (centre), and finally the silver, dielectric and phosphor layers (right).	141
Figure 7-32: Testing the adhesion between layers; silver, dielectric, phosphor and Clevios layers.....	142
Figure 7-33: Testing the adhesion of layer materials to PC.	143
Figure 7-34: The release of Clevios™ from the mould when using ACMOS 82-2405 release spray.	144
Figure 8-1: A diagram showing the basic process and structure; a. the EL layers are applied to the insert film or the mould tool, b. the layers are injection moulded over & c. once ejected, the injected substrate has the layer structure embedded into its surface.....	150
Figure 8-2: The structure of 2-(2-Ethoxyethoxy)ethyl acetate, the component materials which makes up 30-60% of the phosphor layer.	151
Figure 8-3: The three ratios of bonding layer (made using the Clevios PEDOT:PSS) shown against light and dark backgrounds.....	155
Figure 8-4: EL devices made using an additional bonding layer in between the PEDOT:PSS and phosphor. The ratios of PEDOT:PSS to phosphor are A (1:4), B (1:1), and C (4:1); D has no bonding layer.	156

Figure 8-5: A working EL device made with an additional bonding layer in between the PEDOT:PSS and phosphor.	156
Figure 8-6: A diagram showing the sequence of layer application in cross cut test 1; PEDOT:PSS, bonding layer (where applicable), then phosphor.....	158
Figure 8-7: A Clevios™/no bonding layer/phosphor sample showing almost 100% adhesion in cross cut test 1.....	159
Figure 8-8: A diagram showing the sequence of layer application in cross cut test 2: phosphor, bonding layer (where applicable), then PEDOT:PSS.....	160
Figure 8-9: A Clevios™/no bonding layer/phosphor sample showing 100% adhesion in cross cut test 2.	160
Figure 8-10: The 10x10 masking template grid used when making the inserts for the in-mould cross cut test.....	162
Figure 8-11: Clevios™/no bonding layer/phosphor showing almost 100% adhesion in the insert mould cross cut test.	162
Figure 8-12: A moulded part and the grid used to measure adhesion; this part was moulded with ITO-R PEDOT:PSS and a bonding layer.	163
Figure 8-13: The phosphor carrier polymer remains completely separate in the Orgacon™-phosphor bonding layer mixture.....	166
Figure 8-14: The production of injection moulded EL parts using PE inserts.....	169
Figure 8-15: Working injection moulded EL devices fabricated using PE insert moulding.	169
Figure 8-16: A moulded part cut into a silver busbar masking template.	170
Figure 8-17: Masking templates made from moulded parts: left, to make a small device & right, to make a large device.....	171
Figure 8-18: The in-mould layer application sequence. Left to right; silver bus, Orgacon™ PEDOT:PSS, phosphor, dielectric and silver.	171
Figure 8-19: An injection moulded EL part made by applying EL materials directly in-mould.	172
Figure 8-20: An illuminated in-mould EL part seen from the top and side.	172
Figure 8-21: Disruption to layer materials can be seen when moulded over sharp edges.	173
Figure 8-22: A PE insert moulded EL device, both off (left) and on (right).....	174

Figure 8-23: A PE insert moulded EL device that extends over sharp edges; it failed to illuminate.	175
Figure 8-24: The small PTFE insert moulded device; off (left), on viewed from above (centre) and on viewed from the side (right).	176
Figure 8-25: The large PTFE insert moulded device; off (left), on viewed from above (centre) and on viewed from the side (right).	176
Figure 8-26: PC and PP moulded parts.	177
Figure 8-27: The EL layer application: left to right, silver, dielectric, phosphor, PEDOT:PSS and silver bus.	177
Figure 8-28: A working PC EL part made by post mould layer application.	178
Figure 8-29: A working PP EL part made by post mould layer application.	178
Figure 9-1: The saw and polisher used in this project.	187
Figure 11-1: The bought device, illuminated.	218
Figure 11-2: The main effects of frequency and voltage on the illuminance of the bought device.	220
Figure 11-3: The interaction between voltage and frequency on the bought device. .	220
Figure 11-4: A thick film device, illuminated.	221
Figure 11-5: The main effects of frequency and voltage on the illuminance of the thick film devices.	224
Figure 11-6: The interactions between voltage and frequency on the thick film devices.	224
Figure 11-7: An airbrush device, illuminated.	225
Figure 11-8: The main effects of frequency and voltage on the illuminance of the airbrush devices.	227
Figure 11-9: The interactions between voltage and frequency on the airbrush devices.	227
Figure 11-10: A PTFE insert moulded device, illuminated.	230
Figure 11-11: A post mould device, illuminated.	234
Figure 11-12: A curved PTFE insert moulded device operated by batteries and an inverter.	236
Figure 11-13: The average illuminance of each group of devices under different operating conditions.	238

Figure 11-14: The relative standard deviation of each group of devices.	239
Figure 11-15: A cross section of the bought EL device.	242
Figure 11-16: A graph showing the layer thickness of the transparent electrode at five different positions across the bought device.....	244
Figure 11-17: A graph showing the thickness of the phosphor layer at five different positions across the bought device.....	244
Figure 11-18: A graph showing the thickness of the dielectric layer at five different positions across the bought device.....	245
Figure 11-19: A graph showing the layer thickness of the rear electrode at five different positions across the bought device.	246
Figure 11-20: A cross section of a thick film EL device.	247
Figure 11-21: The average layer thicknesses of the thick film group.	248
Figure 11-22: A graph showing the thickness of the PEDOT:PSS layer at five different positions across each of the thick film devices.....	249
Figure 11-23: A graph showing the thickness of the phosphor layer at five different positions across each of the thick film devices.....	250
Figure 11-24: A graph showing the thickness of the dielectric layer at five different positions across each of the thick film devices.....	250
Figure 11-25: A graph showing the thickness of the silver layer at five different positions across each of the thick film devices.....	251
Figure 11-26: A cross section of an airbrush EL device.....	252
Figure 11-27: The average layer thicknesses of the airbrush group.....	253
Figure 11-28: A graph showing the thickness of the PEDOT:PSS layer at five different positions across each of the airbrush devices.	254
Figure 11-29: A graph showing the thickness of the phosphor layer at five different positions across each of the airbrush devices.	255
Figure 11-30: A graph showing the thickness of the dielectric layer at five different positions across each of the airbrush devices.	256
Figure 11-31: A graph showing the thickness of the silver layer at five different positions across each of the airbrush devices.	256
Figure 11-32: A cross section of a PE insert moulded EL device.....	257
Figure 11-33: The average layer thicknesses of the PE insert moulded group.	259

Figure 11-34: A graph showing the thickness of the phosphor layer at five different positions across each of the PE insert moulded devices.	259
Figure 11-35: A cross section of a PTFE insert moulded EL device.....	260
Figure 11-36: The average layer thicknesses of the PTFE insert moulded group.....	261
Figure 11-37: Phosphor layer thickness measurements for each of the PTFE insert moulded devices.	262
Figure 11-38: Dielectric layer thickness measurements for each of the PTFE insert moulded devices.	263
Figure 11-39: A cross section of an in-mould EL device.....	264
Figure 11-40: Sample C of the in-mould devices; the silver layer was not visible.....	265
Figure 11-41: The disruption to the layer structure caused by the injection of the polymer.	265
Figure 11-42: The average layer thicknesses of the in-mould group.	267
Figure 11-43: The dielectric layer thickness measurements for each of the in-mould devices.....	268
Figure 11-44: A cross section of a post mould EL device.....	269
Figure 11-45: The average layer thicknesses of the post mould group.....	270
Figure 11-46: The phosphor layer thicknesses for each of the post mould devices. ...	271
Figure 11-47: The average thicknesses of each layer material produced using each processing technique.	272
Figure 11-48: The combined phosphor and dielectric layer thicknesses produced by each processing technique.....	273
Figure 11-49: A comparison of the illuminance and combined phosphor and dielectric layer thicknesses for each device tested.	278
Figure 11-50: The degradation in the level of light emitted by thick film devices kept in different conditions over a ten week period.	282
Figure 11-51: The degradation in the level of light emitted by airbrushed devices kept in different conditions over a ten week period.	284
Figure 11-52: The light emitted by the airbrushed device kept in damp conditions after one week (left) and for two weeks and longer (right).	285
Figure 11-53: The relative illuminance of each device after the ten week degradation test.....	286

Figure 12-1: A diagram showing the average thicknesses of layers applied in-mould.	289
Figure 12-2: The temperature profile across the EL layers at particular times after injection.....	291
Figure 14-1: 3D electroluminescent injection moulded parts shown from different angles; PTFE insert moulded (left), PE insert moulded (middle) and in-mould layer application (right).....	302

LIST OF TABLES

Table 2-1: Types of <i>smart</i> materials and possible uses for them.	10
Table 3-1: Common abbreviations used in this chapter.	20
Table 4-1: Common examples of thermoplastics and cross-linked plastics	37
Table 4-2: Examples of materials categorised by use/performance.	39
Table 4-3: Some common additives and modifiers used in the plastics industry.	45
Table 5-1: Common thermoplastic processing methods.....	59
Table 5-2: Some variations on the injection moulding process.....	67
Table 5-3: The compatibility of plastic families [127].	76
Table 6-1: Terms used in equations	84
Table 6-2: The values of terms used that remained constant; values associated with geometry and the film material.	87
Table 6-3: Values of terms that were variable; values associated with the polymer substrate and the moulding conditions.	87
Table 6-4: Values used to model different substrate materials	90
Table 6-5: Abbreviations used in the multi-layer model.	94
Table 6-6: Terms used in the multi-layer model.....	95
Table 6-7: Estimated values used in the initial multi-layer model.	99
Table 6-8: The estimated thermal conductivity calculations.....	100
Table 6-9: The boundary interface temperatures at the selected times.....	102
Table 6-10: The temperature of the dielectric material at position x, at each of the selected times.	102
Table 7-1: Materials used to produce electroluminescent devices.....	107
Table 7-2: The oven regimes for the EL layer materials.	116
Table 7-3: A summary of the insert moulding trials and results.....	122
Table 7-4: The molecular structure of water, propanol and MEK.	125
Table 7-5: The molecular structure of the Clevios, phosphor, dielectric and silver layer materials.....	126
Table 7-6: The drying regimes for the MEK-modified materials.....	129
Table 7-7: The drying regime when applying the modified materials in-mould using an airbrush.	140

Table 7-8: The results of the mould release trial.	144
Table 8-1: A table showing the pros and cons of each of the developed methods.	148
Table 8-2: The molecular structure of the component chemicals in Clevios.	152
Table 8-3: The molecular structure of the component chemicals in ITO-R.....	152
Table 8-4: The molecular structure of the component chemicals in Orgacon and its adhesion improver.	153
Table 8-5: The results of the in-mould adhesion observations.	164
Table 8-6: The overall results for the best PEDOT:PSS material to use in-mould.	165
Table 8-7: Drying temperatures and times used when manufacturing PE inserts.....	167
Table 8-8: The drying regime used when producing EL inserts on PTFE film.	175
Table 10-1: The variables used in each trial.....	193
Table 10-2: The illuminance results for the bought EL device.....	194
Table 10-3: The illuminance results for devices made using the thick layer method. .	195
Table 10-4: The illuminance results for the devices made using the airbrush method.	196
Table 10-5: The illuminance results for devices made using the PE insert moulding method.....	197
Table 10-6: The illuminance results for devices made using the PTFE insert moulding method.....	198
Table 10-7: The illuminance results for devices made using the in-mould layer application method.....	199
Table 10-8: The illuminance results for devices made using the post mould layer application method.....	200
Table 10-9: The layer thickness measurements for the bought EL device.....	201
Table 10-10: The layer thickness measurements for thick layer device A.	201
Table 10-11: The layer thickness measurements for thick layer device B.....	202
Table 10-12: The layer thickness measurements for thick layer device C.....	202
Table 10-13: The layer thickness measurements for thick layer device D.	202
Table 10-14: The layer thickness measurements for thick layer device E.....	203
Table 10-15: The layer thickness measurements for airbrush device A.....	203
Table 10-16: The layer thickness measurements for airbrush device B.....	204
Table 10-17: The layer thickness measurements for airbrush device C.....	204
Table 10-18: The layer thickness measurements for airbrush device D.....	204

Table 10-19: The layer thickness measurements for airbrush device E.	205
Table 10-20: The layer thickness measurements for PE insert moulded device B.....	205
Table 10-21: The layer thickness measurements for PE insert moulded device C.....	206
Table 10-22: The layer thickness measurements for PE insert moulded device D.	206
Table 10-23: The layer thickness measurements for PE insert moulded device E.	206
Table 10-24: The layer thickness measurements for PTFE insert moulded device A...	207
Table 10-25: The layer thickness measurements for PTFE insert moulded device B...	207
Table 10-26: The layer thickness measurements for PTFE insert moulded device C...	207
Table 10-27: The layer thickness measurements for PTFE insert moulded device D...	208
Table 10-28: The layer thickness measurements for PTFE insert moulded device E. ...	208
Table 10-29: The layer thickness measurements for in-mould layer application device B.	209
Table 10-30: The layer thickness measurements for in-mould layer application device C.	209
Table 10-31: The layer thickness measurements for in-mould layer application device D.....	209
Table 10-32: The layer thickness measurements for in-mould layer application device E.	210
Table 10-33: The layer thickness measurements for post mould layer application device A.....	210
Table 10-34: The layer thickness measurements for post mould layer application device B.	210
Table 10-35: The layer thickness measurements for post mould layer application device C.	211
Table 10-36: The layer thickness measurements for post mould layer application device D.....	211
Table 10-37: The layer thickness measurements for post mould layer application device E.	211
Table 10-38: The degradation test results for the thick film devices.	212
Table 10-39: The degradation test results for the airbrushed devices.....	214
Table 10-40: The humidity measurements for the environments in which the unencapsulated devices were kept.....	216

Table 11-1: The operating conditions under which each part was tested.	217
Table 11-2: Average illuminance results and standard deviation of the bought device.	219
Table 11-3: The calculation of the main effects that the two parameters have on illuminance of the bought device.	219
Table 11-4: Average illuminance results and standard deviation of the group of thick film devices.	222
Table 11-5: The averages, SDs and RSDs of individual thick film devices.....	222
Table 11-6: Average illuminance results and standard deviation of the group of airbrushed devices.	225
Table 11-7: The averages, SDs and RSDs of the illuminance of individual airbrush devices; device E has been omitted since it failed after one test.....	226
Table 11-8: Average illuminance results and standard deviation of the group of PE insert moulded devices.	228
Table 11-9: The averages, SDs and RSDs of the illuminance of individual PE insert moulded devices; device A has been omitted because it didn't work.	229
Table 11-10: Average illuminance results and standard deviation of the group of PTFE insert moulded devices.	231
Table 11-11: The averages, SDs and RSDs of the illuminance of individual PTFE insert moulded devices.	231
Table 11-12: Average illuminance results and standard deviation of the group of in-mould devices.	232
Table 11-13: The averages, SDs and RSDs of the illuminance of individual in-mould devices; device A has been omitted because it only partially illuminated and D because it failed to illuminate.....	233
Table 11-14: Average illuminance results and standard deviation of the group of post mould devices.	234
Table 11-15: The averages, SDs and RSDs of the illuminance of individual post mould devices.	235
Table 11-16: The illuminance of 3 devices when operated using batteries and an inverter.....	237

Table 11-17: The average, SD and RSD values of the bought device layer thickness measurements.	243
Table 11-18: The average, SD and RSD values for each layer of each of the thick film samples.	247
Table 11-19: The average, SD and RSD values for each layer of each of the airbrush samples.	253
Table 11-20: The average, SD and RSD values for each layer of each of the PE insert moulded samples.	258
Table 11-21: The average, SD and RSD values for each layer of each of the PTFE insert moulded samples.	261
Table 11-22: The average, SD and RSD values for each layer of each of the in-mould samples.	266
Table 11-23: The average, SD and RSD values for each layer of each of the post mould samples.	269
Table 11-24: The group RSD values and average individual RSD values for each material and each processing technique.	274
Table 11-25: A qualitative comparison of the whole multi-layer structure applied using each processing method.	276
Table 11-26: A consideration of the errors occurring in each processing method.	280
Table 12-1: The layer interface temperatures calculated by the model for specific times after injection.	290
Table 13-1: An evaluation of the success of each injection moulding process, in its current state of development.	294

LIST OF EQUATIONS

Equation 1: The surface polymer temperature as a function of time	85
Equation 2: The rate of heat transfer to the film as a function of the polymer temperature	85
Equation 3: The rate of energy transfer to the film as a function of the temperature gradient across the film	85
Equation 4: The temperature gradient across the film as a function of the rate of energy transfer to the film	85
Equation 5: The temperature of the film (at time, t and distance x into the film) as a function of the energy transferred to the film and the temperature of the polymer. ...	85
Equation 6: The temperature of the film (at time, t and distance x into the film) as a function of the mould temperature and the temperature of the polymer at time, t....	86
Equation 7: The temperature of the substrate polymer as a function of time.	96
Equation 8: The thermal conductance of a material as a function of its conductivity and dimensions.	97
Equation 9: The temperature of the substrate polymer w.r.t its thermal conductance.....	97
Equation 10: The rate of energy transfer through a layer as a function of polymer substrate temperature.....	97
Equation 11: The compound thermal conductance of a multi-layer system.	97
Equation 12: The rate of heat transfer through the multi-layer EL system.....	97
Equation 13: The temperature difference across layer L, at time t.....	98
Equation 14: The temperature at position x, across layer L, at time t.	98

Acknowledgements

I would like to acknowledge Dr Vanessa Goodship for her continual advice and guidance, without which this project would not have been successful. I am also grateful to Prof Gordon Smith for the endless enthusiasm and encouragement throughout my studies.

Finally, I would like to thank Tony, who has supported me in every way possible and has made this degree possible.

Declaration

I, Bethany Middleton, hereby declare that this thesis is a presentation of my original work and has not been submitted to any other university for any award. Where other sources of information have been used, they have been acknowledged.

Part of Chapter 6 is published in *Progress in Rubber, Plastics and Recycling Technology*, vol. 27, pp. 85-106, 2011.

Signed:

Date:

Abstract

Electroluminescence is a developing area of research in the fields of display technology and lighting. Solution based processing of organic materials offers the opportunity to manufacture large area, low cost illuminating surfaces but current processes are limited to two dimensions. The ability to apply electroluminescent materials onto three dimensional contoured surfaces would incorporate the illuminating function into objects, enhancing usability and removing the need for an additional light source.

Furthermore, the integration directly into the manufacturing process, such as injection moulding, would have the added benefits of reducing manufacturing time, handling and have environmental and economic savings. Incorporating electronics manufacturing in-mould offers considerable potential for novel research and commercial applications.

Electroluminescent multi-layer structures were constructed on 3D surfaces, applying materials using an airbrush. Novel injection moulded electroluminescent devices were successfully made using insert moulding and in-mould layer application techniques, then characterised and compared to a bought device. Electroluminescent layers were also applied to injection moulded plastic parts as a post mould treatment for further comparison.

In the current state of development, insert moulding using a PTFE carrier film is the most successful method of injection moulding EL parts, producing devices that light up with an average illuminance of 210.2 ± 39.2 lx when operated at 300 V and 400 Hz. A multi-layer thermal model developed in this project confirms that the injected plastic does not transfer enough heat energy to cure materials that are applied directly in-mould. It was also found that, after 10 weeks, the airbrush made devices maintained 27.3 % points more relative illuminance compared to devices made using a conventional method. Problems associated with all of the new processes have been identified and solutions suggested, but with further research these methods could be used to routinely mould plastic parts with the ability to illuminate.

ABBREVIATIONS

Abbreviation	Term
3D	Three Dimensional
AC	Alternating Current
ACTFEL	Alternating Current Thin Film Electroluminescent
av	Mean Average
DC	Direct Current
DSC	Differential Scanning Calorimeter
DTA	Dynamic Thermal Analysis
EIL	Electron Injection Layer
EL	Electroluminescent
ELD	Electroluminescent Device
EML	Emissive Layer
ETL	Electron Transport Layer
F	Frequency
FPD	Flat Panel Display
HIL	Hole Injection Layer
HOMO	Highest Occupied Molecular Orbit
HTL	Hole Transport Layer
HV	High Voltage
IMD	In-Mould Decoration
IML	In-Mould Labelling
IPA	Isopropyl alcohol
ITO	Indium Tin Oxide
LCD	Liquid Crystal Display
LDPE	Low Density Polyethylene
LED	Light Emitting Diode
LEP	Light Emitting Polymer
LUMO	Lowest Unoccupied Molecular Orbit
MEK	Methyl Ethyl Ketone
OLED	Organic Light Emitting Diode
PC	Polycarbonate
PDP	Plasma Display Panel
PE	Polyethylene
PEDOT:PSS	Poly(3,4-ethylenedioxythiophene) poly(styrenesulphonate)
PET	Polyethylene terephthalate
PLED	Polymer Light Emitting Diode
PP	Polypropylene
PTFE	Polytetrafluoroethylene
PU	Polyurethane
PV	Photovoltaic
PVC	Poly (vinyl chloride)
RMS	Root Mean Squared

RSD	Relative Standard Deviation
SD	Standard Deviation
SMOLED	Small Molecule Organic Light Emitting Diode
V	Voltage or Potential Difference
w.r.t.	with respect to
WOLED	White Organic Light Emitting Diode

1 INTRODUCTION

The main topics of this project are plastics processing and *smart* materials, specifically electroluminescent materials will be considered in this thesis. However, the driving forces behind the idea, as is so often the case, are increased part performance, lower costs and reduced environmental impacts. These factors are both important and relevant in a world where so much focus is placed on efficiency and sustainability.

Firstly, addressing the main topics; plastic processing is a global industry and plastic has replaced many traditional materials in a wide range of applications. Plastic can be processed in many different ways and injection moulding is one of the most common techniques; there are a number of variations to it and it continues to develop in order to make more complex parts and improve the overall process.

An exciting development is the integration of *smart* material functionality into the manufacture of plastic parts. *Smart* function has been integrated but mainly by over moulding electronic chips. This work intends to develop a new process for *smart* integration during manufacture.

The types and function of *smart* materials are very wide, hence for the purpose of this work the author has chosen to concentrate on electroluminescence. Solid state lighting by electroluminescence is of interest as a lighting solution of the future; electroluminescence is an efficient mechanism for light emission and devices are low power, thin and can have a large illuminating surface area. The production of inorganic electroluminescent devices involves vacuum deposition techniques which

require highly specialised equipment and extreme environmental conditions; however polymer based electroluminescent materials can be applied using simpler solution based techniques. Current manufacturing processes utilised in making polymer electroluminescent devices are screen printing, spin coating and inkjet printing; all of these application methods apply layers to a flat substrate, albeit sometimes a flexible one. When considering electroluminescence as a lighting option, illuminated strips, sheets and wires can be purchased to include in any situation where required and patterned designs can be specially printed, but again this is in a 2D form. A flat, flexible electroluminescent device cannot always be easily added to items that require illumination due to the shape of the object therefore it would be advantageous to apply the electroluminescent layer structure during the production process. This would enable the manufacture of 3D plastic items with the illuminating materials embedded into the main body of the part; by adding electroluminescent layers in-mould during the moulding cycle, a huge variety of profiles and shapes can be made to illuminate.

With the main topics summarised and the problem identified, the following three paragraphs indicate the relevance of developing this new technique with regards to the three driving forces that motivate a majority of manufacturing research: performance, cost and environmental factors.

The performance of moulded plastic parts will be enhanced by increasing their functionality when adding light emission as an integral property of the moulded structure. This will be done by incorporating electroluminescent layer materials into

the main body of the part as a stage within the injection moulding process. This increased functionality will remove the need for an additional light source.

Reducing the costs associated with making a part can be achieved by a number of methods; firstly, by reducing the number of components by combining the function of many into one has already been suggested in the previous paragraph. Also, by removing manufacturing stages there is an associated cost saving; the entire device production happens in one cycle on one machine so there are no additional pre- or post- process stages or the requirement of component assembly.

There are reduced environmental impacts related to the two previous paragraphs but there are also the benefits directly associated with the materials used in the process. As mentioned earlier, electroluminescence is the most efficient mechanism for light emission, and by making plastic parts illuminate by incorporating the electroluminescent phenomenon, hopefully these will replace objects that use less efficient, more traditional light sources. Also, the solution based processing conditions of the polymeric materials selected for this project have a lesser impact on the environment than the energy devouring, high temperatures and vacuum needed for inorganic electroluminescent processing.

To give an indication of the positive impact this technology could have, some examples of how it could improve road safety are described in this paragraph. Plastic parts that are currently moulded and then require additional lighting can be manufactured to completely illuminate; for example road furniture (traffic cones and bollards) and safety/cycle helmets. This would be more visible than the light emitted by a small additional lamp. Another example is where the function of two

separate parts could be combined into one; for example mudguards on bicycles could also act as lights, or be simply used to make the rider more visible to other road users. Finally, the illuminating function can be used as an additional characteristic to currently moulded parts; for example on a car, the front and rear bumper could illuminate as a more visible alternative to current hazard lights.

From the problems identified earlier, and the anticipated benefits described in the last few paragraphs, the direction of this project is dictated by the following research question:

“Can electroluminescent technology be integrated into the injection moulding process to produce 3D illuminating plastic parts?”

This research question will be answered by meeting the following specific objectives:

- **To determine the optimum electroluminescent structure for an in-mould process; this is the minimum number of layers that will reliably form a working EL lamp.**
- **To develop a method of integrating the application of electroluminescent layer materials into the injection moulding process.**
- **To produce 3D injection moulded plastic parts with electroluminescent capabilities.**
- **To describe any geometric limitations observed in the new process.**

- **To model the temperature conditions undergone by the layer materials during an injection moulding cycle.**
- **To characterise the layer thickness and illuminance of the injection moulded EL devices.**
- **To compare the layer thicknesses and illuminance of devices made using the new injection moulding process with a bought device and a thick film device made using the EL materials in a paste form.**
- **To monitor the degradation of the intensity of light emitted by devices made by the new process with modified materials over a 10 week period. Different conditions and encapsulation options will be considered.**
- **To compare the degradation of the devices made with modified materials to equivalent devices made with materials used as intended.**

To successfully achieve these criteria, firstly, a literature review was carried out across two key areas: recent advancements in electroluminescent technologies, and developments in plastic processing. Practical work began by using commercially available materials, used in a conventional method, to produce flat illuminating EL devices. A method for introducing EL layer materials into the injection mould tool was developed in order to fill the technology gap identified in the literature review. Once the technique had been refined, samples made using both the traditional and novel processing techniques were characterised and compared.

The thesis does not contain a chapter entitled “literature review” but instead has a number of themed chapters covering different key areas; this is because this project covers several separate disciplines and the structure of the thesis shows the

consideration given to each of these and the progression of the project through them.

The thesis starts with a chapter giving an overview of *smart* materials, a group which electroluminescent materials belongs to, and a far reaching, fascinating area of research. There is then a more in depth study into the science behind and recent developments in electroluminescent technology. Since this project is focusing on plastic processing, particularly injection moulding, and polymeric materials are used in some EL systems, there then follows some background information on polymers and plastics. The chapter gives an overview of the fundamental material science and includes a section specifically on electrically conductive polymers, a material utilised in this project. The next logical step is to look at plastic processing; this chapter briefly covers general plastic processing but focuses on injection moulding and the current progress made in injection moulding multi-material parts.

The electroluminescent materials used in this project are not formulated to be used in an injection moulding cycle so it is important to calculate the temperatures they are subjected to. Therefore at this point in the thesis there is a chapter showing the development of a model replicating the in-mould thermal conditions that the layer materials will undergo.

The methodology section follows, and this has been divided into 3 chapters: the scoping experiments, refinement of the new processing technique and the characterisation of parts made using the new method. Next are the experimental results and the analysis of those results. The experimental data is then used in the

model to simulate the temperature profiles experienced by the layer materials when manufacturing a real device.

There is then a discussion evaluating each of the methods developed during the project, suggestions to overcome identified problems and a discussion on the relevance of this project with respects to the wider research area. The key findings are then summarised in the conclusion chapter.

Finally, thoughts on how this research can be continued, ideas on how the novel process can be advanced and suggestions into making the technique more commercially viable are described in the further work chapter.

To give a simple overview to the whole project, a diagram has been constructed representing the progression of work from top to bottom; it shows the key areas of the project and how they relate the each other (see Figure 1-1).

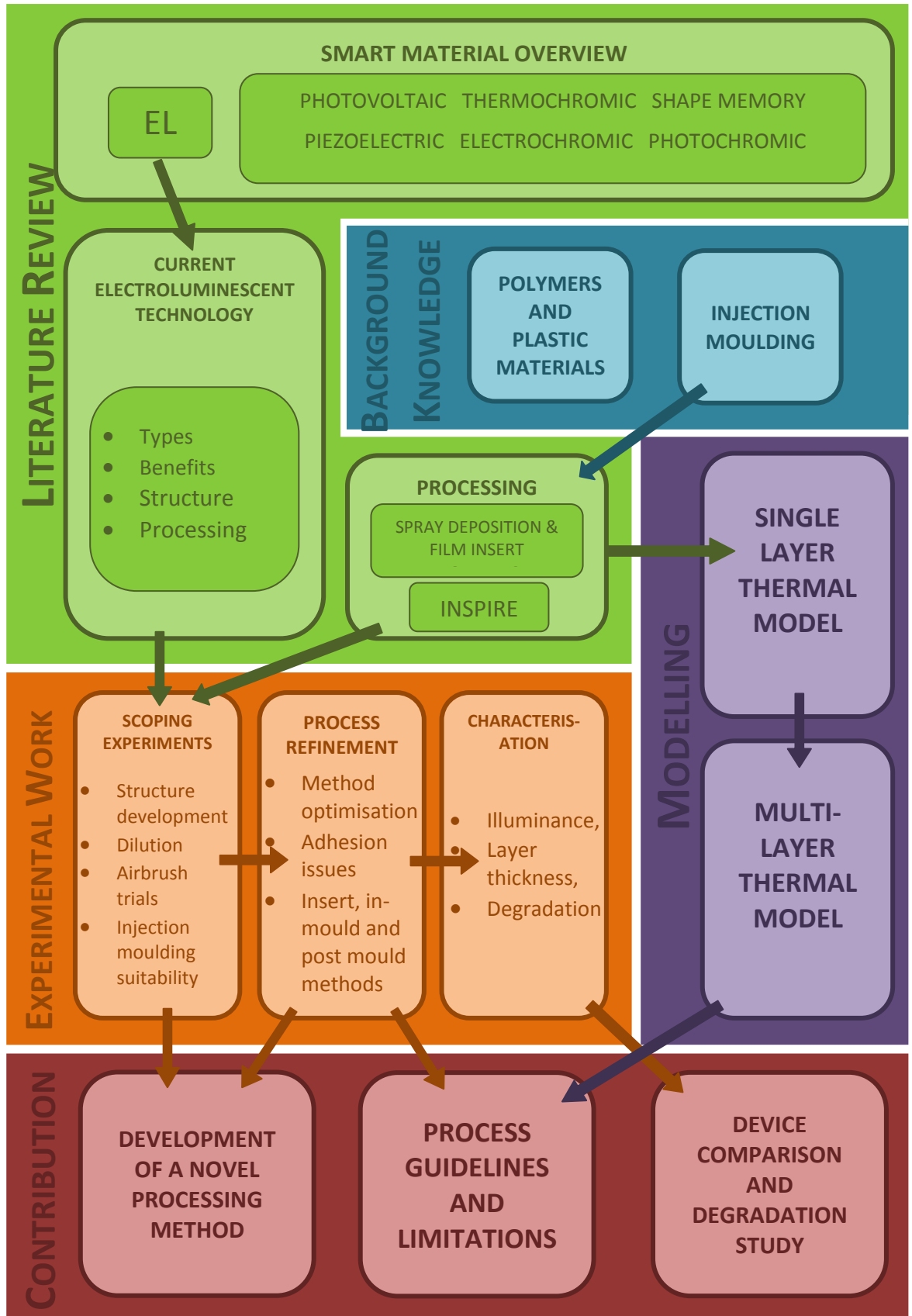


Figure 1-1: An overview of project.

2 SMART MATERIAL SYSTEMS

This project aims to develop a new method of manufacturing electroluminescent devices and the light emitting (luminous) material within them fall into the wider category of *smart* materials. For this reason the literature review begins with a brief chapter introducing *smart* materials, before focusing down to the main themes of the project.

2.1 Definition of *Smart* Materials

The development and study of *smart* materials is a relatively contemporary area of research that has progressed steadily over the last ten years [1]. *Smart* materials have a “coupling between multiple physical domains” [2]; this means that a particular characteristic of a material changes in response to a change in a different field. For example in some materials, an external temperature change can cause a colour change in the material. Vepa describes *smart* materials as “materials that can sense an external stimulus... and initiate a response” [1], however Addington and Schodek draw attention to the fact when people talk about *smart* materials they are actually referring to the reactive device, that may consist of a system of multiple layers of different materials, rather than the single material that exhibits the coupling mechanism [3]. Despite this, it is also stated that due to the “common usage by engineers and designers” it is accepted that some devices may be referred to as *smart* materials [3]. Different *smart* materials have different input and output couplings. The ability to “react” to a stimulus means that *smart* materials can be used to give additional functionality to devices and despite being cutting edge

technology, *smart* material systems are already used in objects found in many homes and workplaces.

2.2 Types of *Smart* Materials

There are a wide range of materials falling within the blanket name of *smart* materials, since there are a large number of combinations of different field couplings. However they can be grouped into three different categories, type 1, 2 and 2(reversible) [3] or they can be referred to as type 1, 2 and 3 [4]. Type 1 materials exhibit a property change; type 2 materials undergo an energy exchange and when this energy exchange is reversible the materials are named type 2(reversible) or type 3.

Table 2-1: Types of *smart* materials and possible uses for them.

Name of <i>Smart</i> Material	Type	Input Stimulus	Output Reaction	Application
Electroluminescent	2	Electric potential	Light emission	Lighting
Electro chromic	1	Electric potential	Colour change	Smart Window
Photochromic	1	(UV) Radiation	Colour change	Tinted Glasses
Photovoltaic	2	(UV) Radiation	Electric potential	Solar Cell
Piezoelectric	3	Physical deformation	Electric potential	Sensor
Thermal Shape Memory	1	Temperature change	Shape change	Stent
Thermo chromic	1	Temperature change	Colour change	Thermometer

With a few exceptions, the names of different *smart* materials are related to the domain coupling they exhibit; the first part of the name relates to the input and the

second part to the output; Table 2-1 shows a number of examples adopting the type 1, 2, 3 nomenclature. A short explanation of some of the different types of *smart* material follows.

Electroluminescent materials emit light upon the application of an electric field [5]. Visible light is emitted and since other parts of the electromagnetic spectrum (e.g. infra-red) are not also emitted, the devices are cool to the touch and energy efficient. The devices have a layer structure which can be applied to thin substrates, as a result the devices are also lightweight and may be flexible; they also have the benefits of being robust as they do not contain easily breakable parts such as a filament [3].

The two main areas of application of electroluminescence are in lighting and display technology. For use in lighting and advertising, multi-layer electroluminescent sheets and strips can be incorporated into items or can be retrofitted to almost any surface or product; different shapes and designs can also be printed to order. Matrix structures of layer materials can be printed to produce thin, lightweight, flexible flat panel displays (FPDs) with improved brightness, viewing angle, efficiency and response times, when compared to previous flat panel technology such as LCDs. Since this particular *smart* material system is the focus of this project, further details follow in the next chapter, Electroluminescent Systems.

Electro chromic, photochromic and thermo chromic materials all respond to different stimuli with a colour change; these are often utilised as a useful visible indication [6, 7] of a normally non-visible change.

Electrochromic materials undergo a permanent but reversible electrochemical reaction which switches the molecule between its reduced and oxidised states [3, 8, 9]. Electrochromic devices have a layered structure where the electrochromic material, an ion storage layer and an electrolyte, are positioned between two transparent electrodes [3, 8, 10] (see Figure 2-1). The application of a potential difference across the electrodes (the switching voltage) induces an electric field between the electrodes. This causes charge to be transferred from the ion storage layer across the electrolyte and into the electrochromic material; which results in either a reduction or oxidation reaction [10].

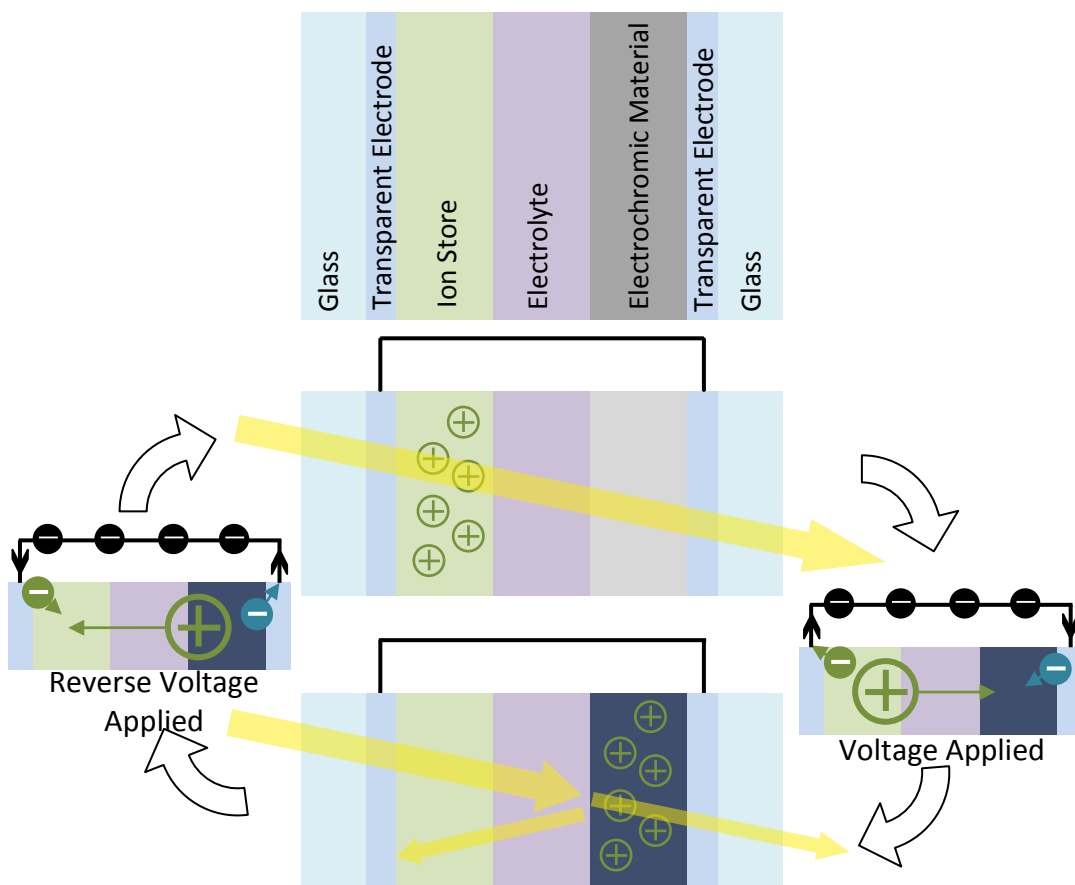


Figure 2-1: A diagram showing how electrochromic windows work.

The change is visible to an observer because the material has different absorption properties in each different state, causing differences in how much light is transmitted or absorbed [6, 9]. The most common transition undergone is between transparent and opaque [6, 9]. The voltage is only required during “switching” [11] and the new state is maintained until the reaction is reversed by applying an opposite voltage or by short circuiting the system [10].

The photochromic mechanism is very similar to that of electro chromism; the molecule can exist in different states, each with different absorption properties [3]. The difference occurs in the stimulus; photochromic materials change state when they are subjected to radiation of a particular wavelength which causes a photochemical reaction to occur [7]. When the radiation is not incident on the material, the substance returns to its original state [3].

When a photochromic material is irradiated it is not only the colour that changes, electrical properties such as conductivity also change and as such there is interest in these materials acting as photo-switches [12].

A thermo chromic device changes colour when there is a change in temperature; they can be made from liquid crystals or dyes. The dyes often only change between colourless and a single colour and as such are often only used when a single change needs to be indicated. The liquid crystal type contain multiple layers of crystals; when the temperature changes, the orientation of the crystals changes and the wavelength (and therefore the colour) of the reflected light changes too [7]. Liquid crystal thermo chromic materials are used when more accuracy is required or to indicate changes over a wide temperature range [3].

Colour changing materials are an example of *smart* systems currently used in a number of common uses within the home; forehead thermometer strips incorporate thermo chromic technology, and reactive lenses (a coating applied to glasses that becomes tinted in sunlight) utilise the photochromic phenomenon [3, 4]. Electro chromic windows are available; a voltage applied at the flick of a switch can change glass from transparent to tinted/opaque and back again [3], further developments include utilising thermo chromic or photochromic layers to produce *smart* windows with the ability to react to the Sun or a buildings environment [10, 13].

Liquid crystals can be used to alter the path of light in order to produce displays; two simple examples are calculator and digital clock screens [7]. Liquid crystal displays (LCDs) are also multi-layer devices; the minimum requirements are polarising layers, transparent electrodes and the liquid crystal layer but there also can be adhesives, protective films and surface treated films [14]. Upon application of an electric field the liquid crystals change orientation which affects the polarisation of light passing through it causing it to switch between transparent and opaque [7, 8] however the current must be maintained in order to keep the material opaque [3]. LCD screens are often accompanied by an electroluminescent backlight.

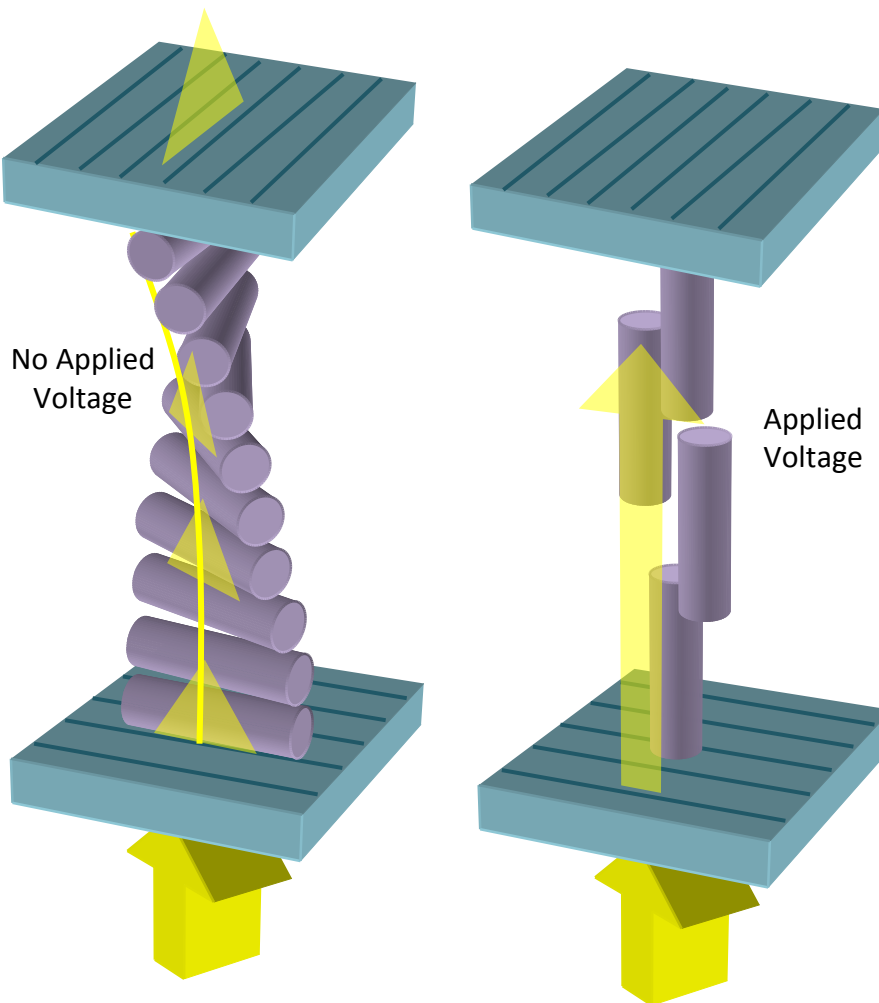


Figure 2-2: A diagram showing how common nematic liquid crystals can (within a multi-layer structure) transmit (left) or block (right) light; the electrode layers have been omitted for simplicity.

The liquid crystal (LC) material is positioned in between two transparent electrodes, and that system is placed in between two polarising films (at 90° to each other) [14]. A common type of LC is twisted nematic and in this, the active bulk layer is comprised of many individual molecular layers of crystals. In the “off” state, the crystals in each layer are positioned horizontally, with the slight difference in each layers alignment resulting in a twisted structure. The twisted crystal architecture rotates the orientation of the entering polarised light through 90° so that it is then aligned with the second polarising film; this means that light can pass through the LCD structure. In the “on” state, the electric field induced by the applied voltage

causes the crystals in each molecular layer to align vertically [14]. In this arrangement, the alignment of the entering polarised light remains unaltered and is therefore blocked by the second polarising film; this means that light is blocked by the LCD structure. Figure 2-2 shows both the transparent and opaque states of an LCD.

Photovoltaic (PV) materials have the ability to generate an electrical energy by absorbing light (specifically UV solar) energy [15]. PV cells have a multi-layer structure with conductive contacts either side of the active layers. Light passes through the contact grid and hits the photovoltaic material causing electrons to be excited into a higher energy band. These electrons, and the resulting “holes”, move to opposite electrical contacts which causes a potential difference between them, which in turn induces a current through the circuit [16].

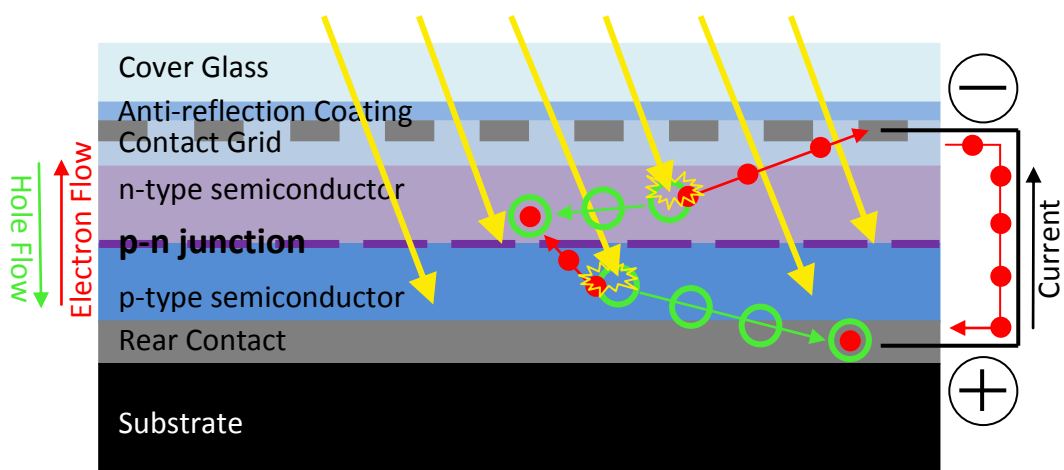


Figure 2-3: A diagram showing the typical structure and mechanism of a PV cell.

Figure 2-3 shows how the PV cells work; the green rings represents holes and the red circles represent electrons, the p-n junction between the two types of semiconductor allows the flow of electrons in only one direction. When a photon

from the Sun's light hits a molecule in the PV semiconductor layer, the energy absorbed from the photon excites an electron into the conduction band. Electrons in the conduction bands of semiconductors can move within the layer and flow in the "n" direction, this results in the apparent flow of the holes in the "p" direction. The movement of the charge carriers in separate directions results in an electric field, which means there is a potential difference between the contacts; so when they are connected, electrons (i.e. a current) flow(s) through the circuit [15, 16].

These so called "solar cells" use PV technology to convert solar energy into more useful electrical energy. Calculators often contain solar cells and arrays of them can be seen on buildings; portable PV devices are also available which are used to charge small electrical items. Current research is also investigating the benefits of photovoltaic/thermal collectors which can simultaneously generate electricity and heat air or water [17-21].

A piezoelectric material has a two-way relationship between the mechanical stress within it (deformation) and the potential difference (voltage) across it [3]. Deformation of the material can cause a voltage across it and an applied voltage can cause the material to deform. Quartz is a common piezoelectric material used in watches; the battery causes a regular oscillation of the quartz which is used to keep time. Airbags contain a piezoelectric sensor; the impact causes a voltage which is detected and the airbag is deployed. Push ignition buttons also utilise this effect, by creating a spark [3]. Due to the mechanical-electrical relationship, piezoelectric materials are often used as sensors and actuators [22].

Shape memory materials have a permanent shape; this shape can be deformed and then the original shape can be recovered when the material undergoes a particular stimulus [23, 24]. Polymers are one type of material that have this ability, and temperature is one of a number of different stimuli that can be used to initiate the shape change; light, moisture and electric fields are other examples [23, 25]. Shape memory polymers that are activated by a temperature change are of particular interest because the temperature at which the shape transition is initiated can be easily controlled [23]. It is hoped that thermal shape memory polymers will be commonly used in the medical industry; there is extensive research into self-expanding stents, self-tightening sutures and drug delivery systems [25, 26].

Overall *smart* materials, and the systems they are part of, are used in a wide range of applications and their use is growing; from common everyday objects to state-of-the-art devices, their “reactive” abilities are utilised extensively however there is further potential considering the new ways of using exploiting additional properties that are being continually discovered.

3 ELECTROLUMINESCENT SYSTEMS

This chapter offers an in-depth review of the overall topic of electroluminescence, which is of particular relevance to this project.

3.1 The Relevance of Electroluminescence

Although it was first observed in 1907 [27], the phenomenon of electroluminescence was not researched in great depth until the latter half of the twentieth century. Since then, there has been significant research into all aspects of the subject including conductive and light emitting materials (*more recently organic as well as inorganic*), device structure and processing techniques. Currently interest in electroluminescence is high, as the benefits over traditional light emission are seen to solve many of the problems relevant in today's energy conscious and performance demanding society, e.g. devices are lightweight, low power and efficient [28]. Research into organic electroluminescent (EL) technology is currently progressing along two different developmental pathways; initially interest into using matrices of devices to create flat panel displays (FPDs) dominated, but now using EL materials to create large area, single colour lighting is catching up [29, 30]. There are many acronyms used in this chapter so a short abbreviations table (Table 3-1) has been included here to aid the reader.

Table 3-1: Common abbreviations used in this chapter.

Abbreviation	Full Term
(AC)TFEL	(Alternating Current) Thin Film Electroluminescence
EL	Electroluminescent/Electroluminescence
ELD	Electroluminescent Device
FPD	Flat Panel Display
PDP	Plasma Display Panel
LCD	Liquid Crystal Display
LED	Light Emitting Diode
LEP	Light Emitting Polymer
OLED	Organic Light Emitting Diode
PLED	Polymer Light Emitting Diode
WOLED	White Organic Light Emitting Diode
SMOLED	Small Molecule Organic Light Emitting Diode
ITO	Indium Tin Oxide
EML	Emissive Layer
HTL	Hole Transport Layer
ETL	Electron Transport Layer
HIL	Hole Injecting/Injection Layer
EIL	Electron Injecting/Injection Layer

Electroluminescent devices are multi-layer structures, where the *smart* light emitting material and often other layers are sandwiched in between two electrodes; an example of such a structure is shown in Figure 3-1.

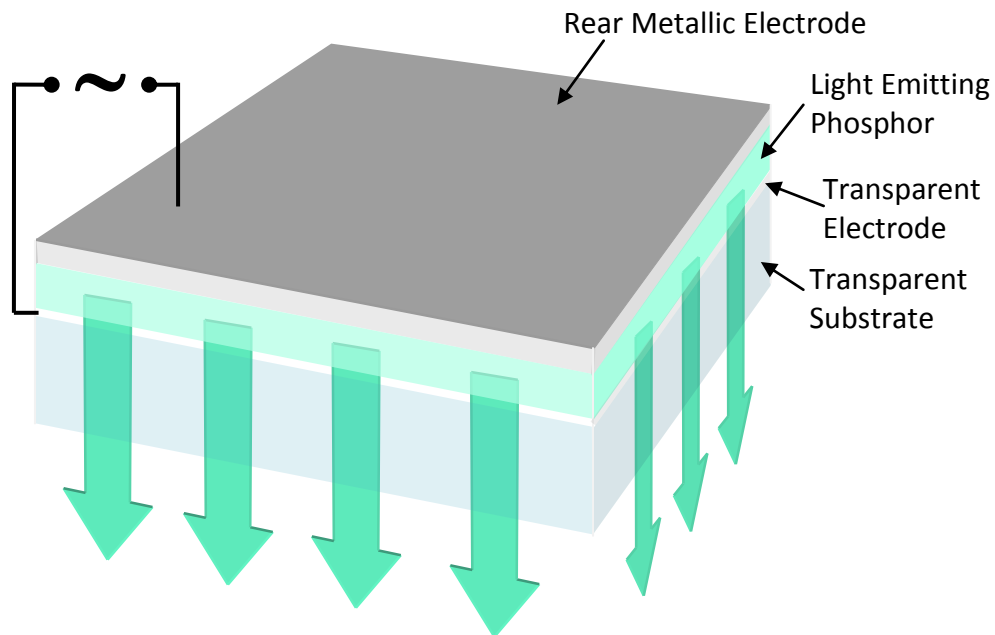


Figure 3-1: An example of a multi-layer electroluminescent structure

3.2 Types of EL Devices

Electroluminescent devices can first be divided into two groups based on the materials they are made from; organic and inorganic. Devices classified as organic are not completely manufactured from organic materials but have a minimum of one organic/carbon/polymer based layer [30]; electrode and charge transport layers can be either organic or inorganic.

A Venn diagram has been constructed showing how electroluminescent devices can be separated into groups; this also indicates the hierarchy of the categorisation and how the groups relate to each other (Figure 3-2). For example, “powder phosphor” electroluminescent devices fall within the “high field” category, which itself is part of the larger “inorganic” group; “injection” devices are also inorganic but do not include and are not related to the “powder phosphor” type.

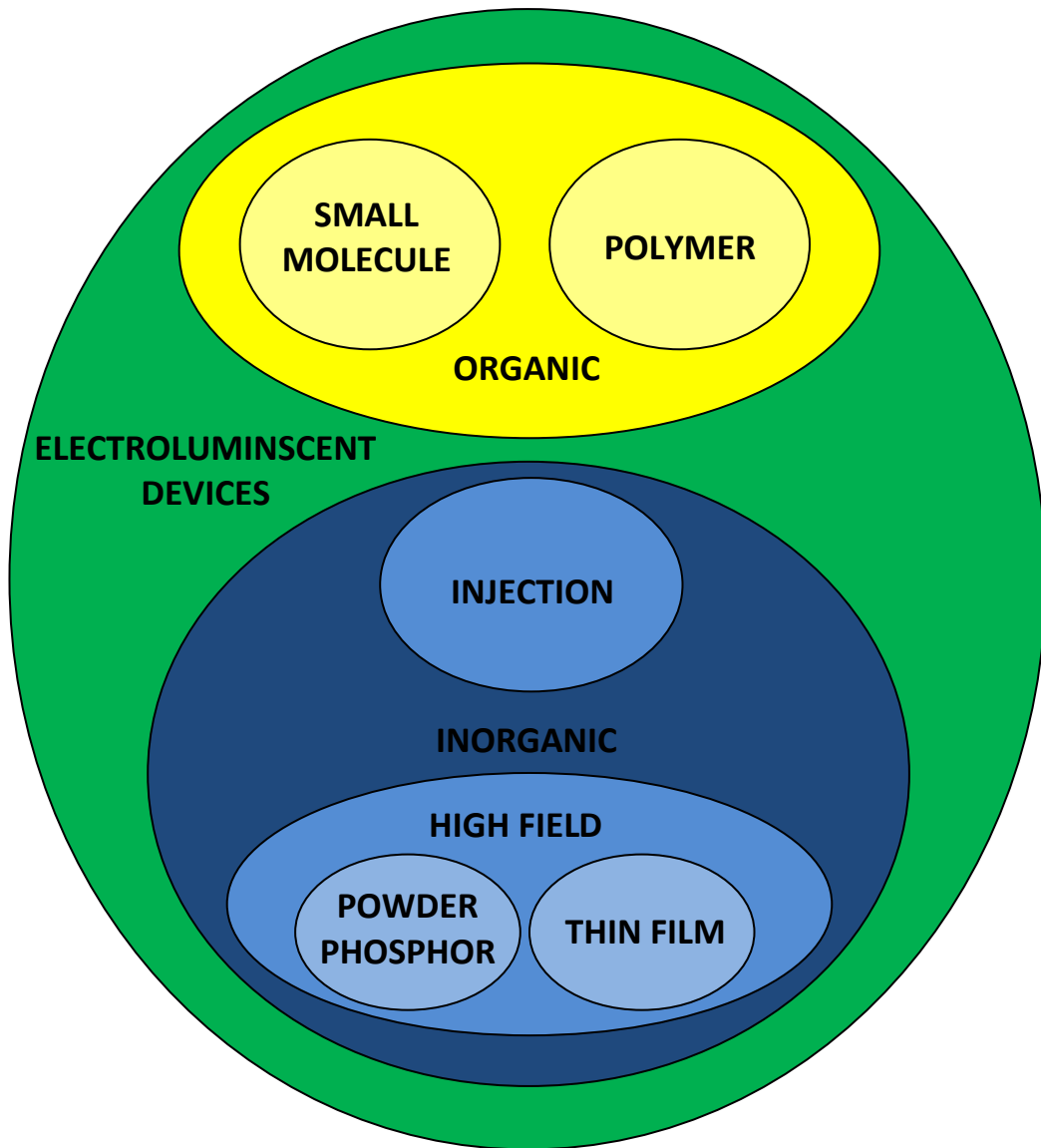


Figure 3-2: A Venn diagram showing the categorisation of electroluminescent devices.

3.2.1 Inorganic

Inorganic EL has a longer history [31] and therefore is further developed than organic EL; early, simple displays on commercial appliances date back to the 1970s and currently high resolution LED flat screen TVs are widely available. Different types of EL devices are suited to different applications; the following sections summarise the range of inorganic EL technology. Inorganic EL can be classified as either high field or injection [5] depending on the mechanism of light emission.

High field ELDs (electroluminescence devices) have a capacitor structure and rely on a strong alternating or direct current electric field to accelerate charge carriers; this category can be further separated into powder phosphor devices and thin film electroluminescence.

Inorganic EL lamps and backlights typically use powder phosphor high field electroluminescence and thin film electroluminescence (TFEL) is used in FPD technology [5, 31, 32]. Alternating current thin film electroluminescent devices (ACTFEL) are preferable over direct current devices due to the poor efficiency and reliability of the latter [5].

Inorganic injection devices generally utilise the recombination mechanism. EL occurs when injected charge carriers meet at a p-n junction; electrons and holes recombine and emit energy in the form of a photon. No overall current flows through this type of device as the active material does not need to be in direct contact with the electrodes; LEDs utilise this type of electroluminescence. [5]

3.2.2 Organic

Organic EL devices contain at least one organic layer within the device architecture/structure [30]. They have diode structure with a p-n junction and can be separated into two categories: small molecule organic light emitting diodes and polymer light emitting diodes [33-36].

3.2.2.1 Small Molecule

The first type of OLED to be developed was using small organic molecules; these are now known as SMOLEDs but can still be referred to as OLEDs due to the fact that initially these were the only type. Deposition of small molecule layers is similar to inorganic devices; vacuum deposition methods are required and as a result production is complicated and expensive [34].

3.2.2.2 Conjugated Polymer

A later development in organic electroluminescence saw the use of conjugated polymers as transparent electrodes, emissive and charge carrier layers. Organic light emitting diodes based on conjugated polymers are known as PLEDs (for polymer light emitting diode). The conjugated polymers in PLEDs are solution based so this type of device can be manufactured by spin coating and printing methods. A more detailed description of conjugated polymers is included in the “Conductive Polymers” section 4.5.

In this project, both conductive polymers and inorganic materials in a polymer matrix were used to produce ELDs with a capacitor structure, operated by the high field mechanism.

3.3 Electroluminescent Emission Mechanisms

Luminescence occurs when energy from an excited EL molecule is emitted in the form of a photon, this is known as radiative relaxation [5]. The excitation can be induced in a number of different ways; by high electric fields, impact from charge carriers and recombination of charge carriers [5].

In high field EL, emitting states are directly excited by a strong AC or DC electric field; electrons from the valence band (the highest occupied molecular orbit or HOMO) of the active molecules gain energy and move to the conduction band (the lowest unoccupied molecular orbit or LUMO) by field ionisation [33].

Impact EL occurs when high electric fields across the device accelerate charge carriers; these charge carriers collide with the active molecule, exciting or ionising them [33].

Recombination EL can occur in a bulk layer (in ELDs) or at a p-n junction (in LEDs) [33]. Electrons are injected by the cathode, holes are injected by the anode and they drift in opposite directions. They meet and recombine in the emissive layer; energy is released by recombination which excites a molecule (forming an exciton) [37]. The molecule is excited because an electron moves into a higher energy state when the recombination energy is absorbed; a higher energy electron then moves to re-fill the ground (most stable) state and causes a photon (light) to be emitted. Recombination can occur at different positions between the electrodes due to differences in the mobility of the electrons and holes [30]. Recombination can also occur at a p-n junction; the mechanism is the same but the charge carriers originate

in the “p” and “n” semi-conductors, rather than been injected from the electrodes [33].

3.4 Uses and Applications

In the early days of commercial applications single colour electroluminescent devices were used for illuminating watch faces and automotive dashboards. The EL phenomenon is now used in a wide range of applications; some examples where the technology has been incorporated are backlighting LCDs, illuminating large advertising boards and providing low intensity feature lighting [38]. In the future it is hoped that large area solid state lighting will be provided by organic EL devices [36, 39] and become the standard method for lighting a building, but as of yet the lifetime and efficiencies of devices do not match that of other lighting technology [34]. Multi-colour matrix arrays of devices are used in inorganic LED TVs and these are becoming commonplace for commercial and domestic use. Small organic multi-colour EL displays are already used commercially in car stereos, MP3 players [29, 30] and mobile phones [34]; an expensive, small OLED TV has been commercially released by Sony but larger organic displays are currently only for demonstration purposes rather than being commercially available [34].

3.5 Benefits of Electroluminescence

Electroluminescence is moving towards replacing existing technology in many areas. Small and large display applications [34, 40], advertising and potentially lighting [29, 30, 36, 41, 42] are utilising the EL mechanism; a number of advantages sees EL outperform traditional technologies. The following sections describe how EL

devices are an improvement on conventional components and how moving towards organic materials offers further benefits.

3.5.1 Benefits of EL over other light sources

Electroluminescence is preferable over traditional lighting mechanisms such as incandescence due to its low power consumption (due to high efficiency), also sources remain cool to the touch, and encapsulated devices are robust, tolerating a range of operating conditions [28]. The prospect of having completely flat, flexible or transparent light features is also appealing [36]. A further advantage is that an EL light source will not undergo instant failure, but get dimmer over its lifetime [33].

3.5.2 Benefits of LEDs in FPD Technology

The use of LEDs in FPDs offers many significant benefits over the commonly available LCDs and PDPs; a wide viewing angle, good contrast, resolution and colour variation result in better quality viewing [28, 35, 43]. The LED displays are very thin and lightweight making appliances less bulky [30, 44]; they are also self-illuminating, and a fast response time means crisper high speed images [33].

3.5.3 Benefits of PLEDs over LEDs

Conventional LEDs based on inorganic crystals (GaAs etc.) are not suited for large areas/arrays; they are brittle and so are unable to be used for flexible displays and the crystals are expensive to grow [39]. SMOLEDs are also produced using high temperature vapour-deposition techniques [34, 35] giving similar processing disadvantages.

There are many manufacturing advantages of using conjugated polymers in OLEDs; solution based processes such as spin coating and printing [34] can be used

resulting in the ability to process large areas, use flexible substrates, and produced patterned electrodes for displays [35]. These production methods are cheaper and easier than vacuum deposition techniques as they can be performed under atmospheric conditions.

Despite all of the benefits of OLEDs for lighting and displays, there are still significant limitations such as operational lifetime, transparency [36] and the need for absolute encapsulation of polymer devices [40].

3.6 Structure of EL Devices

The structure of EL devices can vary greatly but are always multi-layer systems; in addition to the minimum requirement of the emissive layer and two electrodes [30], further layers can be incorporated to increase efficiency [35].

Further differences arise when the use of the device is taken into account; it may be necessary to have a single device with uniform large area layers or to have an array of individually controlled micro devices. When EL is to be utilised as a lighting technology to illuminate or highlight specific areas (including advertising) one large single device is used. These devices are a single colour, cover a large area and are formed in panels, wires and strips; they can also be printed to take on a specific shape (within some constraints). Flat panel displays use a matrix array of micro-devices, each of which can be controlled individually in order to give a large area multi-colour dynamic display [34].

3.6.1 Layer Structures

The simplest layer structure is a single layer device which has one organic layer in between the transparent electrode and the opaque (usually metallic) electrode; an emissive layer (EML) [33]. Double layer devices have two layers in between the electrodes, a hole transport layer (HTL) and an electron transport layer (ETL); these can be categorised by where the light emission occurs, HTL-emissive or ETL-emissive [33]. Basic OLEDs typically have a double layer structure [34].

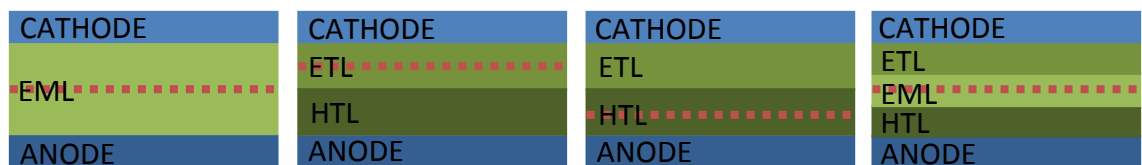


Figure 3-3: OLED devices structures. (L to R); single layer, double layer ETL-emissive, double layer HTL-emissive and triple layer. The dotted red line indicates in which layer emission occurs.

Triple layer devices have HTL and ETL along with a specific EML in between the electrodes [33]. These are the basic ELD structure categories (all shown in Figure 3-3), however further layers have been investigated in the literature [30, 45, 46]. LEDs have “p”-type and “n”-type semi-conductor layers to form the p-n junction.

Devices where the transparent electrode is the first layer to be applied to the transparent substrate will emit light through the substrate material; this is a standard bottom emission device. Layers can be applied in the reverse order, so that the transparent electrode is the last layer to be applied; this is known as a top emission device.

3.7 Device Layers

Each layer within EL devices performs a specific role, the following sections are an overview of the purpose, required properties and examples of suitable materials for each of the layer types. In order to maximise the lifetime of a device, encapsulation of layer materials is essential [35].

3.7.1 Transparent Electrode

It is a requirement of an LED to have a transparent electrode in order for the light emitted by the emission layer to be transmitted out of the device. The transparent electrode is commonly the anode or hole injecting electrode [34, 35]. A common inorganic transparent electrode material is indium tin oxide (ITO); and conductive polymers are also used (details follow in chapter 4). Many OLEDs still use ITO as the transparent electrode and a conductive polymer as the HTL [29, 35, 47]. Polyaniline (PANI), poly(3,4-ethylenedioxy-2,4-thiophene)-polystyrenesulphonate (PEDOT:PSS) and Poly(*p*-phenylene vinylene) (PPV) are all examples of conductive polymer transparent electrode materials [34, 35].

3.7.2 Busbar

A metallic busbar is often included along one edge or surrounding the transparent conductive layer to ensure even charge distribution across the electrode.

3.7.3 Light Emission Layer

As the name suggests, this is the layer from which light is emitted. This is where the charge carriers recombine or collide with luminescent centres. Emissive layer (EML) materials can be light emitting polymers (LEPs) or small molecule phosphors suspended within a polymer matrix, the latter tend to be more efficient emitters

[35]. Two examples of LEPs are Poly(*p*-phenylene vinylene (PPV) and poly(*N*-vinylcarbazole) (PVK) [35]. Zinc sulphide phosphors are commonly used and can be doped with other elements to emit light of different colours.

3.7.4 Buffer Layers

A thin, insulating buffer layer is sometimes required between an electrode and an organic layer; these are added to reduce the energy barrier between them [33]. The result of adding a buffer layer is to reduce degradation caused by chemical interaction, improve device durability [33], increase efficiency and luminance and decrease the turn-on voltage [34, 48-50].

3.7.5 Cathode

There is no need for the cathode (electron injecting electrode) in an LED to be transparent, so it is usually a paste suspension of a metal or other conductive material such as carbon black. Although carbon black is cheaper it is preferable to have a metallic rear electrode as this will reflect emitted light back through the transparent electrode and so improving the light out efficiency. Silver, nickel and carbon based pastes and inks are available for use as rear/opaque electrodes [35].

3.7.6 Transport Layers

To improve the efficiency of LEDs, extra layers can be added into the structure to aid the transport of charge carriers; these are usually called the electron transport layer (ETL) and the hole transport layer (HTL); these can also act as blocking layers for the opposite charge carrier [33]. Additional electron and hole blocking layer (EBLs and HBLs) can be incorporated into the structure; five layer devices like this are called “p-i-n type” [30, 51]; however this contradicts Li, who states the p-i-n

structure is that of a single layer, light emitting electro-chemical cell (LEC) [35]. The purpose of these additional layers is to increase the likelihood that the recombination of holes and electrons occurs in the emissive layer, resulting in more light emission [30].

3.8 Production Methods

This project is focussing on ELDs made using soluble conjugated polymer materials; this section will be limited to the current production methods of this type of device.

The ability to print conjugated conductive polymers results in a number of advantages during processing; solution based printing can be undertaken in atmospheric conditions as opposed to a high temperature vacuum required for depositing inorganic materials [35].

Different methods (both solution based and thermal deposition) can be used to apply different layers and this has often been seen in the literature [52-55]. All of the following methods are carried out on flat substrate materials.

3.8.1 Spin-Coating

Spin-coating is an effective and established method of producing thin films of polymer based materials [34]. An amount of material is placed in the centre of a disc, revolving at a high rate; centrifugal forces cause the material to spread outwards as a film; the film is then cured [56]. The thickness of the film can be controlled by altering the solution and process conditions but the processibility of very thin or very thick films is complex [34]. This method of film production wastes

a large amount of material [29] and does not allow for patterning; it also cannot be used to produce large area devices [34].

3.8.2 Screen Printing

Screen printing is the simplest and least expensive method of layer application used in producing electroluminescent devices. Paste materials are forced through a fine mesh (stretched over a frame) using a squeegee to apply a uniform layer onto a substrate. Large areas can be processed and shapes can be created by masking part of the screen. Displays can be processed using this method but resolution is low [33, 35].

3.8.3 Inkjet Printing

Inkjet printing can be used as a method to apply small drops of solution based layer materials accurately and to a high degree of resolution [57, 58], producing a matrix of individual pixels [34]; and as such is suitable for display processing [35]. Problems associated with inkjet printing are drying time (solvent evaporation), clogging [33, 35] and the requirement to ensure adjacent materials are insoluble to each other [34].

3.8.4 Roll-to-roll

There a number of different roll-to-roll methods of laying down patterned layers of material and these methods can offer the best economic value [35] and high speed [59]. All roll-to-roll processes are continuous, whereby rollers convey the substrate material, transfer the high viscosity liquid and print onto the substrate surface; patterns are created by altering the surface of one of the rollers [35]. Some

examples are gravure printing, doctor blading and flexographic printing [60]. These are effective processes for producing large area devices and high volumes [35].

3.9 Recent Developments in Organic EL Devices

Research into organic EL is progressing down many paths; within the two main areas of lighting and display technology, developments are being made in device production, efficiency and composition. An overview follows.

With the huge potential of using EL as a mechanism for providing efficient solid state lighting there is considerable interest in creating devices that emit white light. Jwo-Huei Jou *et al* have produced a WOLED with a very high colour rendering index (CRI) of 98 by using a double white emitting layer and an addition hole modulation layer [47]. White PLEDs have also been produced using a multi-layer structure with both red and blue emitting layers [45], and the colour tuning of PLEDs to produce a white light has also been investigated using red and green dyes in combination with a blue emitting system [36]. Graphene based materials have also been used to produce an intense blue light which can be used with other colours to produce a white emitting device [61].

Another factor when considering EL for lighting applications is the manufacturing process; the cost, scale and ease of manufacture will play a significant role in the possible up-take of this technology. There is significant research into developing easier solution based processes and techniques that have the ability to manufacture large areas; gravure, inkjet, contact, stamp transfer and roll-to-roll printing are some examples [29, 53, 54, 57, 59]. Soft lithography processing has also been investigated [38, 43] and patterned polymeric anodes have successfully been

created using a peel-off soft lithography method [62]. A combination of production techniques has also been investigated where both spin coating and evaporation techniques are used to apply different layers with no decrease in the device performance [55]. Research is being carried out into processing techniques for display applications; microcontact printing [63] is one such example. The ability to produce flexible devices is well established but more recently there has also been a piece of work into producing EL devices on curved surfaces [64].

If organic EL is to be a viable lighting option, a number of obstacles need to be overcome (obstacles shared with organic photovoltaics); extending operational lifetime, efficiency degradation and encapsulation options are all areas of current research [65-67].

As with any industry, there is also work being carried out into improving the efficiency of EL devices. Some research has been carried out to increase emission within the devices, as well as changing the formation of devices to increase the amount of light that exits the device; these are often called light extraction techniques [68, 69]. There are a number of methods of improving light extraction from LEDs and even though these are not necessarily specific to organic devices, the principles remain the same. Some changes to LEDs that can improve light extraction are: altering the shape of devices, including light reflective layer(s) and surface modification [68, 69]. There is also particular interest in using additional layers within the device structure; efficiency of devices have been improved using a hole modulating layer [47], an additional layer in between HIL and HTL [46], nano-fullerene layers [70] and layers incorporating carbon nanotubes [71, 72]

Stacked devices have also been created that increase illuminance without the need to increase current density; this is done by multiple-photon emission (MPE), i.e. each stacked device emits a photon [73].

3.10 Summary

In summary, it is clear that solution based processes based on polymeric materials offer easier manufacturing (compared to inorganic processing) and the large process areas required to open up the lighting market. Screen printing of EL devices is widely used and materials are commercially available, and despite the inability to transfer this method in-mould, the materials would make a good starting point for this project.

Although research has been carried out to improve the efficiency of devices and develop new processing methods, there is still a very limited ability to produce EL devices on 3D surfaces; and a method of processing EL materials onto a 3D surface of an item during its manufacture was not found.

4 PLASTIC MATERIALS

Plastics are a versatile group of materials utilised to varying degrees in a majority of modern day sectors. They have developed significantly since their origins over 100 years ago and their adaptability means materials with specifically customised properties have been produced and have often replaced the use of traditional materials in many areas [74, 75]. Plastics can be categorised in many different ways; according to their thermal behaviour, the source of their raw materials, and their usage, to name just a few. The most common ways of organising similar plastic materials into groups will be detailed in the next two paragraphs.

Plastics are separated into two main classes: thermoplastics and cross-linked plastics. Thermoplastic materials can be remoulded and cross-linking materials undergo an irreversible reaction [76, 77]. Further differences between the two classes will be described later in this chapter. Some examples of thermoplastics and cross-linked plastics are given in

Table 4-1. These two classes can be further divided into groups depending on their molecular structure; this will also be detailed later.

Table 4-1: Common examples of thermoplastics and cross-linked plastics

Examples of Thermoplastics	Examples of Cross-linked Plastics
Polyethylene (PE)	Epoxy
Polypropylene (PP)	Unsaturated Polyesters
Polycarbonate (PC)	Melamines
Poly(ethylene terephthalate) (PET)	Vulcanised Rubber/Polyisoprene
Acrylonitrile butadiene styrene (ABS)	Phenolics
Polystyrene (PS)	Polybutadiene
Poly(vinyl chloride) (PVC)	Polyurethane
Nylon/Polyamide (PA)	Silicone

Commercially, plastics can also be classified by their cost and performance; they can be divided into the following groups: commodity plastics, engineering plastics, high performance plastics and functional plastics. Examples of each of these groups are given in Table 4-2 on the following page. Commodity plastics are generally the cheapest group and manufactured in bulk, they are standard materials and their properties are poor in comparison to other groups. From commodity to engineering to high performance materials, the mechanical properties improve from group to group; also the cost generally increases and the quantity in which they are manufactured decreases. Functional plastics are speciality materials used because they have properties for a particular purpose; these tend to be expensive and manufactured in smaller quantities than the other groups [76-78].

Table 4-2 follows on the next page.

Table 4-2: Examples of materials categorised by use/performance.

Group of Plastics	Name of plastic	Features; Uses
Commodity	Polyethylene (PE)	Flexible, low density; Packaging, pipes, storage and bags
	Polypropylene (PP)	Impact resistant, flexible; Pipes & fittings, device housings
	Polystyrene (PS)	Transparent; Containers. Expandable grades used in packaging
	Poly(ethylene terephthalate) (PET)	Transparent; Drinks bottles, food trays
Engineering	Acrylonitrile butadiene styrene (ABS)	Tough, good impact strength; helmets, steering wheels
	Poly(butadiene terephthalate) (PBT)	Tough, dimensionally stable; Automobile parts, home appliances
	Polycarbonate (PC)	High strength, tough, clear; Housings for devices, CDs
	Polyamides (PA)	Tough, rigid; Bolts, gears and bearings
High Performance	Polyetherketones (PEK)	High melting temperature, excellent mechanical resistance; Aerospace components, circuit boards
	Polysulphones (PSU)	Transparent, high heat distortion, stiff; resists in semiconductors, automobile parts near engine
	Polyimides (PI)	High use temperatures, dimensionally stable; Construction, bearings, gears
	Polyarylates (PAR)	Tough, good elastic recovery, thermally stable; electrical and construction applications
Functional	Poly(ethylene-co-vinyl alcohol) (EVOH)	Gas barrier properties; Food packaging
	Poly(tetrafluoroethene) (PTFE)	High heat distortion, low surface friction, insoluble; non-stick coatings
	Poly(vinylidene fluoride) (PVDF)	Withstands solvent and chemical attack; O-rings

Plastics are manufactured by combining a polymer foundation with additives in order to make commercially useful materials [75, 77, 79]. The range and function of additives will be discussed later in section 4.4.

4.1 Thermoplastics

Thermoplastics are materials that can be melted, moulded and cooled into a solid shape; this process can be repeated [80, 81] as there are no strong permanent bonds in between chains only relatively weak intermolecular forces that can be overcome with heat energy [76, 82]. Due to the fact that thermoplastics can be remoulded, they are a suitable group of materials for recycling [75] and have the ability to be welded [74]. The internal structure of plastics can vary significantly therefore so can properties such as strength, flexibility, and toughness but common thermoplastics at room temperature are generally flexible and tough with low operating temperatures. Some examples of ways in which the internal structure of the plastic can differ are chain length, branching and symmetry; an example is shown in Figure 4-1.

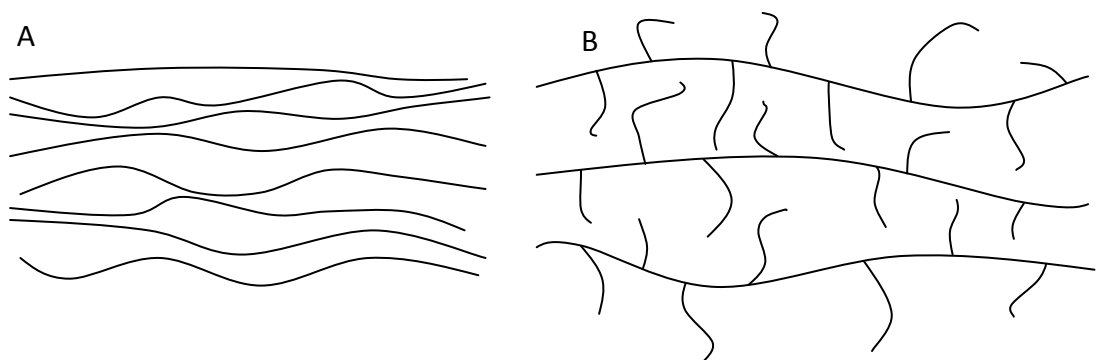


Figure 4-1: A diagram to show both linear (A) and an example of branched (B) chain structures within a thermoplastic.

Examples of thermoplastics are polyethene, polycarbonate, poly(methylmethacrylate), nylon and poly(vinyl chloride) [75, 83]. Thermoplastics have a wide range of uses including food packaging and bottles, laboratory ware, sterilisable medical equipment, containers, pipes and bags [75, 83].

4.2 Cross-linked Plastics; Thermosets and Elastomers

Some types of plastics (elastomers and thermosets) undergo a cross-linking or curing reaction; this can be initiated by high temperature, a catalyst or a specific frequency of electromagnetic radiation. Thermosets and elastomers have cross-linked networks to varying degrees [74], thermosets are highly cross-linked and elastomers to a lesser degree (this can be seen in Figure 4-2).

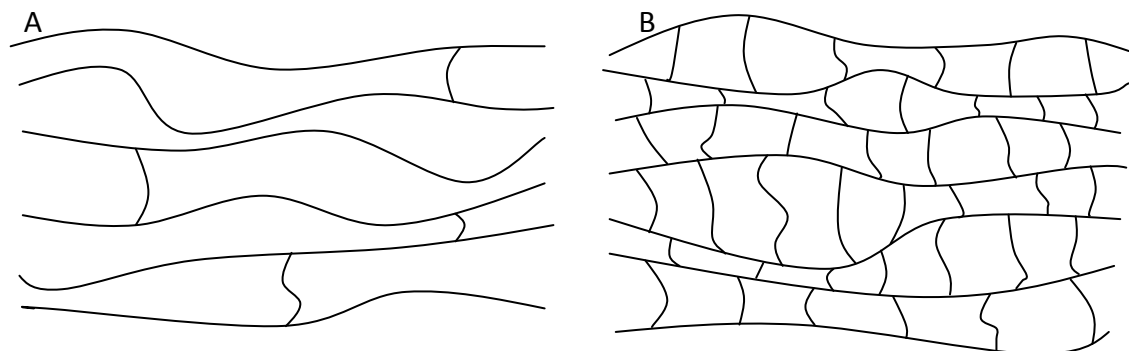


Figure 4-2: A diagram representing partially crosslinked (A) and highly crosslinked (B) chain structures

During the curing reaction strong bonds form between chains creating a three dimensional molecular network [75]; meaning the molecules extend across the whole volume of the material [82]. Once the curing reaction has taken place the plastic cannot be remoulded as the cross-linking bonds are permanent [80]. Due to the cross-linking, thermosetting plastics are generally hard, rigid, strong and brittle at room temperature and can be used at high operating temperatures [74, 76, 84].

Some examples of thermosetting plastics are epoxies, polyurethane, thermoset polyesters and phenolics [75]. Thermosets are used for applications such as adhesives, heat resistant handles and laminates and surface coatings [75, 83].

With elastomers the level of cross-linking is much less than that of a thermoset so the change to properties is to a lesser degree. Elastomers exhibit elastic, rubbery behaviour at room temperature and are able to recover from large deformations [74, 82]. Some examples of elastomers are polyisoprene, silicone, polychloroprene and polybutadiene [83]. Elastomers are used in the production of seals, grips, handles, inner tubes and waterproof liners [75, 83].

Once a curing reaction has occurred, a materials properties are irreversibly changed; it can no longer melt but will decompose upon heating [75, 80].

The transparent electrode in the EL devices made in this research is a conductive polymer that requires curing. Thermally activated crosslinking (as opposed to UV curing) would be easier to initiate in-mould but it may be problematic to achieve the required cure temperatures within the injection mould tool.

4.3 Blends and Alloys

Blends and alloys are mixtures of two or more polymers [85] that make up the plastic material. They are made in order to combine the desirable properties of different materials [76]; for example, a mix of a “glassy” plastic and a “rubbery” plastic results in a commercially attractive material that is both rigid and impact tough [86]. Blends are generally a mixture of chemically incompatible polymers and alloys are compatible mixtures [77].

Composite materials are also a mixture, however these are usually combinations of two or more distinct materials [77]. One material (the reinforcement) is usually distributed amongst the other (the polymer matrix) [80]. Materials such as glass, aramid, carbon and other polymers (usually in a fibre form) [76] are set within the matrix in order to utilise the properties of both constituent materials [78]. There is a huge range of composites since thermoplastic, elastomer and thermoset polymers can all be used as the continuous medium and can be combined with a variety of different reinforcements, configured as short, long or a range of woven fibres and mats [82]. Laminated structures can also be considered as composites; this project includes incorporating different layer materials into the wall of a moulded part, so a brief description of multi-layer materials follows.

4.3.1 Multi-layer Plastics

In order to incorporate the functions of different plastic materials into one item, multi-layer plastics are produced [87, 88]. Multiple materials are combined to form a single piece; it is important that the components remain distinct from each other, often in a layer structure [88]. Multi-layer materials are regularly used for producing packaging; examples of sectors that use multi-layer storage and packaging are food / grocery, healthcare and agriculture / chemical [87]. The layers can be aesthetic, adhesive, have specific functions such as barrier properties, or be a cheap substrate material or a recyclate [87]; Figure 4-3 shows some of the different layers that are often combined in a multi-layer packaging material produced using blow moulding. Six or seven layer materials are frequently manufactured to provide the required properties [80, 87].

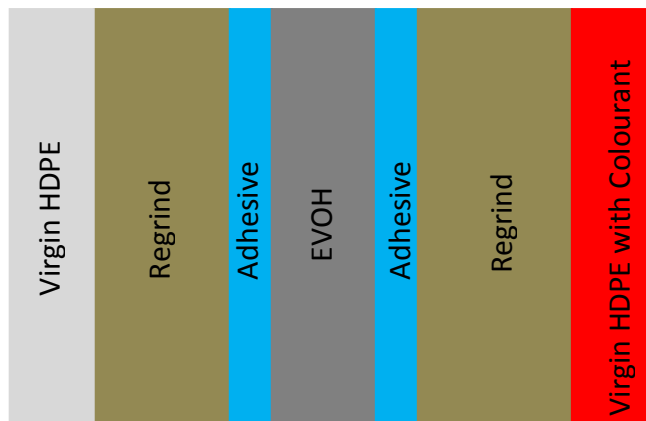


Figure 4-3: A cross-section showing a typical multi-layer plastic structure incorporating recycled material, barrier properties and surface decoration.

Food packaging is a widespread and familiar example of the versatility of multi-layer technology; some properties that can be integrated into materials are barrier properties to ensure long shelf lives, a layer that enables materials to be heat sealed, materials that comply to standards when in direct contact with food, and thermal resistance for containers such as sauce bottles that are filled with hot foodstuffs [80, 87, 89]. By using a multi-layer structure these properties are incorporated into the packaging whilst still retaining features such as flexibility, transparency and low cost.

Some examples of specialist materials commonly incorporated as barrier layers are: ethylene-vinyl alcohol co-polymers (EVOH), which provide good barrier properties for flavour, aroma and oxygen [87, 88]; fluorinated-chlorinated plastics such as polychlorotrifluoroethylene (PCTFE), which provide excellent moisture barrier properties and vinylidene chloride co-polymers (PVDC), which provide both oxygen and water vapour barrier properties to a high degree [87]. Although these materials are expensive, they make up just a thin layer of the overall structure, which makes

the use of it affordable yet still integrating the desired property into the manufactured material.

Multi-layer materials are produced fairly easily by co-extrusion and processes that use extrusion as the first stage [80]. Other processing methods include variations on injection moulding, laminating and coating; some examples will follow in Chapter 5.

4.4 Additives and Modifiers

Additives and modifiers are combined with a polymer to make plastic materials [80]. These improve/impart characteristics in order to make the material more commercially appealing [77]. The additives and modifiers in Table 4-3 are some of the most common used in the plastics industry, but are just a few of the many available.

Table 4-3: Some common additives and modifiers used in the plastics industry.

Additive/ Modifier	Function
Active Filler	Active fillers are also called reinforcing fillers; they are modifiers that have an intentional impact on plastics properties such as strength and stiffness. Carbon black, kaolin and mica are common active fillers [77, 86].
Inactive Filler	To make the plastic material cheaper by adding volume [80]. Some examples are chalk, talc and clay [77, 80, 86].
Coupling Agent/ Compatibiliser	Coupling agents are additives used in plastic materials to improve the bonding between the polymer and fillers [76, 77, 86].
Dyes	A soluble colourant that mixes with the molten plastic [86, 87].
Pigments	An insoluble colourant that remains suspended in the plastic [86, 87].
Plasticisers	Plasticisers are added to plastics to improve the flexibility/reduce brittleness of the final plastic product, and to improve the processibility of the plastic by lowering the viscosity of the material during processing [77, 80, 86, 87].
Reinforcements	Fibres made from carbon, glass and aramid can be added to plastics to improve properties such as rigidity and strength [80]. Chopped strands of fibre can be added to the melt or composites can be made using mats or braided fibres.

Stabilising Agents	Stabilising agents make plastic materials less reactive to external stimuli such as oxidation reactions, degradation due to UV radiation and burning/heat [87]. They slow the aging of the plastic in order to prolong the life of the product [76, 77].
--------------------	--

More recent advances in the plastics industry are around the development of conductive polymers; polymers can be modified to conduct electricity by a number of different methods, one of which is by using fillers. Since conductive polymers are used in this research the following section has been devoted to the different types and the progress being made in that research area.

4.5 Conductive Polymers

Multi-layer *smart* structures such as electroluminescent and photovoltaic devices require a transparent electrode layer and conductive polymers can be used for this function. Polymers have conventionally been considered as electronically insulating but the Nobel Prize winning research of Heeger, MacDiarmid and Shirakawa in 2000 showed that they can be modified to conduct electricity, thus opening up opportunities for further use.

4.5.1 Types

Chanda *et al* state that conductive polymers can be separated into two categories: filled polymers and intrinsically conductive polymers [90], however the “Encyclopaedia of Polymer Science and Technology” includes two further groups: ionomers and charge transfer polymers [87], for completeness a description of all four groups is included.

4.5.1.1 Filled Polymers

Conductive fillers such as carbon black, graphite fibres, silver and copper can be used in high percentage loadings to give a plastic the ability to conduct electricity [87, 89, 91]. These materials are also known as extrinsically conductive polymers. Benefits to this type of conductive polymer are the relative low cost and its ease of processing [87]. However one disadvantage is that properties of the plastic can be negatively affected by the high proportion of filler [91]. Further drawbacks include lack of reproducibility stemming from the inhomogeneity of the material in the micro-scale [87].

4.5.1.2 Ionically Conducting Polymers; Ionomers

An ionomer is a co-polymer of a mixture of organic and ionic monomers; a majority of the macromolecule is formed from the organic monomer and the ionic group occurs in distinct parts of the chain; it is the movement of the ionic species to different positions along the polymer chain that enables conductivity [92]. These types of materials are also called polymer electrolytes [92, 93]. It is the ionic interactions undergone by ionomers that determine their properties [87]. These types of conducting polymers are found in rechargeable batteries and used in LED applications (a use that is of particular interest to this project) [87]. Ionically conducting polymers are easily processed however they are susceptible to moisture damage [87]. Some examples of ionomers used as conductive polymers are poly(3,4-ethylenedioxythiophene), known as PEDOT, and poly(styrenesulphonate), or PSS. These (and other ionomers) can be combined to give a conductive polymer blend. PEDOT:PSS is one of the most commercially developed conductive polymers

and although it has one of the lowest conductivities, it is of interest to this research project.

4.5.1.3 Charge Transfer Polymers

Charge transfer materials are a combination of two constituents, an oxidant and the charge transfer polymer [87]; these act as electron acceptor and electron donor molecules and it is the partial transfer of charge between these that allows the material to conduct [92]. Charge transfer polymers are usually p-type (hole transporting), but there are lower efficiency than n-type polymers [93]. Poly(vinyl carbazole), (PVK) is an example of a charge transfer polymer [93].

4.5.1.4 Intrinsically Conductive Polymers

Intrinsically (or inherently or electrically) conductive polymers consist of delocalised charge carriers along a conjugated polymer chain [87]; the principal polymer material must be doped in order to form the charge carriers that conduct electricity [90]. In the undoped, neutral form the polymers behave as electrical insulators or semiconductors but chemical doping through oxidation and reduction reactions delocalises electrons [87]. Since doping is achieved by oxidation and reduction reactions, it can be reversed which means these polymers can be “switched” between the conductive and neutral state [87, 93]. Conjugated polymers have alternating single and double bonds along the polymer chain; meaning there are unsaturated carbon atoms next to each other within the structure of the polymer [94]. The orbitals of adjacent unsaturated carbons overlap which result in the formation of delocalised π -states; this means the polymers can be easily oxidised/reduced and quasi-charge carriers transfer energy along the chain by the

movement of charge density [94]. Polypyrrole and polyaniline are examples of intrinsically conducting polymers [3].

4.5.2 Uses

Conductive polymers have many uses, it is an area of research that is steadily growing; improved conductivities and processing stability are leading to new applications. Some current uses of filled conductive polymers include electromagnetic interference shielding; items such as PC housings can be moulded using the filled polymer or spray-coated with them [90]. Charge transfer polymers have history of use in photocopying [93, 95]. Other conducting polymers can be utilised in more technologically sophisticated areas such as printed electronics, flexible displays, EL lighting and organic solar cells [95, 96].

4.5.3 Recent Developments

As with the recent developments in OLED technology (as described in Section 3.9), research into conductive polymers is focusing on effectiveness (improving conductive properties), processing techniques and understanding limits to operational lifetime.

Work has been carried out into understanding and overcoming the influence that various external conditions have on conductive polymers such as PEDOT:PSS [97-99], with the aim of improving robustness, reducing degradation and increasing the lifetime of devices utilising them.

Research into improving the properties of conductive polymer films includes developing them into composite materials with other conductive materials such as carbon nanotubes [100, 101], and graphene [102, 103]. The use of post-treatments

on prepared layers [104] and modifying the polymerisation process [105] have all been found to improve the performance of conductive polymer films.

Research into the scope of conductive polymers has been looked at both from a processing perspective and by modifying materials. An investigation into the effect of solvents on polymer films has shown an increase in the conductivity in certain conditions [106] and the feasibility of electro-spraying PEDOT:PSS has been considered as an application method [107].

As an alternative to using polymer (and polymer composite) transparent electrodes, there is considerable research been carried out into producing thin, transparent conductive films from carbon in its various forms; some examples are using carbon nanotubes [108-110], graphene [111, 112], and diamond like carbon [31].

4.6 Plastic Behaviour and Properties

Some of the properties and behaviour of thermoplastics can be attributed to the organisation of the macromolecules in the material. The arrangement of the molecules can range from entirely random (amorphous) through the varying degrees of alignment of semi-crystalline materials [76]. Figure 4-4 shows the arrangement of chains within amorphous and semi-crystalline materials. The amorphous material shows no order whereas the semi-crystalline material has regions where polymer chains have aligned [82]. The following section will highlight the differences in materials with different molecular organisation.

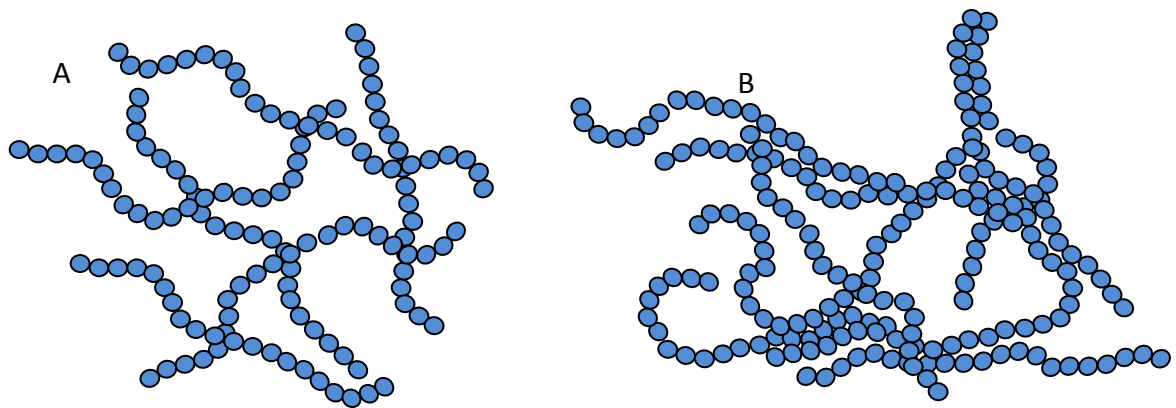


Figure 4-4: A representation of the molecular organisation of A, an amorphous plastic and B, a semi-crystalline plastic.

4.6.1 Amorphous

Some examples of amorphous plastics are poly(vinyl chloride), polystyrene and acrylonitrile-butadiene-styrene. Amorphous materials are generally transparent/clear and, upon heating, they soften over a broad temperature range. Amorphous plastics are often brittle (at room temperature) [74] and have poor chemical and wear resistance; however, they have high impact strength [81] and undergo low shrinkage when processed [76].

4.6.2 Crystalline and Semi-crystalline

There is no completely crystalline polymer but in many plastics there are regions where molecules align and crystallise [89]. Plastics that have a partially or predominantly crystalline arrangement within them are generally tough [74] with good chemical and wear resistance but low impact strength [81]. When processing they have a sharp melting point and shrink considerably [75]. Semi-crystalline plastics are generally opaque or milky, some examples are polyethene, nylon and polyester [76].

4.6.3 Thermal Transitions

When solid, plastics can be entirely amorphous or have distinct areas with crystalline arrangements [83] and upon heating, they pass through different transitions depending on that internal organisation [85].

The glass transition temperature, T_g , is the temperature at which a polymer changes from a brittle material to a rubbery material. Below T_g the plastic is said to be glassy and it is brittle and rigid. Above T_g the material is able to bend like leather. The material is still solid as it cannot flow but it is no longer stiff and inflexible [74, 85]. As a material is heated through the glass transition temperature, chains within the amorphous areas of the material become more mobile, molecules in the crystalline areas do not, so the material remains a solid.

When the heating of a semi-crystalline plastic continues past T_g , the material passes through another transition, the melting point, T_M . Above T_M , the crystalline areas of the plastic are now able to move past each other; since the chains in the entire volume of the material can now move past each other the plastic is now a viscous liquid. If heating continues the liquid becomes less viscous as the temperature increases. Entirely amorphous plastics do not have a melting point, but soften as the temperature increases.

Crystallisation of a plastic occurs at the crystallisation temperature, T_C . As a molten semi-crystalline plastic cools the chains can no longer move past each other, continued cooling past T_C causes the chains to begin to crystallise and become ordered. The plastic is no longer a viscous liquid able to flow but is now a rubbery

solid. T_C is below T_M , since in order for crystals to form the material needs to be more energetically stable [85].

Figure 4-5 shows the thermal transitions experienced by an amorphous (line A), and a semi-crystalline plastic (line B); changes undergone by an entirely crystalline material (line C) has been included for comparison.

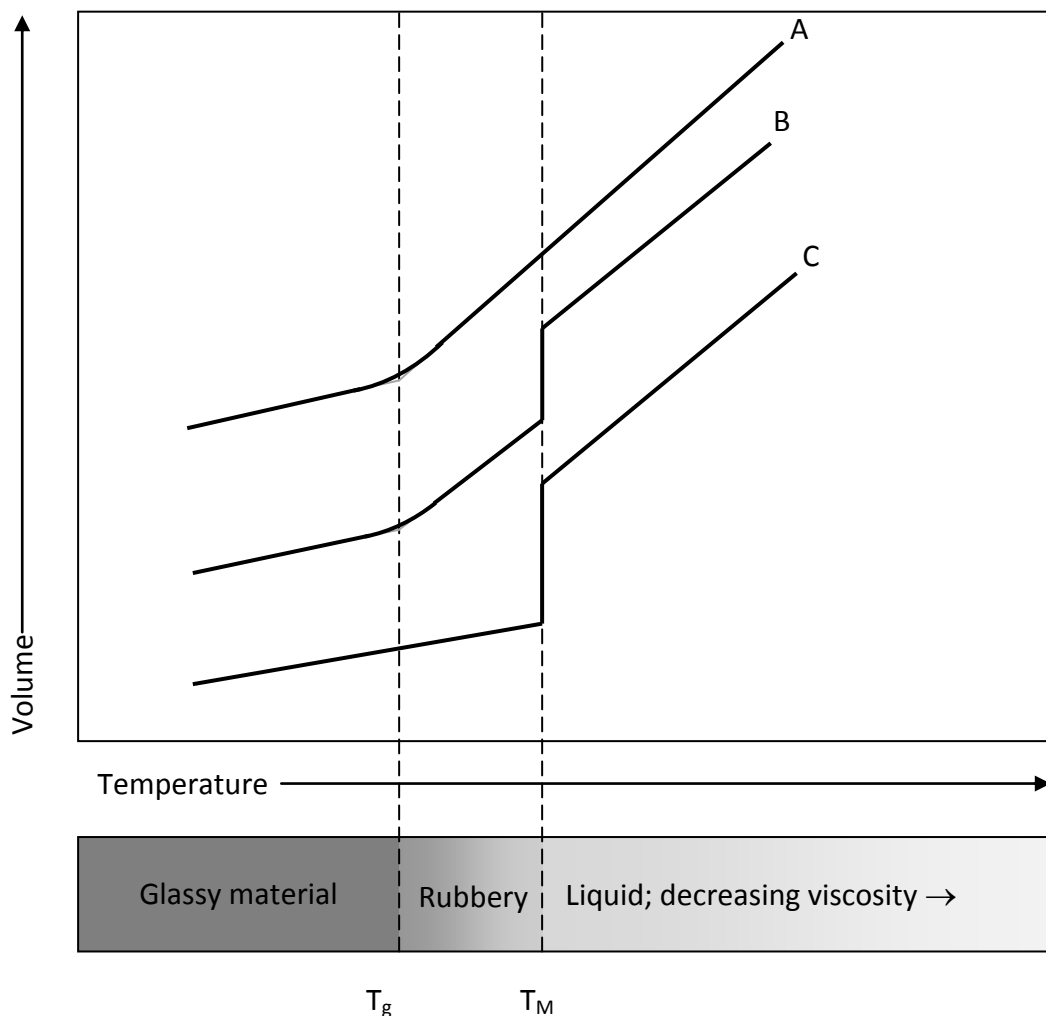


Figure 4-5: A graph to show the change in volume as a function of temperature for A, an amorphous plastic; B, a semi-crystalline plastic and C, a crystalline material. Transitions labelled are T_g , glass transition temperature and T_M , melting point. The schematic below the graph indicates the change in the materials physical behaviour.

From Figure 4-5 it can be seen that if an amorphous plastic is heated from its glassy state it gradually expands as the temperature increases. Past a particular

temperature (the T_g) it will expand at a greater rate; the material will now be rubbery in nature, softening and continuing to expand until it steadily becomes a viscous liquid. Expansion continues further as the viscosity decreases and the temperature increases. A crystalline material will steadily expand in the glassy state as it is heated, but as it passes through T_M the volume will increase dramatically. This happens because crystallised structure becoming disordered and molecules move further apart. Once all order is overcome, energy is again used to increase the temperature of the now viscous liquid; as the temperature increases, viscosity decreases and volume increases.

Most plastic materials have both ordered (crystalline) and disordered (amorphous) regions [74] within them and so incur changes at both transition points. As heated, the glassy semi-crystalline material expands; upon passing through T_g the material becomes rubbery and expands at a greater rate, chains within the amorphous regions can now move past each other. The rubbery material gets softer as the temperature increases. At T_M the chains in the crystalline regions become disordered causing a sharp increase in volume and the material now is a viscous liquid with the ability to flow. Past T_M the liquid's temperature increases, the viscosity decreases and the material continues to expand [74].

4.6.4 Structure and Properties

This section will briefly describe how polymer chain structural differences have an effect on the properties of the plastic material.

For high molecular weight molecules (and therefore longer chains), the melting temperature, T_M , of a plastic material is higher [77]. The tensile strength and the

viscosity of the melt also increases as the molecular weight increases [85]. The regularity of polymer molecules influence the ability of the material to crystallise [86], highly branched polymers are less able to align and become ordered and the presence of side groups also reduces crystallisability. Syndiotactic and isotactic polymers (regularly repeating structures) are more likely to crystallise than atactic (random) molecules [86].

Thermal transitions are also affected by the structure of molecules, factors affecting glass transition temperature T_g are structural changes that affect the flexibility of the backbone of the chain; the presence of side groups and unsymmetrical polymers with different functional groups or substituent atoms reduce the flexibility of backbone and increase T_g [83]. The melting point of a plastic, T_M , is also affected by symmetry; symmetrical molecules can more easily packed together, requiring more energy to overcome attractive forces and have higher melting points [83]. So, unsymmetrical and irregular molecules are more likely to have lower melting points.

Generally chain branching decreases density, lowers melting point and decreases tensile strength of a plastic [75] and crosslinking removes the ability to flow even upon heating [82]. Density is principally affected by molecules' ability to pack closely together with linear polymers being more likely to crystallise and be more dense [85], however in low density (open, random structure) amorphous plastics the presence of heavy atoms such as chlorine increase density [86]. The solubility of a material is defined by the compatibility of functional groups in the solvent and the polymer chain [86].

4.6.5 Testing and Equipment

The testing of polymeric and plastic materials is essential to verify properties and characterise materials to ensure they are sufficient for the required application. A huge range of testing regimes is available; tensile, impact, fatigue and hardness are all common tests that can be carried out but are beyond the scope of this project. The thermal behaviour of materials is more relevant to this research.

4.6.5.1 Thermal Characterisation

Thermal characterisation of plastic materials is important in determining transition points so that processing conditions and operational ranges can be verified. It is also important to see how the material behaviour changes through a temperature range. In addition, knowing values such as specific heat, the coefficient of thermal expansion and thermal conductivity is invaluable for correct processing but also essential when a material is to be used in an environment where temperature extremes or changes may be an issue. Dynamic thermal analysis (DTA) and differential scanning calorimetry (DSC) are two common characterisation techniques used to measure the thermal properties of a plastic material.

Differential scanning calorimetry (DSC) is a thermal analysis technique that compares a small sample against a reference material while the temperature of both is increased; the user can set the temperature range and ramp rate over which the sample will be tested. The DSC measures the amount of energy required to increase the temperature of the sample and compares it to the reference. If the sample passes through a transition point this affects the amount of energy required to increase its temperature by the same amount.

If the sample passes through an endothermic transition, such as melting, more energy is required to change the temperature since additional energy is required to overcome intermolecular forces to melt the material. If an exothermal transition takes place, such as curing, less external energy is required to increase the temperature of the sample since there is some energy released by the bond making during the reaction. The resulting scan shows the heat flow in/out of the sample as a function of temperature.

As well as identifying thermal transition points of materials, DSCs can be used to determine the energy changes occurring during those transitions and can be used to calculate the thermal heat capacity of materials.

Dynamic thermal analysis (DTA) measures the mechanical changes that occur to a material as it is heated over a particular temperature range. The sample to be tested is clamped into position and while the sample is heated over the selected temperature range it is deformed and internal stress/strain is measured. The user can set how the sample is to be deformed, by altering the displacement, frequency of oscillation and mode operation. From the measurements taken, the modulus of the sample is measured and this correlates to the stiffness of the material; shifts in the modulus indicate a thermal transition has occurred. The resulting scan shows the change in modulus as a function of temperature.

4.7 Summary

This chapter has highlighted two interesting aspects to this project; the possible suitability of PEDOT:PSS to in-mould application and the conflict of heating regimes by different polymeric materials.

The ability to dilute PEDOT:PSS without significant detrimental effects (in fact with reported benefits), as well as the use of spray technology lends itself to the possibility of incorporating layer application directly into the injection mould tool. However, the different heating requirements of the materials may make processing them together in one cycle a problem; the heat required to dry and cure EL materials in-mould is inconsistent with the cooling required to solidify the thermoplastic substrate it is applied to.

5 PROCESSING PLASTICS

Plastics are processed into products. There are many different methods, variations of methods and post process techniques that can be used in combination to produce useful, complete plastic goods [77]. An appropriate processing method is determined by the material used and the shape and structure of the final product [76].

Table 5-1: Common thermoplastic processing methods

Processing Method	Overview	Examples of Products
Extrusion	Powder or granule plastics are melted and forced through a die to form a continuous part with a constant cross-sectional shape which can be cut to the desired length.	Pipes, uPVC window sections, guttering, seals.
Calendering	A number of rollers form a polymer melt into thin films or sheets.	Flooring, films.
Press Moulding	Covers a range of processes where large pressures are applied to the moulding. Glass fibre reinforced composites are usually processed this way.	Auto body panels, TV and radio casings, PC housings.
Blow Moulding	A split mould closes around a tubular preform; pressurised gas inflates the plastic to form a hollow part within the tool.	Bottles, drums, fuel tanks.
Rotational Moulding	A heated, closed mould containing a measured amount of resin or powdered plastic rotates through a number of axes. The material distributes evenly within the tool to form a hollow part.	Buoys, bins, traffic cones, balls, storage tanks.
Vacuum Forming	An open tool is raised up to a heated plastic sheet. A vacuum is used to pull the plastic onto the tool.	Blister packs, food trays, vending machine cups.

The full range of processing methods is beyond the scope of this research, so this section will be limited to the processes most relevant to this project; injection moulding, in-mould decoration and tool heating. A brief summary of other common processing methods of thermoplastics can be found in Table 5-1.

5.1 Injection Moulding

As previously mentioned, this research focuses on injection moulding and its variations and developments as the manufacturing method in which to incorporate electroluminescent technology, so the following sections describe injection moulding from the simplest system and through the advances made in the process.

Injection moulding and its variations is one of the most common plastic processing methods [75]. This is due to the ability of the process to make complex, highly repeatable parts in a fast cycle time [82, 89] with just a single stage from raw material to completed product [74, 84]. The process involves the high-speed injection of a measured amount of molten plastic into a closed, cooler mould and kept under pressure until ejection [77, 82]. Injection moulding follows the three key stages of all main thermoplastic melt processes; material softening, shaping and solidification [75, 77, 81, 90]. Before many plastic materials can be processed, they must be dried to remove any moisture that may have been absorbed during transportation and/or storage [75]. Dryers can be incorporated into the design of the injection machine but this can work out more expensive compared to having a separate dryer providing dried material to a number of moulding machines [81].

5.1.1 Machine and Mould Tool

Once the material has been dried and prepared, it can be transferred to the injection moulding machine by way of the hopper [113]. Figure 5-1 shows a simplified diagram detailing the main parts of an injection moulding machine.

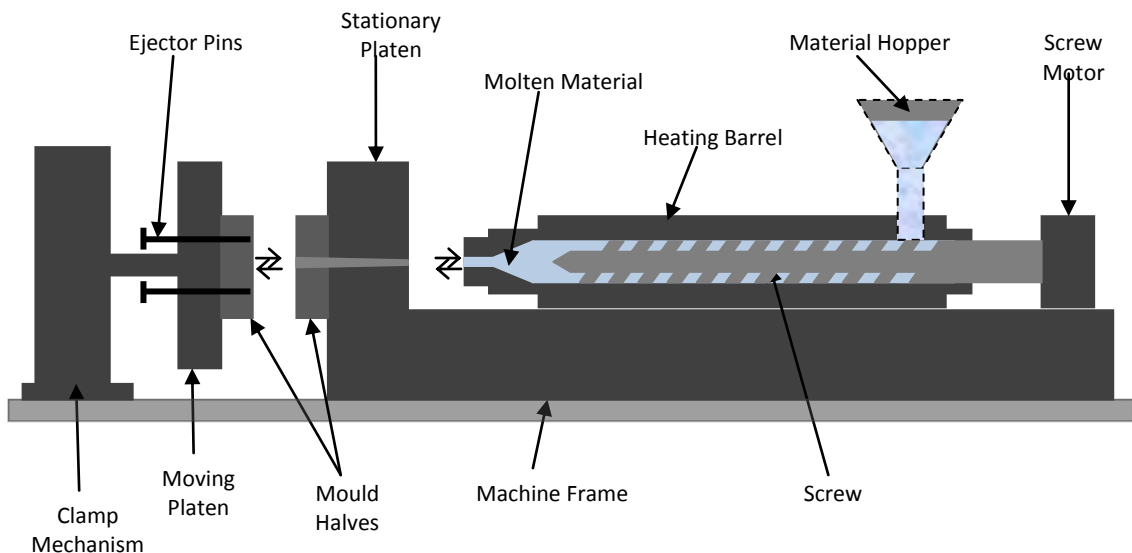


Figure 5-1: An injection moulding machine.

The hopper stores the feedstock and provides a constant supply of material to the injection moulding machine [75]; the force of gravity is utilised to keep material flowing through the throat into the injection barrel [75, 81]. The barrel is where the material is melted and plasticised by the heaters surrounding the cylinder and by the action of the screw [80, 89]. The screw's other function is to move new material from the hopper along the barrel [81]. There are a number of different types of screw design, varying in geometry and the forces applied to the molten polymer; the screw can also be designed to incorporate different stages along the length of the barrel [81]. The screw is operated by the screw motor and the injection hydraulic cylinder at the rear of the machine [74, 82].

At the other end of the machine, the mould halves are attached to the platens; the moving platen is controlled by the clamping unit and runs along bars to ensure it remains aligned with the stationary platen [75, 82]. The clamping unit also operates the ejector pins that remove moulded parts [75, 80].

Channels are incorporated into the design of the mould tool [76]; these carry water or oil in order to keep the temperature of the mould constant [78]. For the moulding of thermoplastics (as has been used in this research) the mould is cooled; without cooling, repeated moulding using hot thermoplastic would heat the mould which results in the parts being unable to solidify sufficiently for ejection.

Since this is highly relevant to this project, mould heating and cooling is considered in further detail later in this chapter.

5.1.2 The Process

Once the material is in the hopper it steadily falls into the barrel. As the screw turns and moves backwards, the material moves along the barrel, melts and becomes homogeneous and collects in front of the screw [84, 90]. The molten material is then ready for injection. The four main stages of injection moulding are shown in Figure 5-2a-d (on the following page). Once the mould has closed, the first stage is injection (Figure 5-2 a), the screw moves rapidly forward, forcing molten material through the nozzle into the mould cavity. During this action, the screw is been operated by the hydraulic injection cylinder [84]. There is then a period where a high pressure is held in the cavity to ensure the volume of the part is maintained; this is because material shrinks during cooling [80].

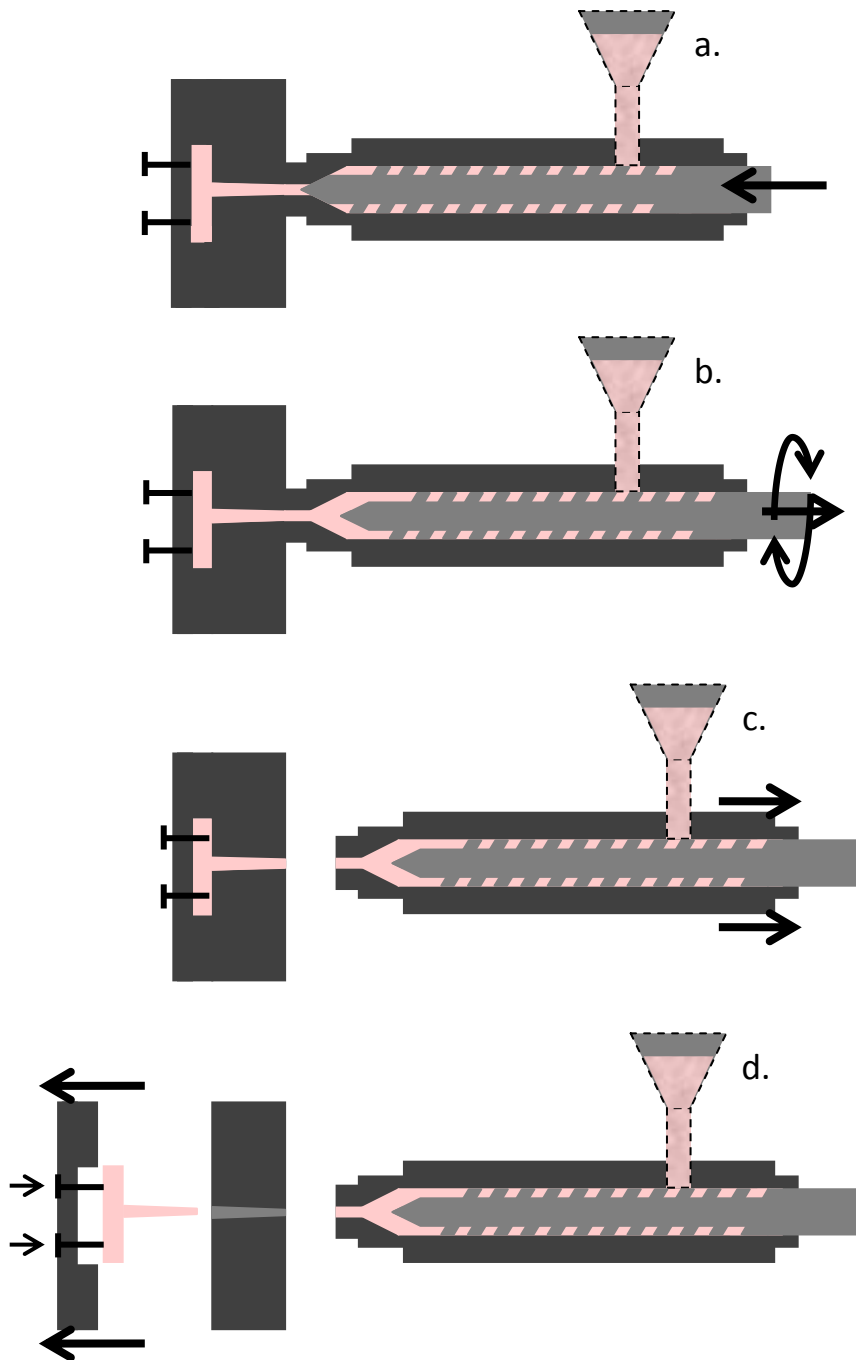


Figure 5-2: The injection moulding process; a, injection and hold; b, screw back; c, unit retraction; d, open and eject.

As soon as the material is injected it begins to cool; during the cooling stage of the process, a number of operations take place. The screw rotates causing it to move backwards, this is known as “screw back” (Figure 5-2 b); this moves the screw into position ready for the next cycle and meters a shot [75]. The whole injection unit is then retracted back, as shown in Figure 5-2 c [75]. Finally, when sufficient cooling has occurred for the part to hold its shape, the clamping unit opens the mould by moving the moving platen and ejects the part using the ejector pins (Figure 5-2 d) [80]. The mould is then closed and the injection unit moves forward ready for the process to repeat [75]; a representation of the injection moulding cycle is shown in Figure 5-3.

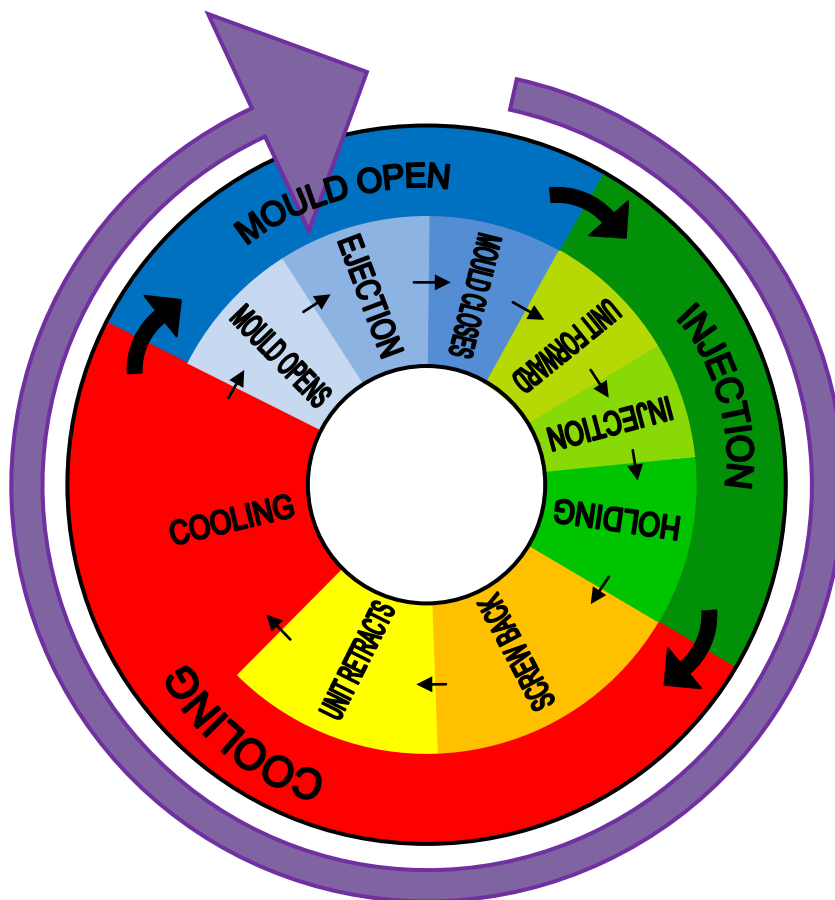


Figure 5-3: The different stages of an injection mould cycle (the diagram is not to scale; the angle of each section does not represent the proportion of time in the cycle it merely shows the cycle sequence).

5.1.3 Tool Heating and Cooling

In order for efficient moulding to take place, the temperature of the mould tool must be able to be controlled throughout the moulding cycle. Different heating and cooling regimes are needed depending upon the process variation and substrate material used; thermosetting plastics require tool heating in order to cure the moulded part and tool cooling is required to counteract the heat transferred to the tool by hot thermoplastics. Mould tool heating is also used for producing parts with a high gloss finish, thin walls and microstructures [114, 115] However, in order to stabilise the shape of the thermoplastic, cooling is required before ejection, meaning some processes require rapid cycling of both heating and cooling.

5.1.3.1 Heating and Cooling in Conventional Injection Moulding (CIM)

Conventional injection moulding utilises a single heat transfer method that is continuous and unidirectional [114]; the cheapest method of both heating and cooling a mould is to pump a fluid through channels machined into the tool in order to transfer heat into or out of the system [116, 117]. Water and oil are the two most common liquids used to transfer heat but both have limitations; water can only heat tools up to 100°C and oil is not efficient in transferring heat [116]. High pressure water can heat tools to above 100°C but can damage the channels it flows through [116]. The cooling of mould tools works using the same principle except chilled liquids are pumped through the channels to transfer heat away from the tool [117]. Electric mould heaters can also be used as an additional heat source [118].

5.1.3.2 Heating methods for Rapid Heat Cycle Moulding (RHCM)

As already mentioned, heating a tool whilst a thermoplastic is being injected offers a number of benefits to the appearance of parts and the dimensions of moulded features. A number of different methods of rapidly heating the mould have been investigated and some are available commercially [119]. The heating method is usually accompanied with channel cooling [116, 118]. Rapid heating of the tool can be carried out by transferring heat directly from hot gases or steam [118, 120, 121] or by non-contact methods such as electromagnetic induction [115, 116, 122], infrared radiation [123, 124] and electrical resistance [125]. Steam can be carried along the same channels as the cooling water (at different times in the cycle) [117, 120, 121] in order to heat the tool or hot gases can be pumped through different channels or directly into the mould cavity [118]. Infrared lamps can be used to heat the surface of the tool while the mould is open; in this set up the tool has a thin conductive layer separated from the rest of the mould by an insulating layer so as not to unnecessarily heat the core of the mould [124]. The combination of an insulating layer and conducting layer on the surface of the mould is also used when heating the surface using electrical resistance; the conductive, metallic layer is so thin that it has a high resistance and a high current is passed through the layer to heat it [125]. Resistive heating is also the heating mechanism utilised in inductive heating. Induction heating of the mould is carried out by inserting an induction coil into the tool cavity; the coil carries a high frequency alternating current which generates an alternating magnetic field. The effect of this rapidly changing magnetic field is to induce current “eddies” in the inner surface of the tool; it is these “eddies” which heat up the tool by resistive heating [116, 122].

5.1.4 Variations on Injection Moulding

Since the injection moulding process was first patented in the 1870's [75, 81] it has grown to become one of the most important processes for the manufacture of plastic parts [74, 77, 82, 84]. As well as the improvement of standard injection moulding, there has also been a number of process variations developed, enabling the moulding of more complex parts [82, 87].

Table 5-2: Some variations on the injection moulding process.

Variation on Injection Moulding	Summary of the Process
Micro-moulding	The injection moulding of very small parts using a special moulding machine.
Gas Assisted Injection Moulding	This produces hollow parts; a reduced shot of material is injected followed by the injection of high pressure gas.
Reaction Injection Moulding	Injection moulding thermosets; a resin and catalyst are mixed in a head and injection moulded, curing occurs in the mould.
Injection Blow Moulding	This makes thin walled, hollow containers; injection moulding produces a preform which is inflated to fit into a different mould cavity.
Foamed Moulding	Lightweight structures are produced; blowing agents are added to a material, the mould is partially filled and gas is released which expands the part.
Over Moulding	Multi-material products are made; pre-moulded plastic sections are placed into the mould and moulded over.
Co-injection Moulding	Multi-layer plastic mouldings are made; two or more materials are injected from separate barrels into the same mould.
Insert Moulding	Pieces incorporating metal, fabrics and decorative films etc. are moulded; the material is placed inside the mould cavity and injected over.

All methods are based on the standard injection moulding processes: material is melted and plasticised in a barrel, a measured amount of molten plastic is injected

at high speed into a closed, cool mould, and then the material is held under high pressure until the part has solidified [75, 77, 81, 82]. A few of the different techniques are summarised in Table 5-2.

Over moulding, co-injection moulding and insert moulding are all methods of producing multi-material parts and as such are of particular interest to this project; so more detail has been included about these techniques in the next sections.

5.1.4.1 Over Moulding

Over moulding produces parts consisting of more than one type of plastic; this is carried out by operating a number of different injection moulding cycles sequentially [80]. This can either be on a multi-shot injection moulding machine, or by injecting over pre-moulded inserts. Figure 5-4 shows the latter; a pre-formed part is placed inside the cavity of the injection mould tool, and a second material is injected over the preform [75]. This process can then be repeated to build up a part comprising of many materials [75, 126].

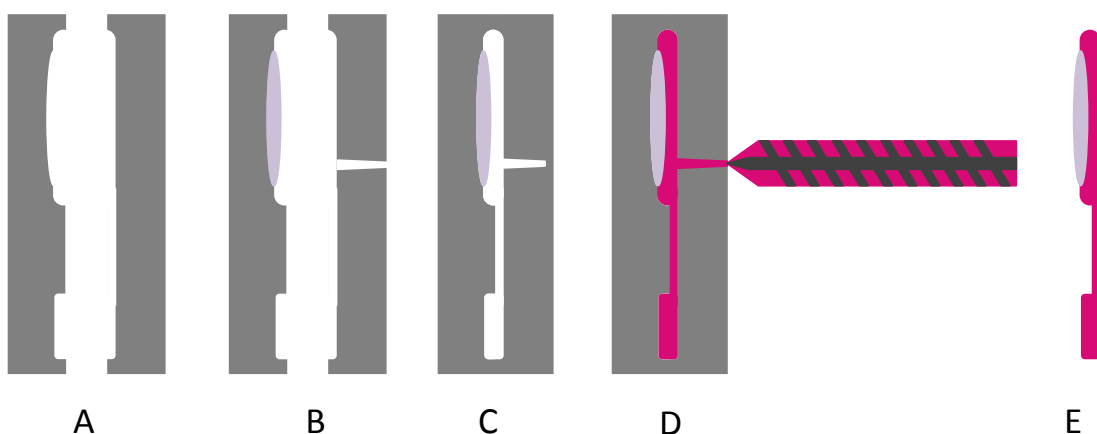


Figure 5-4: The over moulding process; A, an open mould; B, a preform is placed in the mould; C, the mould is closed; D, a different material is injection moulded; E, the ejected two material part.

Although a huge combination of plastic materials can be over moulded, the term often refers to the moulding of a rigid part with a soft, elastomer section; one common example is a toothbrush, a differently coloured soft-feel section can be incorporated into a handle [80]. Injection moulding over other materials, such as metals, can also be called over moulding [127].

5.1.4.2 Co-Injection Moulding

Co-injection moulding requires each material to have separate injection unit [77, 89, 126]; the materials are applied simultaneously [80], or in rapid succession [75, 89], producing a multi-material part in a single process cycle. Components usually comprise of two materials, a core and a skin [89, 90, 126]. By processing more than one material the function of a part can be optimised by utilising properties of different materials [90]. Examples of component materials that can be co-injection moulded are: recycled, foamed or reinforced cores, and soft or tough skins and coloured outer layers [75, 77]. The following benefits are associated with such mouldings/ material combinations:

- Weight reduction,
- Cost reduction by using a cheap core and limiting the use of costly aesthetic “skin” materials,
- Remove the need for additional processes such as painting,
- Combining opposing properties such as rigid core with a soft skin.

Figure 5-5 shows the co-injection moulding process; from top to bottom the diagram shows the different stages of the cycle:

- a. shows the separate barrels holding two different plastics,
- b. and c. show the injection of the skin material,
- d. and e. show the injection of the core material which fills the part and forces the skin material to the edges of the cavity,
- f. shows the second injection of skin material, this flushes any core material from the nozzle ready for the following cycle, and,
- g. shows the finished part with a separate core and skin material.

Figure 5-5 can be seen on the following page.

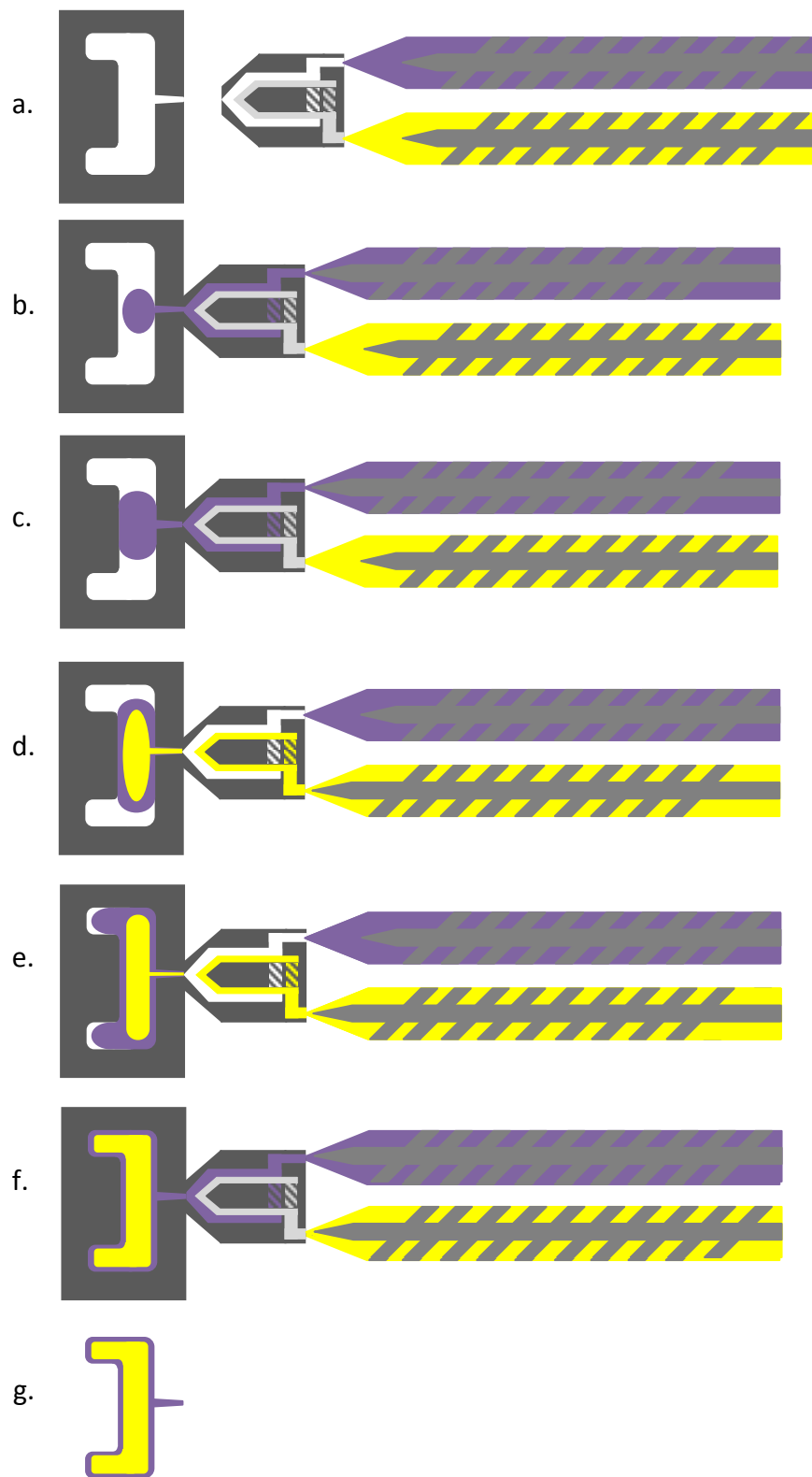


Figure 5-5: The co-injection moulding process; the skin material is injected first followed by the core material to pack the moulding out.

5.1.4.3 Insert Moulding

Many moulded parts require post mould treatments such as assembly, painting and labelling [90]. In order to save money, time and energy many insert moulding techniques have been developed which can apply a number of different materials such as metal components, labels and textiles during the moulding cycle [80].

Insert moulding is a broad term referring to any technique where something is placed in-mould before substrate injection; it is similar to over moulding however the insert in this process can be of any material. For example, textiles are inserted into a tool cavity and are moulded onto to produce items such as auto parcel shelves [82]. In-mould processes eliminate the need for further stages [80]. Also, incorporating materials into the moulding process provides a good bond to the substrate and therefore produces very durable parts [90].

Film insert moulding is a broad term referring to both in-mould transfer decoration and in-mould labelling (IML). These are very similar processes however IML refers mainly to in-mould decoration of packaging and as is often associated with other processes such as blow moulding. Both processes provide high quality decoration of moulded items without the need for further handling [88, 126]. Films are printed and die cut, they are often positioned by a robotic arm and kept in place within cavity by using a vacuum or electrostatic attraction [126].

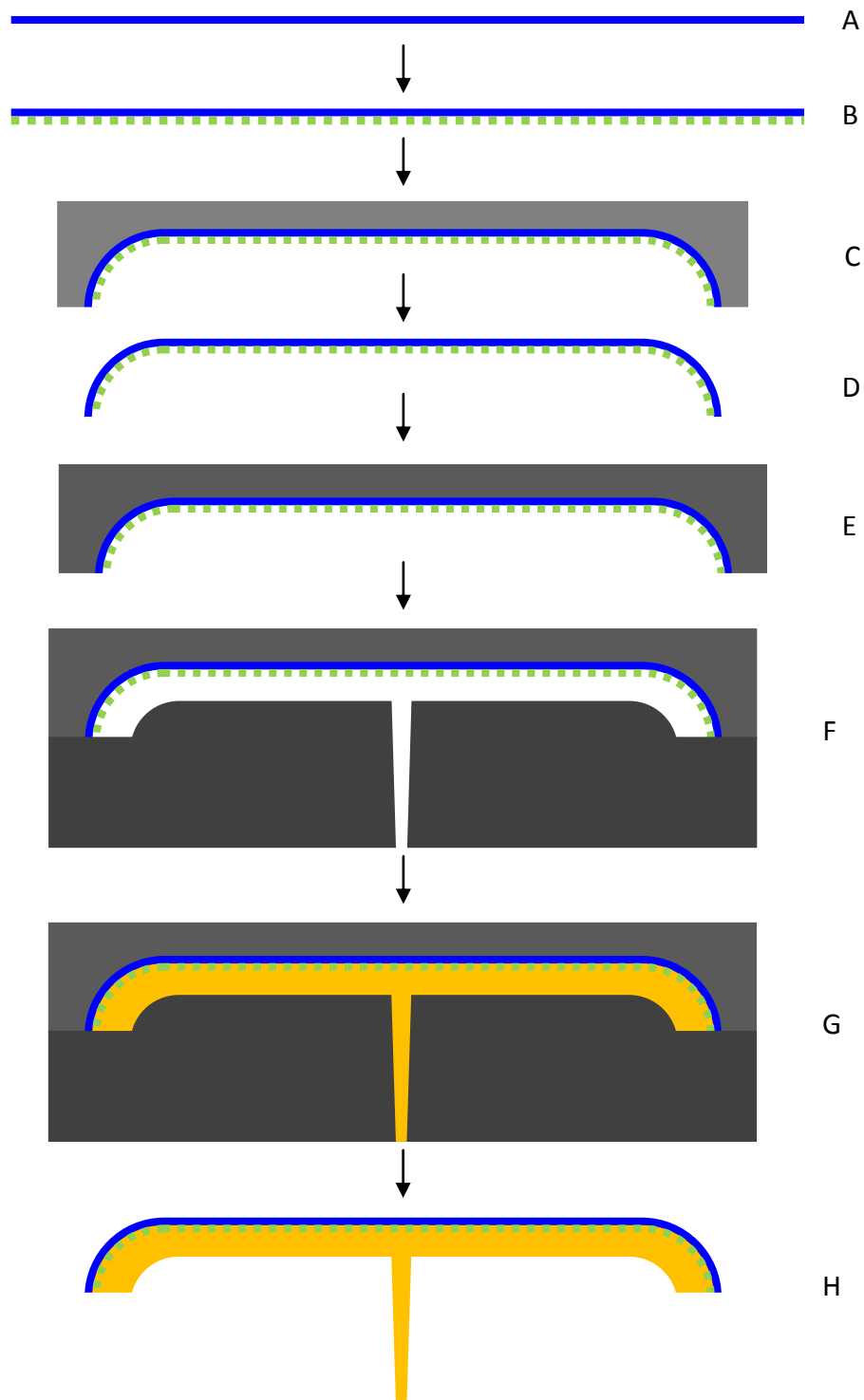


Figure 5-6: Film insert moulding: A, the film substrate; B, the label is printed; C, the label is pre-moulded to the correct shape (this stage is not always required); D, the predecorated film; E, the film is placed in the mould cavity; F, the mould is closed; G, the part is moulded; H, the decorated product.

In transfer decoration the pre-printed film (known as a decal) is the same material as the substrate; once injected, the film bonds with the substrate to make a complete, decorated part [90]. The decoration is within the wall of the plastic item with the film making up the external surface; this results in a very durable decoration. Examples of parts decorated with in-mould decoration are internal car panels and mobile phone components [128]. Figure 5-6 shows the film insert moulding process.

5.1.4.4 Recent Developments in Injection Moulding

A number of developments have been made in injection moulding that are relevant to this project; these include applying layer materials in-mould and incorporating electronics into injection moulded plastic parts.

A novel method developed for manufacturing painted thermoplastic parts is the INSPIRE process; a thermoset powder coating is applied to the cavity of the tool and is then injected with a thermoplastic [129, 130]. The outcome is the application of paint during the injection mould cycle. By moulding and painting in a single manufacturing stage, the requirement for post mould painting is eliminated. The process works by using pressurised air to deliver the thermoset powder into a closed mould, the powder gels on a warm tool and ideally the heat provided by the injected substrate should cure the paint layer during the moulding cycle. However fully cured paint layers have not been achieved in-mould. A technique similar to the INSPIRE method could be used to build up a number of layers sequentially, resulting in multi-layer parts such as the ones required in this project. In this case, solution based EL materials would dry on a warm tool and the heat from the thermoplastic

substrate would cure materials such as PEDOT:PSS. The temperature of layer materials would need to be modelled to ensure cure was achieved in-mould.

Another area of interest to this project is the embedding of electrical functionality into injection moulded parts; this has been carried out by injection moulding over a “printed wiring board” to embed the part and its function into the moulded plastic [131], it is noted that this is old but relevant research. Some later work also highlighted recycling problems when embedding components into a thermoplastic part [132]. This is a problem that could be even more difficult to solve when multi-layer materials are incorporated into the structure of the part rather than distinct components that can be more easily separated. Further research has taken place in this area [133, 134] but, again, it differs from this project by encapsulating a standalone electronic component into the plastic rather than incorporating electro-active materials into its structure.

This overview of research shows that there is currently a knowledge gap in injection moulding multi-layer materials with electrical functionality.

5.1.4.5 Issues Concerning Multi-material Parts

When processing a number of different materials together, it is important that their thermal and physical properties are compatible with each other; for example, processing temperatures, thermal behaviour and miscibility must be considered so that they can be processed together and bond on contact [87]. Bonding between adjacent materials can be achieved chemically, or by adhesion of chemically compatible materials and mechanical methods [127, 135, 136].

5.1.4.5.1 Plastic Compatibility

If a multi-material part is to be robust and withstand appropriate use there must be a good bond between materials. There are different bonding mechanisms that occur at the boundary interface between two plastics depending on whether they are compatible or not. When adjacent materials are chemically compatible there is a high level of interdiffusion which makes a good interfacial bond [127]. Table 5-3 shows the compatibility of different plastic families.

Table 5-3: The compatibility of plastic families [127].

	ABS	ASA	EVA	PA6	PA66	PBT	PC	PE-HD	PE-LD	PET	PMMA	POM	PP	PPOmod	PS-GP	PS-HI	SAN	TPU
ABS	+	+	+			+	+	-	-	+	+	-	-	-	*	*	+	+
ASA	+	+	+			+	+	-	-	+	+	-	-	-	*	-	+	+
EVA	+	+	+					+	+				+		+	+	+	
PA6				+	+	*	*	*	*			-	*	-	-	-	+	+
PA66				+	+	*	*	*	*			-	-	-	-	-	+	+
PBT	+	+		*	*	+	+	-	-	+	-	-	-	-	-	-	+	+
PC	+	+		*	*	+	+	-	-	+		-	-	-	-	-	+	+
PE-HD	-	-	+	*	*	-	-	+	+	-	*	*	-	-	-	-	-	-
PE-LD	-	-	+	*	*	-	-	+	+	-	*	*	+	-	*	-	-	-
PET	+	+				+	+	-	-	+	-	-		-	-	-		+
PMMA	+	+				-		*	*	-	+		*	-	-	-	+	
POM	-	-		-	-	-	-	*	*	-		+	-	-	-	-	-	
PP	-	-	+	*	-	-	-	-	+		*	-	+	-	-	-	-	-
PPO mod	-	-		-	-	-	-	-	-	-	-	-	-	+	+	+	*	-
PS-GP	*	*	+	-	-	-	-	-	*	-	-	-	-	+	+	+	-	-
PS-HI	*	-	+	-	-	-	-	-	-	-	-	-	-	+	+	+	-	-
SAN	+	+	+	+	+	+	+	-	-		+	-	-	*	-	-	+	+
TPU	+	+		+	+	+	+	-	-	+			-	-	-	-	+	+

(-): No adhesion, (*): Poor adhesion, (+): Good adhesion

When plastics are chemically similar and have compatible functional groups they can easily mix; so when two compatible molten plastics are adjacent with each other there is a degree of diffusion of molecules across the boundary [136]. This is called interdiffusion [137] and is classed as a rheological bonding mechanism [135].

This can continue until there is no longer a distinct boundary but a gradual change from one material to the other; when these materials solidify, this interfacial mixing forms a very strong bond [136].

5.1.4.5.2 Other Boundary Interactions

When plastics are incompatible and there is no interdiffusion at the interface, the bond that forms at the boundary is due to molecular and mechanical bonding and thermodynamic conditions [135, 138].

Molecular bonding can only occur if the adjacent materials (and their molecules) are in very close proximity with each other. The bond strength comes from the intermolecular forces that occur between molecules; forces such as Van der Waals and dipole-dipole interactions [135].

Mechanical bonding can influence adhesion by two different methods (and there is some debate about the influence of each); one explanation is that the uneven surfaces at the interface increases the total area over which molecular bonding can take place and the second explanation is that there is an interlocking between the two irregular surfaces [135, 137].

The entanglement of molecules in a transition region between two immiscible polymers can also contribute to the overall interfacial bond and has been reported by Cole *et al* [138]; these materials were compression moulded so this mechanism may not be seen, or may have a lesser effect in other processing methods (such as injection moulding).

The thermodynamic theory describes the importance of surface energy of the two adjacent plastic materials in order to achieve the closest contact between surfaces and some argue that this is a predominant consideration [135, 137]. Without close contact, none of the other bonding mechanisms occur [135, 137].

5.1.4.5.3 Improving Adhesion

If adjoining layer materials are not compatible, adhesives can be incorporated into the structure to bond them together [80, 87]. If the application of an adhesive is not feasible compatibilisers can be added to plastic to make them bond [127]; a compatibiliser is usually a compound that has molecular similarities to each plastic which makes it miscible with both. There are also surface treatments (using solvents, acids and oxidising agents) that can be carried out on plastic surfaces to improve the bond between them. These usually work by forming functional groups that are compatible with the neighbouring material [135].

5.2 Spray Deposition

Spray deposition is a broad term referring to the application of liquid materials by atomisation; dispersion techniques include ultrasonic, electrospray and airbrush [139, 140]. Materials used in this project (polymer EL materials) are solution based and lend themselves to this application method. This is also a method that has the ability to easily apply a series of different layer materials and onto a 3D, contoured surface. Successful research has already been carried out into applying organic electro active, electroluminescent and photovoltaic materials [139-144] using this method and as such it seems a suitable technique for applying EL materials in-mould.

5.3 Summary

A number of areas of interest have arisen from this chapter; specifically the developments of in-mould techniques for injection moulding, the importance of mould temperature during processing, issues regarding multi-material plastic parts and spray deposition techniques.

The INSPIRE process is of particular interest as this is a method relevant to the aims of this project; the application a thin layer (albeit a powder coating) to the surface of an injection moulded part. The INSPIRE research highlights the issues that are likely to occur during this project; specifically the problems faced when thermally incompatible materials are moulded together in a single part and cycle.

The compatibility and adhesion between adjacent polymeric materials is also an important consideration in a multi-layer structure. Without good adhesion between the EL materials and the injected substrate, manufactured parts would not be durable.

Also this review of the literature has shown the suitability of solution based polymer materials to spray deposition techniques and this offers a potential solution to applying EL materials directly in-mould.

6 THERMAL MODELLING

When introducing materials into the injection moulding process that would not normally be used in this environment, it is important to be able to model the situation in order to predict the conditions that the introduced materials will be subjected to and how these change throughout the injection moulding cycle.

Many models are used in engineering and manufacturing to further understand processes and improve them and/or optimise their use. An example of such computer aided engineering is Moldflow [145]. This software is used to simulate the injection moulding process in order to optimise the moulding conditions and cycle times, as well as balancing flows in the tooling. Whilst Moldflow has been developed for a number of different injection moulding processes, unfortunately no add-on exists for modelling the application of thin layers in-mould before moulding. The development of such a model would be beneficial to understand and optimise this novel process.

A single layer model will be generated first to reproduce the changing conditions during the INSPIRE in-mould process, this will then be modified to incorporate multiple layers, like the structure produced when injection moulding electroluminescent materials.

6.1 Single Layer Thermal Model

A novel in-mould decoration process called INSPIRE [129, 130] involves spraying a thermoset powder coating into a warm mould, the powder gels to form a film and then a thermoplastic substrate is injected to produce a fully painted part in a single

manufacturing step. When in-mould painting is carried out using this system (a thermoset coating and a thermoplastic substrate) there is a conflict with the moulding temperature requirements of the two materials. Both require heat to soften, however the coating requires high temperatures to cure as opposed to the substrate which needs to be cooled in order for the part to be solid enough to eject. Ideally, the hot molten thermoplastic substrate would supply enough heat to cure the thin layer of thermoset coating, enabling the mould tool to be kept at a temperature appropriate for the ejection of the part. This would produce a complete, cured painted part with no need for post processing. A thermal model of the system would help establish if this is feasible during a standard injection mould cycle.

6.1.1 The Problem

In order to develop the model, the conditions and the materials in the problem need to be specified and certain simplifications made. The following statements were used to build the simulation:

- The part is predominantly thermoplastic with one side coated by a thermoset film (see Figure 6-1)
- The part is moulded using INSPIRE, the latest in-mould painting technique
- ABS is used as the thermoplastic, a tough engineering plastic commonly injection moulded
- A processing temperature of 200 °C and a tool temperature of 50 °C are used; both are appropriate for moulding ABS

- The thermoset film coating is an unsaturated polyester; many such coatings are commercially available
- The part would be a small, sample moulding, dimensions approximately 7.5 cm x 7.5 cm x 0.3 cm, including a 50 μm layer of thermoset.

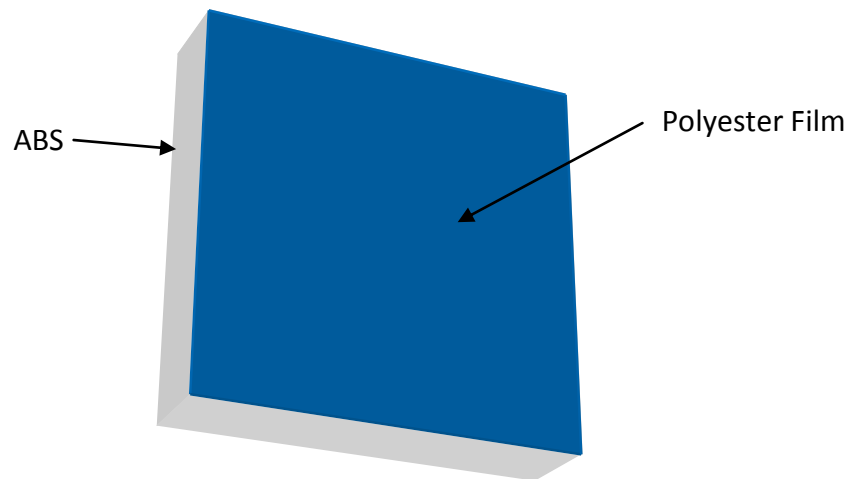


Figure 6-1: A representation of a single side painted sample injection moulded part.

Although the model itself is not original work, the novelty occurs in the application of it to an in-mould painting technique using a thermoplastic-thermoset material combination. To simplify further, the following assumptions have been made:

- At the time of thermoplastic injection the thermoset had reached the isothermal temperature of the mould tool; in the example given in Figure 6-2, this means a temperature of 50 $^{\circ}\text{C}$.
- The effects of the boundary interfaces have been ignored¹.

¹ The importance of considering boundary layer heat transfer coefficients in more complex and accurate models are acknowledged [146] A. Dawson, M. Rides, C. R. G. Allen, and J. M. Urquhart, "Polymer-mould interface heat transfer coefficient measurements for polymer processing," *Polymer Testing*, vol. 27, pp. 555-565, 2008.; however this simple model is adequate to calculate the

- The use of geometric correction factors was also ignored².

Whilst the simplicity of the model is therefore acknowledged, it has been extremely useful in exploring the INSPIRE process and its limits; it also acts as a base on which to develop a multi-layer model.

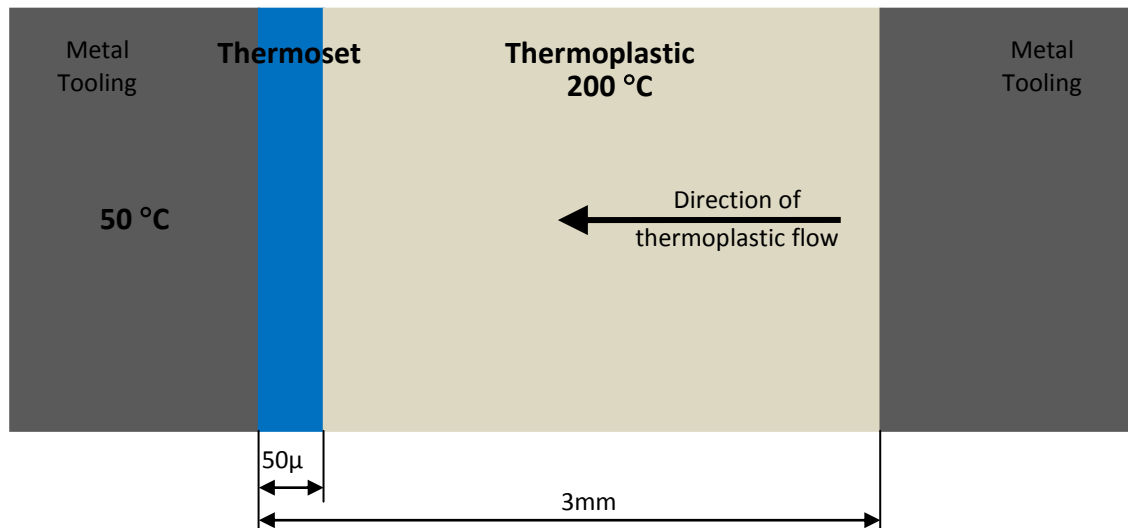


Figure 6-2: A diagram showing a cross-section of the thermoset-thermoplastic system in-mould.

The cooling problem can be considered by a straight forward derivation of cooling times utilised in injection moulding production for obtaining ejection times. From Figure 6-2, the problem can be summarised as:

A 50 μm thickness of polyester thermoset powder coats the inside of an injection moulding tool at 50 °C, the mould cavity has dimensions of 7.5 x 7.5 x 0.3 cm³. An ABS substrate is injected at 200 °C onto it, giving a moulding of total thickness 3 mm.

temperature and time available for thermoset curing, as required to estimate working heat exposure times.

² These would need to be taken into account for more accurate modelling; however geometric correction factors vary widely in the literature [147] J. Z. Liang and J. N. Ness, "The calculation of cooling time in injection moulding," in *Proceedings of the International Conference on Manufacturing Automation, 10-12 Aug. 1992*, Hong Kong, Hong Kong, 1992, pp. 830-5..

From this statement, the values required for the model (such as part dimensions, processing conditions and materials' properties) can be determined.

6.1.2 The Model

Table 6-1 gives the abbreviations of terms used in the equations used in the model.

Table 6-1: Terms used in equations

Term	Symbol
Thickness of Polymer	X_P
Surface Area of Polymer	A_P
Mass of Polymer	m_p
Polymer Specific Heat	c_p
Polymer Thermal Conductivity	k_p
Initial Temperature of Polymer	$T_{P(0)}$
Temperature of Polymer at Time, t	$T_{P(t)}$
Thickness of Film	X_f
Surface Area of film	A_f
Mass of Film	m_f
Film Specific Heat	c_f
Film Thermal Conductivity	k_f
Temperature of Film at Interface at Time, t	$T_{f(t,0)}$
Film Temperature at distance, x from Interface at Time, t	$T_{f(t,x)}$
Temperature of Mould	T_M
Time	t
Distance Across Film from Interface	x

Equation 1 -Equation 5 were used to calculate how the temperature across the thermoset film changed as the part cooled within the mould. The model starts with a cooling equation (Equation 1); this shows how the temperature of the polymer at the surface changes over time.

Equation 1: The surface polymer temperature as a function of time

$$T_{P(t)} = (T_{P(0)} - T_M) e^{-\frac{k_P A_P}{m_P c_P X_P} t} + T_M \quad [1]$$

The temperature of the polymer can then be used in the conduction formula to give the rate that heat energy is transferred to the film (Equation 2):

Equation 2: The rate of heat transfer to the film as a function of the polymer temperature

$$\frac{dQ_f}{dt} = \frac{k_f A_f}{X_f} (T_{P(t)} - T_M) \quad [2]$$

Equation 3 shows how the rate of energy transferred to the film is related to the temperature gradient (over small increments) across the film; this equation can be rearranged in the form of Equation 4 which then in turn integrates with respect to x , to give Equation 5.

Equation 3: The rate of energy transfer to the film as a function of the temperature gradient across the film

$$\frac{dQ_f}{dt} = -k_f A_f \frac{dT_f}{dx} \quad [3]$$

Equation 4: The temperature gradient across the film as a function of the rate of energy transfer to the film

$$\frac{dT_f}{dx} = -\frac{dQ_f}{dt} \frac{1}{k_f A_f} \quad [4]$$

Equation 5: The temperature of the film (at time, t and distance x into the film) as a function of the energy transferred to the film and the temperature of the polymer.

$$T_{f(t,x)} = -\frac{dQ_{f(t)}}{dt} \frac{x}{k_f A_f} + T_{P(t)}^3 \quad [5]$$

³ $T_{P(t)}$ is the integration constant since at $x = 0$ (the thermoset-thermoplastic boundary), $T_{f(t,x)}$ is equal to $T_{P(t)}$.

The equations can be manipulated further to give an overall solution to the differential problem (*Equation 6*); the solution is a linear correlation across the depth of the film, the slope of which decreases over time, however the different stages will be shown for visualisation purposes.

Equation 6: The temperature of the film (at time, t and distance x into the film) as a function of the mould temperature and the temperature of the polymer at time, t .

$$T_{f(t,x)} = - \left(\frac{x}{X_f} \right) (T_{P(t)} - T_M) + T_{P(t)}^4 \quad [6]$$

The results section begins on the following page.

⁴ Equation 2 is substituted into Equation 5 to give, $T_{f(t,x)} = - \left[\left(\frac{k_f A_f}{X_f} \right) (T_{P(t)} - T_M) \right] \left(\frac{x}{k_f A_f} \right) + T_{P(t)}$. The terms $k_f A_f$ cancel out to give equation 6.

6.1.3 The Results

Table 6-2 and Table 6-3 show the values used for the modelling of the initial problem.

Table 6-2: The values of terms used that remained constant; values associated with geometry and the film material.

Film: Unsaturated Polyester			
Term	Symbol	Value	
		Commonly Used Units	SI Units
Thickness of Polymer	X_p	3 mm	0.003 m
Surface Area of Polymer	A_p	120 cm ²	0.012 m ²
Thickness of Film	X_f	50 μm	0.00005 m
Mass of Film	m_f	1 g	0.001 kg
Surface Area of film	A_f	60 cm ²	0.006 m ²
Film Specific Heat	c_f	1.2 ^[17] kJ kg ⁻¹ K ⁻¹	1200 J kg ⁻¹ K ⁻¹
Film Thermal Conductivity	k_f	0.7 ^[17] W m ⁻¹ K ⁻¹	0.7 W m ⁻¹ K ⁻¹

Table 6-3: Values of terms that were variable; values associated with the polymer substrate and the moulding conditions.

Polymer Substrate: ABS; Film: Polyester			
Term	Symbol	Value	
		Commonly Used Units	SI Units
Mass of Polymer	m_p	24.1 g	0.0241 kg
Initial Temperature of Polymer	$T_{P(0)}$	200 °C	473.15 K
Polymer Specific Heat	c_p	1.3 ^[17] kJ kg ⁻¹ K ⁻¹	1300 J kg ⁻¹ K ⁻¹
Polymer Thermal Conductivity	k_p	0.18 ^[17] W m ⁻¹ K ⁻¹	0.18 W m ⁻¹ K ⁻¹
Temperature of Mould	T_M	50 °C	323.15 K

A spread sheet was created using Equation 1, Equation 2 and Equation 5 along with the data from Table 6-2 and Table 6-3; the results were as follows.

The cooling of the injected thermoplastic was calculated using Equation 1, this data was then fed into Equation 2 in the spread sheet and the results of which, the energy rate transfer curve, can be seen in Figure 6-3.

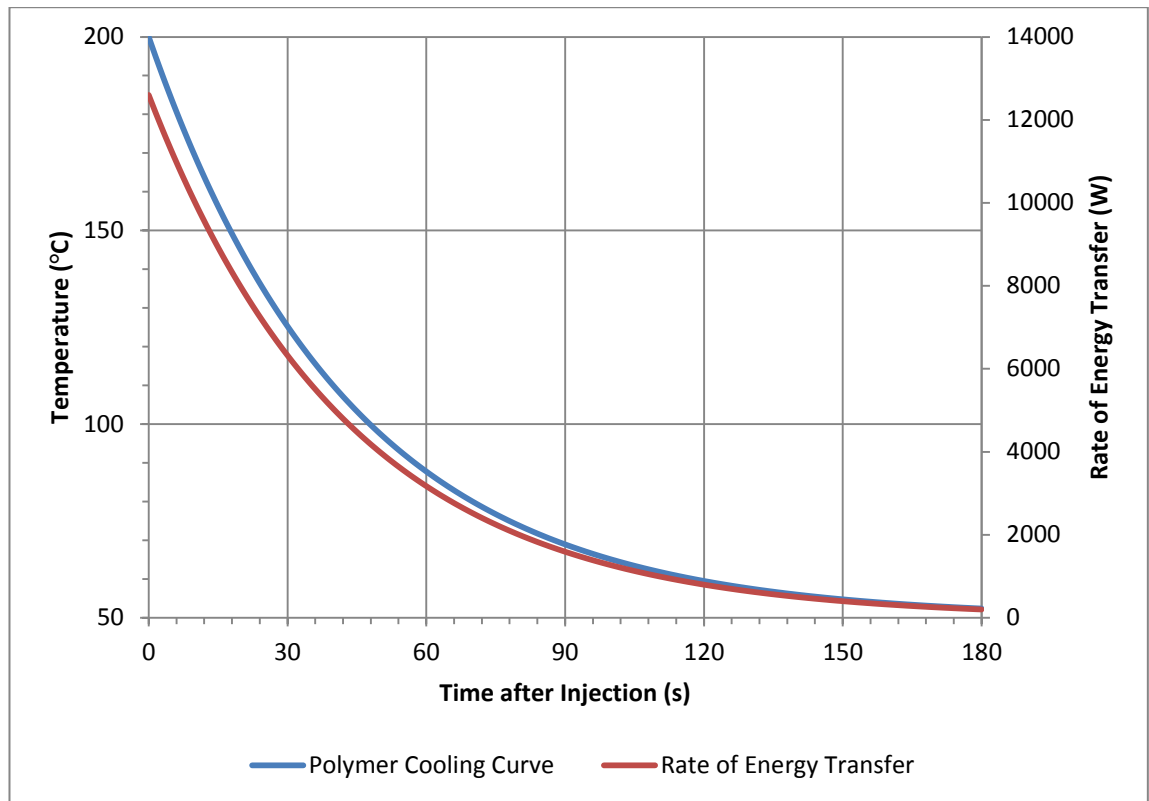


Figure 6-3: A graph showing ABS substrate temperature and the rate of energy transfer to the thermoset film over time.

Once the rate of heat transfer was established, Equation 5 was used to obtain the temperature gradient across the thickness of the thermoset film at any given time; the next step was to plot a graph showing the temperature gradient across the film at different times. A limited number of times were selected in order to clearly present (graphically) the changes during the cycle and to compare the results given by each substrate material within the system. The selected times were the arbitrary values: 0 s, 1 s, 2 s, 5 s, 10 s, 15 s, 20 s, 30 s, 60 s, 120 s and 180 s. This is shown for

a model based on the initial problem of ABS injected at 200 °C with a mould tool temperature of 50 °C in Figure 6-4.

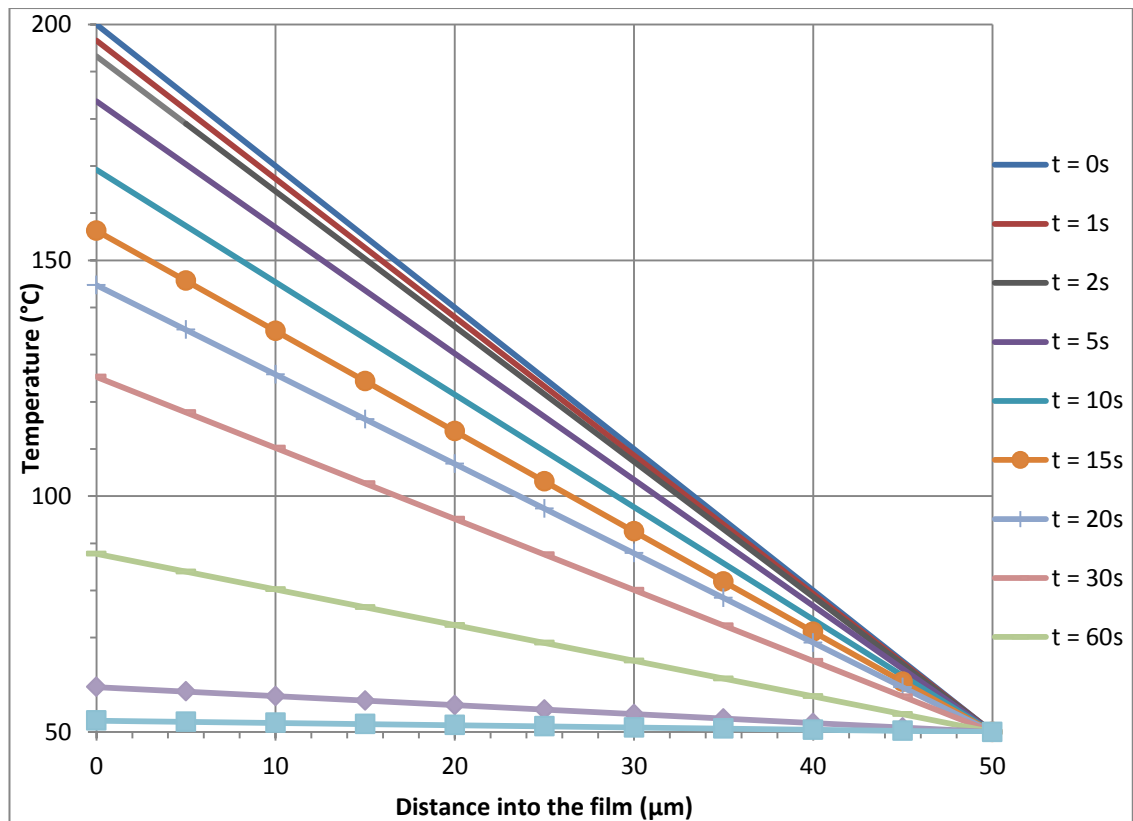


Figure 6-4: A graph showing how the temperature profile across the depth of the thermoset film changes over time.

Figure 6-4 also highlights a further issue with this model in that the film surface contacting the mould tool never rises above 50 °C; this is not the case in practice. Despite that, this model is extremely useful for comparing the thermal conditions provided when using different parameters and substrate materials. The model was easily adjusted to observe how increasing the injection temperature of the ABS by 30 °C affected the heat available for curing.

Further variations of the model with different substrate materials, processing and tool temperatures were carried out with the variables shown in Table 6-4. These initial chosen temperatures reflect a general processing temperature of each of the selected thermoplastics. The other substrate materials that were modelled are: Nylon 6 (PA6), Nylon 66 (PA 66), Polyethylene terephthalate (PET) and Polybutylene terephthalate (PBT).

Table 6-4: Values used to model different substrate materials

Term	Symbol	Values for different substrate materials					Units
		PA 6	PA66	PBT	PET		
Mass of Polymer	m_p	26.2	26.4	30.4	31.7	g	
Initial Temperature of Polymer	$T_{P(0)}$	250	280	260	280	°C	
Polymer Specific Heat	c_p	1.7 ^[17]	1.7 ^[17]	1.3 ^[17]	1.05 ^[17]	$\text{kJ kg}^{-1}\text{K}^{-1}$	
Polymer Thermal Conductivity	k_p	0.29 ^[17]	0.23 ^[17]	0.21 ^[17]	0.24 ^[17]	$\text{W m}^{-1}\text{K}^{-1}$	
Temperature of Mould	T_M	50	85	50	85	°C	

Each of the different substrate thermoplastics was modelled and data gathered regarding the temperature profile across the film at different times; graphs for each substrate material were plotted. Regularly spaced heat exposure times were selected in order to compare the performance of each substrate material within the system; the selected heat exposure times were the arbitrary values: 100 °C maintained for 30 s, 100 °C maintained for 60 s and 150 °C maintained for 30 s. The graphs were interpreted in order to determine to what depths these heat exposure times were maintained for using the different substrates. The results are shown in Figure 6-5.

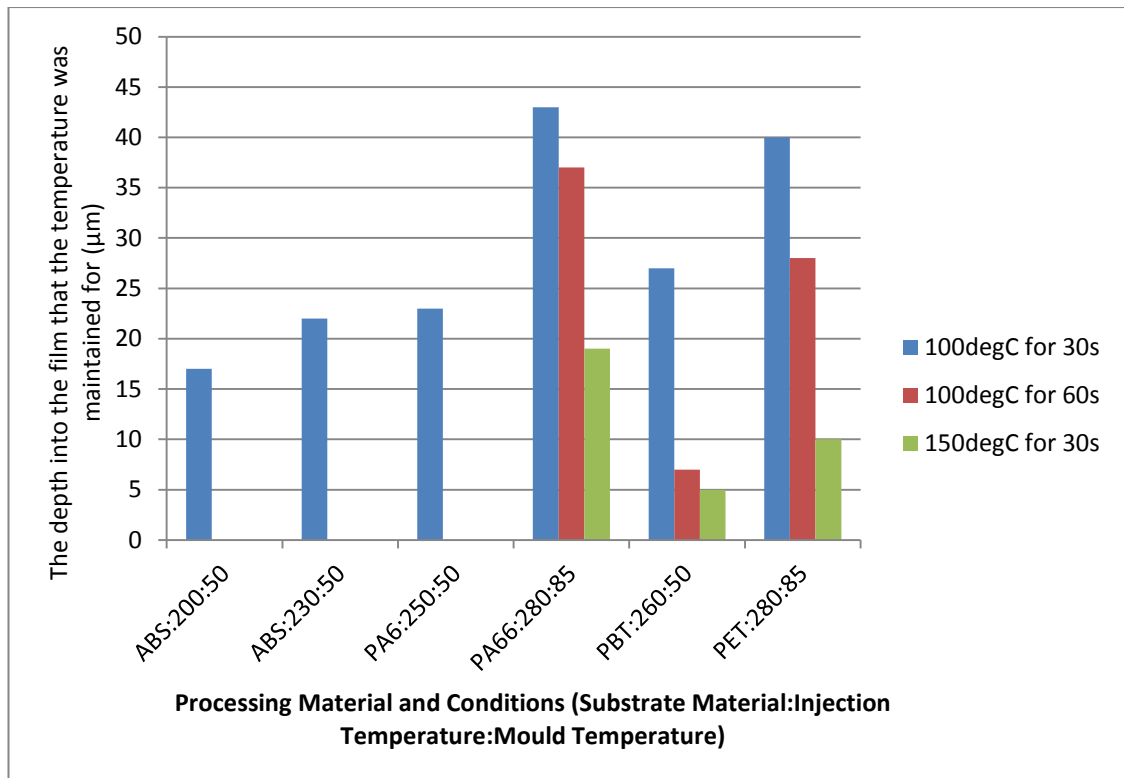


Figure 6-5: A graph comparing the film depth penetrations of heat exposure times using different substrates.

It is clear to see from Figure 6-5 that PA66 provides the best penetration depths for the heat exposure times selected and therefore is most likely to provide adequate heat for cure initiation within the mould.

As well as being a useful tool to more fully understand the changing temperature conditions during the INSPIRE process; the model has been implemented to find the most suitable material combination to be used in practical work.

Using the framework of this successful model, modifications can be made for a more complex system.

6.2 Multi-layer Thermal Model

An electroluminescent lamp is a multi-layer device, so when applying these layers sequentially in-mould, the moulded part comprises of a substrate material topped

with a composite layer structure. Since these materials have different properties, each individual layer must be considered and for this a more complex model is required.

6.2.1 The Problem

Again, the problem needs to be simplified:

- A thermoplastic part is moulded with one side covered with different multiple layers
- The substrate material is injected over the EL materials coating a warm mould tool
- PP is used as the thermoplastic, a commodity plastic commonly injection moulded
- A processing temperature of 220 °C and a tool temperature of 65 °C are used; which are appropriate for PP
- Modified electroluminescent pastes are sprayed in-mould, sequentially
- A bonding layer has been incorporated into the structure in the anticipation that one is required in the injection moulded part (this can be amended/omitted later if required)
- The part would be a small, sample moulding, dimensions approximately 7.5 cm x 7.5 cm x 0.3 cm, including a 44 µm EL multi-layer structure.

The multi-layer structure within the mould tool is shown in Figure 6-6.

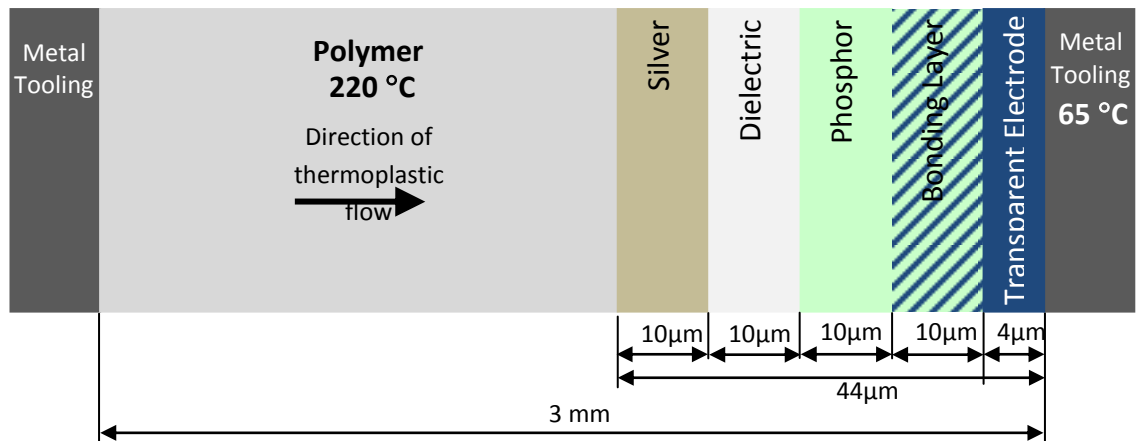


Figure 6-6: A diagram showing the multi-layer structure within the mould tool.

The multi-layer problem can be assumed to be:

A 44 µm thickness of EL device materials coats the inside of an injection mould tool at 65 °C; There is a transparent electrode of 4 µm covered by a bonding layer, phosphor layer, dielectric layer and silver electrode all of 10 µm. The mould cavity has internal dimensions of 7.5 x 7.5 x 0.3 cm³. A PP substrate is injected at 220 °C onto it, giving a moulding of total thickness 3 mm.

6.2.2 The Model

In the multi-layer model there are many more materials so the abbreviations in Table 6-5 are used as subscripts when referring to values in order to differentiate between individual layers, generic layers and the whole multi-layer device.

Table 6-5: Abbreviations used in the multi-layer model.

Material	Abbrev.
Generic Layer	L
A Generic Composite Layer	CL
Whole EL Device (All Layers)	EL
Substrate Polymer / Polymer Interface	P
Silver Electrode	SE
Silver Electrode-Dielectric Interface	SED
Dielectric Layer	D
Dielectric-Phosphor Interface	DPh
Phosphor Layer	Ph
Phosphor-Bonding layer Interface	PhBL
Bonding Layer	BL
Bonding layer-Transparent Electrode Interface	BLTE
Transparent Electrode	TE
Mould / Mould Interface	M

Table 6-6 (on the following page) shows the different terms used in the model; in combination with the subscript abbreviations in Table 6-5 (the # represents the position of the abbreviations).

Table 6-6: Terms used in the multi-layer model.

Term	Symbol
Thickness	$X_{\#}$
Surface Area	$A_{\#}$
Mass	$M_{\#}$
Specific Heat	$c_{\#}$
Thermal Conductivity	$k_{\#}$
Thermal Conductance	$C_{\#}$
Initial Temperature	$T_{\#(0)}$
Temperature at Time, t	$T_{\#(t)}$
Layer Temperature at distance, x from Interface at Time, t	$T_{L(t,x)}$
Time	t
Distance Across Layer from Interface	x

Figure 6-7 shows the abbreviations used for materials and boundaries:

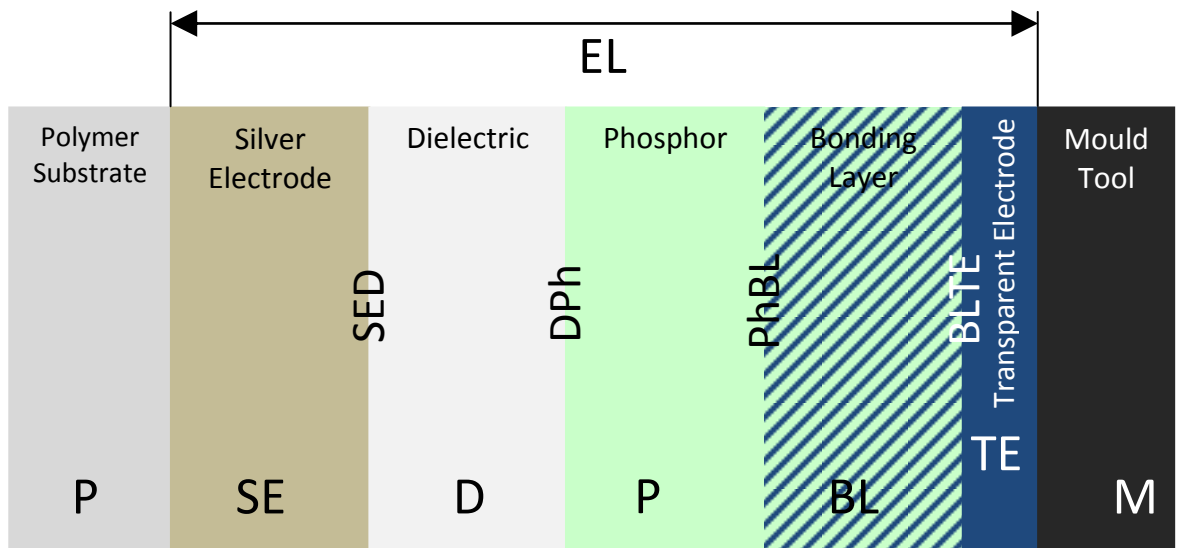


Figure 6-7: A diagram showing the layers and boundary abbreviations.

The similarities between the single layer model and this model are the calculation of the polymer cooling and calculating the temperature gradient across each layer

from the rate of heat transfer through it. The differences in this model stem from the presence of multiple layers. The calculation of the rate of heat transfer through the layers has to take into account the different properties of the materials present in the composite layer and temperatures at layer interfaces must be determined to use in the calculation of each individual layer's temperature gradient. A breakdown of the model process is as follows:

- The calculation of the polymer cooling (w.r.t. time)
- The calculation of the rate of heat transfer across the composite layer (w.r.t. time)
- The calculation the temperature difference across each layer using individual layer thermal conductance (at specific times after injection)
- Use the temperature differences to calculate the layer interface temperatures (at specific times after injection)
- Calculate the temperature gradient across each layer within the structure (at specific times after injection)
- Combine the temperature gradients to give a complete temperature profile across the multi-layer structure (at specific times after injection)

The temperature of the polymer w.r.t. time is calculated using Equation 7.

Equation 7: The temperature of the substrate polymer as a function of time.

$$T_{P(t)} = (T_{P(0)} - T_M) e^{-\frac{k_P A_P}{m_P c_P X_P} t} + T_M \quad [7]$$

The surface area and thickness of a material and its thermal conductivity can be used to calculate its thermal conductance:

Equation 8: The thermal conductance of a material as a function of its conductivity and dimensions.

$$C = \frac{kA}{X} \quad [8]$$

Substituting Equation 8 into Equation 7 gives:

Equation 9: The temperature of the substrate polymer w.r.t its thermal conductance.

$$T_{P(t)} = (T_{P(0)} - T_M)e^{-\frac{C_P}{m_P c_P} t} + T_M \quad [9]$$

The rate of energy transfer through a single layer w.r.t. the polymer temperature is shown by:

Equation 10: The rate of energy transfer through a layer as a function of polymer substrate temperature.

$$\frac{dQ_L}{dt} = \frac{k_L A_L}{X_L} (T_{P(t)} - T_M) = C_L (T_{P(t)} - T_M) \quad [10]$$

In order to take into account the multiple layers, the combined thermal conductance must be calculated. The thermal conductance of a composite layer with n layers can be calculated using Equation 11.

Equation 11: The compound thermal conductance of a multi-layer system.

$$\frac{1}{C_{CL}} = \left(\frac{1}{C_{L1}} + \frac{1}{C_{L2}} + \frac{1}{C_{L3}} + \dots + \frac{1}{C_{Ln}} \right) \quad [11]$$

So by substituting Equation 11 (with the appropriate subscripts) into Equation 10, the rate of heat transfer through the EL device (with a structure as in Figure 6-7) is calculated by:

Equation 12: The rate of heat transfer through the multi-layer EL system.

$$\frac{dQ_{EL(t)}}{dt} = \frac{(T_{P(t)} - T_M)}{\left(\frac{1}{C_{SE}} + \frac{1}{C_D} + \frac{1}{C_{Ph}} + \frac{1}{C_{BL}} + \frac{1}{C_{TE}} \right)} \quad [12]$$

The rate of heat transfer is equal throughout the thickness of the device, therefore the values calculated using Equation 12 can be used as the rate of heat transfer through each individual layer.

Particular times (after injection) are then selected to use in the next part of the model. The temperature differences across each layer at those times are then calculated using Equation 13:

Equation 13: The temperature difference across layer L, at time t.

$$\Delta T_{L(t)} = \frac{\frac{dQ_{EL(t)}}{dt}}{C_L} \quad [13]$$

Using these temperature differences, along with the temperature of the polymer at those times, the temperature at each of the layer boundaries can be calculated (at the selected times).

Using the same equation as the single layer model but with the appropriate values, the temperature gradient across an individual layer can be calculated using Equation 14.

Equation 14: The temperature at position x, across layer L, at time t.

$$T_{L(t,x)} = -\frac{dQ_{EL(t)}}{dt} \frac{x}{k_L A_{fL}} + T_{HOT\ BOUNDARY}^{5\ 6\ 7} \quad [14]$$

This is repeated until the temperature gradient has been calculated for each layer at each of the selected times.

⁵ Where x=0 is at position at the interface of the layer closest to the injected polymer

⁶ HOT BOUNDARY refers to the interface of the layer closest to the injected polymer

⁷ T_{HOT BOUNDARY} is the integration constant since x = 0 is the layer boundary therefore at that point T_{L(t,x)} is equal to T_{HOT BOUNDARY}.

All of the layer temperature gradients can finally be combined to give a complete thermal profile across the entire thickness of the multi-layer device for each of the selected times after injection.

6.2.3 The Results

Table 6-7 shows the values used in the initial model; since the model was created before an injection moulded EL device was produced and characterised, estimations were used. The surface areas, polymer thickness and mass were calculated from the tool cavity dimensions and density and other values were estimated from properties of similar materials.

Table 6-7: Estimated values used in the initial multi-layer model.

Term	Symbol	Values	SI Units						
Mould Temperature	T_M	338.15	K						
Polymer Temperature at time 0s	$T_{P(0)}$	498.15	K	Material Specific Values					
Mass of Polymer	m_p	0.015	kg	Polymer	Silver Electrode	Dielectric	Phosphor	Bonding Layer	Transparent Electrode
Specific Heat Capacity of Polymer	c_p	1800	$J.kg^{-1}.K^{-1}$	P	SE	D	Ph	BL	TE
Thermal Conductivity	k	→	$W.m^{-1}.K^{-1}$	0.4	5	0.1	0.5	0.35	0.2
Surface Area	A	→	m^2	0.0128	0.0018	0.0018	0.0018	0.0018	0.0018
Thickness	X	→	m	0.003	0.00001	0.00001	0.00001	0.00001	0.000004

The intermediate calculations made in the model are detailed in the following few paragraphs; the first stage was to calculate the conductance of each material using Equation 8, the results are shown in Table 6-8.

Table 6-8: The estimated thermal conductivity calculations.

Material	Thermal Conductivity k W.m⁻¹.K⁻¹	Area A m²	Thickness X m	Conductance C W.K⁻¹
Polymer	0.40	0.0128	0.003	1.71
Silver Electrode	5.0	0.00180	0.00001	900
Dielectric	0.10	0.00180	0.00001	18.0
Phosphor	0.50	0.00180	0.00001	90.0
Bonding Layer	0.35	0.00180	0.00001	63.0
Transparent Electrode	0.20	0.00180	0.000004	90.0

Next, the temperature of the polymer (w.r.t. time after injection) was calculated using Equation 9 (a cooling equation). The calculated values were used in Equation 12 to calculate the rate at which energy is transferred through the electroluminescent layers; taking into account combined conductance's of the different materials within the composite layer. The polymer temperature and the rate of heat transfer are both shown in Figure 6-8, as a function of time after injection.

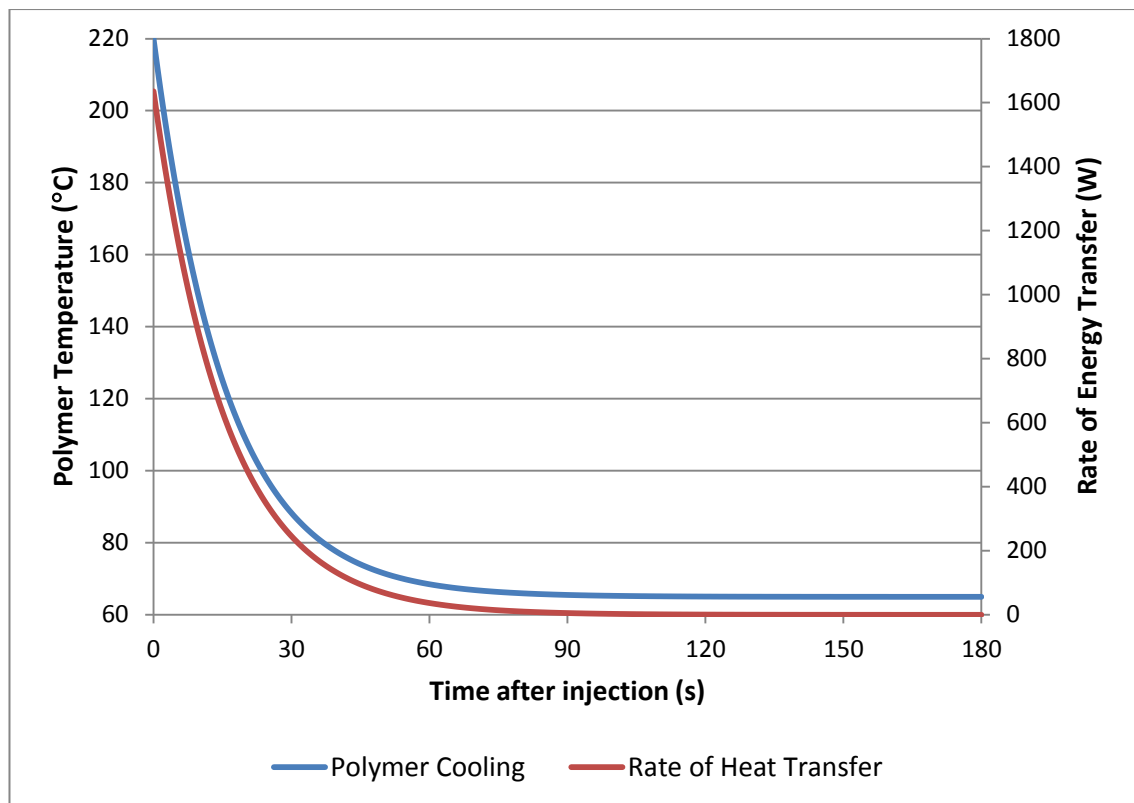


Figure 6-8: The substrate polymer temperature and the rate of heat transfer through the multi-layer EL system as a function of time.

Using Equation 13, the individual material properties and the calculated rate of energy transfer, the temperature difference across each individual layer can be calculated. Again, a limited number of times were selected in order to clearly present (graphically) the changes during the cycle; the selected times were the arbitrary values: 0 s, 1 s, 2 s, 5 s, 10 s, 20 s, 30 s, 45 s, 60 s, 90 s, 120 s and 180 s.

Using the temperature differences across each layer and the polymer temperature at each of the specified times, the temperature at each layer interface was calculated; these values could be verified by the final interface (the mould tool) being calculated to be the tool temperature value input into the model (in this case 65 °C). Table 6-9 shows the incremental interface temperatures.

Table 6-9: The boundary interface temperatures at the selected times.

t(s)	$T_{P(t)}$	$\Delta T_{SE(t)}$	$T_{SED(t)}$	$\Delta T_{D(t)}$	$T_{DPh(t)}$	$\Delta T_{Ph(t)}$	$T_{PhBL(t)}$	$\Delta T_{BL(t)}$	$T_{BLTE(t)}$	$\Delta T_{TE(t)}$	$T_{M(t)}$
	(K)										
0	493.2	-1.8	491.3	-90.9	400.5	-18.2	382.3	-26.0	356.3	-18.2	338.2
1	483.7	-1.7	481.9	-85.3	396.6	-17.1	379.6	-24.4	355.2	-17.1	338.2
2	474.7	-1.6	473.1	-80.1	393.1	-16.0	377.0	-22.9	354.2	-16.0	338.2
5	451.1	-1.3	449.8	-66.2	383.6	-13.2	370.3	-18.9	351.4	-13.2	338.2
10	420.5	-1.0	419.6	-48.3	371.3	-9.7	361.6	-13.8	347.8	-9.7	338.2
20	381.9	-0.5	381.4	-25.7	355.8	-5.1	350.6	-7.3	343.3	-5.1	338.2
30	361.4	-0.3	361.1	-13.6	347.5	-2.7	344.8	-3.9	340.9	-2.7	338.2
45	347.2	-0.1	347.1	-5.3	341.8	-1.1	340.7	-1.5	339.2	-1.1	338.2
60	341.6	0.0	341.6	-2.0	339.6	-0.4	339.1	-0.6	338.6	-0.4	338.2
90	338.7	0.0	338.7	-0.3	338.4	-0.1	338.3	-0.1	338.2	-0.1	338.2
120	338.2	0.0	338.2	0.0	338.2	0.0	338.2	0.0	338.2	0.0	338.2
180	338.2	0.0	338.2	0.0	338.2	0.0	338.2	0.0	338.2	0.0	338.2

The next stage of the model involves calculations for each individual layer; Equation 14 was used to calculate the temperature gradient across the thickness of each layer at each of the specified times. Table 6-10 shows the temperature gradients for the dielectric layer; the same calculations were carried out for each layer.

Table 6-10: The temperature of the dielectric material at position x, at each of the selected times.

x (μm)	$T_{D(0,x)}$	$T_{D(1,x)}$	$T_{D(2,x)}$	$T_{D(5,x)}$	$T_{D(10,x)}$	$T_{D(20,x)}$	$T_{D(30,x)}$	$T_{D(45,x)}$	$T_{D(60,x)}$	$T_{D(90,x)}$	$T_{D(120,x)}$	$T_{D(180,x)}$
	(K)											
0	491.3	481.9	473.1	449.8	419.6	381.4	361.1	347.1	341.6	338.7	338.2	338.2
1	482.2	473.4	465.1	443.2	414.7	378.9	359.8	346.5	341.4	338.6	338.2	338.2
2	473.2	464.9	457.1	436.6	409.9	376.3	358.4	346.0	341.2	338.6	338.2	338.2
3	464.1	456.4	449.1	429.9	405.1	373.7	357.1	345.5	341.0	338.6	338.2	338.2
4	455.0	447.8	441.1	423.3	400.2	371.2	355.7	344.9	340.8	338.5	338.2	338.2
5	445.9	439.3	433.1	416.7	395.4	368.6	354.3	344.4	340.6	338.5	338.2	338.2
6	436.8	430.8	425.1	410.1	390.6	366.0	353.0	343.9	340.4	338.5	338.2	338.2
7	427.7	422.2	417.1	403.5	385.8	363.5	351.6	343.4	340.2	338.5	338.2	338.2
8	418.6	413.7	409.1	396.8	380.9	360.9	350.2	342.8	340.0	338.4	338.2	338.2
9	409.5	405.2	401.1	390.2	376.1	358.3	348.9	342.3	339.8	338.4	338.2	338.2
10	400.5	396.6	393.1	383.6	371.3	355.8	347.5	341.8	339.6	338.4	338.2	338.2

The data from in Table 6-10 is shown in Figure 6-9.

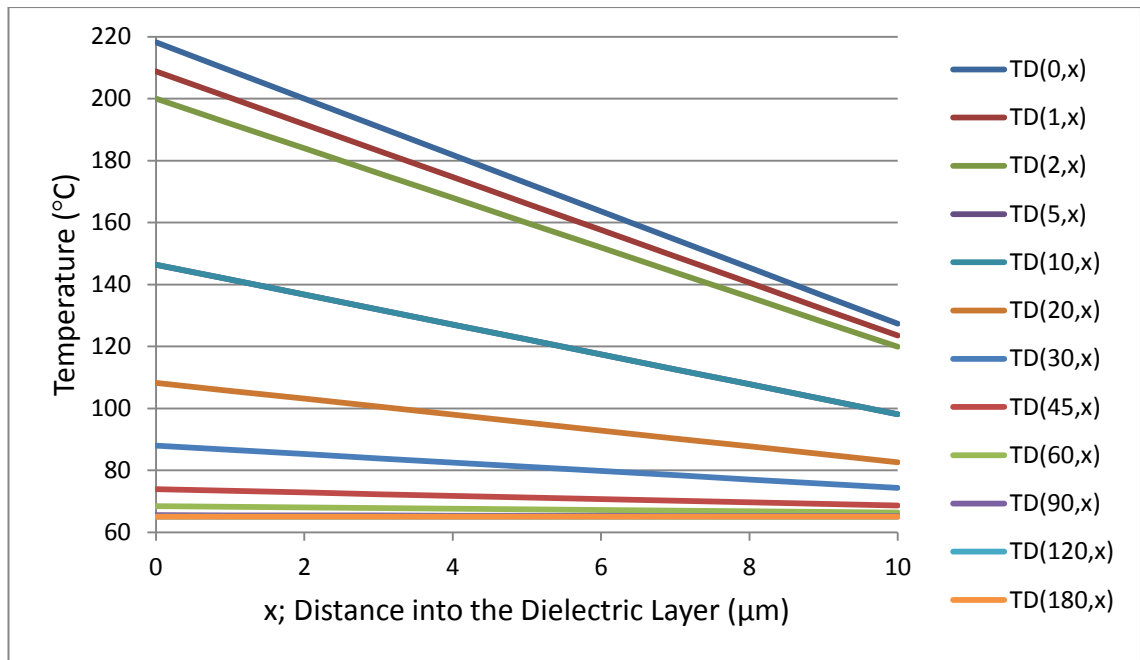


Figure 6-9: The temperature gradient across the dielectric layer at each of the selected times.

The calculated temperature gradients across individual layers combine to give a thermal profile across the entire multi-layer device at each of the selected times; Figure 6-10 shows the changing temperature profile changing as time progresses.

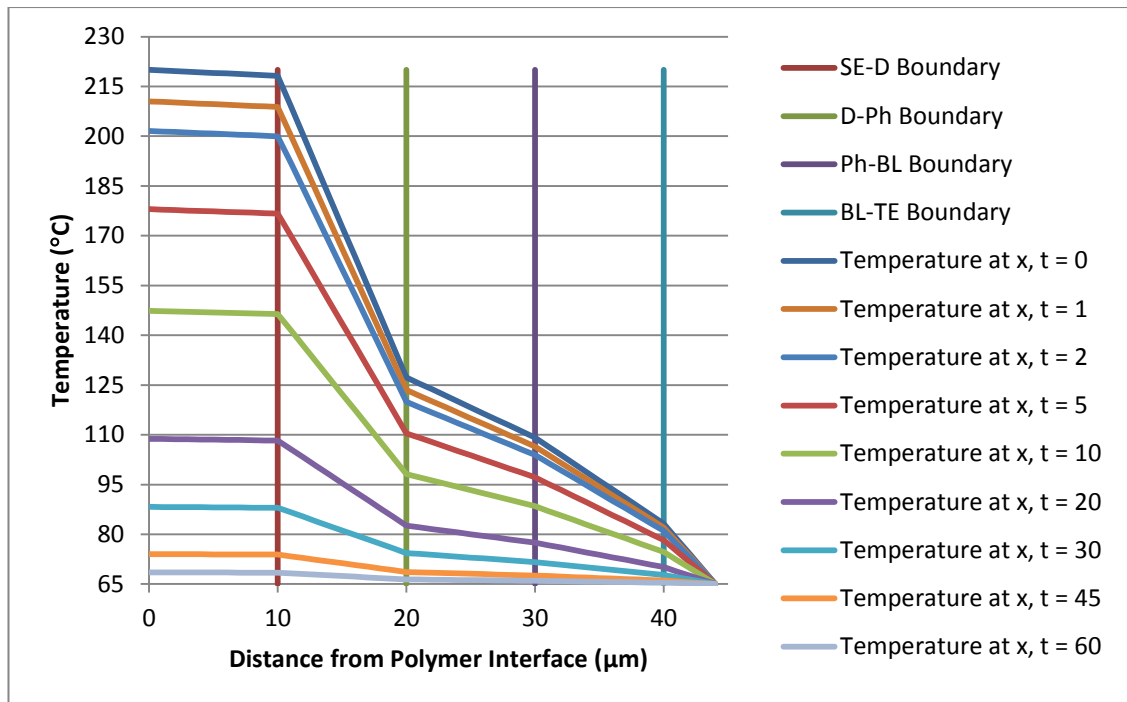


Figure 6-10: The complete temperature profile across the multi-layer EL system at selected times after injection.

Although this model uses approximate values, it appears from the results the model works as a guide to temperatures experienced by each layer and can be modified to incorporate real, measured values in future work. This will be helpful in understanding in-mould material behaviour with respect to the processing conditions.

7 SCOPING EXPERIMENTS

The aim of the project is to determine whether electroluminescent layers can be applied during the manufacturing process (specifically injection moulding) and if three dimensional (3D) surfaces can be produced with electroluminescent capabilities. No existing methodology relating to such a novel process was found. A sequence of initial scoping experiments was planned and carried out in order to develop the process method and ultimately be able to apply the layers sequentially in-mould. The following chapter provides an explanation of the experimental work carried out throughout the initial developmental stages; this preliminary work begins with a multi-layer structure recommended by H C Starck, a supplier of one of the materials [148]. The recommended structure can be seen in Figure 7-1; from the bottom up it comprises of:

- a clear substrate material, PC or PET (shown in pale blue),
- a Clevios™ PEDOT:PSS transparent electrode (shown in dark blue),
- a silver busbar surrounding the Clevios™ (shown in beige),
- a light emitting phosphor layer (shown in green),
- one or more dielectric layers (shown in pale grey),
- a Clevios™ PEDOT:PSS layer (again, shown in dark blue), and finally,
- a silver rear electrode (again, shown in beige).

Figure 7-1 also shows the direction of light emission (represented by the pale yellow arrows), originating in the phosphor layer and exiting the device through the transparent electrode and the substrate.

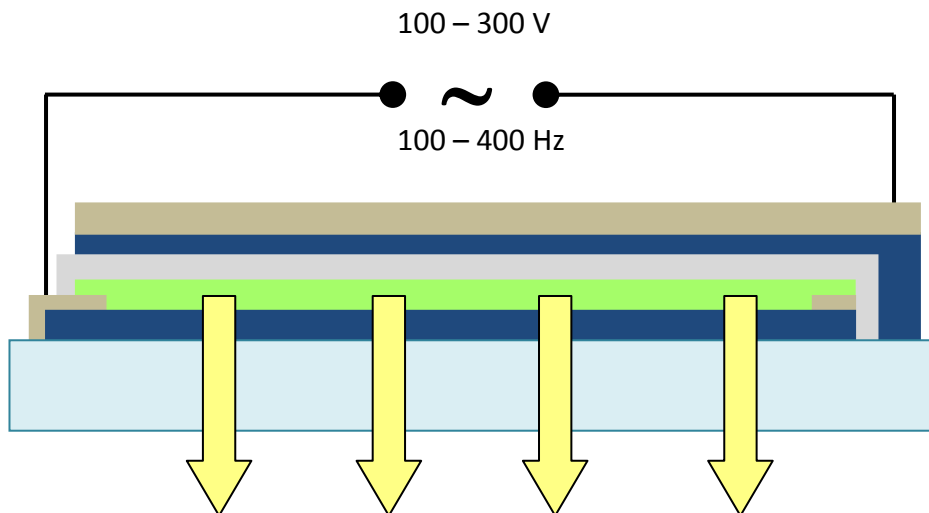


Figure 7-1: The EL structure and operating conditions as recommended by H C Starck.

7.1 Materials and Equipment

The equipment and materials used throughout the project are detailed in this section; some items were already available in the workshop and laboratory and some speciality materials and equipment were bought in for this specific project.

7.1.1 Materials

Commercially available materials were sourced and their use/versatility investigated. The electroluminescent materials are produced with the intention of them being used for the screen printing method (a common method currently utilised commercially as described in section 3.8.2). These materials were then adapted to be used in the methods developed as part of this project. The electroluminescent (and associated) materials used in this project are detailed in Table 7-1.

Table 7-1: Materials used to produce electroluminescent devices.

<i>Material</i>	<i>Supplier</i>	<i>Information</i>	<i>Function within Device</i>
PEDOT:PSS	H C Starck	CLEVIOS™ S V3 conductive polymer	Transparent Electrode
Phosphor Paste	Electra Polymers	ZnS:Al ₂ O ₃ with Cu activator suspended within a polymer matrix	Light Emission Layer
Dielectric Paste	Electra Polymers	Not Supplied	Non conducting layer to give capacitor structure
Silver Paste	Electra Polymers	Silver particles suspended within a polymer matrix	Rear (opaque) Electrode
PEDOT:PSS	AGFA Materials	Orgacon™ conductive polymer	Alternative transparent electrode material
PEDOT:PSS	Electra Polymers	ITO-R conductive polymer	Alternative transparent electrode material
Clear UV curable thermoset polymer	Electra Polymers	Coverlay	Clear protective layer applied over the device
ER1 Reducer	Electra Polymers	Solvent	To reduce the viscosity of materials to enable them to be used with an airbrush
Polyurethane Clear Coat	PlastiCote	Air drying PU	Clear protective layer applied over the device
MEK	VWR International	Solvent	To reduce the viscosity of materials to enable them to be used with an airbrush

Propanol	Laboratory Stores	Solvent	“
Distilled Water	Laboratory Stores	Solvent	“
Clear PC sheet	SABIC Innovative Plastics	3 mm Lexan™ Sheet	Flat substrate material
Polypropylene	SABIC	PP granules	Injection moulding substrate
Polycarbonate	SABIC	PC granules	Injection moulding substrate
LDPE Film	Laboratory Stores	Transparent film	Insert substrate
PET Film	Laboratory Stores	Semi-transparent film	Insert substrate
PTFE coated woven mat	Laboratory Stores	Non-stick mat	Insert substrate
0.05 mm PTFE Film	RS Components	Non-stick film	Insert substrate
12.7 mm Copper Bus	DCC Supplies	Copper tape with conductive adhesive	Electrode connection point

Further details of the chemical composition of the materials can be found in section 7.3. Initially the electroluminescent materials were used as they were supplied, using the application method they were intended for; then the paste materials were diluted and sprayed using an airbrush with air compressor.

7.1.2 Equipment

The central equipment used in developing processes by which an EL device can be produced by injection moulding include; the oven, the airbrush and compressor and the injection moulding machine. A brief description of each is given in this section.

The oven used for drying the electroluminescent materials is made by Pickstone Ovens with a maximum temperature of 600 °C.

The airbrush and compressor were purchased from Absolute Airbrush; the compressor runs from mains electricity (220-240 V, 50 Hz) and has an air output of

23 L/min and a working pressure of 43-53 PSI (3-4 bar). The airbrush is a dual action airbrush with push button activation and has a nozzle diameter of 0.30 mm. It is used in conjunction with 22 cc glass jars with suction lids; a separate glass jar is used for each of the layer materials. The compressor, airbrush and jars can be seen in Figure 7-2.

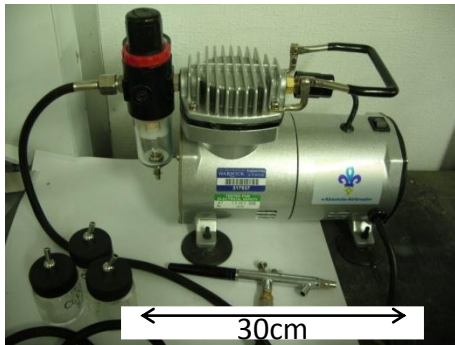


Figure 7-2: The compressor, airbrush and jars used to apply the layer materials.

The injection moulding machine used in this project is a Sandretto Micro 30 and has a maximum clamping force of 30 tonnes, for this project the mould is heated by electric cartridge heaters: the machine can be seen in Figure 7-3.

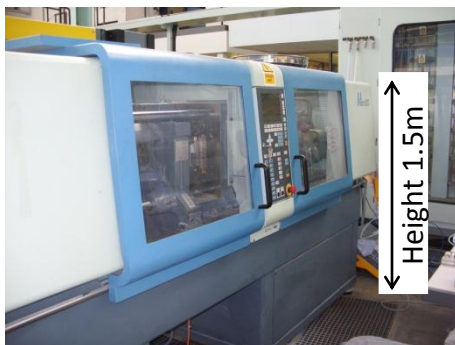


Figure 7-3: Sandretto Micro 30.

The mould tool used in this project had a range of geometrical features to help determine the scope of the new process; there are flat regions, a shallow curved

area and sharper edges (the mould cavity is shown in Figure 7-4 and the geometry of the mould tool is shown in Figure 7-6).

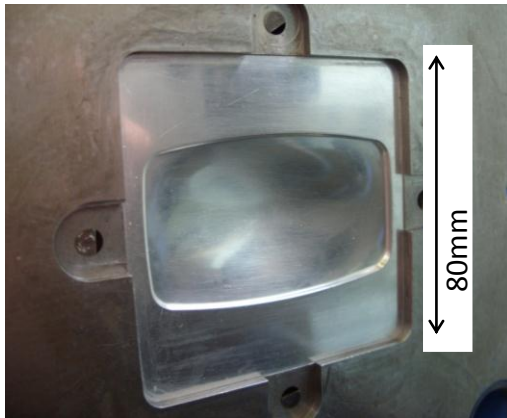


Figure 7-4: The mould cavity.

An example of parts produced by this mould is shown in Figure 7-5. The various part geometries of the front face can clearly be seen; a basic flat base with a raised central shape. The mould is centre fed and the sprue is located on the reverse of this part, in the centre.



Figure 7-5: An example of a part moulded in the tool used in this project.

In order to identify any dimensional limitations of the new process it is important to know the dimensions of the moulded parts, these are shown in Figure 7-6.

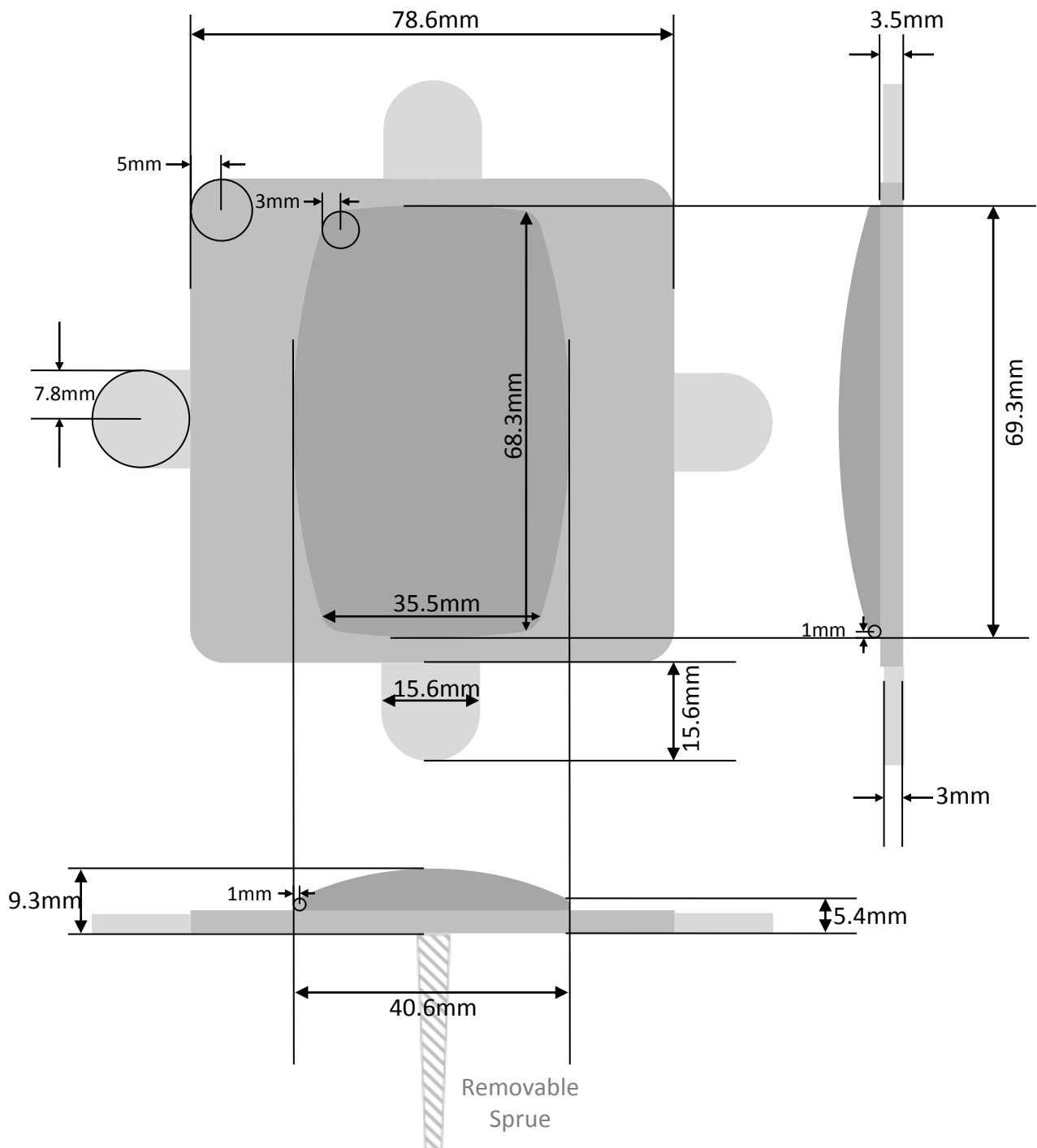


Figure 7-6: The dimensions of the moulded parts made in this project; the removable sprue dimensions have not been included.

To power and test the manufactured devices, an AC power supply was made in-house by technical staff. The device could supply variable RMS voltages and frequencies; its ranges were 100-300 V and 100-400 Hz.

For testing and characterisation carried out later in the project, a Velleman HPS10 handheld oscilloscope and probe were purchased; as was a ST-1301 light meter and a ST-321 humidity and temperature probe.

7.2 Thick Layer Application Method

It was essential to first use the materials as they were supplied in order to determine that the acquired materials and selected structure produced a working electroluminescent device. The layers were applied using the method for which these materials had been designed, a screen printing method; so the next stage was to select suitable equipment from a range available.

7.2.1 Equipment Selection

The screen printing method uses a mesh screen to apply a layer of paste with a uniform thickness, areas where materials is not required are masked off and a squeegee scraper is used to force the paste through the mesh (Figure 7-7 shows a diagram illustrating the method). Since an electroluminescent device contains a number of different materials applied sequentially, the mesh screen would need to be cleaned between each layer application wasting a lot of material and result in a very slow process. By carefully selecting equipment it was thought that an even layer could be applied in a similar method without the need for a mesh screen, and so reducing the amount of equipment needed, reducing waste and speeding up process time.

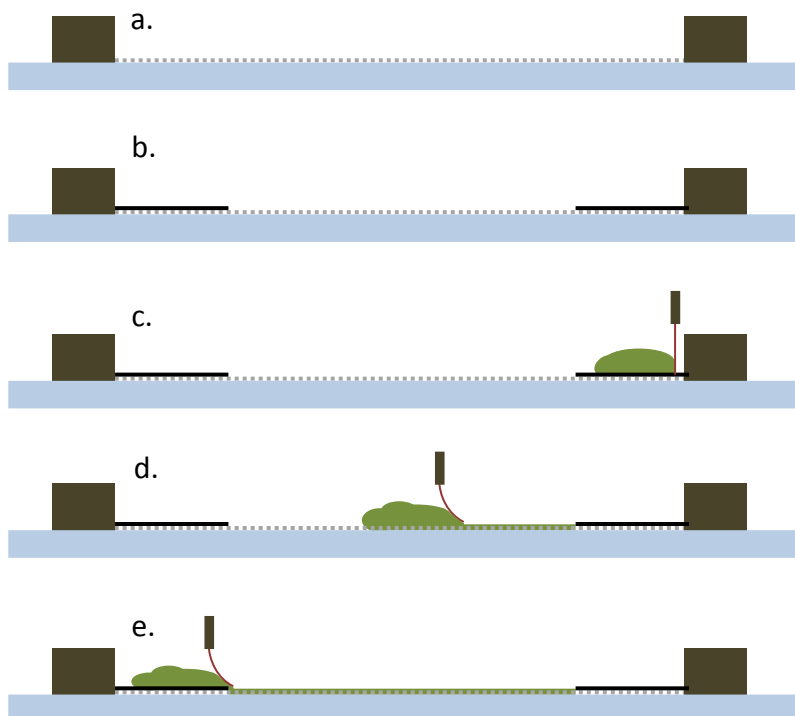


Figure 7-7: The screen printing technique. From top to bottom: a) a mesh screen is placed on a substrate, b) areas of the screen may be masked off, c) a viscous liquid is applied on the mesh, d) the flexible scraper forces material through the mesh, e) across the whole frame.

The equipment that needed to be selected was a tool to carry out the function of the screen printing squeegee (i.e. to be used for material layer application) and the materials required for masking off areas where particular layer materials need not be applied.

From some initial trials, the equipment that produced the most even layers and masked areas effectively to give the best edge definition were a rigid material applicator and self-adhesive PVC film masking templates. These sufficiently replicated the screen printing process and were used to make the thick film devices.

7.2.2 Masking Template Design

The initial number of layers and layer shape was followed from a document produced by H C Starck (the supplier of the transparent electrode) [148]. Figure 7-8 and Figure 7-9 show the layer design used in these initial trials. Also included in the

process guide was curing regimes, operating parameters and substrate material suggestions; 3mm polycarbonate sheet was selected as it was readily available and its rigidity was suitable for the screen printing type layer application.

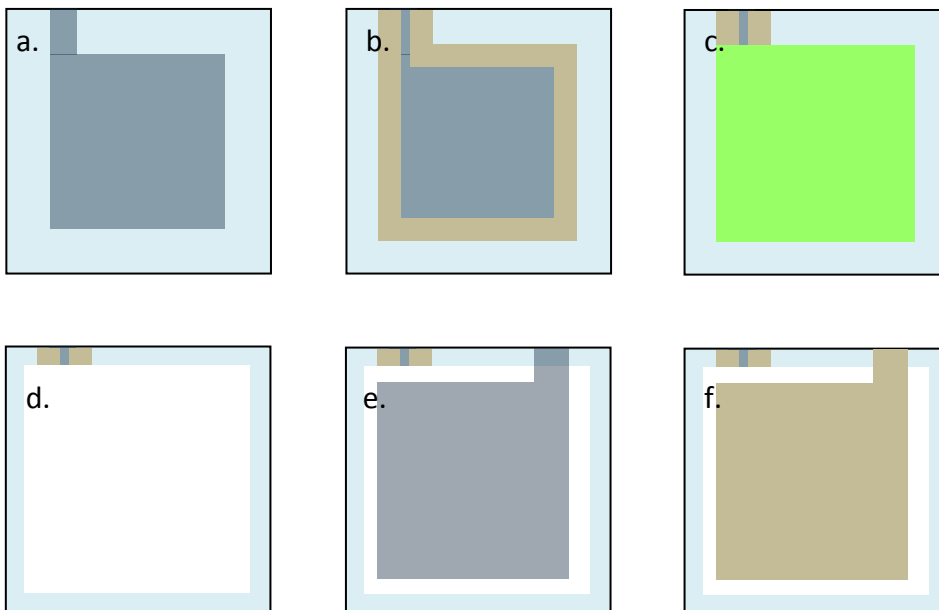


Figure 7-8: The suggested layer design; a) Clevios™ PEDOT:PSS, b) silver bus, c) phosphor, d) dielectric, e) Clevios™ PEDOT:PSS and f) silver.

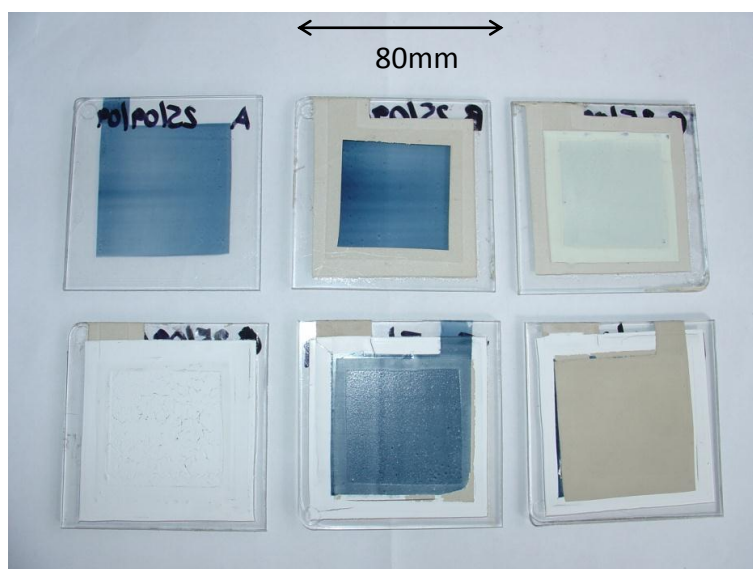


Figure 7-9: The real layer by layer build up.

7.2.3 Structure Investigation

The next stage was to determine the simplest possible layer structure that produced a working device. Since a transparent electrode, a light emitting layer and a rear electrode are essential components of the device (see page 29) this is the simplest structure that was tested; the dielectric layer and silver bus bar were added to see if they were required or not. Test plaques using the four following structures were constructed:

- (PC Substrate) Clevios™ PEDOT:PSS – phosphor – silver
- (PC Substrate) Clevios™ PEDOT:PSS – phosphor – dielectric – silver
- (PC Substrate) Clevios™ PEDOT:PSS – silver bus bar – phosphor – dielectric – silver
- (PC Substrate) Clevios™ PEDOT:PSS – silver bus bar – phosphor – dielectric – Clevios – silver

The devices were assessed to be successful if they sustained illumination for a minimum of 1 minute. Upon testing it was discovered that a silver bus bar is not required as the device illuminated without one, however a dielectric layer is needed. Devices constructed without a dielectric layer were unreliable; some failed to illuminate, some flickered and failure occurred when operated at high voltages. Devices also worked when the rear Clevios™ layer was removed.

The structure was simplified to a four layer architecture. After using the recommended shapes for the initial process development, the template shape was modified to simpler shapes (shown in Figure 7-10) in order to simplify the layer application process.

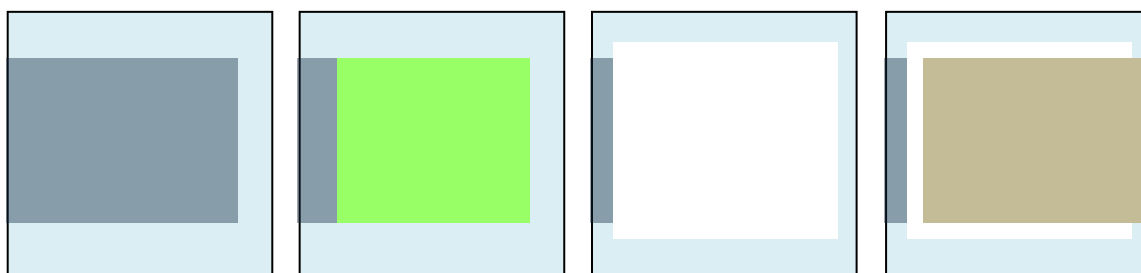


Figure 7-10: The simplified EL structure consisting of four layers.

The materials were applied using the rigid scraper and a self-adhesive masking template, then dried and following regimes recommended by the suppliers [148]; these are shown in Table 7-2.

Table 7-2: The oven regimes for the EL layer materials.

Material	Oven Temperature (°C)		Drying Time (min)	
	Range Given	Value Used	Range Given	Value Used
Clevios™	80-130	130	15-30	15
Phosphor	110-130	130	2-10	3
Dielectric	110-130	130	2-10	4
Silver	110-130	130	2-10	2

A working device was produced with a four layer structure; Clevios™, phosphor, dielectric and silver layers, this is shown in Figure 7-11.

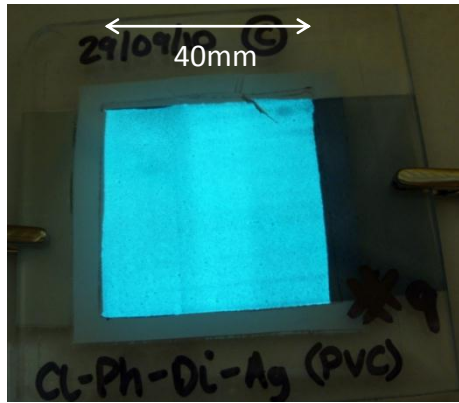


Figure 7-11: A four layer working EL device made on a PC substrate using a rigid scraper.

Further variations were constructed to investigate the versatility of the structure. The dielectric paste layer was replaced with an adhesive PVC film; this was carried out to see if generic insulative materials could be used as an alternative. The device lit but needed a larger voltage to emit the equivalent level of light, and areas remained unlit where air bubbles under the film prevented contact between layers.

A semi-transparent device was constructed by using Clevios™ for both front and rear electrodes and a clear adhesive PVC film was used for the dielectric. The device lit and light was emitted from both sides but again equivalent light levels were only achieved using higher voltages.

Patterning the silver electrode results in an illuminated shape/logo; it is essential that there is contact between different characters/elements of the logo so that there is electrical connectivity across the whole shape of the electrode. The patterned device can be seen in Figure 7-12.

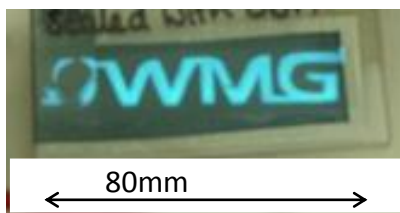


Figure 7-12: A shaped EL device made using a rear electrode shaped like the WMG logo.

7.2.4 Suitability to Injection Moulding

Some experimental work was then undertaken to investigate the suitability of introducing these EL materials into the injection moulding process. Since the materials are paste and gel consistencies initially they were painted into an open mould using a brush. This was done because the previously selected rigid material applicator would not successfully apply materials across the contours of the mould cavity. Each layer of the device structure needs to be dried/cured before the next can be added; a mould heater was used at 65 °C to speed up the drying, but since the tooling on the machine did not have the capability of cooling, the temperature had to be limited to a suitable ejection temperature of the thermoplastic moulding material.

Polypropylene was the moulding material used in these trials as this is a cheap, commodity plastic, is very stable throughout the process, does not require drying prior to processing and has relatively low processing temperatures. Since PP is fairly opaque, the finished part should be a top emitting device, i.e. the layer structure was applied in the sequence that results in the transparent electrode forming the outer surface of the moulded part (shown in Figure 7-13).

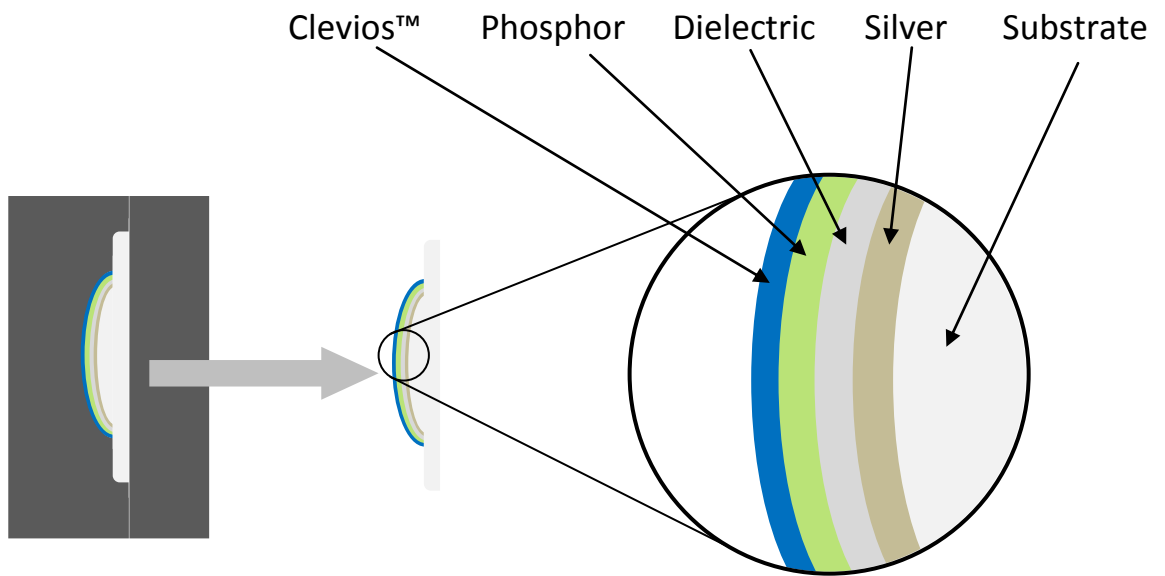


Figure 7-13: A diagram showing the order that the layer materials are applied in-mould and appear on the final part.

Figure 7-14 shows the sequential build-up of the material layers; the brush applied a thick layer, each of which was dried in between application.



Figure 7-14: The in-mould layer application. Left to right; Clevios™, phosphor, dielectric and silver.

After moulding, it was immediately clear that some of the materials had transferred onto the part, but the Clevios™ PEDOT:PSS material remained in the mould. Upon closer inspection, it could be seen that the silver, dielectric and most of the phosphor had successfully been transferred to the part during moulding (see Figure 7-15).

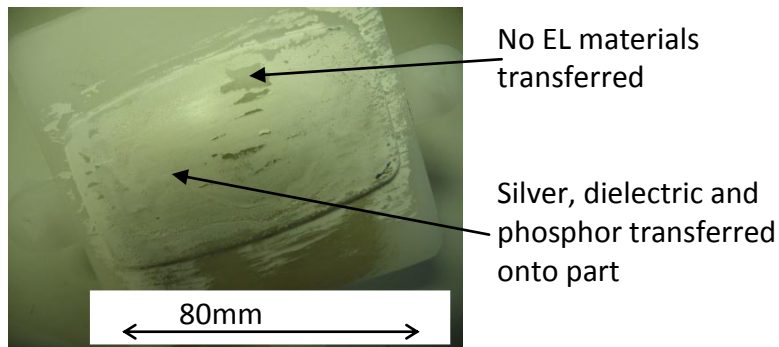


Figure 7-15: A moulded part with phosphor, dielectric and silver transferred onto it.

Next, the part was connected to an AC supply to see if there was any illumination. A crocodile clip was connected to the exposed area of the rear, silver electrode and due to the lack of a transparent electrode a probe was used to make contact with intact sections of the phosphor. Despite the complete lack of a transparent electrode layer illumination did occur at the electrical contact point; this initial experiment shows (with considerable improvements to the process) it is feasible for these materials to be used in the injection moulding process. Figure 7-16 shows the small but significant illuminated spot on this injection moulded part.

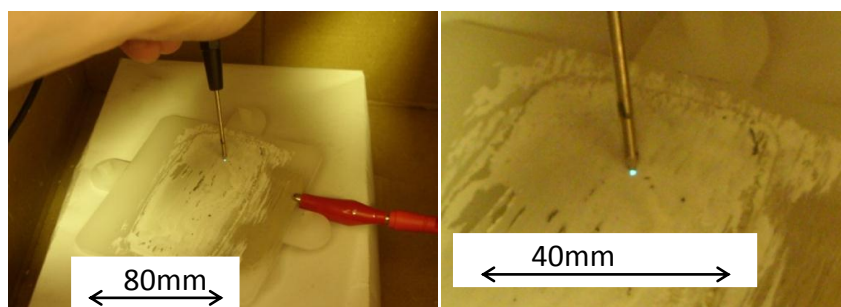


Figure 7-16: The illumination of the phosphor at the electrical contact point.

The Clevios™ PEDOT:PSS material was also applied independently as a single layer, and moulded using PP; again the material remained in the mould after ejection. Clevios™ is most compatible with polyester or polycarbonate so this was not entirely unexpected; also PP has poor adhesion to many materials [135]. The ability to utilise PP in this process however, would be an extremely good development step if it could be overcome as it would open up new markets with cheaper substrate materials.

From this initial trial experiment it can be seen that the problems that need to be overcome in order to make the process successful are:

- the adhesion between layers and the substrate material,
- the release of materials from the mould tool, and
- the uneven coverage due to the method of layer application.

7.2.5 Early Insert Moulding Trials

Since applying the EL layers directly into the mould tool caused some of the materials to remain in the mould after a part was moulded and ejected, experiments were carried out applying EL layers using insert moulding. The electroluminescent device structure was built up on an insert substrate; this insert was then placed in the mould and the plastic was injection moulded over it in order to produce a moulded part with the insert (and EL materials) formed over the surface.

Three different insert substrates were tested, PTFE coated woven mat, PET Film and LDPE, these were all readily available and further selection details are given in Table

7-3. During preparation the insert substrates were mounted on aluminium plates to alleviate any problems associated with handling such thin, flexible materials, e.g. during transfer to/from the oven. Reusable non adhesive templates were used in place of single use self-adhesive templates since removal of the adhesive templates was damaging both the substrate film and previous layers. During the preliminary equipment selection trials, it had already been discovered that the screen printing type method forces material under the edges of the non-adhesive template and if electrode layers spread it could cause a short circuit. To avoid this, a temporary application method was devised in order to quickly test the feasibility of using insert moulding as a processing technique. The alternative application method was sponge stippling; this was determined to produce the best coverage and edge definition.

Table 7-3: A summary of the insert moulding trials and results.

<i>Insert Material</i>	<i>Selection Reason</i>	<i>Insert Characteristics</i>	<i>Processibility (Layer drying and moulding)</i>	<i>Moulded Part</i>
PTFE coated woven mat	Non-stick so it will easily release from the materials and part after processing	Flexible, woven texture	Withstands 130 °C, moulded well	Some Clevios™ came off with the insert. Woven texture to the surface. Part successfully illuminated.
PET Film	PEDOT:PSS adheres well to PET and it is a material commercially used in insert moulding	Thick, fairly inflexible film, very smooth surface	Withstands 130 °C, PET film (and Clevios layer) remained in the mould when the part was ejected	An incomplete layer structure was left on the surface and there were crease marks from the film. Part did not illuminate
LDPE Film	Due to a low	Very flexible,	Significant	The PE sealed

	melting point, there will be diffusion at the surface during injection, forming a bond with the injected Polypropylene encapsulating the layers	smooth surface	shrinkage at 130 °C, can be made on pre-shrunk film ⁸ , moulded well	with the PP encapsulating the EL area. Part successfully illuminated.
--	---	----------------	---	---

Working parts were produced using both the PTFE and PE insert techniques. With PE, copper strips were used as a means of providing an electrical connection to the electrode materials sealed under the film; the strips of copper were added to the insert when electrode layers were dried in the oven and simply overhung the edge. Although this method worked occasionally, the copper strips easily detached from the insert. A working example of a PE insert moulded part can be seen in Figure 7-17.

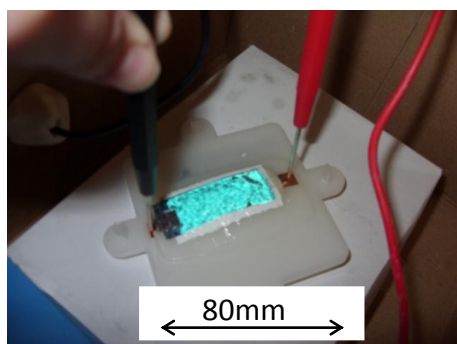


Figure 7-17: A working insert moulded EL device.

This experiment shows a plastic part with a 3D curved electroluminescent surface can be produced using an insert moulding process (using both PTFE coated woven

⁸ An oversized piece of PE was used and pre-heated; heating the PE actually benefitted the layer application process, as the PE formed to the aluminium plate and gave a flatter surface to apply layers to; the PE easily peeled from the aluminium after cooling and trimming to the correct size. However, some samples were too deformed to use.

mat and LDPE film), as an alternative to applying layers directly into the mould tool. However in order for this method to be truly successful many improvements and developments are required:

- a more even layer application method,
- a non-woven alternative to the PTFE mat, and
- an improved electrical connection option for encapsulated layers.

7.3 Airbrush Layer Application

To improve the speed of processing and the quality of layers it was decided that a compressor driven airbrush spray would be used to apply layer materials; this would result in faster produced and more easily repeatable, thin, even layers. It also has the benefit of enabling further improvement by automation and the ability to apply layers over a contoured surface. The EL materials needed to be modified to be suitable for use with an airbrush. The materials needed to flow better (i.e. be less viscous) so they required dilution with a compatible solvent.

The centipoise (cP) is a common unit for measuring viscosity of paints, inks and coatings; using this unit the viscosities of water, propanol and MEK are 1 cP, 1.9 cP and 0.4 cP respectively. An online airbrush information sheet published by a paint manufacturer states that the ideal viscosity for airbrushing is 35-60 cP [149]. The viscosity data for the exact materials used in this project were unavailable from the supplier but research has been carried out on similar materials which are used here to provide a good estimate. A W-BUS white silver, Dielectric-O and Blue Phosphor were measured to have viscosities (at zero stress) of 123 Pa.s, 80 Pa.s and 80 Pa.s respectively [150]; this is the equivalent to 123000 cP and 80000 cP. This shows that

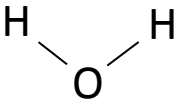
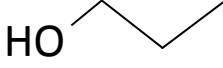
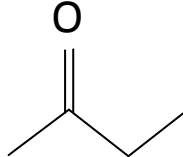
the screen printing materials used in this project need considerable “thinning” to make them suitable for use with an airbrush.

7.3.1 Dilution

Initial dilution trials of the electroluminescent materials were carried out with the readily available solvents of distilled water, propanol and MEK;

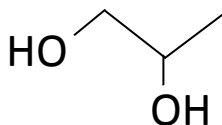
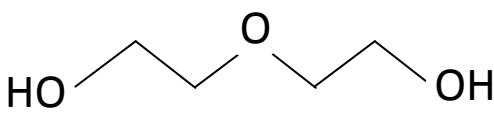
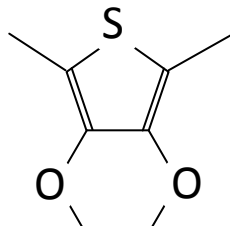
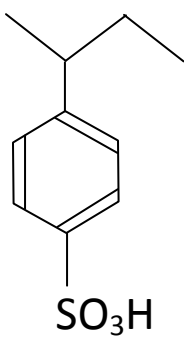
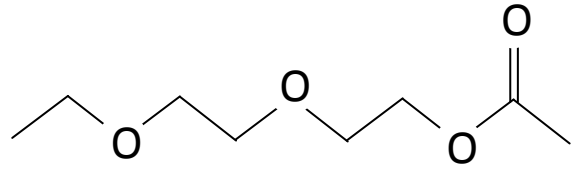
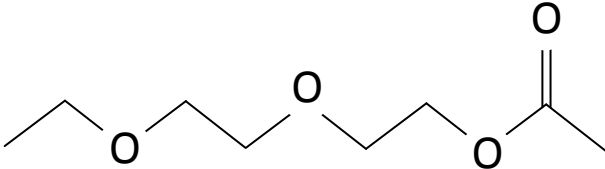
Table 7-4 shows the chemical composition of these. Comparing functional groups of the solvents and layer materials indicates which solvent is best suited for the dilution of the pastes.

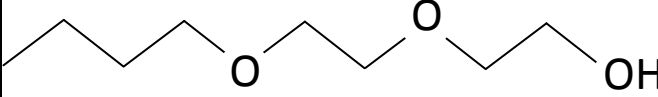
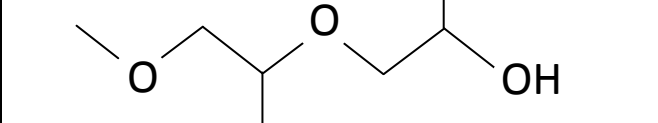
Table 7-4: The molecular structure of water, propanol and MEK.

Solvent Name	Chemical Formula	Chemical Structure
Water	H ₂ O	
Propan-1-ol	C ₃ H ₇ OH	
MEK; Methyl ethyl ketone	CH ₃ C(O)C ₂ H ₅	

The chemical composition and structure of the component materials within each layer are given in Table 7-5 (the names of the components shown in the table are the names given on the suppliers MSDS; these are not always the IUPAC name and in some cases there are a number of different names for the same compound).

Table 7-5: The molecular structure of the Clevios, phosphor, dielectric and silver layer materials.

Name	Component Chemical	% by Weight	Chemical Structure
Clevios™ SV3	Propane-1,2-diol	65.6	
	2,2'-Oxydiethanol	15	
	PEDOT – Poly(3,4-ethylene dioxithiophene)	1.1	
	PSS – Poly(styrenesulphonate)		
Phosphor ELX10	2-(2-Ethoxyethoxy)ethyl acetate	30-60	
	Phosphor	Not Given	ZnS:Cu
Dielectric ELX80	2-(2-Ethoxyethoxy)ethyl acetate	30-60	
	Ceramic	Not Given	Undisclosed

Silver ELX30	2-(2-Butoxyethoxy)ethanol	5-10	
	Methoxypropoxypropanol	10-30	
	Silver Powder	60-100	Ag

The Clevios™ PEDOT:PSS material has OH functional groups in both of the solvents present in it; propanol therefore appears to be best suited to dilute Clevios™ since this also has an OH group, however water could also act as a diluent. The solvent in the phosphor material is an acetate, as is the solvent in the dielectric. The C=O group present in MEK makes it the most obvious solvent to dilute these materials who also possess the C=O in the acetate group. Two components of the silver paste also have an OH group therefore propanol is most likely to be best suited to dilute the silver as well. Since MEK is most suitable for the phosphor and dielectric, it will also be tested for suitability with the Clevios™ and silver paste.

First Clevios™ was initially diluted to a 1:1 ratio of paste to solvent; further solvent was added gradually if the airbrush did not draw up the liquid. Although this method of dilution was trial and error, it was deemed the most favourable for a number of reasons; the measuring and mixing of a number of small batches of thick paste materials resulted in a lot of waste of expensive materials, measuring the viscosity for every type of material each time it is mixed would have been very time consuming (and again wasteful) and when mixtures were not used for a period of

time the viscosity would have to be re-measured and re-adjusted. The following observations of the modified material were made:

- The Clevios™ and propanol mix diluted but had solid granules in, it did not spray easily,
- The Clevios™ and water mix diluted well, it also sprayed well but was incompatible with the PC substrate. This can be seen in Figure 7-18, the materials pulled away from the substrate surface giving a streaky appearance. The polar nature of the water molecules means that the cohesion between them is greater than the adhesion to the PC, causing the water rich Clevios™ mixture to pull together into streaks.
- The Clevios™ and MEK mix diluted well (with a few solid granules remaining), it sprayed and dried well, Figure 7-18 shows the modified Clevios™ sprayed layers.

MEK also proved to be the most suitable solvent for the other layer materials; again dilution was started at a 1:1 ratio and then adding more solvent if required:

- The phosphor and MEK mix diluted well but separated quickly; it recombined upon shaking, sprayed well but needed to be shaken to remain well mixed. The layer shrunk when drying and cracked if over dried,
- The dielectric and MEK mix diluted well, again this material cracked if over dried,
- The silver and MEK mix diluted well but separated, it recombined upon shaking, the mixture sprayed well and air dried but was fragile to touch, it hardened when heated in an oven.

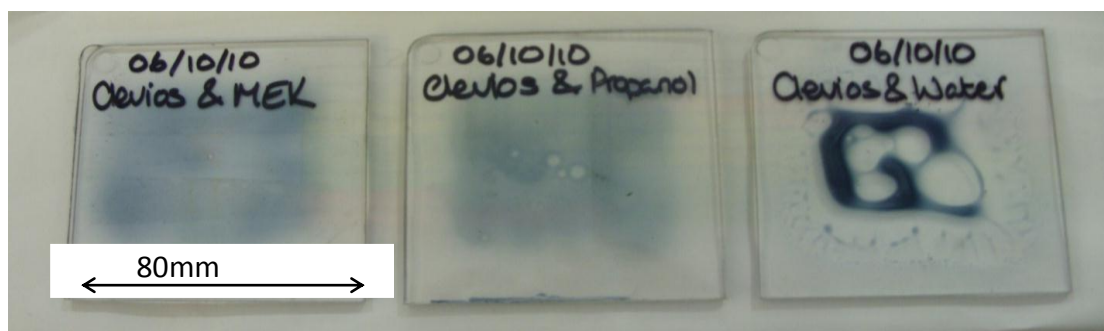


Figure 7-18: Dilution of Clevios with MEK, propanol and water and the resulting layers.

The solvent used to dilute the EL materials in order for them to be sprayed with an airbrush is MEK, also from these experiments, new drying regimes were established for the diluted, MEK modified materials, and these are shown in Table 7-6.

Table 7-6: The drying regimes for the MEK-modified materials.

Material:MEK Mix	New Airbrush Drying Regime	
	Oven Temperature (°C)	Time (min)
Clevios™ PEDOT:PSS	130	5
Phosphor	130	2
Dielectric	130	2.5
Silver	130	1.5

7.3.1.1 ER1 Reducer V MEK

Following the initial dilution experiments, a commercially available diluent specifically designed to be used with the purchased electroluminescent materials was acquired; it was called ER1 and was 100 % 2-Butoxyethyl acetate (see Figure 7-19).

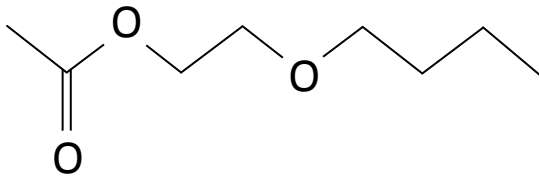


Figure 7-19: The molecular structure of ER1.

It was used to dilute the EL materials and compared with the results produced using the MEK solvent.

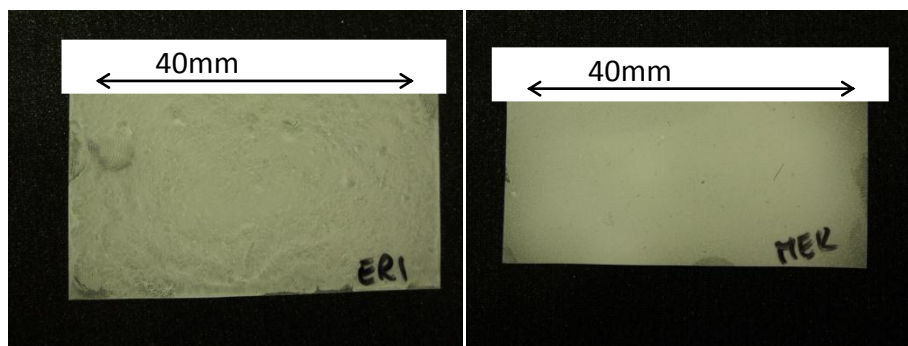


Figure 7-20: The poor coverage of materials when diluted with ER1 compared to the good coverage with MEK.

At the level of dilution required for use in an airbrush, it was found that using ER1 caused materials to dry with a patchy coverage (this can be seen in Figure 7-20) and devices made with these layer materials failed to illuminate when connected to a power source. The technical datasheet supplied with the EL paste materials states that over dilution with reducer could affect its print properties, as it had done here. MEK remained the solvent of choice for the rest of the project.

7.3.2 Layer Build Up

Initially the same four layer structure was used that was developed in section 7.2.3; each electrode extends to opposite sides of the PC substrate plaque, the phosphor

layer covers the area where the electrodes overlap and the dielectric layer covers an area larger than the phosphor to ensure the separation of the two electrodes (a diagram can be seen in Figure 7-10 on page 116). When using this structure with airbrush applied layers, two significant problems were encountered; the dielectric layer cracked when dried and when connected to an AC supply, the Clevios™ PEDOT:PSS layer burned where the teeth of the crocodile clip connected with the material. The dielectric material only cracked where it overlapped the edge of the phosphor layer so this problem was overcome by extending the size of the phosphor area to match that of the dielectric. The new structure can be seen in Figure 7-21.

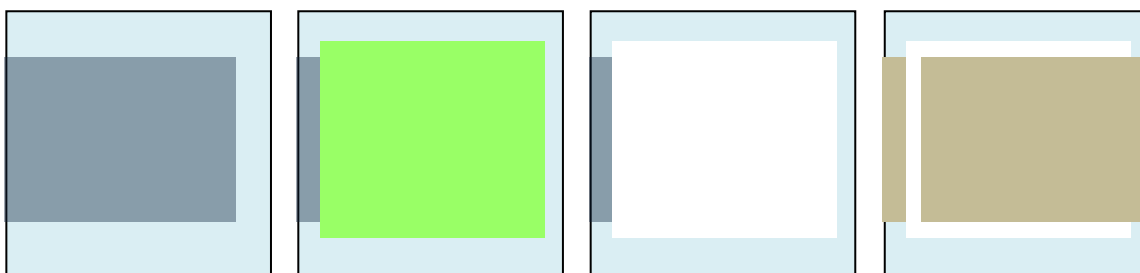


Figure 7-21: The adapted four layer structure; including a larger phosphor layer and a silver bus.

The burning of the Clevios™ at the contact point was most likely caused because the layer applied using the airbrush is much thinner than the paste method, this can be seen from the lighter colour and greater transparency of the layer. A thinner layer would give an overall smaller cross-sectional area at the contact point, resulting in a greater electrical resistance and more heating associated with the resistance, causing burning. Another explanation is that it could be a negative impact of diluting the paste materials to such a high degree. This problem was overcome by adding a silver busbar across the width of the electrode to increase

the contact area with the Clevios™. Although it was determined that this element of the structure was not required using the paste method, it seems it is required when using the airbrush layer application process.

A further problem was found with the diluted dielectric material, a few days after mixing a solid congealed at the bottom of the container; when sprayed the coverage looked complete but upon drying it could be seen that the layer was patchy and uneven. This problem could be overcome; the mixture could be recombined using vigorous mechanical mixing or more simply, small batches of dielectric were mixed as required.

A working device made using the airbrush method can be seen in Figure 7-22.

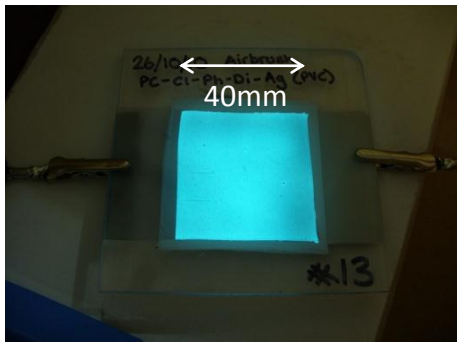


Figure 7-22: A working EL device made using the airbrush application method.

7.4 Airbrush Produced Inserts

Following the success of producing working airbrush devices the next logical step was to produce devices on a thin insert material that can be over moulded – this would determine if the modified materials and thinner structure could withstand the conditions of the injection moulding process and still illuminate when taking on

a 3D, curved profile. Insert substrates can either remain as part of a moulded product or can be removed following moulding; both options were investigated.

The methodology developed during the early insert moulding was adopted, mounting the insert material onto aluminium plates and using re-useable non-adhesive masking templates with the new airbrush application and drying regime. The same three insert materials were tested with the airbrush layer application method; that is LDPE film, PET film and PTFE woven mat. Some PTFE film was also purchased and tested as a smooth alternative to the textured PTFE mat.

7.4.1 LDPE Film

The airbrush materials sprayed evenly onto the PE giving uniform layers on the film; and when moulded produced devices with a smooth surface finish. However, there were flow lines evident in the underlying layers and these became more apparent when illuminated (this can be seen in Figure 7-23).

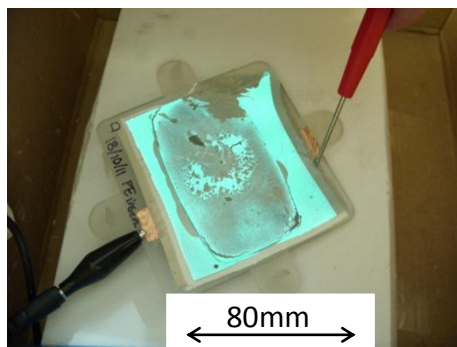


Figure 7-23: An illuminated EL device manufactured using a LDPE insert; flow lines are visible.

As with the initial insert trials using LDPE, devices were sprayed onto oversized pre-heated PE film and cut to size before moulding; although this method worked on some occasions, there were still some random failures when further distortion

occurred when drying individual layers. The use of copper contact points was repeated but this time adhesive copper was used to improve the adhesion to the insert and it also provided the added function of securing the insert into the mould during the cycle. The copper electrical contact point design still had problems; the adhesive copper that overlapped the film remained adhered to the tool during ejection and therefore pulled a section of the insert away from the part, disrupting the layer structure (as shown in Figure 7-24).

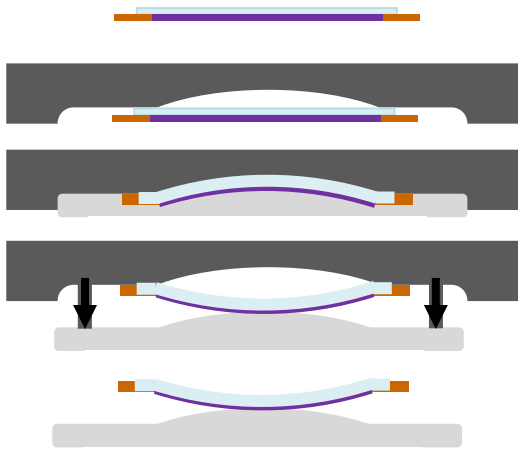


Figure 7-24: A diagram showing how the insert pulled away from the part during ejection. The purple represents the EL layers on the pale blue LDPE with orange copper strips.

To overcome this problem, the copper was then bent around the edge of the film; but during moulding, the force of the injected material often displaced it from the film (as in Figure 7-25).

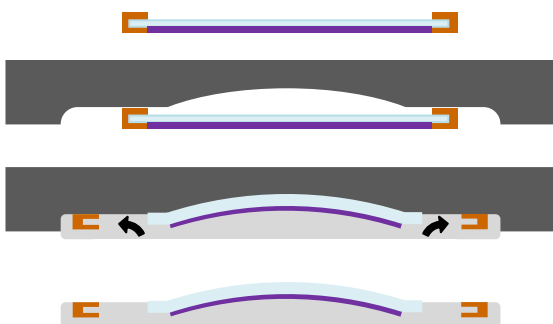


Figure 7-25: A diagram showing the displacement of the copper connectors, separating them from the electrode layers.

Once the connection points had become displaced, the rest of the device was sealed by the PE film and could not be operated. Despite these problems, some PE inserts did mould successfully, however, there are still some problems with the method that need to be overcome:

- The fast drying times provided by the high oven temperatures are not beneficial enough to warrant the number of inserts that fail during manufacture, so a cooler, longer drying time will be used.
- An improved method of providing electrical connection points will also need to be developed.

7.4.2 PET Film

PET film can be printed onto and is used in a number of laminate structures; these qualities suggest that this is an appropriate material to use in this process where a multi-layer structure is made by airbrushing layer materials onto an insert film and then injection moulding of the insert. The Clevios™ transparent electrode material used in this project also readily adheres to polyesters.

Upon moulding it was clear that the thickness and stiffness of the PET film caused significant creases over the 3D curve of the part, the PET film did not bond to the PP and separated (along with the Clevios™) from the rest of the part; this can be seen in Figure 7-26.

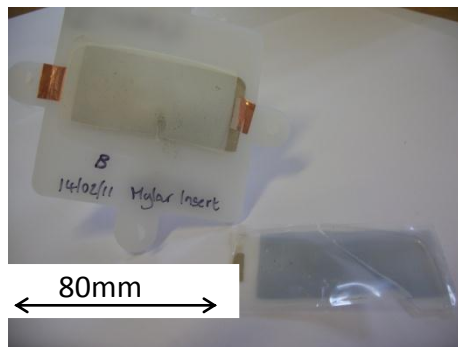


Figure 7-26: The PET film and Clevios™ did not adhere to the part.

The lack of adhesion to the PP substrate, the thickness of the material and the separation that occurred between the EL layer materials were all problematic. These problems could be overcome by using a much thinner and more flexible PET insert film and a PET injected substrate; but since LDPE film and PP substrate were both readily available and also produced an encapsulated device, this was the option that was continued.

7.4.3 PTFE Coated Woven Sheet

PTFE is a chemically inert, hydrophobic material with a low coefficient of friction which is well known for its non-stick properties. The sheet used here is a very flexible woven mat coated in PTFE. The PTFE coated woven sheet was selected because its non-stick properties make it a suitable choice to use as a carrier film; the EL materials would transfer completely onto the moulded part and not remain on the film when it is removed. The materials applied well to the sheet, forming even coatings and these did not readily peel off when handling the insert.

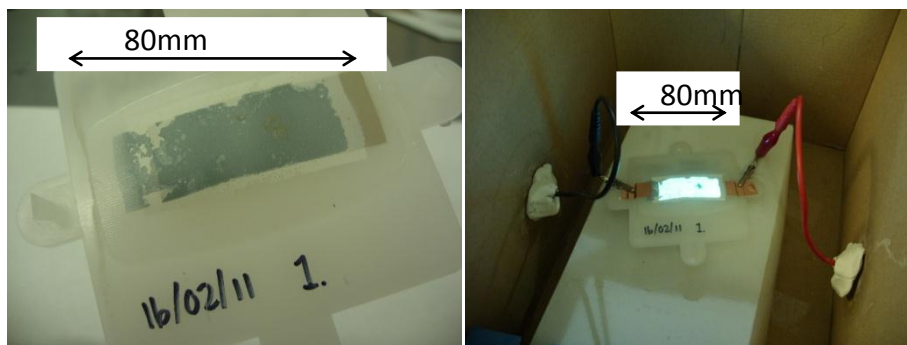


Figure 7-27: An injection moulded EL device made using PTFE coated woven mat inserts.

Upon removal of the insert, some material did pull away from the part but there were enough of the layers intact to make a working EL device (this can be seen in Figure 7-27). However the woven texture of the mat also left an undesirable pattern on the surface of the part. There was some burning of the Clevios™ material where the electrical connection was made with the surface; a copper strip was added to increase the contact area which eliminated the problem. In future, a silver busbar along the length of the transparent electrode will be incorporated into the structure which will remove the need for the later addition of a copper strip.

7.4.4 PTFE Film

Some PTFE film was trialled as an improvement on the PTFE coated woven mat; the film, retains all of the benefits associated with being a non-stick material, however the thin (0.05 mm), flexible film has a very smooth surface finish which will transfer onto the moulded part.

When applying the first layer of material onto the film (the Clevios™ PEDOT:PSS), spraying at a close distance caused an uneven dispersion of the liquid. The non-stick

nature of the film caused the material to pull away leaving uncoated regions (see Figure 7-28), however subsequent layers coated evenly.

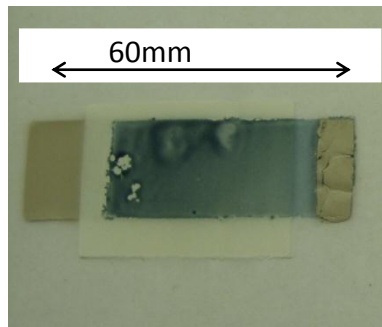


Figure 7-28: If sprayed at a close distance, Clevios™ did not coat the PTFE evenly.

It was found that, when applying the Clevios™ PEDOT:PSS layer, a fine spray over a longer application time gave more uniform material coverage; this was achieved by diluting the material further and by holding the airbrush at a greater distance away from the film surface (15-20 cm).

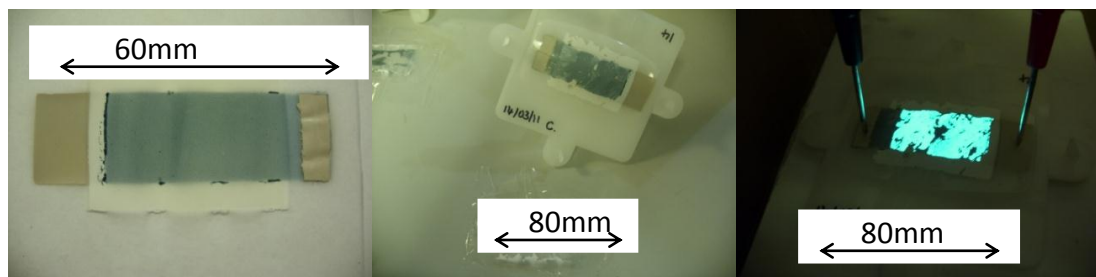


Figure 7-29: A more even coated PTFE insert, after insert moulding and illuminated.

Figure 7-29 shows that working parts were successfully made using a PTFE insert; the surface finish is smoother than when the woven mat was used, however there is still not a complete transfer of material to the part.

7.4.5 Summary

The parts produced using polyethylene inserts do not suffer from the adhesion problems and layer separation that the other insert materials do; this is because the PE remains on the part and bonds to the PP injection substrate. PE also has the benefit of acting as a protective layer encapsulating the electroluminescent materials, and although there are problems associated with providing electrical contact points to the sealed device this is a viable insert material to use in this method. The PET film neither bonded to the part nor transferred all of the layers to the part due to compatibility with Clevios™ and its incompatibility with the PP substrate. It also left crease marks on the part because of the thickness and inflexibility of the film. A complete PET system could work as a solution but both thin flexible PET film and granular PET injection moulding substrate would need to be purchased.

The PTFE woven sheet and PTFE film are insert materials that are designed to act as a medium to transfer the EL materials onto the moulded part and as such are removed following processing. During removal, the poor adhesion between the transparent electrode material and the emissive layer causes the Clevios™, in part, to remain on the insert film. Despite some Clevios™ layer damage, working 3D injection moulded electroluminescent devices were produced using PTFE woven sheet and PTFE film. The PTFE sheet gave the best surface quality of the transferred layers, so this along with PE were both further investigated as insert film options.

7.5 In-mould layer Application

After producing working 3D plastic products with electroluminescent capabilities using pre-prepared airbrushed inserts in the injection moulding process, the next step was to introduce the layers into the mould directly.

The airbrush was used to spray directly in-mould the EL layer structure that is shown in Figure 7-13 on page 119; each of the thin layers was dried before the next was applied; the drying times varied slightly due to variation in layer thickness and mould temperature (the drying regime can be seen in Table 7-7).

Table 7-7: The drying regime when applying the modified materials in-mould using an airbrush.

Material:MEK Mix	In Mould Drying Regime	
	Mould Tool Temperature(°C)	Time (min)
Clevios™	65-70	2-2.5
Phosphor	65-70	1.5-2
Dielectric	65-70	2-2.5
Silver	65-70	1-1.5

The same adhesion and release problems encountered in the initial in-mould trials occurred here but not to such a great extent (see Figure 7-30). Again, there was a burning of the Clevios™ material at the electrical contact point so a silver busbar will have to be incorporated into the structure to avoid this.

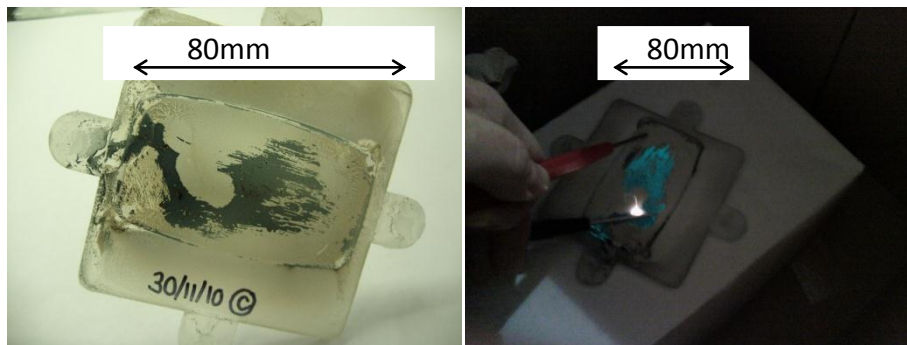


Figure 7-30: EL layer materials on a plastic part made directly in-mould

The next step was to apply individual layer materials sequentially to determine at which boundary the problems occur.

7.5.1 Adhesion between Layer Materials and the Substrate

The EL materials were applied in-mould starting with a single layer and increasing the number of layers each time to determine which interfaces had adhesion problems.

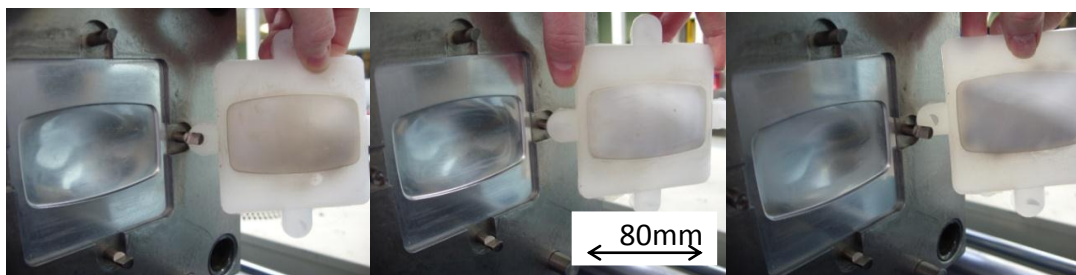


Figure 7-31: The adhesion between layers is investigated. Silver layer only (left), the silver and dielectric layers (centre), and finally the silver, dielectric and phosphor layers (right).

The mould tool was heated to 65 °C to dry the layers; firstly a silver layer was applied and then moulded. The silver material adhered to the PP and released from the mould. Next the dielectric followed by silver was moulded and then phosphor, dielectric and silver. All had no adhesion problems or any material left in the tool (see Figure 7-31).

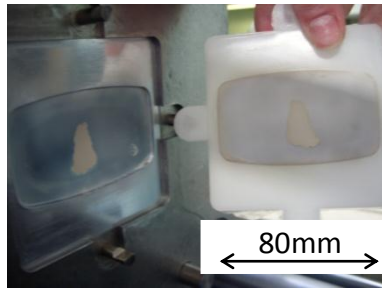


Figure 7-32: Testing the adhesion between layers; silver, dielectric, phosphor and Clevios layers.

Finally, all layers were applied in-mould; Clevios™ was applied followed by the phosphor, dielectric and silver and then moulded. The Clevios™ layer remained in the mould after ejection and separated from the phosphor; some of the other layer materials also separated from the part at the injection point (see Figure 7-32).

Two different options can be tried to overcome the adhesion problem; a different injected polymer could be trialled and a mould release can be used on the tool.

7.5.2 Changing the Injection Substrate Material

Clevios™ PEDOT:SS is recommended to be applied to a PC substrate (as stated in the H C Starck processing guide [148]) so PC was also trialled as the injection material and compared to parts produced using PP. From the samples produced it was apparent that there was no improvement in the adhesion between the layer materials and a PC substrate compared to the PP substrate.

In fact, the higher the number of layers that were moulded over, the less material transferred onto the part (see Figure 7-33).

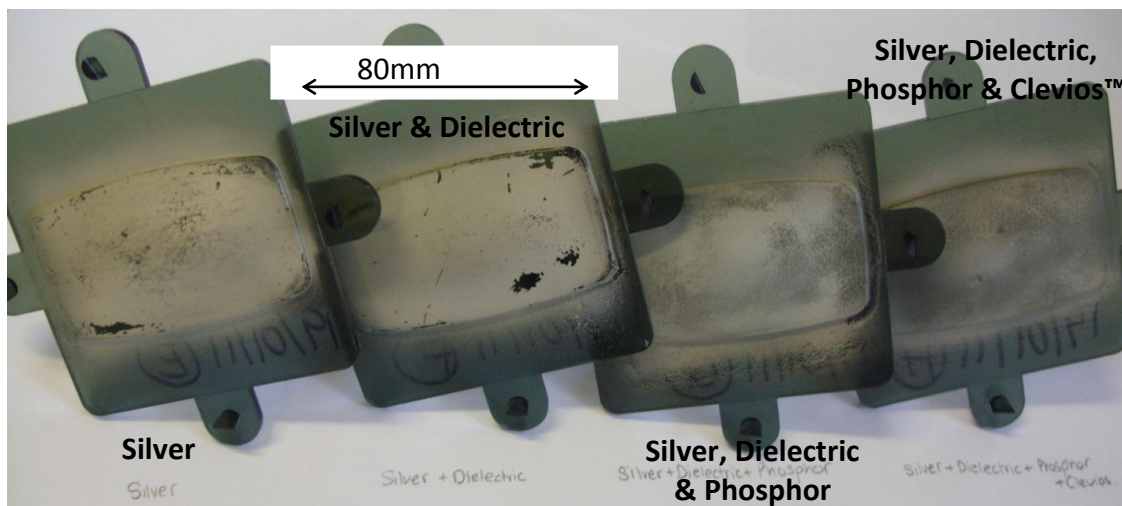


Figure 7-33: Testing the adhesion of layer materials to PC.

However, the material directly adjacent to the substrate is the silver electrode so it may be irrelevant that Clevios™ bonds better to PC; in addition to that, the materials are already in their cured/dried states when the substrate is injected over them. In their solid state they would be less likely to bond to the substrate compared to been applied wet and dried or cured on the surface.

Since PP is cheaper and easier to mould than PC and there appears to be no adhesion benefits to using PC, PP will remain as the substrate materials to be injected.

7.5.3 Mould Release

A number of different mould releases were available in the workshop and were trialled as release options; they were judged by how well the Clevios™ PEDOT:PSS released for the tool (see Table 7-8). Each time the mould release was applied as per the manufacturer instructions and a layer of Clevios™ was sprayed in-mould, onto a tool at 65 °C. The Clevios™ was allowed to dry for 2-3 minutes and then PP

was injected at 220 °C. Finally the mould tool was cleaned in between each test to avoid contamination.

Table 7-8: The results of the mould release trial.

<i>Name</i>	<i>Type</i>	<i>Release Effectiveness</i>	<i>Effect on Surface Finish</i>
Finish Kare #1165	Wax	About 60% of the Clevios™ released	Lines were visible due to uneven coverage of the wax from the sponge applicator
Ambersil PTFE	Spray	No Clevios™ released	N/A
Ambersil Formula 20	Spray	No Clevios™ released	N/A
ACMOS 82-2405	Spray	About 85% of the Clevios™ released (see Figure 7-34)	The surface finish was slightly duller
ACMOS 82-7007	Liquid	No Clevios™ released	N/A

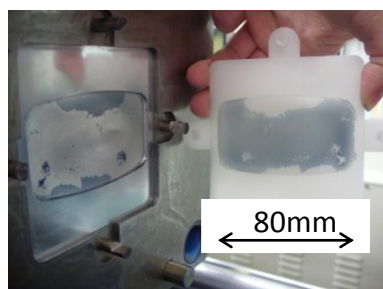


Figure 7-34: The release of Clevios™ from the mould when using ACMOS 82-2405 release spray.

The result of this set of experiments is that ACMOS 82-2405 release spray is the most suitable for preventing Clevios™ from sticking inside the mould tool during the injection moulding process. The ACMOS 82-2405 mould release is a film forming release and is designed for the release of Poly(methylmethacrylate) (PMMA) [151], but it is not immediately obvious why this particular release works the best with PEDOT:PSS.

7.6 Findings from Scoping Experiments

When making devices using the commercially bought paste materials:

- A dielectric layer is required; devices fail at high operating voltages without one, probably due to a short circuit across the electrodes.
- A silver busbar is not required; devices light evenly across the surface (although the illuminating area is only 4 cm x 4 cm) and there is no damage to the transparent electrode material at the electrical connection point.
- Other insulative materials can be used in substitution to the supplied dielectric; an adhesive PVC film was used successfully to produce a standard device structure and a semi-transparent structure where light is emitted from both sides of the device. Both of these devices produced a dimmer light; this is possibly due to a lower electric field produced by an equivalent RMS voltage due to a greater distance between the electrodes (a thicker dielectric layer).
- Shaped illuminated areas can be produced by shaping one of the electrodes or the phosphor layer.
- When applied in-mould, Clevios™ sticks inside the tool cavity.
- There are major adhesion problems between Clevios™ and PP, PC substrates and its neighbouring layer material phosphor. PET should be trialled in future injection moulding tests if it is available.
- Despite some problems, it can be said that the EL materials can withstand the temperatures and pressures of the injection moulding process as working parts have been made using an insert moulding technique.

When applying diluted materials using an airbrush and compressor:

- MEK is a suitable diluent for all of the layer materials; approximately 40 % paste; 60 % MEK mix (by volume) airbrushed well.
- Even layers are achieved and working devices can be made using this material application technique.
- A silver busbar is required to protect the transparent electrode material at the electrical connection point.
- PE inserts can be made and moulded but high drying temperatures destroy many samples and the development of a method of gaining electrical contact to the encapsulated electrode layers is required.
- Further dilution and a large spray distance are required when applying layers onto PTFE film for insert moulding.
- There are still adhesion problems at the phosphor-PEDOT:PSS interface; some transparent electrode is removed with the PTFE after moulding (this should not happen)
- ACMOS 82-2405 spray provides the best release of the transparent electrode from the mould tool when applying materials directly in-mould.

7.6.1 Summary

The work described in this section shows that it is possible to produce an injection moulded part with a working electroluminescent structure on the surface. The PE and PTFE inserts both produce working EL devices but each have issues that need to be addressed in order to produce more reliable parts. The in-mould layer application has also produced parts that have the EL layer structure on the surface

(albeit not complete) and work has been carried out to overcome this problem by improving the release of the electroluminescent materials from the mould tool. The basic method of producing injection moulding EL parts has been developed (both insert and in-mould) but there needs to be considerable refinement of the techniques if the process is to be viable and this will be explored in Chapter 8.

8 PROCESS REFINEMENT EXPERIMENTS

A basic methodology has now been developed to produce injection moulded EL devices using in-mould and insert moulding techniques but both methods have specific problems that need to be addressed and they will be covered in this chapter where each technique will be refined. Each method has benefits and drawbacks associated with it (see Table 8-1) and both can be improved by overcoming similar problems.

Table 8-1: A table showing the pros and cons of each of the developed methods.

	Benefits	Drawbacks
In-Mould Layer Application	<ul style="list-style-type: none"> Truly is a one stage process; no pre- or post-processing required. 	<ul style="list-style-type: none"> Conflict of heating regimes between the layer and injected materials Very long cycle time Separation between PEDOT:PSS and phosphor due to poor adhesion
Insert Moulding	<ul style="list-style-type: none"> Short moulding time achieved by pre-preparing inserts 	<ul style="list-style-type: none"> An additional manufacturing stage is required to make inserts PTFE inserts: Separation between PEDOT:PSS and phosphor due to poor adhesion PE inserts: Problems providing a reliable electrical connections to the electrodes

Problems with the in-mould layer application and PTFE insert moulding both stem from poor adhesion between the PEDOT:PSS and phosphor layers; removal of the insert and ejection from the mould tool causes separation between the PEDOT:PSS and the phosphor.

The insert moulded and in-mould processes have so far used the following basic layer structure:

- A PEDOT:PSS transparent electrode (with a silver busbar),
- A phosphor layer,
- A dielectric layer, and
- A silver rear electrode.

These layers are applied using an airbrush either directly into the injection mould cavity or onto an insert film which is placed in the cavity; the layers are injection moulded onto and the resulting moulded part has a top emitting EL structure in its surface (this is shown in Figure 8-1).

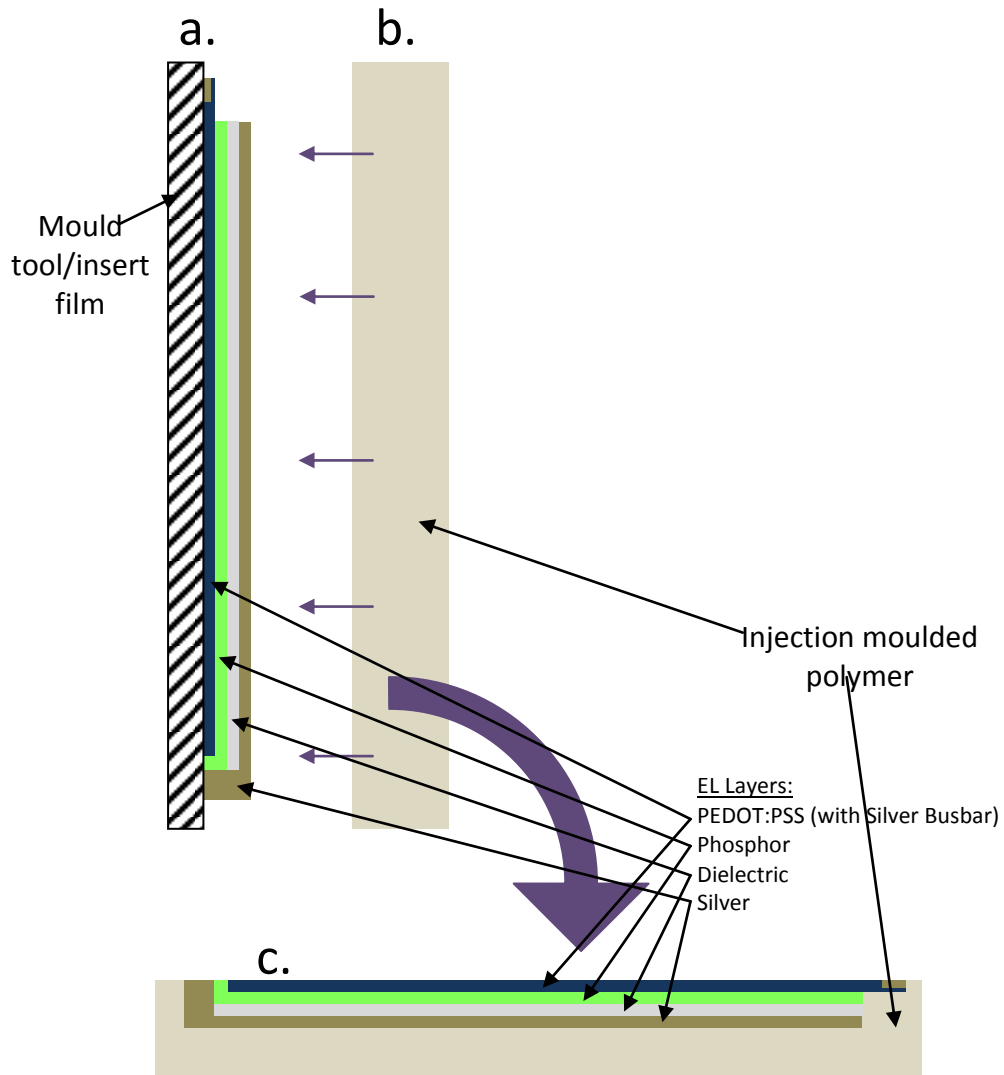


Figure 8-1: A diagram showing the basic process and structure; a. the EL layers are applied to the insert film or the mould tool, b. the layers are injection moulded over & c. once ejected, the injected substrate has the layer structure embedded into its surface.

Two different techniques were trialled as methods to improve the adhesion between the PEDOT:PSS and phosphor layers; the use of more compatible electrode materials and adding an extra layer into the structure (an additional bonding layer in-between the two incompatible layers). Improving the adhesion between the PEDOT:PSS and phosphor layers would improve both the in-mould and PTFE insert moulding technique.

8.1.1 Using Different PEDOT:PSS Brands

The transparent electrode material used in the EL structure is PEDOT:PSS conductive polymer; the brand used so far (that has separated from the phosphor layer) is H C Starck's Clevios™ S V3. Two further brands of PEDOT:PSS were purchased; Orgacon™ from AGFA(with an adhesion improver) and ITO-R from Electra Polymers (the supplier of the phosphor, dielectric and silver pastes).

Comparing the molecular structure of the components of each PEDOT:PSS brands and the phosphor material may give an indication as to which is likely to give the best adhesion. The MSDS provided by Electra Polymers [152] shows the predominant chemical component (30-60 %) in the phosphor layer material is 2-(2-Ethoxyethoxy)ethyl acetate; the structure of which is shown in Figure 8-2:

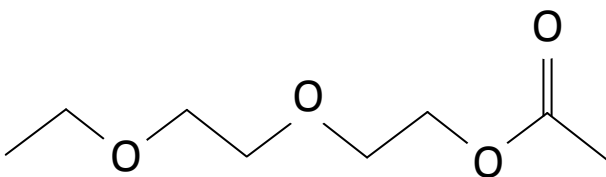
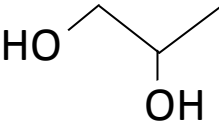
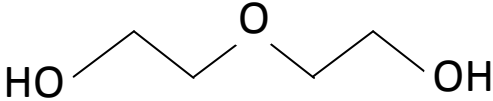


Figure 8-2: The structure of 2-(2-Ethoxyethoxy)ethyl acetate, the component materials which makes up 30-60% of the phosphor layer.

The chemical composition and structure of the three different transparent electrode materials are given in Table 8-2 to Table 8-4; in each table PEDOT:PSS has not been included as this is common in all three materials and makes up just a small percentage of the overall material (1.1 % in Clevios™, 1-5 % in ITO-R and the value was not given for Orgacon™). If required, the structure can be seen in Table 7-5 on page 126. The names of the components shown in the table are the names given on the suppliers MSDS; these are not always the IUPAC name and in some cases there

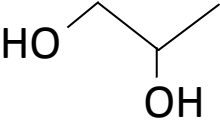
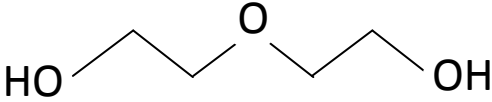
are a number of different names for the same compound. The structure of the component chemicals in Clevios are given in Table 8-2.

Table 8-2: The molecular structure of the component chemicals in Clevios.

Component Chemical	Percentage by Weight (%)	Chemical Structure
Propane-1,2-diol	65.6	
2,2'-Oxydiethanol	15	

The indium tin oxide replacement (ITO-R) supplied by Electra Polymers was selected based on the compatibility with their other electroluminescent materials, as stated in the data sheet. The molecular structures of the components of ITO-R are given in Table 8-3.

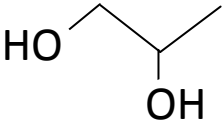
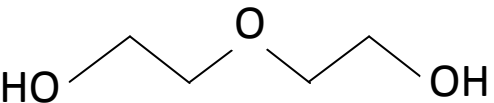
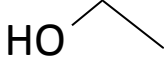
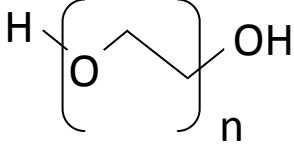
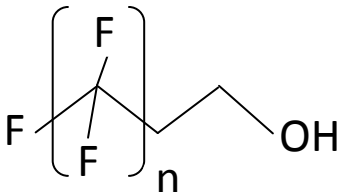
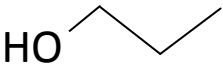
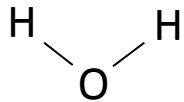
Table 8-3: The molecular structure of the component chemicals in ITO-R.

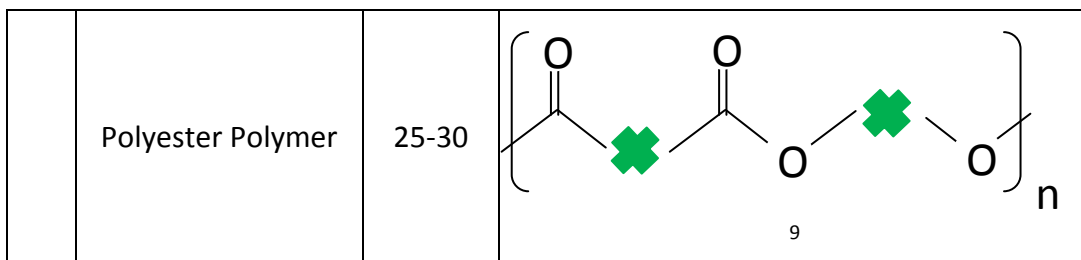
Component Chemical	Percentage by Weight (%)	Chemical Structure
Propane-1,2-diol	60-100	
2,2'-Oxybis ethanol	10-30	

It was identified that Clevios™ S V3 and ITO-R have the same component solvents in them, albeit in a different proportion and different versions of the name are stated in each MSDS.

Orgacon™ supplied by AGFA Materials was selected because an adhesion improver could also be purchased and mixed with it. The structure of the component materials of both Orgacon™ and its adhesion improver are given in Table 8-4.

Table 8-4: The molecular structure of the component chemicals in Orgacon and its adhesion improver.

	Component Chemical	% by Weight	Chemical Structure
Orgacon™	Propylene Glycol	60-80	
	Diethylene Glycol	5-10	
	Ethanol	1-5	
	Poly(oxy-1,2-ethanediyl), α -hydro-, ω -hydroxy-, ether WITH Poly(difluoromethylene), α -fluoro, ω -(2-hydroxyethyl) (1:1)	0.1-0.5	 
Adhesion Improver	Propan-1-ol	1-3	
	Water	60-80	



Once again Orgacon™ has two of the same solvents as the other two brands of PEDOT:PSS (again in a different amount and a different name); however, it also has a small amount of a blend including a highly polar fluoro-polymer. When mixed with the adhesion improver, is the most chemically compatible PEDOT:PSS brand to the phosphor; this is mainly due to the presence of the CO=O present in the polyester.

Each of the PEDOT:PSS brands were diluted with MEK and applied using an airbrush in adhesions tests to determine which was the most suitable to use when producing injection moulded EL devices.

8.1.2 Intermediate Bonding Layer

In addition to testing alternative PEDOT:PSS brands, the use of a bonding layer will also be investigated. It is important that the material used as the bonding layer does not disrupt the electroluminescent mechanism; it would be useless to produce a well adhered part if it does not light up.

The material trialled as the intermediary layer between the PEDOT:PSS and the phosphor materials was a mixture of the two materials. Three different ratios were tested; 1:4 (A), 1:1 (B) and 4:1(C) (the ratios given are volume of diluted PEDOT:PSS

⁹ Since the exact polyester was not given, the structure of a generic polyester has been shown for visualisation of the functional groups; the green crosses represent any section of polymer chain.

to the volume of diluted phosphor). The miscibility, drying time, transparency and adhesion to adjacent layers are all important factors when considering if this mixture and in what ratio is suitable for use in the EL devices; but more importantly the inclusion of a bonding layer must still produce a working device.

Figure 8-3 shows the bonding layers against light and dark backgrounds respectively; it can be seen that from A to C the mixtures are darker in colour but more transparent. The layers sprayed evenly and were dried at 130 °C in 3 minutes.

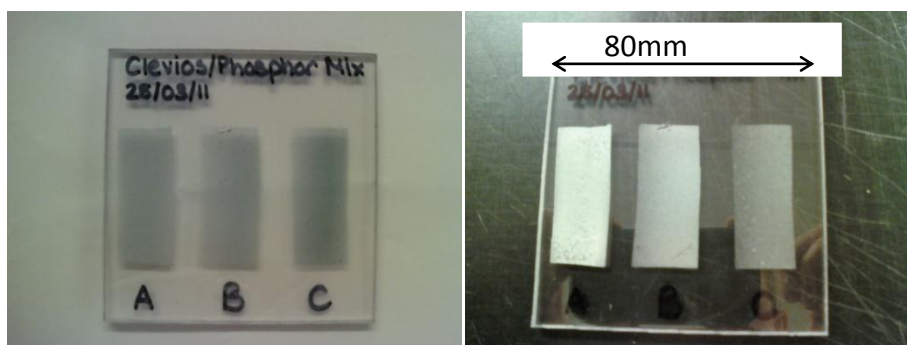


Figure 8-3: The three ratios of bonding layer (made using the Clevios PEDOT:PSS) shown against light and dark backgrounds.

Electroluminescent devices were produced using all three different mix ratios (A, B and C) along with a device with no bonding layer (D) for comparison; these can be seen in Figure 8-4. These tests highlighted one possible problem when using an additional bonding layer; some of the mixtures did not mix completely homogeneously and this had implications in the appearance of the device and caused blockages in the airbrush. This is discussed further in section 8.1.4.

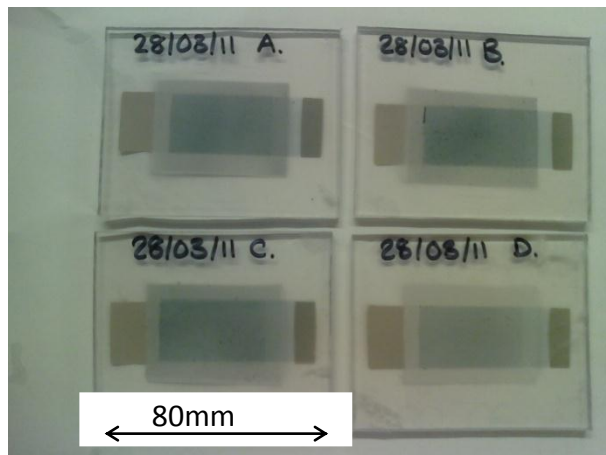


Figure 8-4: EL devices made using an additional bonding layer in between the PEDOT:PSS and phosphor. The ratios of PEDOT:PSS to phosphor are A (1:4), B (1:1), and C (4:1); D has no bonding layer.

The devices made all illuminated successfully (an example can be seen in Figure 8-5); this shows that including a PEDOT:PSS-Phosphor mix bonding layer in the structure is a viable route to follow so this option will also be used in the adhesion tests.

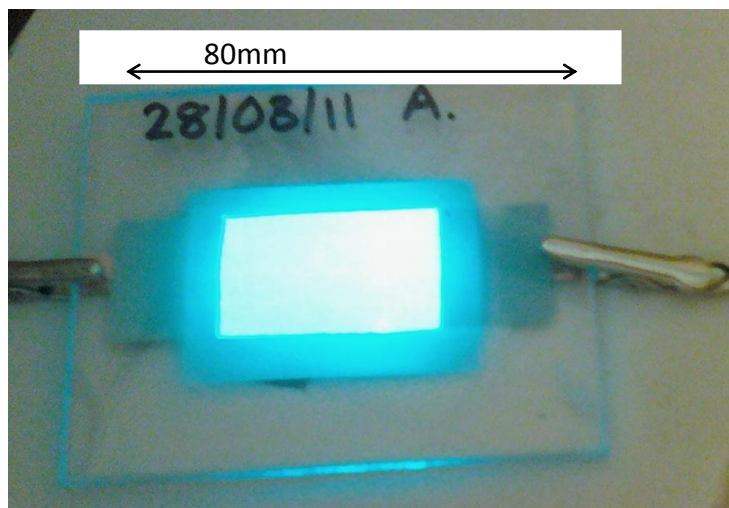


Figure 8-5: A working EL device made with an additional bonding layer in between the PEDOT:PSS and phosphor.

Adhesion tests were then carried out investigating both the use of different PEDOT:PSS brands and the addition of a bonding layer (using each transparent electrode material); the aim of these tests was to quantify the adhesion to determine the best combination to use in the injection moulding process.

8.1.3 Adhesion Tests

Since the problems experienced during in-mould layer application and insert moulding are due to poor adhesion between the transparent electrode and the emissive layer, a set of experiments were designed to determine the layer combination with the best adhesion by varying the electrode material and use of a bonding layer.

An experimental plan was designed to compare the adhesion of different layer combinations; three transparent electrode materials (ITO-R, Orgacon™ and Clevios™) and four bonding layer options (1:4, 1:1, 4:1 electrode-phosphor mixes and no bonding layer) were considered. Each bonding layer option was replicated with each electrode material (giving 12 different permutations) and repeated 3 times (totalling 36 test samples).

Since the layers to be tested were thin (in the region of 10's of microns) and the forces required to separate them were small, a peel test was deemed unsuitable. It was decided that a cross cut adhesion test would be the most suitable in this situation. Layers would be applied using an airbrush, a 10 x 10 grid is scored into the surface and then an adhesive tape is applied and removed; this test is defined in ISO 2409 [153].

Counting adhered squares would provide a percentage adhesion result and a comparison between samples could be made. The only layers to be applied in the tests were the transparent electrode, the phosphor and the bonding layer (where appropriate); this was because during experimentation there were no adhesion problems at the silver-dielectric and dielectric-phosphor boundaries. Since only the PEDOT:PSS-phosphor interface is of interest, test can be carried out on any suitable substrate material.

8.1.3.1 Cross Cut Test 1

The layers were applied to a polycarbonate substrate as this is compatible with the EL materials and the same material that was used to make the traditional, thick layer and airbrush devices; this differs from the injected substrate material but the important measurement in this test was solely the adhesion between the PEDOT:PSS and the phosphor so it was irrelevant what substrate material the layers are mounted on. In order to match the adhesion test as closely as possible to the method used during experimentation, the EL materials were applied in the same order as both the in-mould method and insert production; first the PEDOT:PSS transparent electrode, then the bonding layer and phosphor respectively (see Figure 8-6). This was done because any curing/drying that occurs during the process may affect adhesion so the drying sequence was replicated exactly.

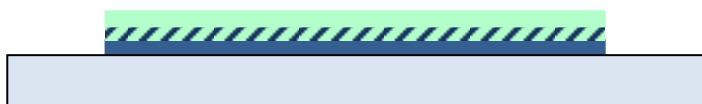


Figure 8-6: A diagram showing the sequence of layer application in cross cut test 1; PEDOT:PSS, bonding layer (where applicable), then phosphor.

One set of samples were made (using the Clevios™ brand of PEDOT:PSS) and testing began; the sample was scored and the tape applied and removed. Despite the fact that this was a layer combination (Clevios™ and no bonding layer) that separated during experimentation there was 100 % adhesion in this test (the sample is shown in Figure 8-7). Two other samples of the same combination were tested but they both had 100% adhesion, it was clear the test was not valid.

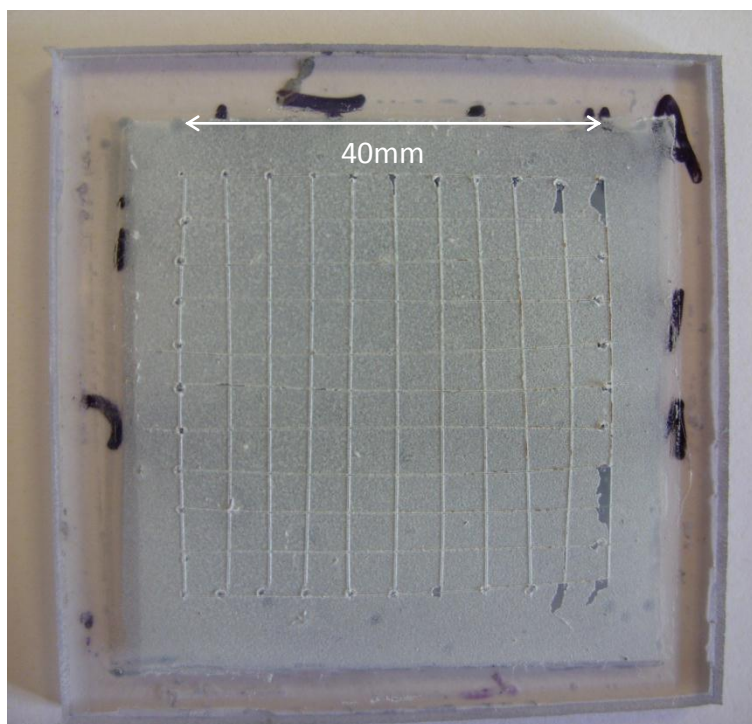


Figure 8-7: A Clevios™/no bonding layer/phosphor sample showing almost 100% adhesion in cross cut test 1.

In order to improve the adhesion test some modifications to the method were made. Since the ejection and insert removal normally occurs when the sample is still relatively hot, following production, the samples were all scored then heated in an oven to 130°C (temp. of part approx. 30s after injection). The adhesive tape was

added and removed while still hot but the result was the same, 100 % adhesion was achieved between materials that do not adhere in-mould. The test was redesigned.

8.1.3.2 Cross Cut Test 2

After further consideration it was decided to perform the same cross-cut test (The ISO 2409 [153]) but with the layers applied in the reverse order; first the phosphor, then the bonding layer and the transparent electrode respectively (see Figure 8-8). This was justified because during ejection and insert removal, the transparent electrode is the outermost layer, so this was replicated in this adhesion test.

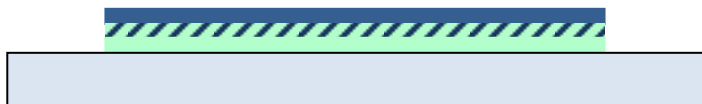


Figure 8-8: A diagram showing the sequence of layer application in cross cut test 2: phosphor, bonding layer (where applicable), then PEDOT:PSS.

As in cross-cut test 1, a layer combination that separated during experimentation (Clevios™ transparent electrode and no bonding layer) remained 100 % adhered after the tape was removed (as seen in Figure 8-9); again this meant that the test was not valid.

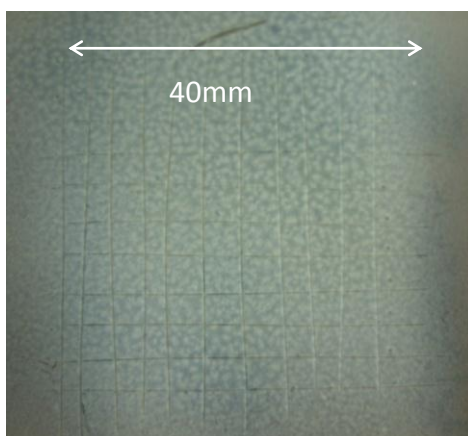


Figure 8-9: A Clevios™/no bonding layer/phosphor sample showing 100% adhesion in cross cut test 2.

Even incorporating similar heat conditions the devices undergo during part ejection and insert removal, the test samples are not adequately imitating the process conditions of the entire process occurring during experimentation. Other factors such as temperatures, pressures and shear forces that occur during injection moulding must be affecting the adhesion between the transparent electrode and the phosphor, and these need to be considered when designing an adhesion test.

The ISO 2409 [153] cross cut test was clearly unsuitable and a new (non-standard) test was designed. A test was needed that incorporates injection moulding conditions but retains the variable combinations and the easily measured percentage adhesion result.

8.1.3.3 Insert Moulded Cross Cut Test

Initial thoughts to improve the adhesion test were to transfer the cross cut test in-mould, but there would be problems when scoring the layers with the 10x10 grid; either the mould tool could be damaged if the test was performed directly in-mould or the substrate film could be perforated if an insert moulding method was used.

The problem associated with scoring the grid was overcome by using a masking template producing a 10 x 10 matrix of squares when applying the transparent electrode layer (see Figure 8-10); this provides the one hundred square grid that will allow for an easy percentage measurement/quantification of adhesion. The use of a template limits the test to using an insert as the template does not follow the contour of the mould tool so a PTFE film insert method was used.

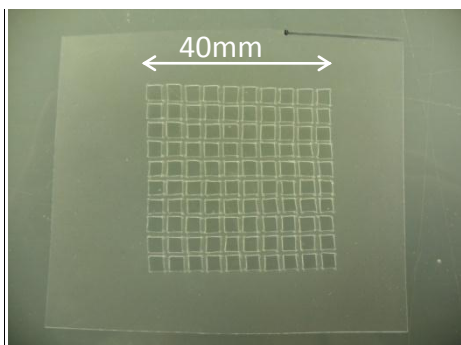


Figure 8-10: The 10x10 masking template grid used when making the inserts for the in-mould cross cut test.

The layer order was the same as if a working device was being produced (first the grid patterned PEDOT:PSS electrode, then the bonding layer (where applicable) and the phosphor respectively).

It was soon clear that this method of testing is also not valid. Figure 8-11 shows a test that again measures 100 % adhesion between Clevios™ PEDOT:PSS and the phosphor (no bonding layer); once again, this differs greatly to the adhesion achieved in-mould during experimentation.

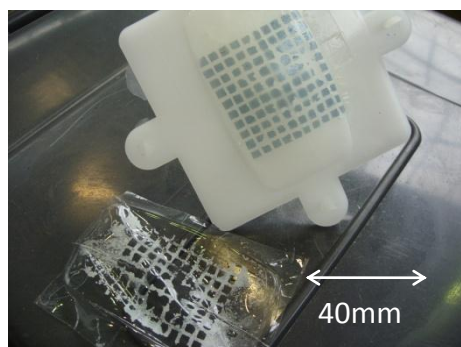


Figure 8-11: Clevios™/no bonding layer/phosphor showing almost 100% adhesion in the insert mould cross cut test.

Since none of the methods used so far have adequately recreated the conditions when applying the materials in-mould, independent cross-cut adhesion tests will be

terminated, and an alternative method of measuring the best layer adhesion will be used.

8.1.3.4 In-mould Adhesion Observations

The adhesion problem still remains and since none of the cross cut tests adequately recreate the conditions that occur in-mould, the solution must be to manufacture full structure devices in-situ and compare the resulting layer adhesion. Full structure devices (PEDOT:PSS, phosphor, dielectric and silver layers) were applied in-mould onto a 65 °C tool using an airbrush and moulded over using PP at 220 °C; the ACMOS release spray was used in each case as it had already been established that this significantly improves the release of the PEDOT:PSS from the tool. Each transparent electrode material was used both with and without a 1:1 (PEDOT:PSS phosphor mix) bonding layer; further bonding layer ratios could be tested if the presence of a bonding layer shows a significant improvement to adhesion. To quantify the adhesion, a 20 x 10 grid was drawn onto a transparent film, this was placed over the moulded part and size of the successfully adhered area was visually measured; this can be seen in Figure 8-12.

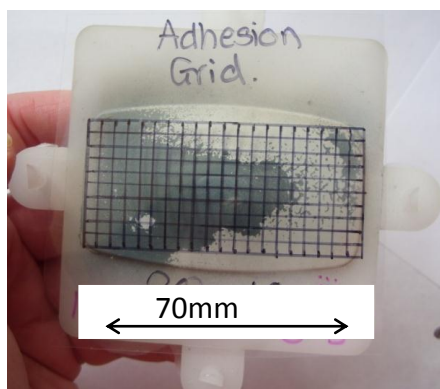


Figure 8-12: A moulded part and the grid used to measure adhesion; this part was moulded with ITO-R PEDOT:PSS and a bonding layer.

Measurements were made for all PEDOT:PSS and bonding layer options and combined with other observations to analyse the effectiveness of the adhesion improvement ideas.

8.1.4 Solution to Adhesion Problems

Adhesion measurements were taken from 18 moulded samples; the 3 different PEDOT:PSS brands were moulded both with and without (1:1) bonding layers and repeated 3 times. The results can be seen in Table 8-5.

Table 8-5: The results of the in-mould adhesion observations.

		Variables						
		PEDOT:PSS →	Clevios™ S V3		ITO-R		Orgacon™ (with adhesion improver)	
		Bonding Layer →	None	50:50 Mix	None	50:50 Mix	None	50:50 Mix
Sample Number	i	Adhered Squares Number Count	56	169	154	172	200	199
		% Adhesion	28.0	84.5	77.0	86.0	100.0	99.5
	ii	Adhered Squares Number Count	176	200	58	73	200	197
		% Adhesion	88.0	100.0	29.0	36.5	100.0	98.5
	iii	Adhered Squares Number Count	161	119	61	115	187	191
		% Adhesion	80.5	59.5	30.5	57.5	93.5	95.5
AV	Adhered Squares Number Count	131	163	91	120	196	196	
	% Adhesion	65.5	81.3	45.5	60.0	97.8	97.8	

From Table 8-5 it is clear to see that Orgacon™ (with adhesion improver) provides the best adhesion for in-mould layer application, and although the presence of a bonding layer is beneficial when used in combination with the other PEDOT:PSS brands, it is not necessarily required with Orgacon™. The adhesion results, along with how well the materials mix with both the solvent and the phosphor, were used to score each PEDOT:PSS brand to determine the best option to use. The results are shown in Table 8-6.

Table 8-6: The overall results for the best PEDOT:PSS material to use in-mould.

Scoring Categories¹⁰	Clevios™	ITO-R	Orgacon™
Adhesion	3	2	5
Dilution with MEK	3	4	5
Miscibility in Bonding Layer	2	3	0
Total	8	9	10

The scores were objectively decided by the author; the adhesion scores were based on the adhesion test results from Table 8-5, and the dilution scores were based on the quality of the mixtures made with MEK and the phosphor material.

When diluting with MEK, both Orgacon™ and ITO-R mixed more homogeneously than Clevios™. Orgacon™ scored highest and this is explained by the condition in which the materials are supplied; Orgacon™ is supplied as a smooth, homogeneous

¹⁰ A 0-5 score was given in three categories; MEK dilution, bonding layer miscibility and adhesion. 0=Very Poor, 1=Poor, 2=Adequate, 3=Good, 4=Very Good, and 5=Excellent

thick liquid but Clevios™ and ITO-R are both thick, granular pastes. When diluted, Orgacon™ was the only material that completely mixed, with no remaining solid granules; the quality of the MEK mix also had an impact on the quality of the bonding layer mix. The granules present in both the ITO-R and Clevios™ MEK mixes remained in the bonding layer mixes; with the Clevios™ to a much greater degree than the ITO-R. Although there were no PEDOT:PSS granules in the Orgacon™ mix, it was clear that it was completely immiscible with the phosphor carrier polymer; this can be seen in Figure 8-13.



Figure 8-13: The phosphor carrier polymer remains completely separate in the Orgacon™-phosphor bonding layer mixture.

Table 8-6 shows that Orgacon™ has achieved the highest possible scores in both the adhesion and MEK dilution categories; although it cannot mix with phosphor to form a bonding layer, the results in Table 8-5 show that in the case of Orgacon™ the presence of a bonding layer provides no improvement to adhesion. This analysis indicates that Orgacon™ was the best PEDOT:PSS material to use in-mould and therefore was used for all remaining experiments.

8.2 Improvements to PE Insert Production

In order to improve the number of successful parts made using a PE inserts, two different issues needed to be dealt with; the layer drying temperature needed to be reduced and an improved method of providing electrical contact points needed developing.

Since the shrinkage occurring at 130 °C is unpredictable and renders some samples unusable the layer materials will be dried for a longer period of time at a cooler temperature. 100 °C was trialed and although the PE did not pull away and break at the edges, significant distortion still occurred making it difficult to apply subsequent layers. At 80 °C (which is the lowest cure temperature for PEDOT:PSS) there was a little rippling of the film caused by the expansion of the material at elevated temperatures but this diminished upon cooling. The new drying conditions for applying layer materials onto a PE film are given in Table 8-7.

Table 8-7: Drying temperatures and times used when manufacturing PE inserts.

Material: MEK Mix	PE Insert Drying Regime	
	Oven Temperature (°C)	Time (min)
PEDOT:PSS	80	10
Phosphor	80	5
Dielectric	80	8
Silver	80	5

Although the new drying conditions significantly increase the insert manufacture time, the benefit of having a minimal number of failures due to material warpage

outweighs the increased processing time (this could also be offset by manufacturing more inserts simultaneously).

The next step was to improve the design of the electrical contact points; during moulding these need to remain connected to the electrode layers and be accessible outside of the sealed EL structure.

This has been achieved using a technique shown in Figure 8-14. Firstly the PE insert is cut to size (Figure 8-14a). Then two holes were cut into the PE film (b) and small adhesive copper strips were added to one side of the PE film (c). The EL layer structure is then applied onto the other side of the film ensuring the two electrode layers make contact (through the holes in the PE) with the separate copper connection points; the PEDOT:PSS layer is applied (d) followed by the phosphor (e), dielectric (f) and silver (g). Each layer is dried using the heating regime specified in Table 8-7. When the film is over moulded, the EL layers are sealed to the part by the PE film and the copper strips are on the outer surface to allow easy connection to an electrical supply (seen in (h)).

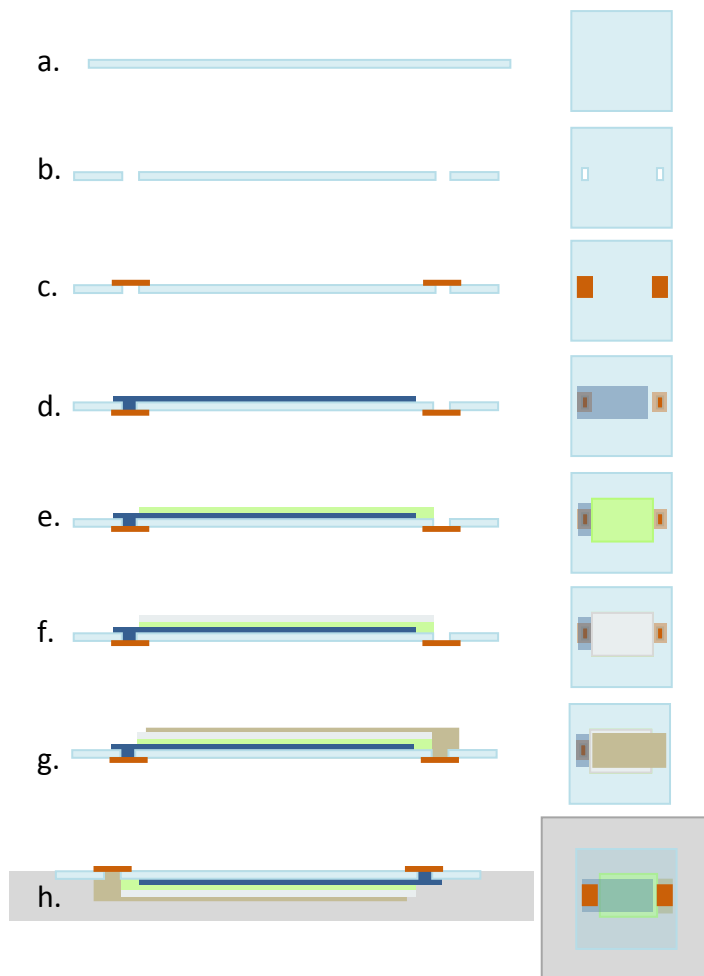


Figure 8-14: The production of injection moulded EL parts using PE inserts.

These inserts moulded well and produced working EL parts (shown in Figure 8-15); this option is a neat, easy to produce, repeatable solution to the electrical connection problem.

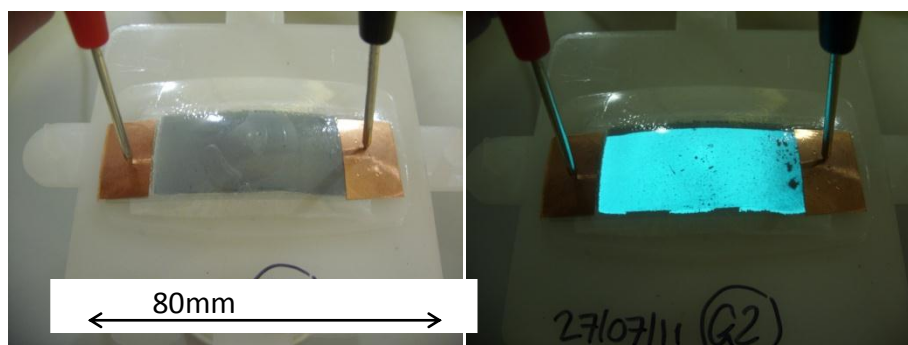


Figure 8-15: Working injection moulded EL devices fabricated using PE insert moulding.

8.3 Implementation of the Optimised Processes

The optimal structure, material selection and process refinements were then used to produce 3D moulded parts by both in-mould application and insert moulding. The layer structure used was PEDOT:PSS, followed by phosphor, dielectric and finally silver.

8.3.1 In-Mould Layer Application

Templates have been used throughout this project to apply layer materials to the required areas; especially to ensure that there is no contact between the two electrode layers. Thin, flat templates have been used so far however since the inside of the mould tool is contoured this type of template will not sufficiently mask off areas, allowing material to seep under it. To overcome this problem, parts were moulded and templates cut from the moulded parts; these templates then fit tightly into the mould tool and effectively mask off the appropriate areas (an example of a template in the mould is shown in Figure 8-16).

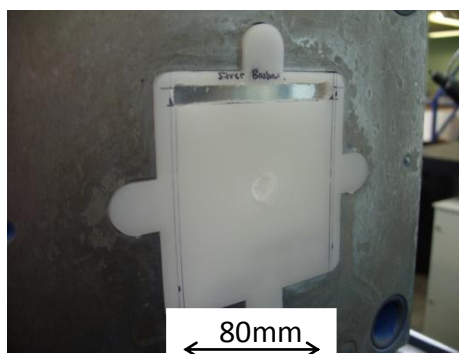


Figure 8-16: A moulded part cut into a silver busbar masking template.

Two sets of templates were made; one to produce a small device over the shallow curve of the part and one set that produces a large device that covers a majority of

the surface of the moulded part, (extending over the sharp edges of the central shape). These templates are shown in Figure 8-17.



Figure 8-17: Masking templates made from moulded parts: left, to make a small device & right, to make a large device.

Figure 8-18 shows the build-up of the layer structure of the small device within the mould tool; the mould tool was heated to approximately 65 °C and each layer was allowed to dry before the next layer was applied. The drying times (which had previously been determined through experimental work) for the Orgacon™ was 2 minutes, the phosphor was 1.5 minutes, the dielectric layer was 2 minutes and the silver dried in 1 minute. After all layers had been applied and dried, PP was injected at 220 °C; the ejected part is shown in Figure 8-19.



Figure 8-18: The in-mould layer application sequence. Left to right; silver bus, Orgacon™ PEDOT:PSS, phosphor, dielectric and silver.

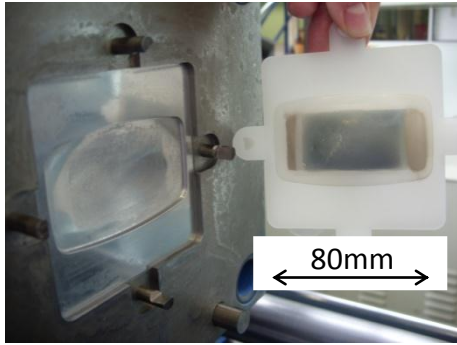


Figure 8-19: An injection moulded EL part made by applying EL materials directly in-mould.

In Figure 8-19 a residue can be seen in the mould tool after ejection, however this appears to be the mould release rather than any of the EL materials; this is explained by the fact that the mould release is described as a film forming medium.

The part ejected with intact layers and successfully illuminated when connected to an AC supply. The illuminated part can be seen in Figure 8-20 from above and a side view shows the curve over which the device covers.

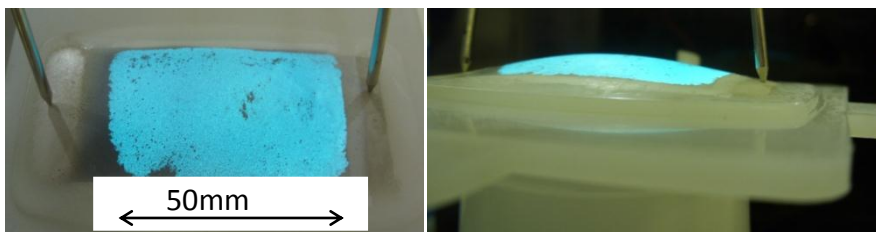


Figure 8-20: An illuminated in-mould EL part seen from the top and side.

The large device was constructed in the same way but with the larger templates; although the part ejected with 100 % layer adhesion, there had been some disruption to the layers during injection. There was a discontinuation along the

layers and due to this the device did not illuminate when connected to an AC source; this can be seen in Figure 8-21.

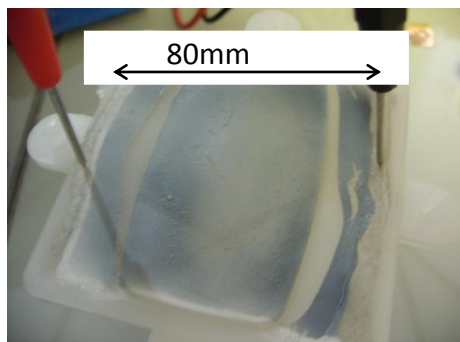


Figure 8-21: Disruption to layer materials can be seen when moulded over sharp edges.

8.3.2 Insert Moulding

The PEDOT:PSS brand determined to have the best adhesion was Orgacon™ with the adhesion improver. Working insert moulded devices had already been made using the original PEDOT:PSS brand (Clevios™) however in order to carry out fair comparisons all devices should be made using the same PEDOT:PSS brand. However, when inserts were made using the Orgacon™ PEDOT:PSS, the inserts failed to illuminate. Upon closer inspection it could be seen that when the phosphor layer dries, shrinkage occurs; this pulls on the Orgacon™ layer below and causes a fracture across the PEDOT:PSS electrode. This was not seen to happen with the other brands of PEDOT:PSS so ITO-R was selected to be used, since this diluted more homogeneously with MEK.

8.3.2.1 PE Encapsulating Film

PE inserts were made using the ITO-R transparent electrode, the new drying regime (Table 8-7 on page 167) and the new external copper connections; small and large layer structures were made to cover different geometries of the tool.

Figure 8-22 shows the small device insert moulded and working; it illuminated evenly and had a good finish; this size of insert is moulded over a shallow curve.

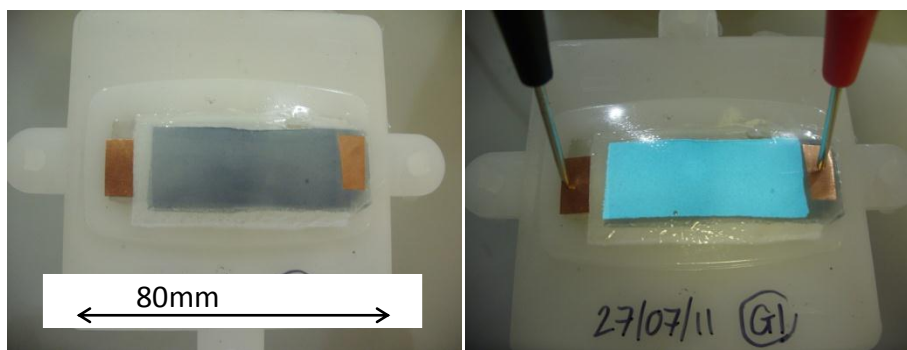


Figure 8-22: A PE insert moulded EL device, both off (left) and on (right).

The large device insert appeared to have moulded well (Figure 8-23) but it failed to illuminate when connected to a power supply. A number were moulded but all failed to illuminate; these layers extended over both the shallow curve and sharper edges. There are clearly geometric curvature limitations to this process. Large devices on PE inserts have produced working parts before (Figure 7-23 on page 133) when moulded over the sharper edges (albeit with significant flow lines), so further investigation would be needed to make the process more consistent when moulding over more extreme contours.

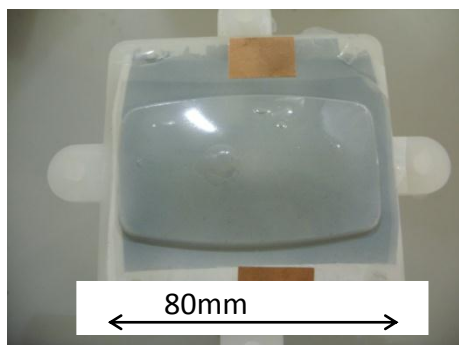


Figure 8-23: A PE insert moulded EL device that extends over sharp edges; it failed to illuminate.

8.3.2.2 PTFE Carrier Film

Inserts were also made on PTFE film; silver bus bars were applied along the length of one side of the ITO-R which increased the area of the electrical contact to the transparent electrode. The layers were dried at the higher temperature of 130 °C, using the drying temperature shown in Table 8-8.

Table 8-8: The drying regime used when producing EL inserts on PTFE film.

Material:MEK Mix	PTFE Insert Drying Regime	
	Oven Temperature (°C)	Time (min)
PEDOT:PSS	130	4
Phosphor	130	2
Dielectric	130	2.5
Silver	130	1.5

The inserts (with both large and small devices) moulded well, all of the transparent electrode transferred onto the part giving a smooth surface finish and illuminated evenly as shown in Figure 8-24 and Figure 8-25.

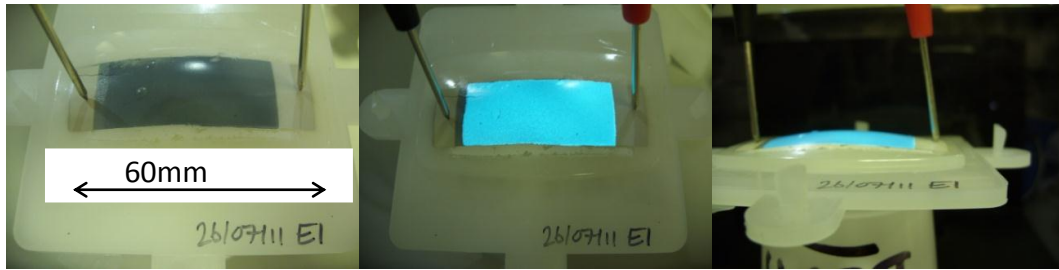


Figure 8-24: The small PTFE insert moulded device; off (left), on viewed from above (centre) and on viewed from the side (right).

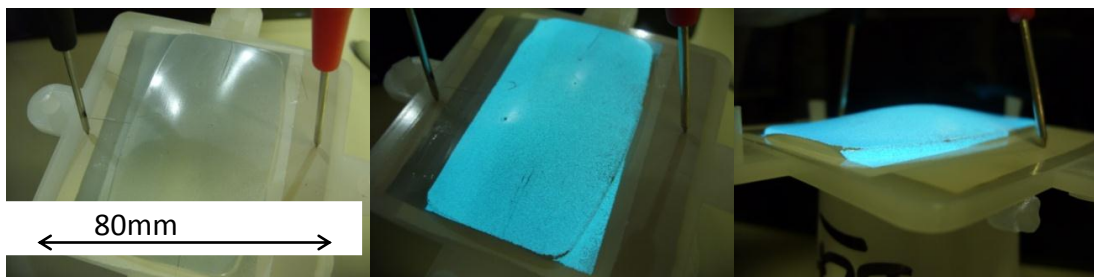


Figure 8-25: The large PTFE insert moulded device; off (left), on viewed from above (centre) and on viewed from the side (right).

The larger devices again extended over the more acute angles at the edge of the central moulded shape and despite some slight layer fractures in sections where the insert is stretched over a corner, the device works as intended.

The large device also showed slight surface defects where the PTFE film had creased when moulded over but these were less apparent when illuminated.

8.4 Post Mould Layer Application

As well as producing injection moulded 3D EL parts by applying layers within the mould during processing, an alternative post production method using the airbrush spraying technique was investigated. The feasibility of spraying materials onto pre-manufactured plastic parts was studied; this differs from current retrospective

addition of EL capability by applying each layer individually rather than attaching a pre-manufactured EL sheet. A benefit of the new method would offer greater conformity over the contours of the entire part.

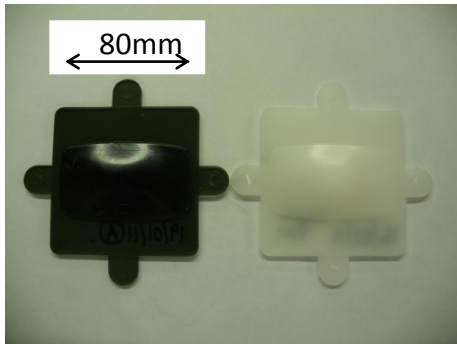


Figure 8-26: PC and PP moulded parts.

Layers were built up on both PP and PC plastic parts (Figure 8-26); the PP is fairly opaque and the PC available to use was a dark colour so it was decided to apply the layers in reverse order as a top emitting device. In this configuration the light is emitted from the surface of the part rather than through the main substrate material; this also reproduced the same device orientation produced by the in-mould and insert moulding processes described earlier.



Figure 8-27: The EL layer application: left to right, silver, dielectric, phosphor, PEDOT:PSS and silver bus.

Figure 8-27 shows the silver electrode applied first followed by the dielectric, phosphor, PEDOT:PSS and finally a silver busbar was applied to the transparent

electrode. The finished and working devices are shown in Figure 8-28 and Figure 8-29.

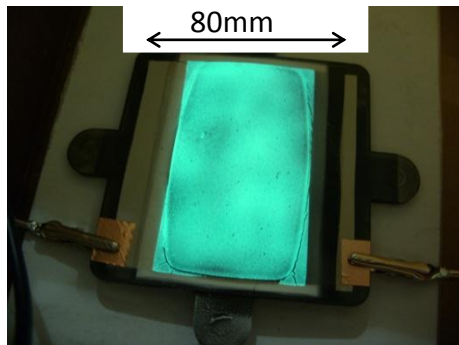


Figure 8-28: A working PC EL part made by post mould layer application.

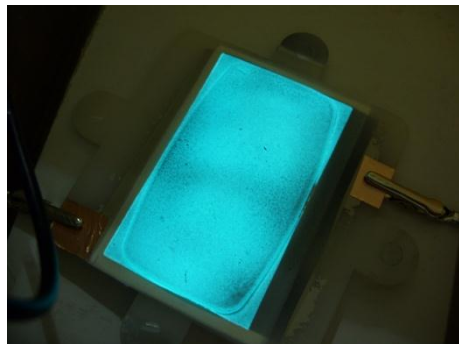


Figure 8-29: A working PP EL part made by post mould layer application.

The layers adhered well to the part and to each other and were dried at 130 °C, following the same drying regime as the airbrush plaques (Table 7-6 on page 129). There is some cracking that occurred at the edges of the PC these are not evident on the PP part and were probably due to variations in the layer application. At high voltages there was some burning at the position of the cracks.

The PP part has a more uniform layer coverage and illumination (Figure 8-29); this was achieved by increasing the distance between the airbrush and the surface to ensure a more even coating of the sprayed material.

8.5 Findings from Process Refinement Experiments

The process refinement experiments have highlighted some interesting findings:

- A bonding layer can be made by mixing the MEK diluted phosphor and PEDOT:PSS materials; incorporating the bonding layer in between the PEDOT:PSS and phosphor does not impair the devices ability to illuminate.
- When spraying EL materials directly in-mould, Orgacon™ provides the best adhesion to the phosphor layer; there is 97.8 % adhesion between Orgacon™ and phosphor both with and without the use of a bonding layer.
- The presence of a bonding layer improves adhesion to the phosphor layer for both Clevios™ and ITO-R; the bonding layer provides a 24 % increase in adhesion for Clevios™ and 32 % increase for ITO-R.
- Different brands of PEDOT:PSS are suited for different techniques; due to its superior adhesion, Orgacon™ is the most suitable brand to use in-mould but when making inserts the drying phosphor fractures the Orgacon™ PEDOT:PSS layer. ITO-R is the most suitable PEDOT:PSS brand for the insert moulding techniques.
- A lower drying temperature of 80 °C is more appropriate when manufacturing PE inserts.

- PE insert moulding can produce plastic parts with EL layers over a shallow curve but there are some problems with devices that extend over sharp edges.
- PTFE insert moulding has the ability to produce moulded plastic parts with an EL layer structure over both a shallow curve and sharper edges. The PTFE film produces a part with a very smooth, glossy surface.
- In-mould layer application is successful in producing moulded plastic parts with an EL surface applied over a shallow contour but layers applied over sharper edges (radius of 1 mm) are disrupted during injection.
- When applying layers directly in-mould, the surface finish and uniformity of illumination is of a lower quality than that of devices produced by insert moulding.
- It has also been determined that using the airbrush layer application; the multi-layer EL structure can be successfully applied directly onto existing 3D plastic parts as a post mould technique.

8.5.1 Summary

Improved methods of injection moulding electroluminescent parts have been successfully developed. Insert moulding using PE and PTFE inserts, and in-mould layer application have all produced plastic parts with a working EL structure over a 3D curved surface; some dimensional limitations have also been identified. There is some variation in surface finish and uniformity of illumination across the range of processes so the next important stage is to characterise parts produced using these novel processes and compared them to parts made using current technology and

bought EL devices. The post mould layer application method will also be included in the comparison, because if this gives comparable results to in-mould methods it offers another option of producing 3D EL devices by adding electroluminescent capabilities to existing moulded plastic parts.

9 CHARACTERISATION EXPERIMENTS

The research for the development of novel methods of injection moulding EL devices has been completed and the next stage is to determine how effective, reliable and robust the manufactured parts are. This will be done by characterising the brightness of manufactured parts and by observing the effect different conditions have on their effectiveness as a lamp. Individual layer thicknesses within each device will also be measured to give an indication of the reliability of the layer application process.

To determine if the processes developed in this project are reliable and repeatable characterisation of devices made in-house (using both traditional and novel techniques) and a commercially available EL device were carried out and compared.

The degradation investigation carried out will quantify how the EL lamps made using the modified materials and the airbrush are affected by different humidity conditions and different encapsulating options; the investigation will observe and measure the degradation of the light level emitted over time.

9.1 Device Characterisation

Characterisation of the devices produced using the novel injection moulded methods, and other methods developed, is required for a number of reasons. The characterisation of a number of different devices made using the same method gives an indication of how repeatable the process is and how consistent each part is. A bought device was purchased and 5 devices were made using each of the different methods used in this project:

- Traditional thick film method (as described in section 7.2)
- Basic Airbrush method (as described in section 7.3)
- PE Insert moulded (as described in section 8.3.2.1)
- PTFE Insert moulded (as described in section 8.3.2.2)
- In-mould application (as described in section 8.3.1)
- Post mould layer application (as described in section 8.4)

Information regarding the manufacturing technique and materials used in the bought device were unavailable.

Although one of the objectives of this project was to produce a 3D contoured EL surface, the characterised moulded parts were made on a flat surface to ensure a fair comparison to the flat bought, basic airbrush and thick film devices.

The devices were characterised with regards to the brightness of the light emitted by them and the thickness of individual layers.

9.1.1 Illuminance

Since the predominant feature of the injection moulded parts is to light up, it is evident that quantifying the intensity of the light is essential in the analysis of the parts made during the project.

The standard method for characterising light emitting devices are current-voltage-luminance (IVL) measurements; for a range of voltages applied to the device, the current flowing through it and the light emitted from it are measured [35]. Current density is also often calculated from the current. The Oxford dictionary defines luminance as “the intensity of light emitted from a surface per unit area in a given

direction” [154] and it is measured in candela per square metre (cd/m^2). These measurements are carried out using specialised equipment such as the SEA IVL Test Platform [155].

Since this equipment was not available to the author but a light meter (measuring lux) was, a compromise was made. The quantity measured in the unit lux is illuminance, this is defined as “the amount of luminous flux per unit area” [156], so the illuminance of each device was measured along with the voltage and frequency applied. Illuminance was being measured as an indication of the brightness of the light emitted from the manufactured parts and although it is not the standard characterisation method it will enable direct comparison of the parts made using different methods.

A battery and inverter were also used to determine if the novel illuminating devices could be portable.

9.1.1.1 Equipment

In order to illuminate the manufactured parts an AC supply was constructed with variable frequency and voltage (RMS) outputs. The frequency of the alternating current could be varied between 100 and 400 Hz and the RMS voltage driving the current could be set to any value between 100 and 300 V. These operating values were taken from the HC Starck processing guide [148] used with the initial material system. The power supply unit has analogue dials to change each value so a handheld oscilloscope was used to measure the frequency and voltage accurately.

A light meter was used to measure the illuminance (in lux) of each device; the light meter was cradled in a holder (made in house) whilst characterising the samples.

The holder kept the detector at the same distance above each sample and ensured the samples were positioned correctly underneath it.

During testing, the sample and light meter were housed within a black-out box to prevent any external light from invalidating the test.

9.1.1.2 Method

An experiment was designed to determine the effect that two variables have on the illuminance of the part; the RMS voltage (V) and the frequency of oscillation (F) of the AC supply.

- V: 0 = 100 V, 1 = 300 V
- F: 0 = 100 Hz, 1 = 400 Hz

Two variable with 2 levels results in an experiment with 4 trials; 5 repetitions were done for each trial. Each reading was taken 1 minute after illumination; this was because the intensity of light given out increased in the time immediately after illumination, but soon levelled out.

9.1.2 Layer Thickness

The different EL devices made in house, and the bought device, were analysed to measure the thickness of the layers within the multi-layer electroluminescent structure; 5 devices made by each method were measured in 5 different positions on every device. The measurement positions were equally spaced across the device, with one in the centre. The centre position was nearest the sprue and was the position where the EL layers would experience the greatest shear during injection, 2 further measurements were taken radially out in opposite directions orientated with the polymer flow. This analysis enabled a comparison of the layer

thicknesses produced by each method, and by measuring the layer thicknesses in different positions on individual devices, the uniformity of layer thickness across a single part and consistency of layer thickness when repeating a method were all determined from the data.

The layer thicknesses was measured using an optical microscope; each layer material is a different colour so an optical microscope was sufficient to determine the interface between two layers and measure the thicknesses

9.1.2.1 Equipment

The equipment that was used to section the samples was a Buehler IsoMet 5000 saw fitted with a 30HC diamond edge blade (Figure 9-1 left); some samples first required an acrylic SamplKwick encapsulating layer. A set of balances, a fume cupboard, mixing cups, stirring sticks, silicon release liquid and 30mm diameter mounting cups were used to prepare the mounting material. EpoHeat epoxy resin was the material used to mount the samples which was cured in a Buehler heating oven. Grinding was carried out on a Buehler Phoenix 4000 sample preparation system (Figure 9-1 right) using silicon carbide papers and diamond slurry on a Trident polishing cloth.

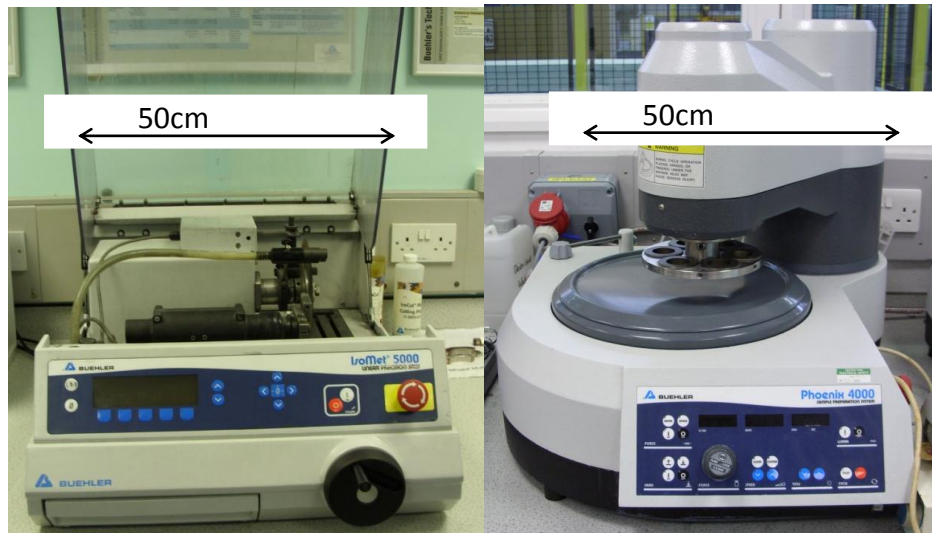


Figure 9-1: The saw and polisher used in this project.

A Zeiss AxioLab A1 microscope was later used to observe the samples and measure the individual layer thicknesses.

9.1.2.2 Method

The following method was used to section, mount and polish sample from each of the EL devices:

- Firstly, some devices required the application of an encapsulating material to protect the EL layers:
 - The following steps took place in a fume cupboard,
 - A small quantity of SamplKwick acrylic was mixed (approximately 2:1 mix of powder to liquid hardener) in a disposable mixing cup and stirred with a wooden stirring stick for 10-20 seconds,
 - The mixed acrylic was poured over Post Mould, In-mould and PE insert moulded parts (these parts had the most delicate PEDOT:PSS

layer and required protecting before cutting), the acrylic was spread across the EL device and this was done in batches.

- 15 minutes was allowed for the acrylic to cure.
- Each of the devices was then sectioned:
 - The sample was clamped into the IsoMet 5000,
 - The blade speed was set at 4000rpm and the feed speed to around 6mm/min.
 - A sample was cut approximately 2cm x 1cm from the centre of the EL devices.
- The sectioned pieces were then mounted:
 - Each section needed to be positioned with the surface of interest facing down, this was done using a stainless steel SamplKlip,
 - Each section was placed into a 30mm diameter SamplKup which had been coated with silicon mould release,
 - The epoxy resin was then prepared to fill the cups, this was carried out in batches of 4 samples and within a fume cupboard,
 - 60g of resin and 15g of hardener were measured into a disposable mixing cup, the cup was then tilted and a slowly stirred using a wooden stick in a folding motion to combine the two components together. Stirring was complete when any streakiness disappeared,
 - The epoxy was then carefully poured into each cup, tapping the cup against the work surface to remove any air pockets,
 - A label was placed on the top of the epoxy and the mounted samples were placed in an oven at 50°C for 3 hours.

- When every sample was mounted and removed from the cups, they were ground and polished:
 - The following settings were applied on the grinder:
 - Single force set at 12N,
 - Complimentary rotation,
 - Rotation speed of 200rpm,
 - Cycle time of 1 minute,
 - Water on.
 - A P320 silicon carbide paper was applied to the metal plate, taking care to avoid trapping any air bubbles, and then placed on the platen,
 - Water was squirted over the surface of the grinding paper,
 - The arm was swung over the paper and the head lowered,
 - 6 samples were placed in the head and a cycle started,
 - This was repeated with all samples and followed with P600 and P1200 papers,
 - After each stage the samples were sprayed with detergent and rinsed with clean water,
 - the following settings on the polisher were then changed:
 - Contra-rotating,
 - Cycle time of 3 minutes 30 seconds,
 - Water off.
 - A Trident polishing cloth was applied to the platen, and 3 μ m diamond slurry was squirted onto the cloth,

- A cycle was run, adding more slurry during the cycle,
- After polishing, each sample was sprayed with detergent, rinsed with clean water, sprayed with IPA and then the surface was blasted with hot air.

After preparing the samples, each was viewed under a Zeiss AxioLab A1 microscope; AxioVision 4.8 software was used to measure the thickness of the layers observed on screen.

9.2 Degradation Investigation

Comparing the intensity of the light emitted by the different devices is important but it is also necessary to determine how the long term performance of the devices is affected by modifying the materials applied using an airbrush. Electroluminescent devices (particularly the conductive polymers that form the transparent electrode) are prone to degradation caused predominantly by humidity. A short experiment was carried out to indicate if dilution of the EL materials had any negative impact on the lifetime of the EL devices. Six near identical devices were kept in different humidity conditions, and their performance monitored over a 10 week period. The different conditions were:

- Low Humidity (no encapsulation)
- Atmospheric Humidity (no encapsulation)
- Atmospheric Humidity (PVC encapsulated)
- Atmospheric Humidity (PU encapsulated)
- Atmospheric Humidity (Coverlay encapsulated)
- High Humidity (no encapsulation)

These tests were carried out using both unmodified and modified materials; 6 thick film devices using the materials as pastes were monitored along with 6 airbrushed devices using materials diluted with MEK solvent. By comparing the two sets of results, it could be determined whether the loss in light emission is due to the solvent dilution or an inherent behaviour of the EL materials.

9.2.1.1 Equipment

The devices were made using equipment used for the thick film layer application method as described in section 7.2.3 and the airbrush method as described in section 7.3.2.

In each set of 6 devices, in addition to the standard equipment and layer materials, the following items were required: a UV curing clear Coverlay and UV lamp, some PVC self-adhesive film and an air drying PU spray, also 2 airtight containers, silica gel crystals, distilled water and absorbent material.

The illuminance of the devices were measured using the same equipment as described in section 9.1.1.2; an AC power supply, a blackout box and a light meter (positioned in a holder at a set distance from the part), a hand held oscilloscope was used to verify the operating V and F. A humidity meter was used to measure the humidity of each of the environmental conditions.

9.2.1.2 Method

The degradation test was designed to measure the decrease in the level of light emitted by EL devices over a ten week period. Devices were made using both modified and unmodified materials and the test was carried out as follows:

- Twelve devices were made on 3mm thick PC plaques, six using the basic airbrush method and six using the thick film method Each device had an illuminated area of 16 cm² (4 cm x 4 cm),
- The illuminance of each device was measured 1 minute after connection to a 300 V, 400 Hz AC supply,
- For each set of six samples, different storage conditions were tested:
 - Low Humidity (samples were kept in a sealed container with Silica gel crystals),
 - High Humidity (samples were kept in a sealed container with absorbent material soaked in water), the samples were dried of condensation before testing,
 - Environmental conditions (samples were are kept on the lab bench with no encapsulation layer),
 - PVC encapsulated (devices were covered with a film of self-adhesive PVC film),
 - Coverlay encapsulated (devices were sprayed with Coverlay, this is cured using 3 x 1 minute exposures under a UV lamp),
 - PU encapsulated (devices were sprayed with PU which was air dried for 10 minutes),
- Each week the samples were tested, illuminance was measured at 300 V and 400 Hz, 1 minute after connection,
- The test was repeated for weeks 1 to 10.

10 RESULTS

10.1 Device Characterisation

In order to compare the electroluminescent devices, each needed to be characterised. Both the illuminance and the thickness of the layers applied using each method were measured, the results follow

10.1.1 Illuminance

The illuminance of each different device was measured; the variables investigated were the frequency and voltage of the AC electrical supply. Table 10-1 shows the experimental design and Table 10-2 to Table 10-8 shows the results. For each trial and repetition, the illuminance was measured in lux and the recorded value was taken one minute after illumination. Each device had an illuminated area of 16cm² (4cm x 4cm).

Table 10-1: The variables used in each trial.

		Variables			
		F		V	
		frequency		voltage	
Trial	1	+	400	+	300
	2	-	100	+	300
	3	+	400	-	100
	4	-	100	-	100

Table 10-2: The illuminance results for the bought EL device.

		Bought Device Illuminance (lx)	
Trial	1	i	492
		ii	452
		iii	457
		iv	476
		v	459
	2	i	135
		ii	132
		iii	134
		iv	129
		v	131
	3	i	116
		ii	112
		iii	109
		iv	112
		v	107
	4	i	34
		ii	35
		iii	35
		iv	33
		v	32

Table 10-3: The illuminance results for devices made using the thick layer method.

			Thick Layer Device Illuminance (lx)				
			A	B	C	D	E
Trial	1	i	158	171	185	160	190
		ii	155	163	179	158	189
		iii	152	170	170	155	185
		iv	159	166	176	153	193
		v	154	172	173	156	182
	2	i	58	61	60	50	62
		ii	52	62	58	49	58
		iii	60	58	58	51	61
		iv	57	58	57	50	59
		v	59	56	61	48	60
	3	i	13	20	24	20	21
		ii	14	19	25	19	20
		iii	11	18	23	17	19
		iv	12	18	23	17	23
		v	13	21	22	18	22
	4	i	5	8	9	7	8
		ii	5	7	9	7	7
		iii	5	7	9	7	9
		iv	6	7	10	6	9
		v	5	8	9	7	8

Results

Table 10-4: The illuminance results for the devices made using the airbrush method.

			Airbrush Device Illuminance (lx)				
			A	B	C	D	E*
Trial	1	i	293	302	324	231	
		ii	277	310	320	225	
		iii	280	305	328	235	
		iv	287	312	336	236	
		v	284	308	317	248	
	2	i	73	90	85	72	
		ii	78	80	90	75	
		iii	75	84	89	76	
		iv	76	81	84	79	
		v	79	85	89	76	
	3	i	61	64	68	79	
		ii	59	62	70	75	
		iii	63	65	68	78	
		iv	60	59	67	76	
		v	58	62	68	75	
	4	i	23	21	24	24	21
		ii	20	20	21	23	
		iii	19	20	24	23	
		iv	20	21	23	24	
		v	20	20	22	23	

**Sample E failed after one trial 4 test*

Table 10-5: The illuminance results for devices made using the PE insert moulding method.

			PE Insert Moulded Device Illuminance (lx)				
			A*	B	C	D**	E
Trial	1	i		159	102	85	145
		ii		160	99		140
		iii		165	102		144
		iv		161	100		151
		v		163	97		149
	2	i		72	44		60
		ii		71	41		61
		iii		67	42		58
		iv		75	38		62
		v		71	37		62
	3	i		48	31	28	43
		ii		47	28	24	46
		iii		53	31		42
		iv		51	29		39
		v		50	29		45
	4	i		16	9	10	14
		ii		17	8	9	14
		iii		15	10		14
		iv		15	12		15
		v		16	10		14

*Sample A failed to illuminate

**Sample D failed after 5 tests

Table 10-6: The illuminance results for devices made using the PTFE insert moulding method.

			PTFE Insert Moulded Device Illuminance (lx)				
			A	B	C	D	E
Trial	1	i	236	248	148	204	187
		ii	251	258	153	205	192
		iii	240	260	147	210	200
		iv	255	251	151	211	195
		v	250	256	148	208	191
	2	i	73	71	43	65	58
		ii	76	74	44	62	58
		iii	74	75	39	62	65
		iv	78	75	43	64	58
		v	74	70	46	65	61
	3	i	52	56	44	50	58
		ii	56	58	45	55	56
		iii	53	59	48	46	58
		iv	55	57	48	52	53
		v	56	62	52	50	56
	4	i	16	17	14	15	17
		ii	17	17	15	15	18
		iii	16	17	14	15	16
		iv	16	19	13	15	16
		v	18	17	13	16	16

Results

Table 10-7: The illuminance results for devices made using the in-mould layer application method.

			In-Mould Device Illuminance (lx)				
			A*	B	C	D**	E
Trial	1	i		38	35		61
		ii					
		iii					
		iv					
		v					
	2	i		15			30
		ii		14			
		iii		20			
		iv					
		v					
	3	i		8	8		16
		ii		10			18
		iii					
		iv					
		v					
	4	i		6	5		10
		ii		4			12
		iii		7			
		iv					
		v					

All working samples failed during trial 1

**Only a partial area of sample A illuminated so it would not be a fair comparison to other*

***Sample D failed to illuminate*

Table 10-8: The illuminance results for devices made using the post mould layer application method.

			Post Mould Device Illuminance (lx)				
			A	B	C	D	E
Trial	1	i	71	121	143	192	82
		ii	68	116	139	185	74
		iii	70	113	138	194	78
		iv	66	114	143	198	82
		v	70	111	142	191	77
	2	i	26	37	43	55	22
		ii	23	33	43	55	23
		iii	21	32	37	49	19
		iv	20	32	41	47	21
		v	20	33	40	54	20
	3	i	23	35	43	50	22
		ii	21	36	38	58	23
		iii	24	35	40	56	21
		iv	24	35	37	57	22
		v	22	31	39	55	21
	4	i	7	11	14	16	7
		ii	8	10	14	18	7
		iii	7	11	14	19	7
		iv	8	11	13	17	7
		v	7	11	12	16	7

10.1.2 Layer Thickness

Each of the devices that had its illuminance characterised also had its layer thicknesses measured at 5 different positions. The 30 devices made in-house (5 samples made using each of the 6 methods), as well as the bought device, were cross-sectioned and observed under a high powered microscope; the layer thicknesses were measured using the microscope software. The results are shown in Table 10-9 to Table 10-37.

10.1.2.1 *Bought Device*

Table 10-9: The layer thickness measurements for the bought EL device.

Bought Device					
Layer Material	Thickness (μm)				
	i	ii	iii	iv	v
Rear Electrode	10.78	10.05	11.51	10.49	11.72
Dielectric	40.90	20.08	40.06	36.91	41.23
Phosphor	18.61	41.49	18.01	21.85	15.68
Transparent Electrode	2.95	2.81	3.54	2.51	4.41

10.1.2.2 *Thick Layer Devices on 3mm PC Sheet*

Table 10-10: The layer thickness measurements for thick layer device A.

Layer Material	Thickness (μm)				
	i	ii	iii	iv	v
Silver	50.44	43.84	42.00	40.88	42.75
Dielectric	41.63	49.69	54.12	46.76	46.39
Phosphor	93.95	93.49	97.95	120.42	106.77
Transparent Electrode	3.33	5.15	5.52	4.05	4.80

Results

Table 10-11: The layer thickness measurements for thick layer device B.

Layer Material	Thickness (μm)				
	i	ii	iii	iv	v
Silver	66.67	73.65	68.48	70.31	65.38
Dielectric	73.32	56.32	60.37	61.52	61.24
Phosphor	57.83	70.36	79.88	102.70	130.30
Transparent Electrode	5.17	6.63	5.52	6.27	7.76

Table 10-12: The layer thickness measurements for thick layer device C.

Layer Material	Thickness (μm)				
	i	ii	iii	iv	v
Silver	58.27	64.78	63.68	69.20	63.70
Dielectric	30.57	30.55	29.83	28.00	30.94
Phosphor	36.16	48.22	72.52	32.52	62.94
Transparent Electrode	3.68	4.05	6.63	4.05	7.00

Table 10-13: The layer thickness measurements for thick layer device D.

Layer Material	Thickness (μm)				
	i	ii	iii	iv	v
Silver	64.39	61.95	64.35	67.00	64.82
Dielectric	38.49	33.59	41.06	52.3	42.04
Phosphor	98.35	79.18	58.66	104.57	61.18
Transparent Electrode	4.79	5.17	5.15	6.26	5.90

Table 10-14: The layer thickness measurements for thick layer device E.

Layer Material	Thickness (μm)				
	i	ii	iii	iv	v
Silver	64.42	68.51	72.51	67.00	64.82
Dielectric	62.21	65.73	48.61	59.63	66.32
Phosphor	52.31	39.03	38.28	29.10	104.66
Transparent Electrode	8.47	8.83	8.10	8.47	5.90

10.1.2.3 *Airbrush Layer Devices on 3mm PC Sheet*

Table 10-15: The layer thickness measurements for airbrush device A.

Layer Material	Thickness (μm)				
	i	ii	iii	iv	v
Silver	13.93	20.15	17.19	15.67	14.01
Dielectric	26.87	33.22	31.96	27.79	23.97
Phosphor	26.43	51.32	39.80	28.51	24.76
Transparent Electrode	3.39	4.07	3.75	5.53	5.99

Results

Table 10-16: The layer thickness measurements for airbrush device B.

Layer Material	Thickness (μm)				
	i	ii	iii	iv	v
Silver	8.10	22.11	14.76	10.37	11.87
Dielectric	15.46	17.67	13.62	16.57	15.31
Phosphor	26.88	30.95	55.29	28.38	40.36
Transparent Electrode	5.15	6.27	4.72	7.74	5.21

Table 10-17: The layer thickness measurements for airbrush device C.

Layer Material	Thickness (μm)				
	i	ii	iii	iv	v
Silver	16.58	18.07	16.95	20.64	15.84
Dielectric	17.30	24.69	28.00	33.57	18.07
Phosphor	36.82	25.79	32.41	39.04	50.83
Transparent Electrode	4.79	2.21	2.60	2.97	4.43

Table 10-18: The layer thickness measurements for airbrush device D.

Layer Material	Thickness (μm)				
	i	ii	iii	iv	v
Silver	12.88	10.67	15.46	19.15	10.31
Dielectric	13.70	16.20	16.93	17.68	18.79
Phosphor	26.14	27.97	24.67	15.11	24.67
Transparent Electrode	5.52	4.42	6.63	5.53	5.15

Table 10-19: The layer thickness measurements for airbrush device E.

Layer Material	Thickness (μm)				
	i	ii	iii	iv	v
Silver	12.15	14.37	11.42	15.67	12.89
Dielectric	20.84	27.25	20.66	23.87	16.97
Phosphor	37.5	35.71	20.62	15.84	25.13
Transparent Electrode	6.26	5.89	7.03	6.26	7.00

10.1.2.4 PE Insert Moulded

N.B. There are no layer thickness measurements for sample A because it was damaged during the cutting and mounting process.

Table 10-20: The layer thickness measurements for PE insert moulded device B.

Layer Material	Thickness (μm)				
	i	ii	iii	iv	v
Silver	9.71	10.83	11.94	11.75	9.49
Dielectric	19.85	23.08	24.39	23.09	21.96
Phosphor	23.15	19.63	15.80	19.58	20.86
Transparent Electrode	2.99	2.23	2.67	2.51	3.11

Results

Table 10-21: The layer thickness measurements for PE insert moulded device C.

Layer Material	Thickness (μm)				
	i	ii	iii	iv	v
Silver	13.35	8.43	9.32	7.83	14.38
Dielectric	22.67	23.54	21.30	25.41	22.97
Phosphor	19.08	8.14	17.61	11.67	18.04
Transparent Electrode	2.53	3.28	2.38	3.10	2.53

Table 10-22: The layer thickness measurements for PE insert moulded device D.

Layer Material	Thickness (μm)				
	i	ii	iii	iv	v
Silver	10.45	11.61	11.82	8.34	12.67
Dielectric	22.67	23.54	25.20	28.49	31.09
Phosphor	17.48	24.82	19.66	18.02	16.17
Transparent Electrode	2.64	2.89	2.13	3.42	2.60

Table 10-23: The layer thickness measurements for PE insert moulded device E.

Layer Material	Thickness (μm)				
	i	ii	iii	iv	v
Silver	12.41	22.01	20.27	17.59	9.88
Dielectric	28.16	28.25	20.70	29.51	32.55
Phosphor	28.81	14.56	20.18	17.14	14.61
Transparent Electrode	2.67	4.29	2.87	2.55	2.23

10.1.2.5 PTFE Insert Moulded

Table 10-24: The layer thickness measurements for PTFE insert moulded device A.

Layer Material	Thickness (μm)				
	i	ii	iii	iv	v
Silver	9.01	18.62	11.37	17.15	14.91
Dielectric	24.36	25.57	39.27	27.14	20.08
Phosphor	32.33	33.22	12.55	29.55	36.46
Transparent Electrode	1.77	3.85	1.48	1.77	1.62

Table 10-25: The layer thickness measurements for PTFE insert moulded device B.

Layer Material	Thickness (μm)				
	i	ii	iii	iv	v
Silver	10.48	12.40	14.78	13.88	8.71
Dielectric	19.34	15.06	20.37	25.25	18.04
Phosphor	37.35	49.9	45.32	42.96	49.30
Transparent Electrode	1.92	1.62	2.22	3.55	2.66

Table 10-26: The layer thickness measurements for PTFE insert moulded device C.

Layer Material	Thickness (μm)				
	i	ii	iii	iv	v
Silver	11.36	10.92	9.53	8.66	14.85
Dielectric	14.83	16.13	17.40	18.67	14.98
Phosphor	16.04	18.37	14.71	23.54	23.61
Transparent Electrode	2.55	1.80	1.04	2.02	2.07

Table 10-27: The layer thickness measurements for PTFE insert moulded device D.

Layer Material	Thickness (μm)				
	i	ii	iii	iv	v
Silver	10.19	10.20	10.33	11.81	11.51
Dielectric	16.24	22.89	18.01	18.90	23.18
Phosphor	46.50	44.29	41.04	42.22	40.30
Transparent Electrode	1.18	1.33	1.48	1.63	1.77

Table 10-28: The layer thickness measurements for PTFE insert moulded device E.

Layer Material	Thickness (μm)				
	i	ii	iii	iv	v
Silver	11.52	6.50	11.22	8.41	11.41
Dielectric	24.97	30.04	28.64	30.90	25.50
Phosphor	25.24	27.03	25.99	25.56	26.96
Transparent Electrode	1.62	2.36	1.78	1.81	2.07

10.1.2.6 *In-Mould Layer Application*

N.B. There are no layer thickness measurements for sample A because it was damaged during the cutting and mounting process.

Table 10-29: The layer thickness measurements for in-mould layer application device B.

Layer Material	Thickness (μm)				
	i	ii	iii	iv	v
Silver	20.63	17.84	15.48	10.51	18.89
Dielectric	18.47	13.07	22.15	24.23	19.80
Phosphor	32.54	35.92	29.81	31.48	33.2
Transparent Electrode	8.26	4.49	5.8	5.16	6.65

Table 10-30: The layer thickness measurements for in-mould layer application device C.

Layer Material	Thickness (μm)				
	i	ii	iii	iv	v
Silver*					
Dielectric	13.93	21.68	11.96	17.45	15.06
Phosphor	30.90	27.72	35.14	31.05	36.31
Transparent Electrode	11.38	9.70	7.84	5.17	6.68

**The silver layer was not visible under the microscope.*

Table 10-31: The layer thickness measurements for in-mould layer application device D.

Layer Material	Thickness (μm)				
	i	ii	iii	iv	v
Silver	12.57				
Dielectric	13.03				
Phosphor	36.58				
Transparent Electrode	3.1				

The multi-layer structure was too disrupted to determine individual layer thicknesses apart from at one location.

Table 10-32: The layer thickness measurements for in-mould layer application device E.

Layer Material	Thickness (μm)				
	i	ii	iii	iv	v
Silver	14.01	29.22	6.21	19.00	15.53
Dielectric	27.91	24.44	31.06	17.12	17.28
Phosphor	17.69	20.56	23.94	57.13	44.00
Transparent Electrode	5.19	5.76	5.76	6.79	5.76

10.1.2.7 *Post mould Layer Application*

Table 10-33: The layer thickness measurements for post mould layer application device A.

Layer Material	Thickness (μm)				
	i	ii	iii	iv	v
Silver	7.97	8.56	10.20	7.39	10.04
Dielectric	10.63	18.16	5.62	13.73	15.21
Phosphor	9.01	6.64	10.04	4.87	4.89
Transparent Electrode	4.73	3.54	3.25	3.55	4.28

Table 10-34: The layer thickness measurements for post mould layer application device B.

Layer Material	Thickness (μm)				
	i	ii	iii	iv	v
Silver	16.07	19.25	16.28	20.08	18.17
Dielectric	9.47	11.44	9.80	9.02	10.05
Phosphor	7.85	7.47	16.69	8.27	8.42
Transparent Electrode	2.55	2.90	2.43	3.69	3.04

Table 10-35: The layer thickness measurements for post mould layer application device C.

Layer Material	Thickness (μm)				
	i	ii	iii	iv	v
Silver	14.33	16.04	11.52	11.37	14.48
Dielectric	17.58	15.65	15.94	19.23	18.19
Phosphor	12.40	21.70	20.24	18.31	12.26
Transparent Electrode	3.10	3.55	3.84	3.69	3.10

Table 10-36: The layer thickness measurements for post mould layer application device D.

Layer Material	Thickness (μm)				
	i	ii	iii	iv	v
Silver	10.49	11.25	18.96	13.29	19.63
Dielectric	13.91	15.12	12.59	12.58	17.07
Phosphor	20.69	7.68	15.68	13.61	12.18
Transparent Electrode	1.48	2.53	2.21	2.07	2.38

Table 10-37: The layer thickness measurements for post mould layer application device E.

Layer Material	Thickness (μm)				
	i	ii	iii	iv	v
Silver	14.36	15.09	12.89	14.73	15.83
Dielectric	16.56	16.95	19.15	13.30	12.60
Phosphor	9.94	16.20	9.94	29.73	13.62
Transparent Electrode	4.76	2.94	6.99	6.63	5.15

10.2 Degradation Test

The degradation test measured the illuminance of 2 sets of 6 devices; one thick film set made using the EL materials as they were supplied and one set made using an airbrush applying modified materials. The samples within each set were produced at the same time then kept in 6 different conditions over 10 weeks; the illuminance was measured in lux at 300 V and 400 Hz, 1 min after illumination. The results are shown in Table 10-38 and Table 10-39.

Table 10-38: The degradation test results for the thick film devices.

		Illuminance of Thick Film Samples (lx)						
		A	B	C	D	E	F	
		Low Humidity	High Humidity	Atmospheric	PVC Film Encapsulated	Coverlay Encapsulated	Polyurethane Encapsulated	
Week	0	i	228	282	252	247	208	223
		ii	236	288	256	242	211	224
		iii	222	293	255	237	210	219
		iv	218	291	259	236	205	222
		v	220	287	250	240	202	214
	1	i	94	0	121	200	162	111
		ii	98	0	116	196	165	108
		iii	103	0	120	198	163	109
		iv	95	0	116	193	162	111
		v	100	0	125	201	162	110
	2	i	91	0	111	188	147	100
		ii	90	0	112	192	154	98
		iii	89	0	105	186	146	92
		iv	92	0	112	196	152	102
		v	92	0	117	198	150	105
3	i	83	0	115	186	148	94	
	ii	88	0	117	191	150	96	

		iii	88	0	114	190	149	97
		iv	90	0	116	188	151	96
		v	87	0	114	189	148	98
	4	i	87	0	108	187	146	88
		ii	93	0	109	185	145	90
		iii	85	0	111	184	146	91
		iv	85	0	112	184	143	84
		v	82	0	112	188	144	92
	5	i	85	0	110	184	147	86
		ii	85	0	113	185	143	87
		iii	87	0	108	181	139	89
		iv	86	0	109	182	141	85
		v	87	0	111	182	142	87
	6	i	87	0	105	180	139	85
		ii	84	0	111	181	142	86
		iii	85	0	108	181	140	85
		iv	85	0	109	185	143	84
		v	86	0	106	182	138	87
	7	i	86	0	104	178	136	84
		ii	83	0	98	180	138	85
		iii	85	0	110	184	138	87
		iv	88	0	107	180	140	83
		v	87	0	103	179	137	86
	8	i	88	0	105	182	138	82
		ii	85	0	108	184	138	84
iii		87	0	100	183	140	85	
iv		89	0	106	183	138	83	
v		86	0	107	178	137	82	
9	i	85	0	100	180	135	83	
	ii	84	0	104	178	135	82	
	iii	85	0	101	181	138	85	
	iv	83	0	105	180	139	83	
	v	87	0	104	183	136	82	
1	i	84	0	104	181	133	84	

Results

	0	ii	86	0	103	179	137	81
		iii	83	0	101	178	134	82
		iv	83	0	99	181	135	83
		v	84	0	102	177	135	82

Table 10-39: The degradation test results for the airbrushed devices.

		Illuminance of Airbrushed Samples (lx)						
		A	B	C	D	E	F	
		Low Humidity	High Humidity	Atmospheric	PVC Film Encapsulated	Coverlay Encapsulated	Polyurethane Encapsulated	
Week	0	i	621	620	698	652	630	796
		ii	625	618	663	669	666	840
		iii	648	625	703	700	664	837
		iv	635	622	692	681	650	790
		v	628	623	685	670	656	822
	1	i	434	14	496	532	576	564
		ii	440	15	533	535	596	529
		iii	441	17	492	501	593	551
		iv	440	15	500	530	582	545
		v	435	16	511	515	591	550
	2	i	418	2	493	498	578	519
		ii	429	2	502	501	551	545
		iii	423	2	499	488	566	531
		iv	420	2	495	491	559	541
		v	425	2	499	500	570	525
	3	i	418	1	496	488	563	528
		ii	430	1	500	458	553	518
		iii	413	1	501	464	549	520
		iv	419	1	500	471	561	516
		v	422	1	498	470	550	530
4	i	409	1	500	468	560	525	

		ii	402	1	496	447	537	540
		iii	394	1	489	456	545	520
		iv	405	1	499	450	550	532
		v	401	1	493	462	542	524
		i	400	1	498	442	519	502
	5	ii	385	1	479	455	542	535
		iii	396	1	484	451	522	507
		iv	395	1	481	445	528	518
		v	394	1	493	453	529	509
		i	380	1	496	432	495	485
	6	ii	382	1	484	447	506	501
		iii	373	1	489	438	508	502
		iv	383	1	491	434	508	500
		v	374	1	492	445	500	491
		i	381	1	492	435	513	499
	7	ii	370	1	488	439	524	494
		iii	375	1	487	442	515	493
		iv	380	1	488	445	513	498
		v	371	1	490	436	522	491
		i	379	1	495	433	520	496
	8	ii	368	1	481	440	522	502
		iii	379	1	472	439	497	488
		iv	377	1	480	435	518	491
		v	372	1	485	439	510	499
		i	380	1	465	439	510	487
9	ii	363	1	476	422	506	468	
	iii	363	1	470	433	504	485	
	iv	368	1	474	429	505	482	
	v	370	1	467	433	508	476	
	i	364	1	463	435	508	485	
10	ii	366	1	469	436	499	498	
	iii	359	1	457	438	507	499	
	iv	363	1	461	435	501	490	
	v	365	1	466	434	510	496	

Results

The humidity of the three different environments that the unencapsulated devices were kept in, were measured, these are shown in the Table 10-40.

Table 10-40: The humidity measurements for the environments in which the unencapsulated devices were kept.

	Conditions		
	High Humidity (%)	Atmospheric (%)	Low Humidity (%)
i	100 (saturation)	41.8	32.1
ii	100 (saturation)	44.2	31.3
iii	100 (saturation)	46.7	30.9

11 ANALYSIS

This chapter mathematically analyses the data obtained to characterise individual devices, groups of devices and the degradation tests carried out on both modified and unmodified materials. This analysis, along with qualitative considerations will be used in chapter 13 to evaluate the best method of producing injection moulded 3D electroluminescent devices.

11.1 Device Characterisation

Individual devices were characterised by the intensity of the light emitted by them and by the thickness of the layers produced using that method. The analysis that follows includes a comparison of parts made using the same method and parts made using different methods.

11.1.1 Illuminance

The illuminance of each device was measured in lux by a light meter. Two parameters that affect the illuminance were investigated; the RMS voltage and frequency of the AC power supply. The four different operating conditions tested are shown in Table 11-1; each trial was carried out five times.

Table 11-1: The operating conditions under which each part was tested.

		Variables			
		F		V	
		Frequency (Hz)		Voltage (V)	
Trial	1	+	400	+	300
	2	-	100	+	300
	3	+	400	-	100
	4	-	100	-	100

11.1.1.1 *Bought Device*

One EL lamp was bought and tested under the same conditions as the devices made in-house. Since only one device was bought there are only one set of results in this group. The illuminated device can be seen in Figure 11-1.

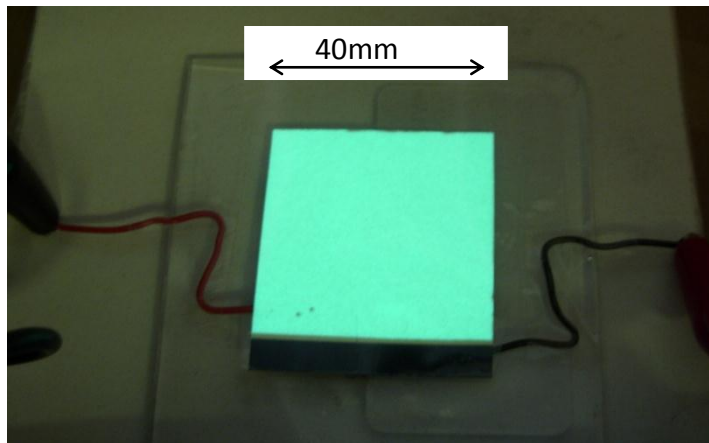


Figure 11-1: The bought device, illuminated.

The bought device had very uniform illumination across the surface and was the brightest device tested; with an average illuminance (on the highest V and F settings) of over 467 lx (see Table 11-2). This is not completely unexpected as the performance of the commercially available device would be optimised in the design stage and it would have been manufactured by an automated process which would be more reliable than hand manufacture. The bought device also had small standard deviations (except for trial 1) indicating a small variation in the illuminance when tested, meaning that device emits a consistent level of light when operated at a particular frequency and voltage.

Table 11-2: Average illuminance results and standard deviation of the bought device.

Trial	Parameter		Illuminance (lx)				RSD (%)
	F	V	av	SD	av-SD	av+SD	
	1	+	+	467.2	16.54	450.7	
2	-	+	132.2	2.387	129.8	134.6	1.81
3	+	-	111.2	3.421	107.8	114.6	3.08
4	-	-	33.80	1.303	32.50	35.10	3.86

Trial 1 has the highest mean value by far so it is expected that there would be a larger variation in the results and the highest standard deviation; to overcome this issue the relative standard deviation has been calculated. When looking at the relative standard deviation in Table 11-2, all of the trials have a small relative standard deviation (RSD) suggesting a there is little variation in the results. Since all of these results were gathered from one device it expected that the RSD would be small; any variation that has occurred may be due to human error, a slight difference in the positioning of the device under the light meter, a variation in the F and V settings or a difference in the time between illumination and when the measurement is taken. Overall, the device may be sensitive to small changes in the operating conditions.

Table 11-3: The calculation of the main effects that the two parameters have on illuminance of the bought device.

Main Effects (lx)						
Trial	Variable	F	V	av	Effect	
1	3	F	1	±	289.2	206.2
2	4		-1	±	83.00	
1	2	V	±	1	299.7	227.2
3	4		±	-1	72.50	

Looking at Table 11-3 and Figure 11-2, it can be seen that (over the parameter range tested in this project) a change in voltage has a greater effect (227.2 lx) on the illuminance than frequency (206.2 lx), although there is only a small difference.

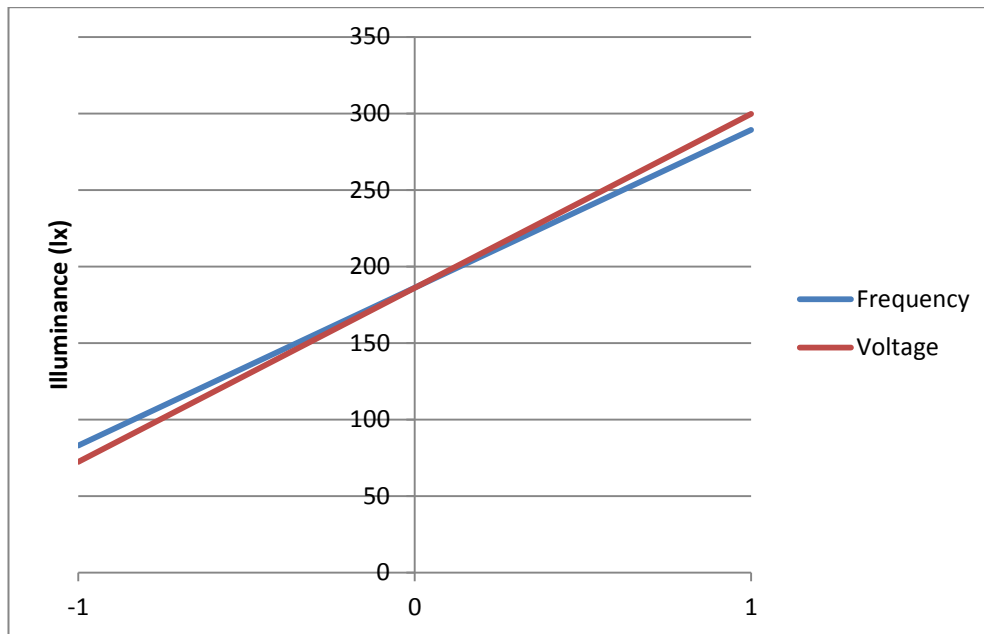


Figure 11-2: The main effects of frequency and voltage on the illuminance of the bought device.

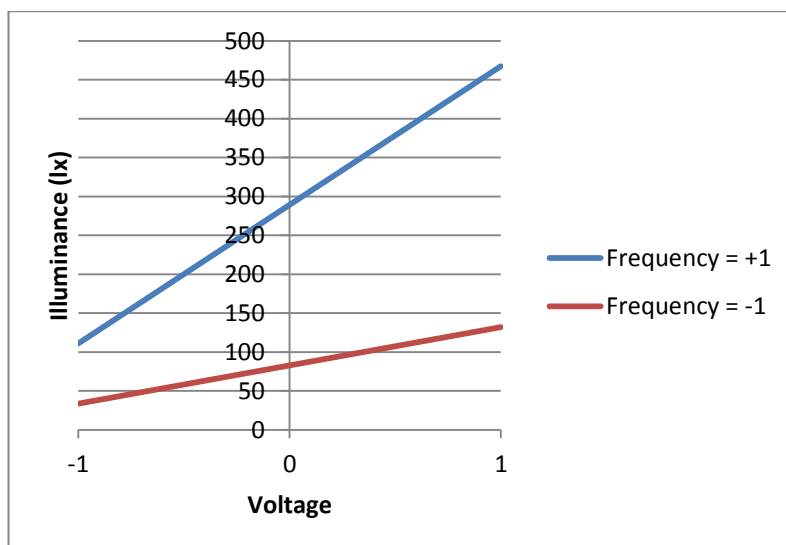


Figure 11-3: The interaction between voltage and frequency on the bought device.

Figure 11-3 shows the interaction between voltage and frequency; since the lines are not parallel with each other it indicates that there is an interaction between

them. At higher frequencies, a change in voltage has a greater effect on the illuminance of the device; the reverse is also true.

11.1.1.2 *Thick Film Devices*

The thick film devices were made with the unmodified materials supplied by Electra Polymers and using a method similar to screen printing; an example of a thick film device is shown in Figure 11-4. The technical data sheet supplied by Electra Polymers states that when operated at 100 V and 400 Hz (trial 3), the phosphor should illuminate with a brightness of 300 lx (blue) and 400 lx (green) [152]. The phosphor used in these trials was blue-green so it should illuminate with a brightness somewhere in between those values. The illuminance achieved by these thick film devices was a fraction of the suggested value (56.92 lx at 100 V and 400 Hz); this shows that perhaps they were not constructed to a high enough standard but they will still offer a good comparison to other devices. The bought device only achieved 111 lx under the trial 3 operating conditions so it could also suggest that the Electra Polymers brightness values may be a little optimistic.

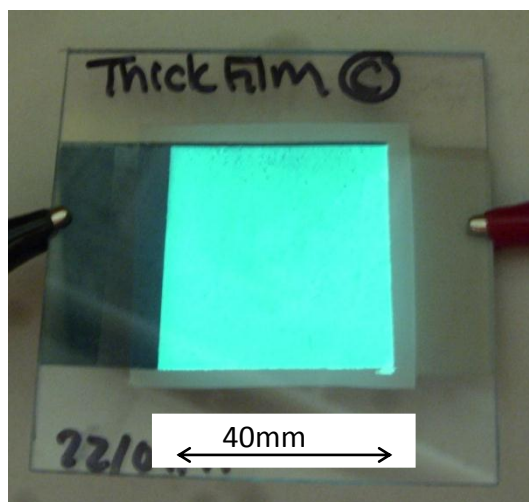


Figure 11-4: A thick film device, illuminated.

From Table 11-4 it can be seen that the group of thick film devices have larger RSD than the bought device; the RSDs range from a reasonable 7.56 % to a fairly high 20.47 %. Although these devices are made by hand, which would increase the variation in manufacture; there is a more important reason for the increase in RSD. Given that there was only one device in the “bought” group, and 5 devices in the other groups; it is reasonable to assume that there is going to be more variation in illuminance between different devices than the illuminance of one.

Table 11-4: Average illuminance results and standard deviation of the group of thick film devices.

Trial	Parameter		Illuminance (lx)				RSD (%)
			av	SD	av-SD	av+SD	
	F	V					
1	+	+	169.0	13.03	155.9	182.0	7.71
2	-	+	56.92	4.300	52.62	61.22	7.56
3	+	-	18.88	3.866	15.01	22.75	20.47
4	-	-	7.360	1.469	5.891	8.829	19.95

The separate averages, SDs and RSDs of individual thick film devices are shown in Table 11-5. By looking at group and individual statistics it can be seen if the variation in illuminance is across the group or within each device.

Table 11-5: The averages, SDs and RSDs of individual thick film devices.

Trial	Device A			Device B			Device C			Device D			Device E		
	av (lx)	SD (lx)	RSD (%)	av (lx)	SD (lx)	RSD (%)	av (lx)	SD (lx)	RSD (%)	av (lx)	SD (lx)	RSD (%)	av (lx)	SD (lx)	RSD (%)
1	155.6	2.88	1.85	168.4	3.78	2.25	176.6	5.77	3.27	156.4	2.70	1.73	187.8	4.32	2.30
2	57.2	3.11	5.44	59.0	2.45	4.15	58.8	1.64	2.79	49.6	1.14	2.30	60.0	1.58	2.64
3	12.6	1.14	9.05	19.2	1.30	6.79	23.4	1.14	4.87	18.2	1.30	7.16	21.0	1.58	7.53
4	5.2	0.45	8.60	7.4	0.55	7.40	9.2	0.45	4.86	6.8	0.45	6.58	8.2	0.84	10.20

The RSD values for individual devices are much smaller than the group values indicating that the variation is across the group. Some of the individual device RSDs

are comparable to those calculated for the bought device suggesting these devices also emit a consistent level of light but trials 3 and 4 have much higher values. This can be explained by the fact that the mean values for trials 3 and 4 are low, so even a small standard deviation represents a large percentage of the small mean. For example, Device A: Trial 4 has a standard deviation of just 0.45 lx, however with a mean of just 5.2 lx the RSD calculates to a moderate 8.6 %. Another factor affecting the SD of trials 3 and 4 is in the method of measurement. The light meter measured brightness in integer values, so a variation of one digit has a greater effect on the SD of a group of low value numbers than a group of high value numbers.

The variation that occurs when lighting a single device was due to the same factors affecting the bought device. The one factor that would have an increased effect in the handmade devices is the position of the device under the light meter; there is slight variation in the brightness across the surface of the thick film lamp which could cause variation in the measurements. However, it can be assumed the variation that occurs between devices is due to inconsistencies in the manufacturing process since these were all made by hand.

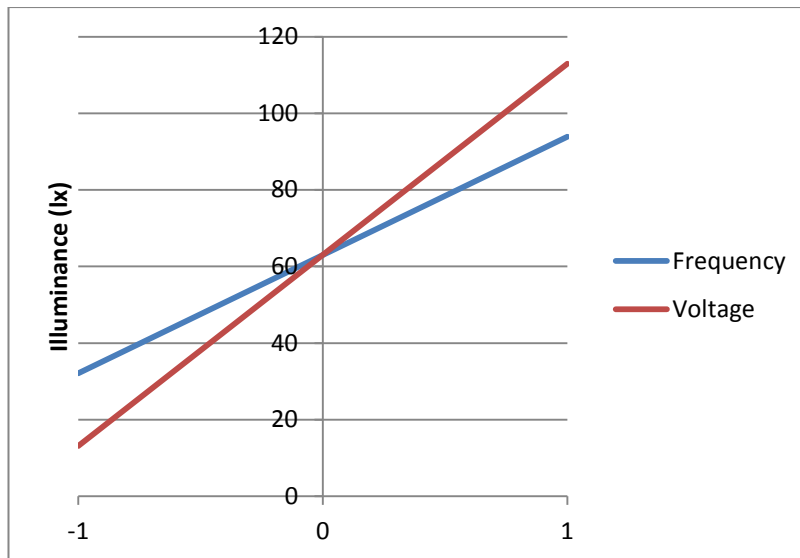


Figure 11-5: The main effects of frequency and voltage on the illuminance of the thick film devices.

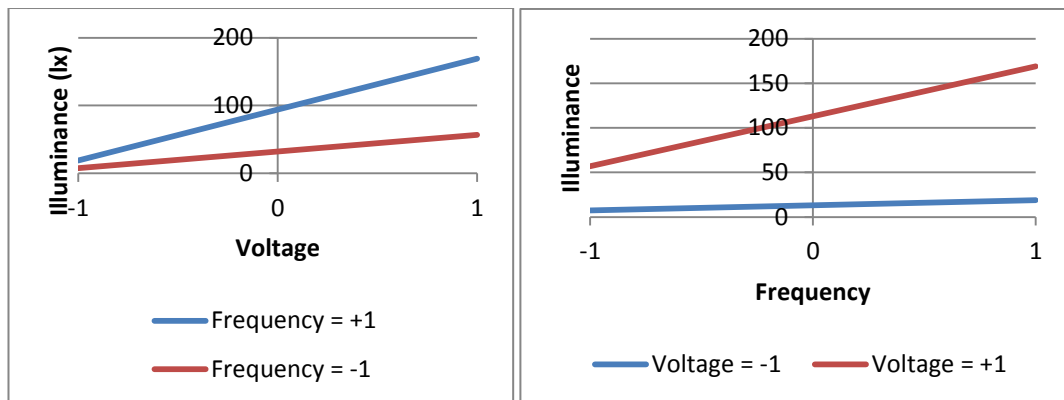


Figure 11-6: The interactions between voltage and frequency on the thick film devices.

Similarly to the bought device, voltage has a greater effect than frequency on the illuminance of the thick film devices, however to a greater degree (see Figure 11-5). Frequency has a 61.78 lx effect and voltage has a 99.82 lx effect; these were calculated using the same method as the bought device. Once again there is an interaction between voltage and frequency (see Figure 11-6); a change in voltage has a greater effect at high frequencies and vice versa.

11.1.1.3 Airbrush Devices

The airbrush devices were made using the modified materials and example of one can be seen in Figure 11-7. Again in this analysis, the RSD of the group of materials and the individual devices are examined.

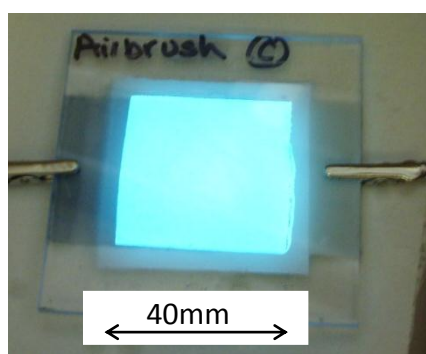


Figure 11-7: An airbrush device, illuminated.

From Table 11-6, it can be seen that the modified materials applied using an airbrush produced much brighter devices. At the highest operating conditions the airbrush devices are on average 70 % brighter than the thick film devices; but they still only emit light just over 60 % of the brightness of the bought device.

Table 11-6: Average illuminance results and standard deviation of the group of airbrushed devices.

Trial	Parameter		Illuminance (lx)				RSD (%)
	F	V	av	SD	av-SD	av+SD	
1	+	+	287.9	35.22	252.7	323.1	12.23
2	-	+	80.80	5.845	74.95	86.65	7.23
3	+	-	66.85	6.722	60.13	73.57	10.06
4	-	-	21.71	1.678	20.03	23.39	7.73

From Table 11-6, it can be seen that the RSDs of the airbrush trials (~7-12 %) are generally lower than those of the thick film devices (~7-20 %), indicating a lower

variation across the group, which may mean it is a more consistent manufacturing method.

Table 11-7: The averages, SDs and RSDs of the illuminance of individual airbrush devices; device E has been omitted since it failed after one test.

Trial	Device A			Device B			Device C			Device D		
	av (lx)	SD (lx)	RSD (%)									
1	284.2	6.22	2.19	307.4	3.97	1.29	325.0	7.42	2.28	235	8.46	3.60
2	76.2	2.39	3.13	84.0	3.94	4.69	87.4	2.70	3.09	75.6	2.51	3.32
3	60.2	1.92	3.20	62.4	2.30	3.69	68.2	1.10	1.61	76.6	1.82	2.37
4	20.4	1.52	7.43	20.4	0.55	2.68	22.8	1.30	5.72	23.4	0.55	2.34

Looking at the RSD values in Table 11-7, many are a similar magnitude to the bought device (up to 4 %) showing that these devices emit a fairly consistent light level when operated at certain power levels. As with the thick film method, any variation in the illuminance of individual devices is most likely due to the lack of uniformity in light emission across the surface and slight discrepancies in F and V measurements. The variation across the group is probably due to differences in layer application; although all devices were made using the airbrush, the material coverage was judged by eye and is therefore open to error. Since the insert moulded, in-mould and post mould devices are all based on the basic airbrush method it will be particularly useful to compare those results to this set.

Once again the voltage had a greater effect on the illuminance than frequency, as seen in Figure 11-8; but there is less of a difference than with the thick film device. Frequency affected the illuminance by 126 lx and voltage affected it by 140 lx.

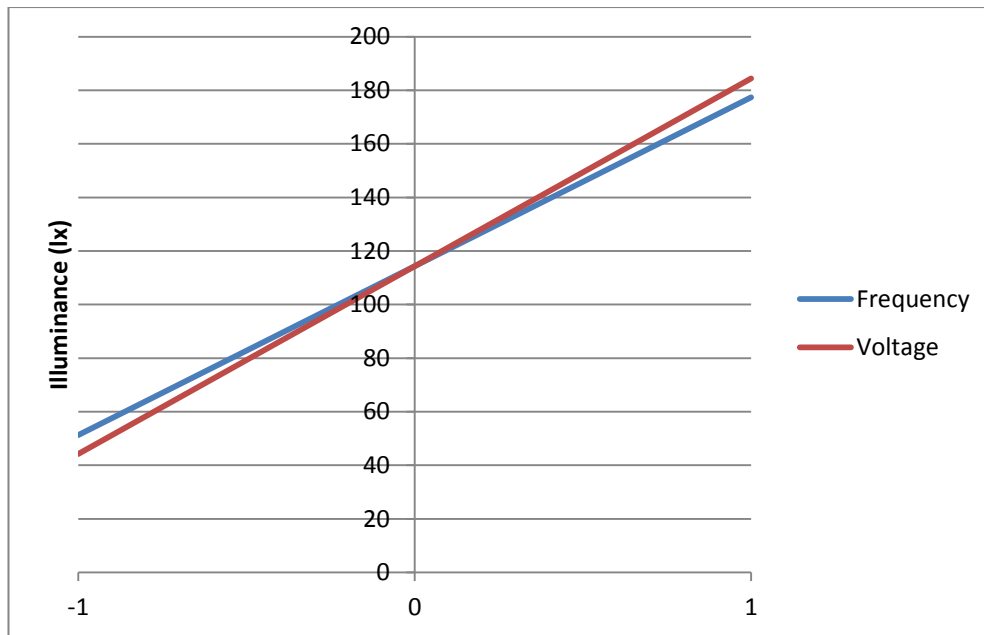


Figure 11-8: The main effects of frequency and voltage on the illuminance of the airbrush devices.

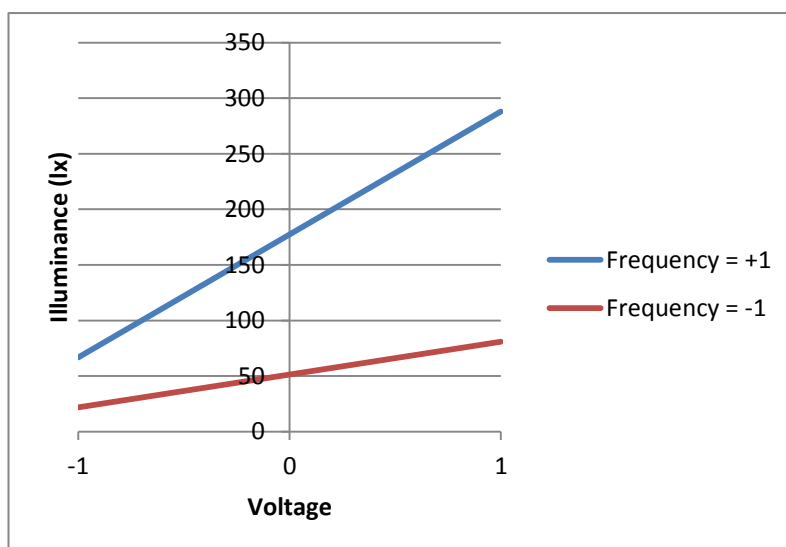


Figure 11-9: The interactions between voltage and frequency on the airbrush devices.

Again, similarly to the thick film device, there is an interaction between frequency and voltage. It can be seen that a pattern is emerging; whilst there is an interaction between the two variables, the operating voltage has a greater main effect on the illuminance of the devices and this is true for the bought device and the ones made in-house. It is also clear that the devices made in-house are not emitting an equivalent level of light as the bought device.

11.1.1.4 PE Insert Moulded

The PE moulded inserts performed quite badly in the illuminance tests; Table 11-8 shows that the illuminance (at the highest operating parameters), is less than half of that of the unmoulded airbrush devices. Not only were the PE insert moulded devices much duller than the basic, unmoulded airbrushed ones but there is a huge variation across the group. Each trial has a RSD of over 20 % showing there is little consistency of the performance of devices made using this method. Once again the results of each individual device were analysed; this data can be seen in Table 11-9.

Table 11-8: Average illuminance results and standard deviation of the group of PE insert moulded devices.

Trial	Parameter		Illuminance (lx)				RSD (%)
	F	V	av	SD	av-SD	av+SD	
1	+	+	132.6	29.18	103.4	161.8	22.00
2	-	+	57.40	13.43	43.97	70.83	23.40
3	+	-	39.06	9.718	29.34	48.78	24.88
4	-	-	12.82	2.899	9.924	15.72	22.61

By examining the data from individual devices (Table 11-9) a number of important points can be made:

- The process appears to be very unreliable; out of five devices, A failed to illuminate, D failed before the end of the tests, and of the working devices C has an average brightness considerable lower than B and E.
- The working devices have fairly low individual RSDs, indicating each illuminates with consistent brightness.
- The high RSD value for device C: trial 4 can be partly attributed to a low average value.

- The very low brightness achieved by device D increased the group’s overall variation by a considerable amount, resulting in high RSD values for the group.

Table 11-9: The averages, SDs and RSDs of the illuminance of individual PE insert moulded devices; device A has been omitted because it didn’t work.

Trial	Device B			Device C			Device D			Device E		
	av (lx)	SD (lx)	RSD (%)	av (lx)	SD (lx)	RSD (%)	av (lx)	SD (lx)	RSD (%)	av (lx)	SD (lx)	RSD (%)
1	161.6	2.41	1.49	100.0	2.12	2.12	85.0	N/A	N/A	143.8	3.56	2.48
2	71.2	2.86	4.02	40.4	2.88	7.13	N/A	N/A	N/A	60.6	1.67	2.76
3	49.8	2.39	4.79	29.6	1.34	4.53	26.0	2.83	10.88	43.0	2.74	6.37
4	15.8	0.84	5.30	9.8	1.48	15.14	9.5	0.71	7.44	14.2	0.45	3.15

Overall, the PE insert moulded devices were much duller than the ones where materials were airbrushed directly onto PC. Individually devices illuminated consistently but there was little reliability across the group; there is a lot of variation in the level of illuminance between devices and a high failure rate.

Once again variation between devices is probably due to the differences in the hand manufacture of each of the inserts, but also because of the additional stage of injection moulding. Although moulding parameters were kept the same for each cycle, a slight change in the position of the insert within the mould could result in very different flow behaviours over the insert. There is also a possibility the conditions endured by the materials during the injection moulding cycle are causing the reduction in illuminance between these and the un-moulded airbrush devices.

The PE insert moulded devices followed the same pattern set by the previous devices; there is an interaction between the parameters tested and of the two, voltage had a greater main effect (69 lx compared to 51 lx for frequency).

11.1.1.5 *PTFE Insert Moulded*

An example of a PTFE insert moulded device is shown in Figure 11-10, and although the illuminance of these devices (~210 lx) was not at the same level as the airbrush devices (~288 lx) they are much brighter than the PE insert moulded parts (~133 lx). This suggests that the injection moulding cycle conditions do not have such a detrimental effect on the illuminance of devices as first thought; the variation is more likely to be due to the lack of repeatability of the hand operated airbrush layer application. If the cycle conditions were the cause of the low illuminance of the PE inserts then similar illuminance levels should be seen here, but they are not (see Table 11-10).

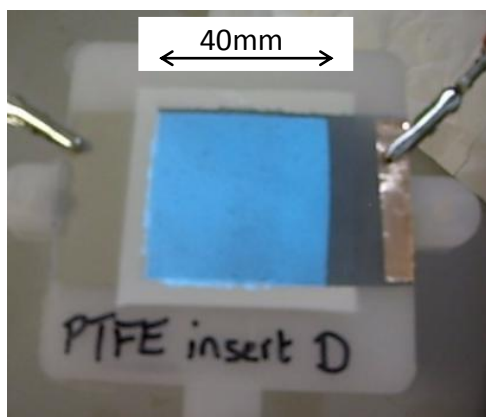


Figure 11-10: A PTFE insert moulded device, illuminated.

At the highest operating conditions the PTFE inserts moulded devices are on average over 58 % brighter than the PE inserts and the lower RSDs shown in Table 11-10 show there is less variation in illuminance across the groups, indicating greater illuminance reliability using this method of production. However, 18 % is

still a high RSD so individual data will also be examined; this is shown in Table 11-11.

Table 11-10: Average illuminance results and standard deviation of the group of PTFE insert moulded devices.

Trial	Parameter		Illuminance (lx)				RSD (%)
	F	V	av	SD	av-SD	av+SD	
1	+	+	210.2	39.22	171.0	249.4	18.66
2	-	+	63.00	11.84	51.16	74.84	18.79
3	+	-	53.40	4.664	48.74	58.06	8.73
4	-	-	15.92	1.498	14.42	17.42	9.41

Studying the individual illuminance results for the PTFE insert moulded group of devices (in Table 11-11) it can be seen that device B was the brightest achieving an average of approximately 255 lx under trial 1 conditions; looking back at section 11.1.1.3, device D made using the airbrush method, under the same operating conditions, achieved a brightness of 235 lx. This confirms that the injection moulding process does not have a significant negative effect on the light emission and that the variation in illuminance is probably due to inconsistencies in the hand manufacture of layer structure.

Table 11-11: The averages, SDs and RSDs of the illuminance of individual PTFE insert moulded devices.

Trial	Device A			Device B			Device C			Device D			Device E		
	av (lx)	SD (lx)	RSD (%)	av (lx)	SD (lx)	RSD (%)	av (lx)	SD (lx)	RSD (%)	av (lx)	SD (lx)	RSD (%)	av (lx)	SD (lx)	RSD (%)
1	246.4	8.02	3.25	254.6	4.98	1.96	149.4	2.51	1.68	207.6	3.05	1.47	193.0	4.85	2.51
2	75	2.00	2.67	73.0	2.35	3.21	43.0	2.55	5.93	63.6	1.52	2.38	60.4	2.88	4.77
3	54.4	1.82	3.34	58.4	2.30	3.94	47.4	3.13	6.60	50.6	3.29	6.49	56.2	2.05	3.65
4	16.6	0.89	5.39	17.4	0.89	5.14	13.8	0.84	6.06	15.2	0.45	2.94	16.6	0.89	5.39

The RSD values of individual devices are again quite low, showing that parts made using this method illuminate consistently at particular operating conditions.

The PTFE insert moulded devices once again continued the main effects and interaction pattern; there is an interaction between the voltage and frequency, and voltage had a greater main effect (102 lx compared to 92 lx for frequency).

11.1.1.6 *In-Mould Layer Application*

Although a method has been developed to make an EL device in-mould, and illuminating parts have been made, it is clear from the data in Table 11-12 and Table 11-13 that currently the process is flawed and very unreliable. The average illuminance at the highest operating conditions was merely 45 lx, only 15 % of the illuminance of the basic, unmoulded airbrush group. The large RSDs for all trials in Table 11-12 show a huge variation in illuminance between parts made using this process. Individual device data is shown in Table 11-13 but little more can be analysed since much of the data is missing due to device failure.

Table 11-12: Average illuminance results and standard deviation of the group of in-mould devices.

Trial	Parameter		Illuminance (lx)				RSD (%)
	F	V	av	SD	av-SD	av+SD	
1	+	+	44.67	14.22	30.44	58.89	31.85
2	-	+	19.75	7.320	12.43	27.07	37.06
3	+	-	12.00	4.690	7.310	16.69	39.09
4	-	-	7.333	3.077	4.257	10.41	41.96

Only three out of the five parts illuminated over the whole area of the EL device and all of those failed at the highest operating conditions; because of this, large amounts of data are missing and averages and SDs could not be calculated. In Table 11-13, of the SD values that are shown, only device B trial 2 and 4 have 3 values, the rest are only calculated from two values and as such are not true standard

deviations but give an indication of the data range. From the RSDs that were calculated (shown in Table 11-13), the values are quite high indicating that even individual devices do not consistently illuminate. There is also the fact that at such low values, a one digit change has a greater effect on the SD and RSD than on high value groups.

Table 11-13: The averages, SDs and RSDs of the illuminance of individual in-mould devices; device A has been omitted because it only partially illuminated and D because it failed to illuminate.

Trial	Device B			Device C			Device E		
	av (lx)	SD (lx)	RSD (%)	av (lx)	SD (lx)	RSD (%)	av (lx)	SD (lx)	RSD (%)
1	38.00	N/A	N/A	35.00	N/A	N/A	61.00	N/A	N/A
2	16.33	3.21	19.68	N/A	N/A	N/A	30.00	N/A	N/A
3	9.00	1.41	15.71	8.00	N/A	N/A	17.00	1.41	8.32
4	5.67	1.53	26.96	5.00	N/A	N/A	11.00	1.41	12.86

From the data that was collected, the in-mould moulded devices followed the same pattern as the others; there is an interaction between the two test parameters and voltage had a greater main effect (23 lx compared to 15 lx for frequency).

Overall, from this characterisation analysis it can be seen that this method in its current state of development is only capable of unreliably producing relatively dim devices that cannot operate at high voltages.

11.1.1.7 Post Mould Layer Application

The plastic parts that had the EL layer materials added as a post mould process were also characterised (one example can be seen in Figure 11-11) and although all of the parts illuminated successfully, the light that they emitted was not as bright as the basic airbrushed devices on PC. At the highest operating conditions the post mould devices were only 41 % the brightness of the basic airbrushed device.

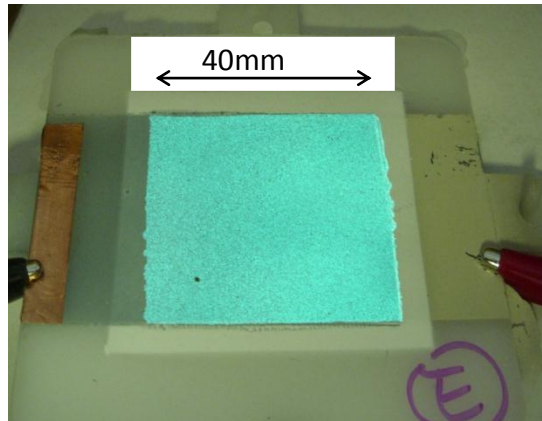


Figure 11-11: A post mould device, illuminated.

The RSDs of the four trials performed on the post mould group of devices, are shown in Table 11-14 and are all over 35 %; this shows that there is huge variation within the group.

Table 11-14: Average illuminance results and standard deviation of the group of post mould devices.

Trial	Parameter		Illuminance (lx)				RSD (%)
	F	V	av	SD	av-SD	av+SD	
1	+	+	119.1	45.66	73.46	164.8	38.33
2	-	+	33.84	12.16	21.68	46.00	35.95
3	+	-	34.72	12.64	22.08	47.36	36.42
4	-	-	11.16	3.965	7.194	15.13	35.53

Most of the RSDs for individual devices are fairly low (below 8 %) showing that each device illuminated consistently and that the high group RSDs are due to a large variation between parts. The illuminance of devices during trial 1 range from 69 lx to 192 lx confirming the large variation; once again this likely to be due to differences during layer application since there is no real processing difference between the post mould and basic airbrush method. Trial 2 on device A has a higher

RSD than others but since this is an isolated result it is more than likely due to human error when taking and/or recording measurements.

Table 11-15: The averages, SDs and RSDs of the illuminance of individual post mould devices.

Trial	Device A			Device B			Device C			Device D			Device E		
	av (lx)	SD (lx)	RSD (%)	av (lx)	SD (lx)	RSD (%)	av (lx)	SD (lx)	RSD (%)	av (lx)	SD (lx)	RSD (%)	av (lx)	SD (lx)	RSD (%)
1	69.00	2.00	2.90	115.00	3.81	3.31	141.00	2.35	1.66	192.00	4.74	2.47	78.60	3.44	4.37
2	22.00	2.55	11.59	33.40	2.07	6.21	40.80	2.49	6.10	52.00	3.74	7.20	21.00	1.58	7.53
3	22.80	1.30	5.72	34.40	1.95	5.67	39.40	2.30	5.84	55.20	3.11	5.64	21.80	0.84	3.84
4	7.40	0.55	7.40	10.80	0.45	4.14	13.40	0.89	6.67	17.20	1.30	7.58	7.00	0.00	0.00

The post mould layer application devices had an interaction between the parameters tested, just as the other devices did but out of voltage and frequency there was little difference in the effect of each on illuminance (both at approximately 54 lx).

11.1.1.8 Using a Battery and Inverter

An inverter was also used to measure the illuminance of a number of the characterised devices when they are powered by batteries (a non-characterised part is shown in Figure 11-12); this was done to determine whether the brightness when operated by a battery is comparable to when the device is driven by the HV AC supply.

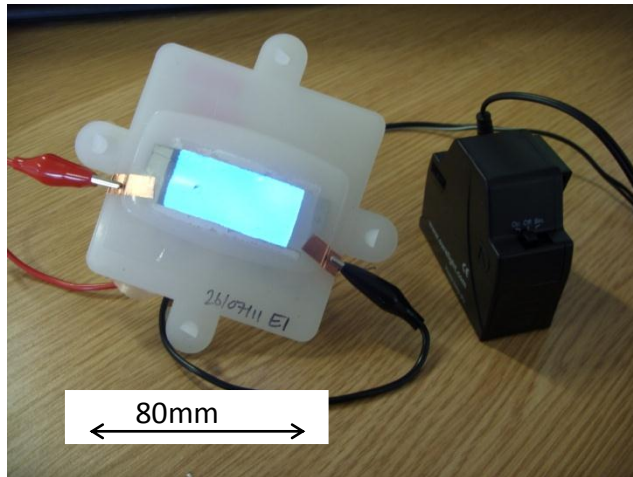


Figure 11-12: A curved PTFE insert moulded device operated by batteries and an inverter.

Four AAA (1.5 V) batteries were used, which had a total voltage of 6 VDC; when connected to the inverter, the AC supply was measured as 122 V and 4 kHz (this was measured using a hand held oscilloscope). The devices selected to compare were:

- The bought device because this is likely to be the most reliable device to test,
- An airbrush applied method because this is the brightest device that utilises the modified materials, and
- A PTFE insert moulded device because out of all of the moulded devices the PTFE insert produced the brightest light.

The results for these tests are shown in Table 11-16; it can be seen that in each case, when operated using the batteries and inverter, the devices emitted light 90 % or more of the brightness compared to when they are at the highest operating conditions on the AC power supply.

Table 11-16: The illuminance of 3 devices when operated using batteries and an inverter.

Device Tested	Illuminance (lx)		Comparison % illuminance (batteries & inverter compared to AC supply)
	Operated by AC supply: 300V & 400Hz	Operated by batteries & inverter: 122V & 4kHz	
Bought	467	419	90
Airbrush	288	266	92
PTFE insert moulded	210	201	96

So far in this analysis, in almost every group of devices the voltage has the greater effect on the illuminance however this test shows that if a sufficiently high frequency (4 kHz) is used, a near equivalent illuminance ($\geq 90\%$) can be achieved even at a low voltage (122 V). This shows that the voltage only has a greater effect than frequency over the operating range suggested on the H C Starck processing guide [148]. This implies that in order to draw more reliable conclusions about the main effects of voltage and frequency, further experimentation should be carried out using *Design of Experiments* to include a greater number of levels over a larger range for both parameters.

11.1.1.9 Illuminance Comparisons

As well as independently analysing the data from each group of devices it is also useful to compare them. Both the average magnitude of the illuminance and the variation within each group were compared; this will help to determine the most successful process (the method that produces the brightest devices and has the lowest variation) developed during this project. Figure 11-13 shows a graph comparing the illuminance of the light emitted by each group of devices.

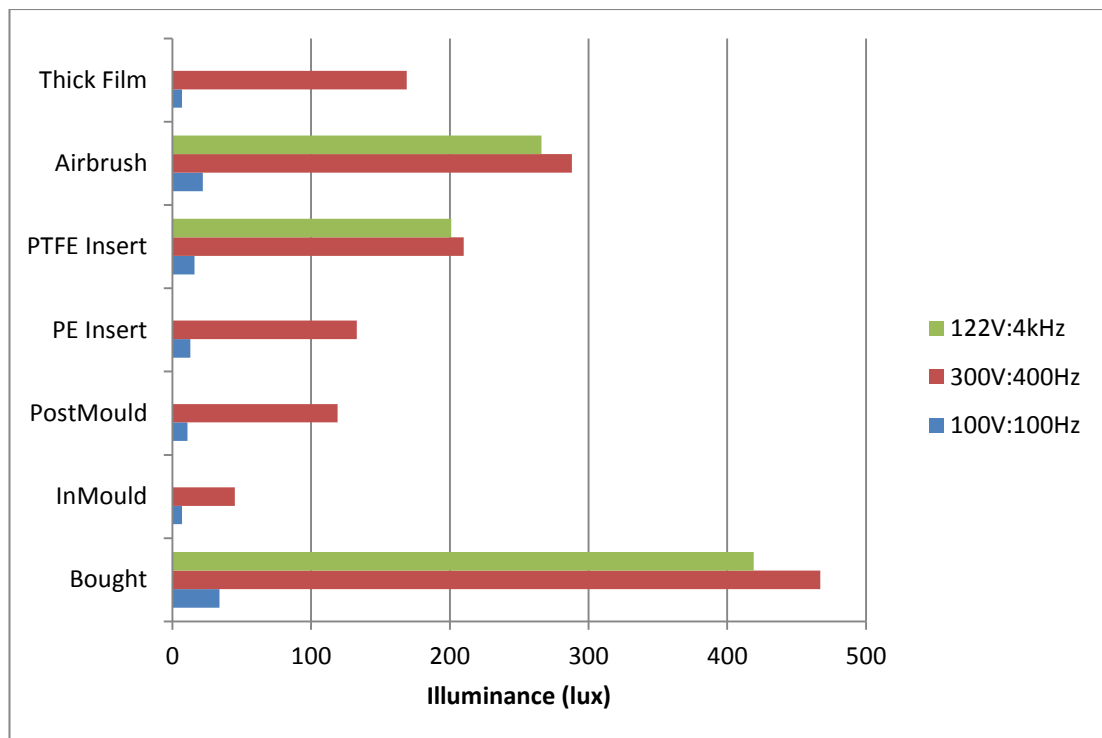


Figure 11-13: The average illuminance of each group of devices under different operating conditions.

Clearly Figure 11-13 shows that the bought device emits a significantly brighter light than any of the devices made in-house and it also shows that the novel airbrush application method developed during this project (using the MEK modified materials) produces brighter devices than those made using the thick film method. Figure 11-13 also shows that the brightest injection moulded devices are the ones made using the PTFE insert moulding method. However, it also confirms that the in-mould method makes devices that emit the lowest light levels, by a significant amount.

The basic airbrush, PTFE and PE insert moulding, post mould and in-mould methods all utilise airbrush spraying as the layer application method, however they all have different average illuminance levels. The most likely explanation for this variation

(both between and within groups) is a difference in structure caused by inconsistencies in manual manufacture.

The second part of this analysis is the comparison of the variation within each group; Figure 11-14 shows the RSDs of each group of devices for each trial.

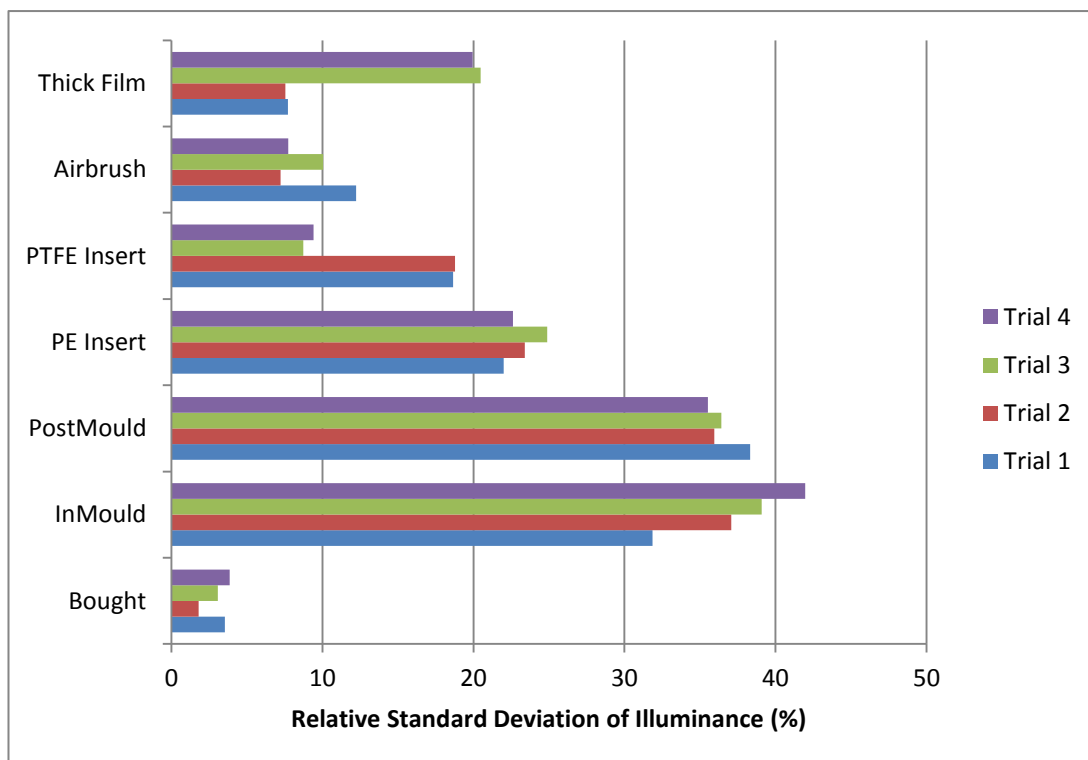


Figure 11-14: The relative standard deviation of each group of devices.

Unsurprisingly the bought group has the lowest variation, however as explained earlier this group contains only one device and therefore it will have a lower variation than a number of different devices. To make a fairer comparison between the commercially available EL lamps and the devices made in-house, a number of different bought devices should be characterised so that the variation within the group can be calculated. This is because if the newly developed methods are to compete with existing process techniques, it is not only important to match the

average magnitude of illuminance of the parts but also in the reliability with which that process can produce a device that emits that level of light. Therefore, it is important to note that the variation of a group of bought devices is likely to be greater than that shown in the graph.

Figure 11-14 shows that the greatest variation in illuminance occurs in the groups made using the post mould and in-mould processes; this indicates that these methods are the least repeatable. Even though the post mould process produces parts with a large variation in the illuminance, every part successfully illuminated (even at high voltages) and this is in sharp contrast to the in-mould devices, that all failed either before or during characterisation. Of the two different insert moulding groups, the PE inserts had a larger variation in the illuminance of the group and had a higher failure rate than the PTFE inserts implying that it is currently a more unreliable process. When comparing the thick film and basic airbrush methods the variation within each group is fairly comparable (when taking into account the large RSD values resulting from the small averages in the thick film group), however the airbrush method produced brighter devices. Overall, when comparing the level of illuminance and reliability with which that method can produce that illuminance, the hand-made methods used during this project are rated best to worst as:

1. Basic Airbrush Method
2. Thick Film Method
3. PTFE Insert Moulded
4. Post Mould Layer Application
5. PE Insert Moulding

6. In-Mould Layer Application Method

Therefore the injection moulding technique that is the most reliable and produces the brightest parts is the PTFE insert moulding technique; this list also shows that applying EL layers as a post mould or retrospective technique is a viable option.

11.1.2 Layer Thickness

Although the illuminance of the parts is the primary characteristic by which the devices and processing methods are judged, it is also important to measure the thicknesses of the layer applied using each technique. These measurements will give an indication of the reliability and repeatability of the application method and give an insight into the reasons for the differences in illuminance. The distance between the two electrodes (i.e. the combined thickness of the phosphor and dielectric layers) will affect the magnitude of the alternating electric field and as such will affect the amount of light emitted by the device.

Devices were sectioned, mounted, polished and the layer thicknesses measured under a microscope; the results and associated analysis follow.

11.1.2.1 Bought Device

The bought device was thin enough to cut with a blade before mounting so it was unnecessary to use the saw; Figure 11-15 shows a cross section of the device and an example of layer measurements taken. From Figure 11-15 it can be seen that whilst the transparent electrode, rear electrode and dielectric layer are homogeneous, the phosphor layer contains particulates of material within a uniform matrix. The presence of these phosphor particles within this layer will limit

how thin this layer can be and may have a significant effect on the variation in thickness across the individual layer and across the group.

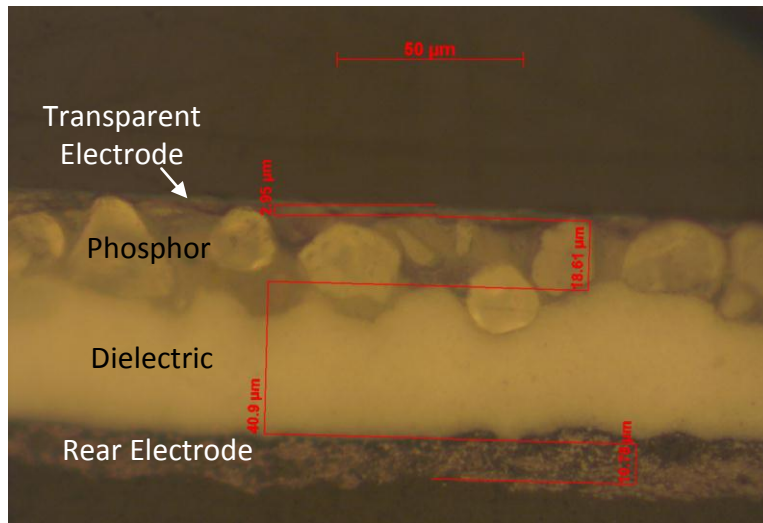


Figure 11-15: A cross section of the bought EL device.

The layer thickness was measured at five different positions and the results, averages and variation are shown in Table 11-17. The measurements were calculated by the computer but the positions were selected by eye; in each case the position that was selected had both good boundary definition and was judged to represent an “average” layer thickness of the section viewed on screen.

The dielectric layer is the thickest, followed by phosphor, silver and finally the transparent electrode is the thinnest.

The RSDs range from 6 % to 45 %, showing that even a bought device (probably made using a controlled, automated process) has a large variation in the thickness of some layers.

Table 11-17: The average, SD and RSD values of the bought device layer thickness measurements.

Layer Material	Layer Thickness (μm) at different positions							RSD (%)
	i	ii	iii	iv	v	av	SD	
Transparent Electrode	2.95	2.81	3.54	2.51	4.14	3.19	0.65	20.38
Phosphor	18.61	41.49	18.01	21.85	15.68	23.128	10.50	45.40
Dielectric	40.90	20.08	40.06	36.91	41.23	35.836	8.97	25.03
Rear Electrode	10.78	10.05	11.51	10.49	11.72	10.91	0.70	6.42

It is clear to see from Table 11-17 that the layer with the greatest variation in thickness is the phosphor; this is unsurprising since it has already been identified that the presence of “lumps” within the layer would cause a wide range of thicknesses across the coverage of the layer. The next greatest variation is within the dielectric layer. This is also to be expected since this layer is directly adjacent to the phosphor (and usually the next to be applied) and as such any fluctuations in the surface of the phosphor would affect the thickness of the dielectric material.

The transparent electrode has a quite a large RSD (~20 %), the variation in the layer thickness can be seen in Figure 11-16. The actual standard deviation is quite low (0.65 μm), but since the average layer thickness is so small it represents a large percentage of it. Part of the variation in the layer thickness could also be due to error in measurements; on such a thin layer, small discrepancies in positioning the marker by eye would have a large impact on the variation of the measurements.

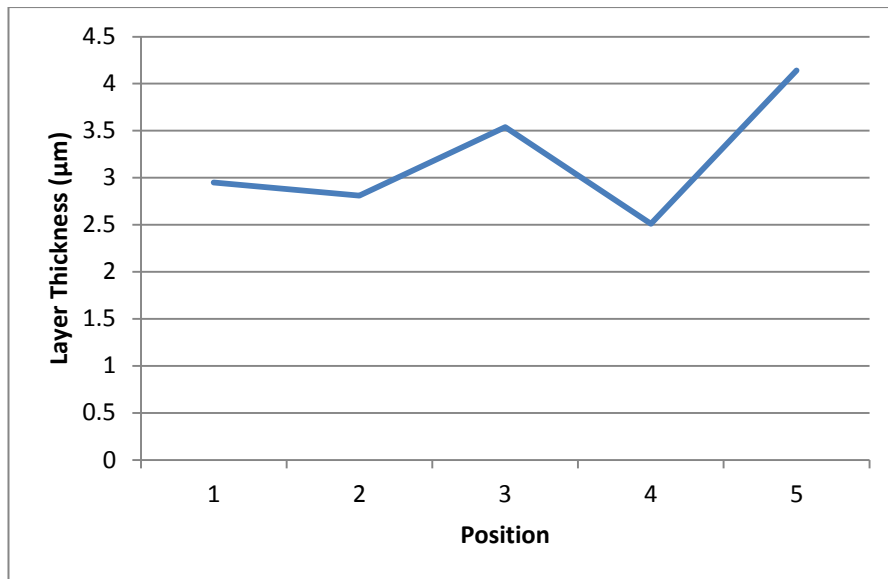


Figure 11-16: A graph showing the layer thickness of the transparent electrode at five different positions across the bought device.

The thickness of the of the phosphor layer is shown in Figure 11-17; it can clearly be seen that there is a large variation across the surface and this is most likely due to the grains of material within the layer.

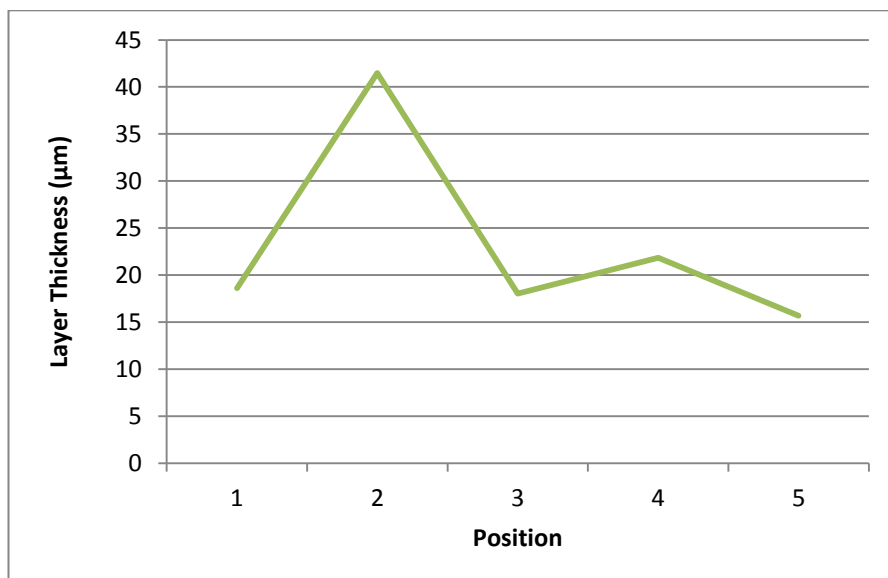


Figure 11-17: A graph showing the thickness of the phosphor layer at five different positions across the bought device.

The dielectric layer thickness is shown in Figure 11-18; this graph shows how the variation in the phosphor layer thickness has an effect on the dielectric layer. The dielectric layer is thin where the phosphor is thick and vice versa; this is because during manufacture where there was a raised “bump” in the phosphor (such as position 2) this would result in a thinner layer of dielectric to be applied in that area.

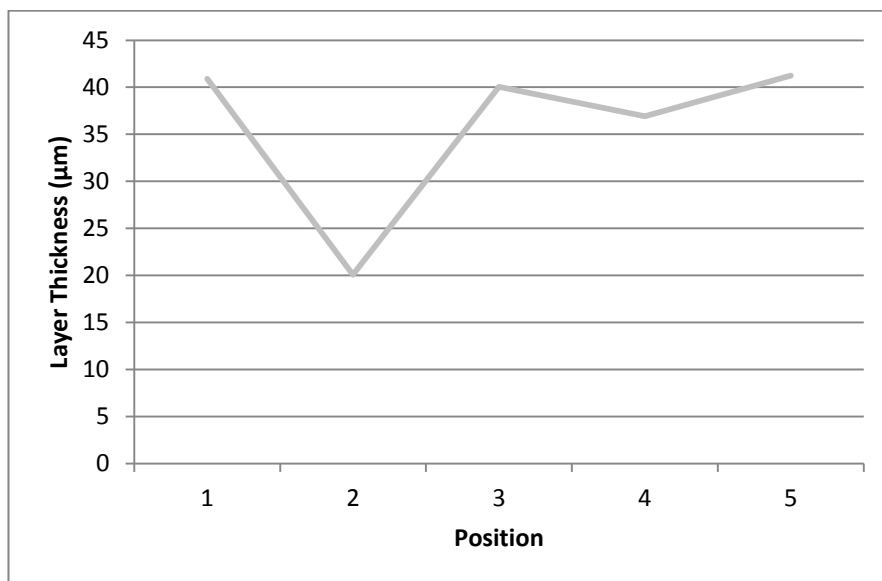


Figure 11-18: A graph showing the thickness of the dielectric layer at five different positions across the bought device.

The rear electrode has the lowest RSD value (6.42 %) indicating there is little variation in the layer thickness; this is confirmed by the graph shown in Figure 11-19.

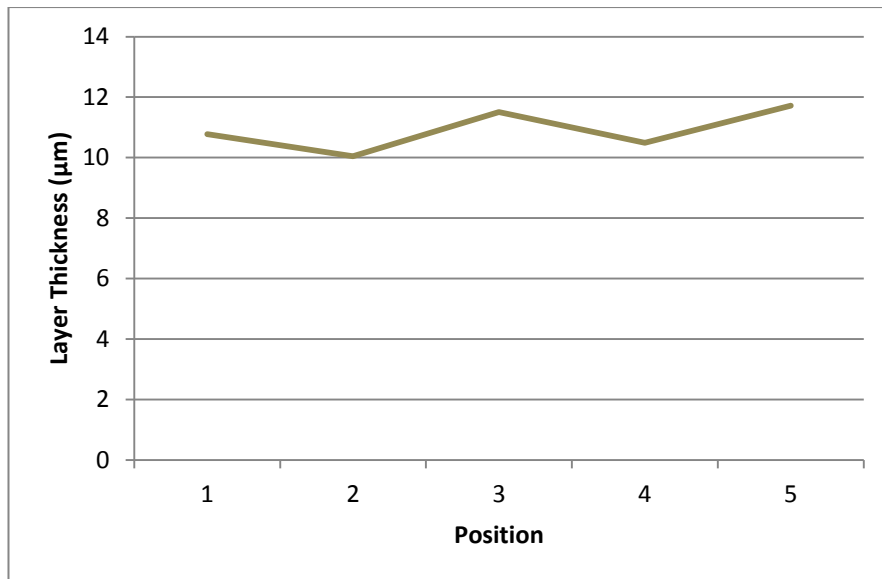


Figure 11-19: A graph showing the layer thickness of the rear electrode at five different positions across the bought device.

Overall there is a moderate amount of variation in the thickness across the individual layer of the bought device. Unfortunately since there was only one bought device it is not possible to compare the layer thicknesses between devices; this would have determined if the manufacturing method produces consistent layer thicknesses each time.

11.1.2.2 *Thick Film Devices*

The thick film devices cut well on the saw, with no damage and there was no requirement for an encapsulation layer. A cross section of a typical sample is shown in Figure 11-20; each of the layers can clearly be seen but there are a number of voids present within the phosphor layer. There are also distinct particles within the phosphor layer in these devices.

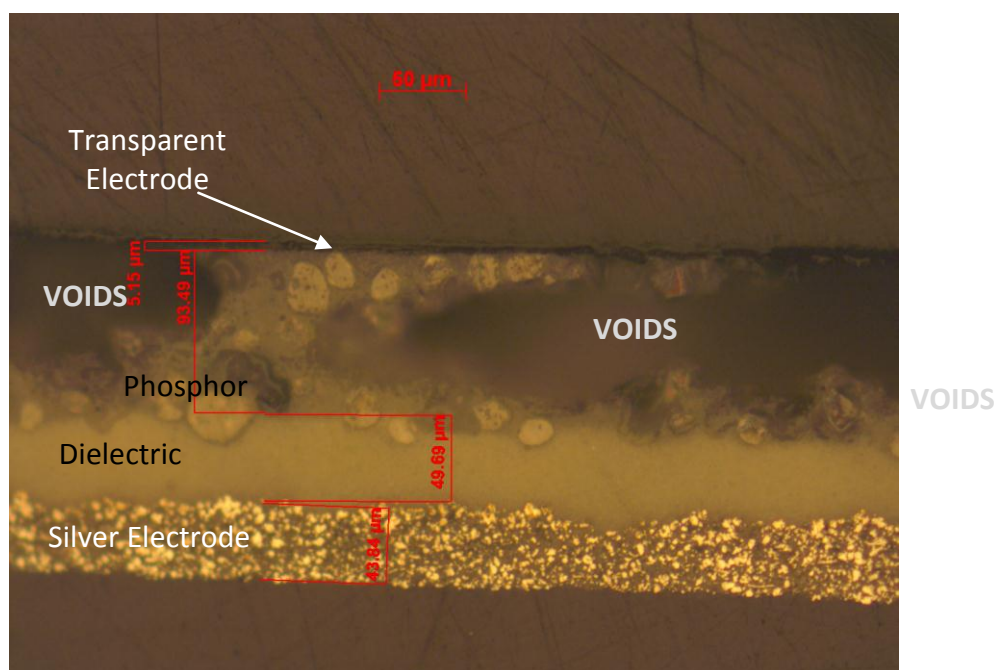


Figure 11-20: A cross section of a thick film EL device.

The individual layer thicknesses (Table 11-18) show that when devices are made using the thick film method the phosphor is the thickest layer followed by silver, dielectric and finally the PEDOT:PSS, however the phosphor measurements are likely to be an over estimate since this layer includes the voids. The presence of voids within the layer structure may contribute to the lower illuminance of the hand-made devices compared to the bought device.

Table 11-18: The average, SD and RSD values for each layer of each of the thick film samples.

Sample	Layer Thickness Data (μm)											
	PEDOT:PSS			Phosphor			Dielectric			Silver		
	av	SD	RSD (%)	av	SD	RSD (%)	av	SD	RSD (%)	av	SD	RSD (%)
A	4.57	0.88	19.26	102.5	10.14	9.89	47.72	8.71	18.26	43.98	7.14	16.23
B	6.27	1.02	16.19	88.21	25.66	29.09	62.55	12.07	19.29	68.90	6.15	8.92
C	5.08	1.59	31.38	50.54	15.24	30.16	29.98	2.23	7.44	63.93	7.38	11.54
D	5.38	0.56	10.35	80.39	18.71	23.27	41.50	13.01	31.36	61.93	4.65	7.51
E	7.95	1.18	14.80	52.68	27.03	51.30	60.50	13.60	22.49	67.45	6.21	9.21
GROUP	5.85	1.57	26.90	74.87	29.34	39.19	48.45	13.41	27.69	61.24	9.66	15.78

The large RSD values in Table 11-18 show that there is a large amount of variation in the layer thicknesses. However it is not just the group RSDs that are large but the individual devices each have quite high values for each layer; this suggests that each device displays moderate to large variation across layers in addition to there being a large difference in thickness between samples.

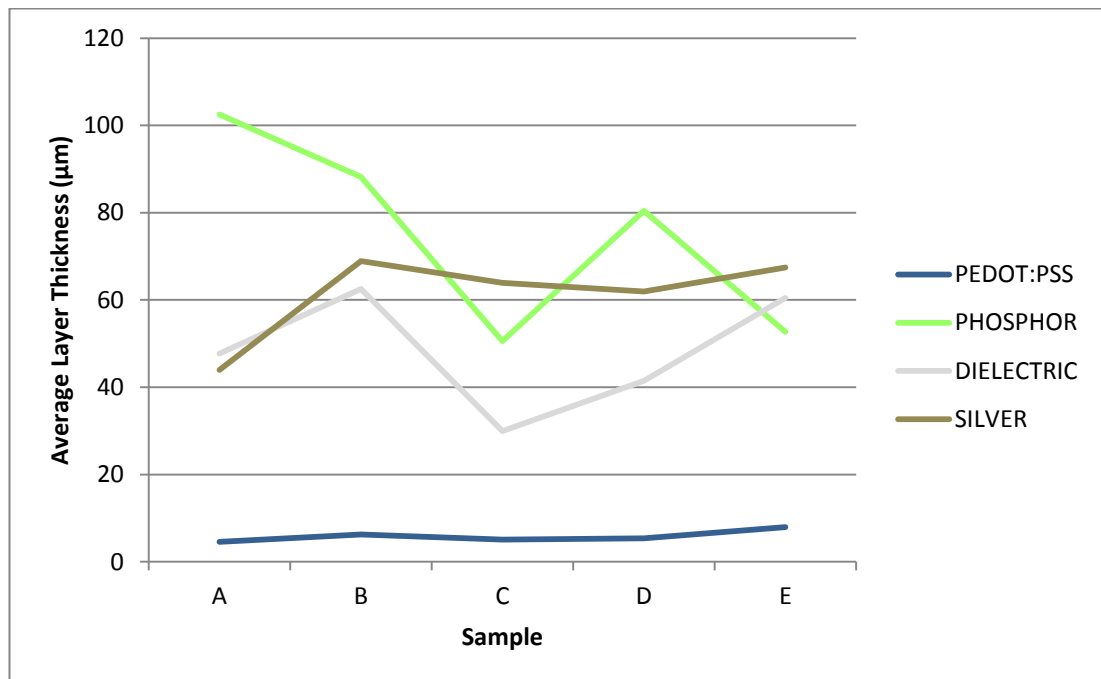


Figure 11-21: The average layer thicknesses of the thick film group.

Figure 11-21 shows the variation in average layer thicknesses across the group; the thick film method appears to apply consistent PEDOT:PSS layers and apart from sample A, there is little silver layer variation between the samples. The dielectric and phosphor layers show a large variation between samples. In order to perform further analysis, each thickness measurement was plotted, showing the variation across each layer; these can be seen in Figure 11-22 to Figure 11-25.

Figure 11-22 shows the thickness of the PEDOT:PSS layer for each sample. There is a moderate amount of variation across the layer and this is probably caused by an uneven pressure on the scraper whilst the layer was applied. Sample E is generally thicker than the others and this was probably due to the application of a lower scraper pressure during manufacture.

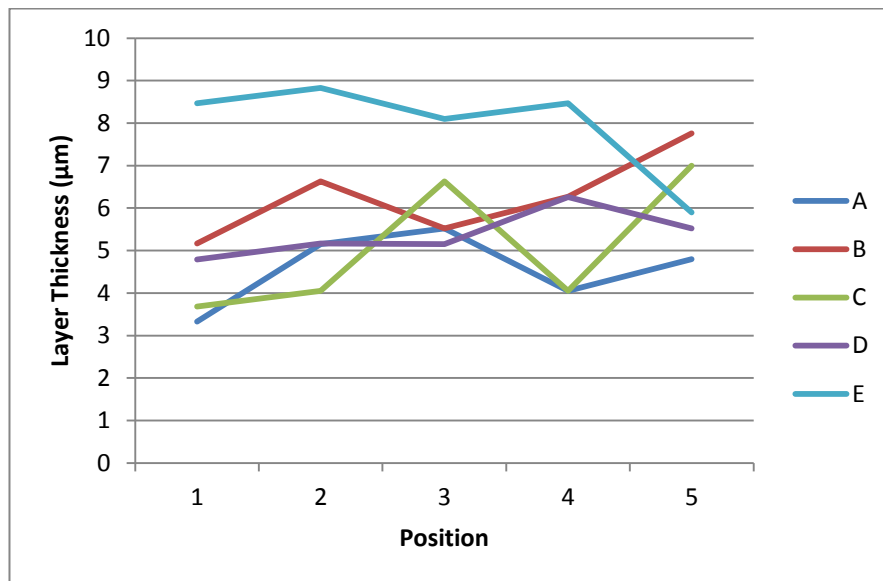


Figure 11-22: A graph showing the thickness of the PEDOT:PSS layer at five different positions across each of the thick film devices.

The phosphor layer thicknesses shown in Figure 11-23 indicates that there is a lot of variation both across each layer and in between layers. As well as the previously identified reasons of differences during manufacture there are also there added effects of the phosphor particles and the voids; these combine to produce a large variation in the phosphor layer thicknesses.

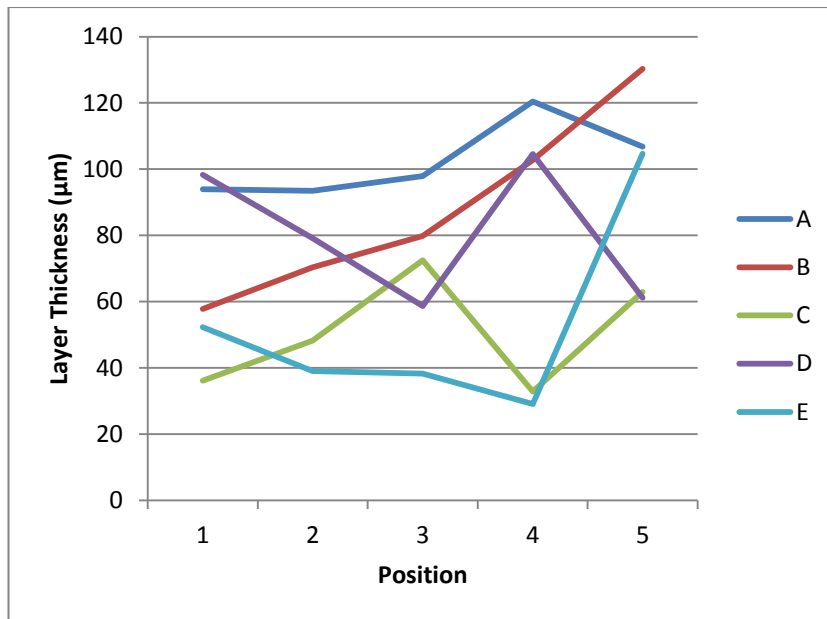


Figure 11-23: A graph showing the thickness of the phosphor layer at five different positions across each of the thick film devices.

An uneven phosphor layer could affect the next layer to be applied which was the dielectric. The dielectric layer thicknesses are shown in Figure 11-24 and it shows a moderate amount of variation across each layer.

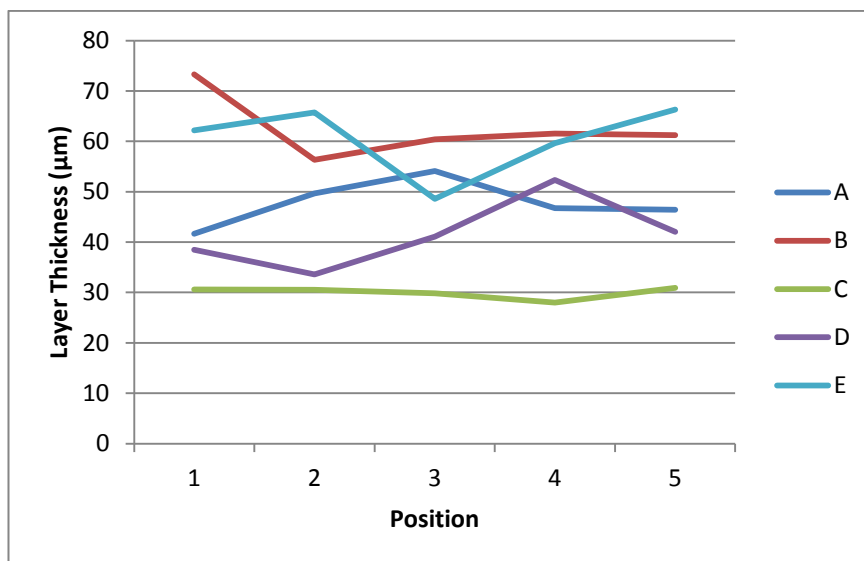


Figure 11-24: A graph showing the thickness of the dielectric layer at five different positions across each of the thick film devices.

Although there is a reasonable amount of variation across each layer, thin areas do not correspond to thick areas of the phosphor so difference in thickness of the dielectrics is likely just to be due to variation during hand layer application.

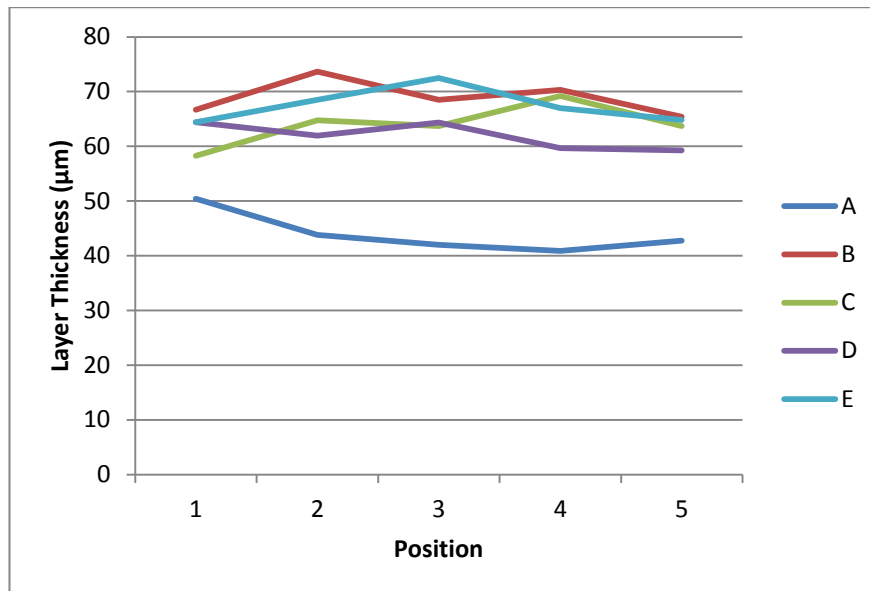


Figure 11-25: A graph showing the thickness of the silver layer at five different positions across each of the thick film devices.

The silver layers (Figure 11-25) are quite consistent across each device and most devices have silver layers of a similar thickness. Device A has a thinner silver layer than the rest of the group and this was probably caused by using an increased pressure during the layer application.

Generally the thick film layer application method applies layers with a reasonably uniform thickness and this is probably because the method utilises a template which provides some control during hand manufacture by limiting how close the rigid material applicator can get to the substrate below. There is however large

variation between devices which is probably caused by the application of different pressures to the material applicator (scraper) each time.

11.1.2.3 Airbrush Devices

The airbrush devices cut well on the saw, with no damage and no requirement for an encapsulation layer. A cross section of one device can be seen in Figure 11-26.

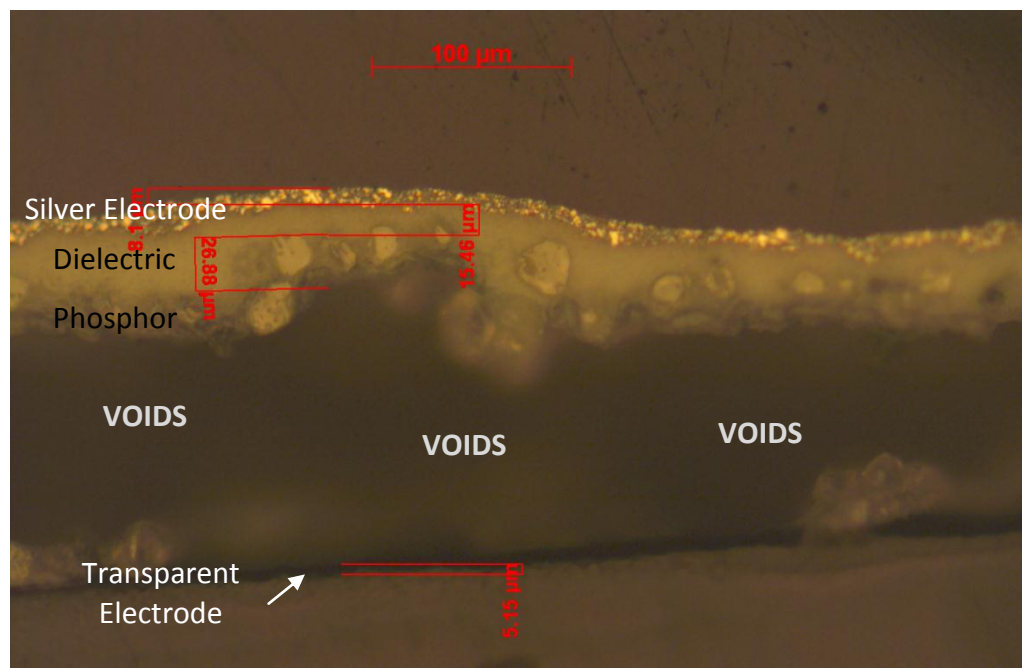


Figure 11-26: A cross section of an airbrush EL device.

Once again, the phosphor layer has distinct particles within it and there are large voids present, both of which would affect the layer thickness measurements and variation. The voids may once again have a negative effect on the illuminance level of device. The layer thickness data for the airbrush devices are shown in Table 11-19.

Table 11-19: The average, SD and RSD values for each layer of each of the airbrush samples.

Sample	Layer Thickness Data (μm)											
	PEDOT:PSS			Phosphor			Dielectric			Silver		
	av	SD	RSD (%)	av	SD	RSD (%)	av	SD	RSD (%)	av	SD	RSD (%)
A	4.55	1.15	25.20	34.16	11.25	32.93	28.76	3.79	13.19	16.19	2.59	15.99
B	5.82	1.22	20.91	36.37	11.80	32.45	15.73	1.51	9.63	13.44	5.42	40.29
C	3.40	1.14	33.64	36.98	9.25	25.01	24.33	6.85	28.15	17.62	1.87	10.63
D	5.45	0.80	14.66	23.71	5.00	21.07	16.66	1.91	11.48	13.69	3.68	26.87
E	6.49	0.50	7.77	26.96	9.42	34.94	21.92	3.86	17.59	13.30	1.72	12.91
GROUP	5.14	1.43	27.72	31.64	10.35	32.71	21.48	6.18	28.77	14.85	3.54	23.81

Similarly to the thick film devices the phosphor layer is the thickest; the average layer thicknesses can be seen in Figure 11-27. The individual and group RSDs vary suggesting an intermediate amount of variation in the thickness of layer applied using the airbrush method.

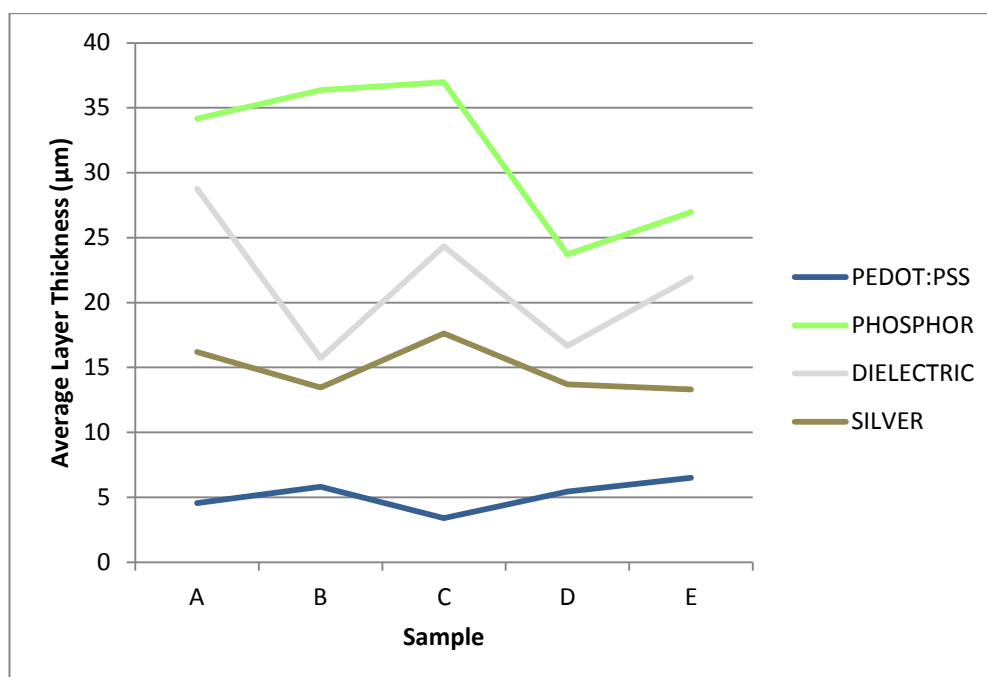


Figure 11-27: The average layer thicknesses of the airbrush group.

Following a similar pattern to the thick film devices, the phosphor and dielectric layers show more variation between samples than the PEDOT:PSS and silver. The PEDOT:PSS layer thickness measurements are shown in Figure 11-28 and this shows a greater degree of variation than thick film layers.

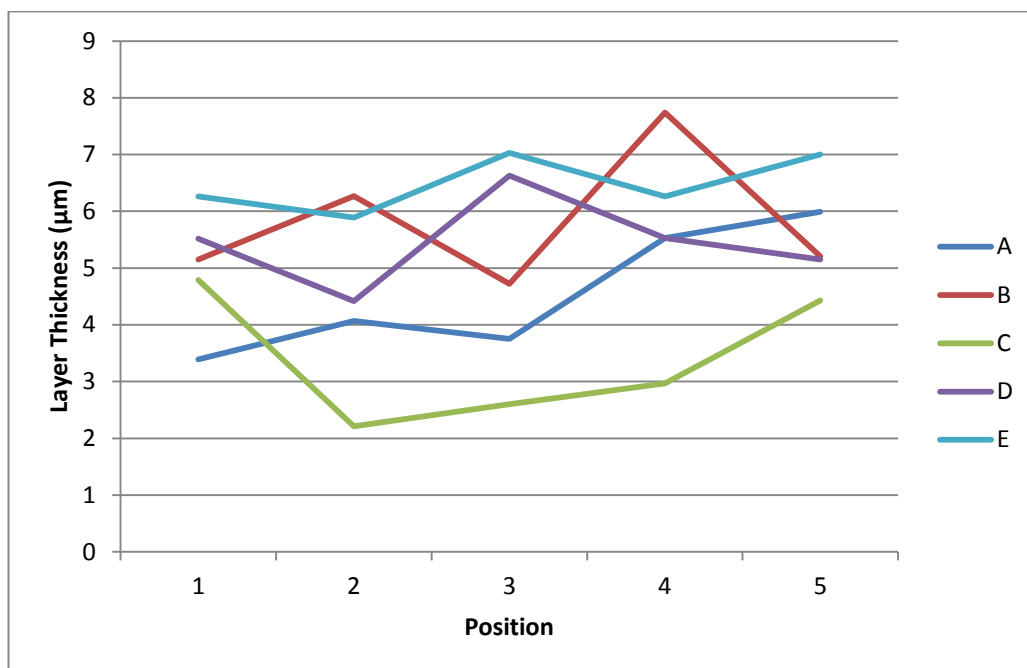


Figure 11-28: A graph showing the thickness of the PEDOT:PSS layer at five different positions across each of the airbrush devices.

One explanation for the increase in variation is that the thickness of each layer is determined by the flow of the material from the airbrush and how long the airbrush is aimed at a particular area (rather than the uniform thickness of a template). Since these devices were made by hand and during manufacture the material coverage was judged by eye, there is likely to be a large variation both across the surface of each layer and between layers on different devices. The flow rate would vary depending on the type of material that is being sprayed, the level of dilution, and

how well it has been mixed; all of these factors would cause variation across a surface and between devices.

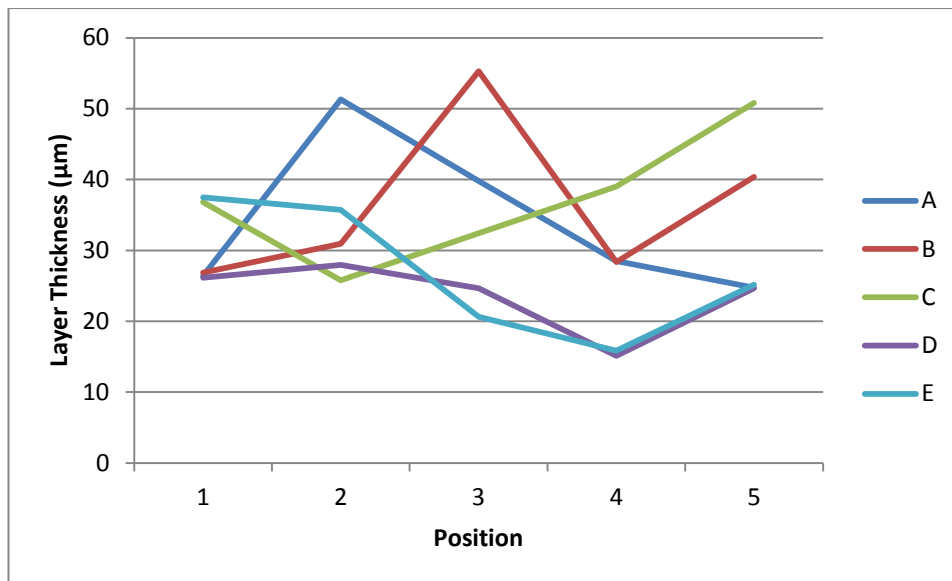


Figure 11-29: A graph showing the thickness of the phosphor layer at five different positions across each of the airbrush devices.

There is a large amount of variation across the phosphor layers (Figure 11-29); as well as the manufacturing reasons already identified there is also the presence of large particles & the added difficulty of measuring this layer due the presence of voids in/near it.

The dielectric material also has a large layer thickness variation between devices, but the individual layers are more uniform than the phosphor (see Figure 11-30).

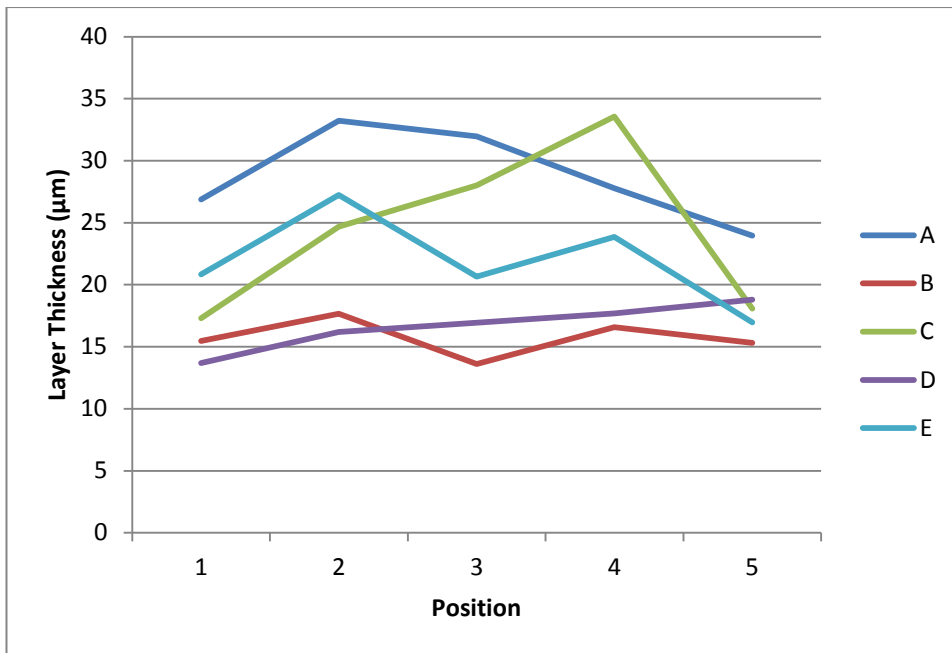


Figure 11-30: A graph showing the thickness of the dielectric layer at five different positions across each of the airbrush devices.

Figure 11-31 show that there is also a moderate amount of variation both across and between silver electrode layers.

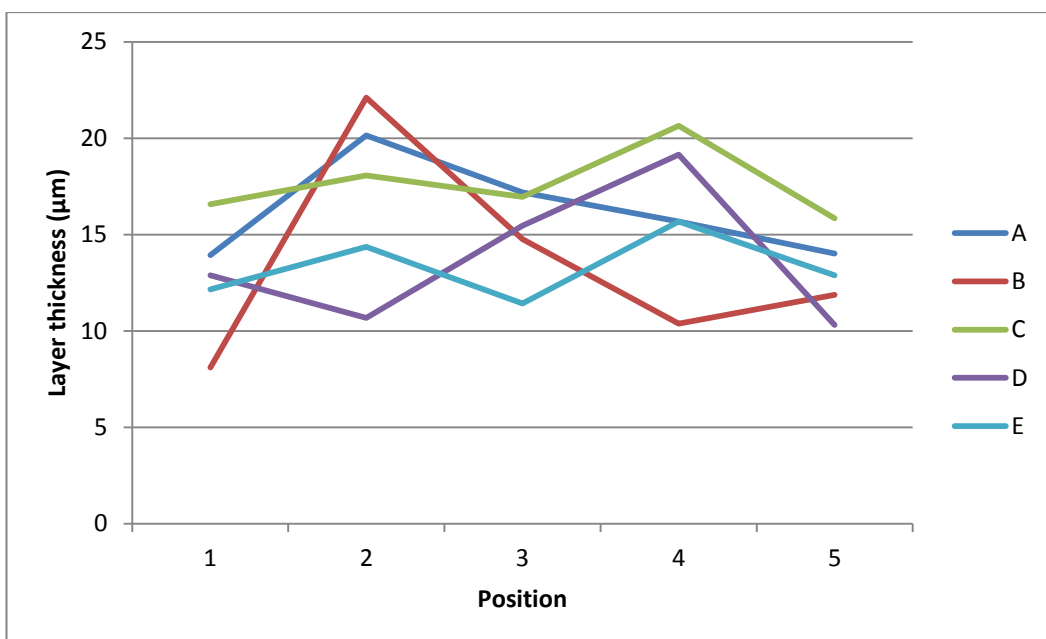


Figure 11-31: A graph showing the thickness of the silver layer at five different positions across each of the airbrush devices.

Overall, the airbrush applies material in layers that exhibit a moderate amount of variation. The variation can be seen across each layer and in between layers. The cause of this variation is likely to be due to differences in airbrush use by the human operator.

11.1.2.4 *PE Insert Moulded*

Upon cutting, the first PE insert film peeled away easily from the device; the exposed PEDOT:PSS layer underneath flaked away from the remaining structure. Due to this, further devices had the PE removed and an acrylic encapsulating layer applied; when samples had been fully sectioned, the PP substrate easily detached from the layers leaving the EL multi-layer structure on the acrylic. This may account for the uneven silver surface that can be seen on the cross section shown in Figure 11-32.

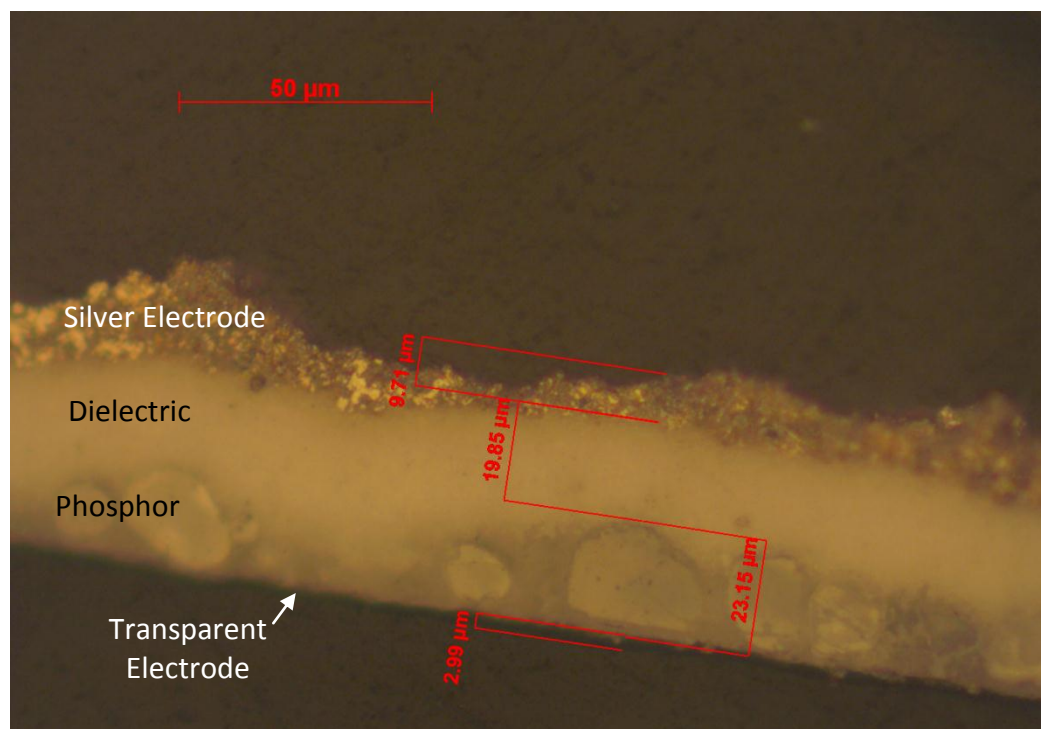


Figure 11-32: A cross section of a PE insert moulded EL device.

There were no voids observed in the PE insert moulded devices and this is probably because the large pressure of injection during the moulding cycle eliminated them. Although the PE insert moulded samples had no voids, they also had a lower illuminance than the bought device (in fact even lower than the non-moulded airbrushed devices); this is not to say that the voids in the other handmade devices did not contribute to the low illuminance but simply that it is not the only factor.

Sample A was damaged during the sectioning and mounting process, so there were no measurements taken and the data is missing from the table.

Table 11-20: The average, SD and RSD values for each layer of each of the PE insert moulded samples.

Sample	Layer Thickness Data (µm)											
	PEDOT:PSS			Phosphor			Dielectric			Silver		
	av	SD	RSD (%)	av	SD	RSD (%)	av	SD	RSD (%)	av	SD	RSD (%)
A	-	-	-	-	-	-	-	-	-	-	-	-
B	2.70	0.36	13.22	19.80	2.67	13.46	22.47	1.70	7.57	10.74	1.13	10.50
C	2.76	0.40	14.43	14.91	4.76	31.96	23.18	1.50	6.45	10.66	2.99	28.08
D	2.74	0.47	17.21	19.23	3.37	17.50	27.59	3.60	13.05	10.98	1.67	15.25
E	2.92	0.80	27.35	19.06	5.92	31.05	27.83	4.37	15.68	16.43	5.15	31.37
GROUP	2.78	0.50	17.94	18.25	4.48	24.52	25.27	3.76	14.90	12.20	3.82	31.34

The RSDs shown in Table 11-20 are lower than other groups of devices which means that this method of production has the lowest variation in layer thickness so far. Figure 11-33 shows that the variation across the group is quite low and the PEDOT:PSS layer thickness is particularly consistent over the group. It is also clear from this graph that just like the bought device the dielectric layer is thicker than the phosphor.

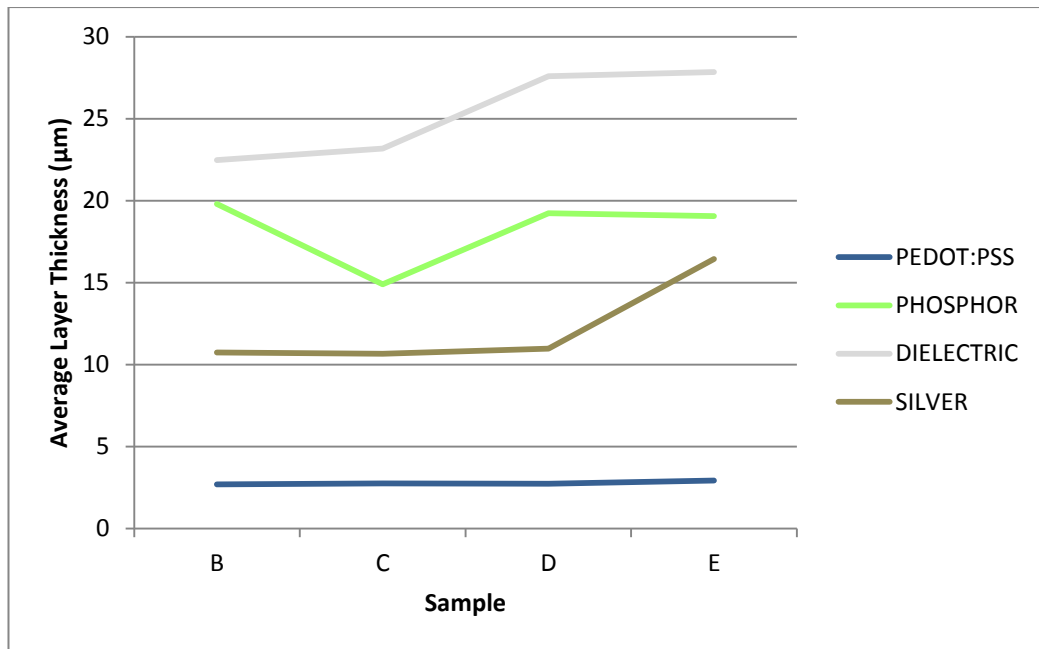


Figure 11-33: The average layer thicknesses of the PE insert moulded group.

The PEDOT:PSS layers of each device were fairly uniform, as were the dielectric and silver; there was a noticeable variation across the phosphor layers (see Figure 11-34) but less than that of other groups.

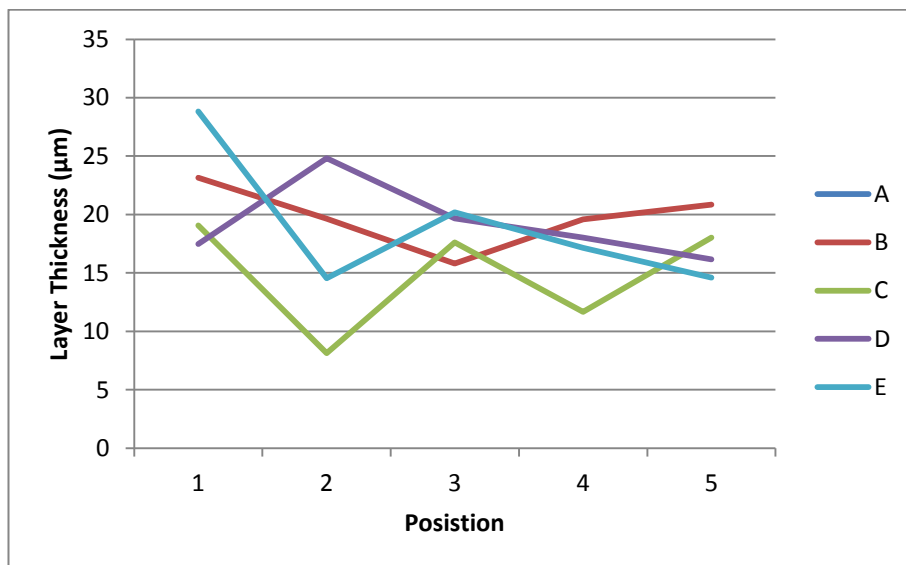


Figure 11-34: A graph showing the thickness of the phosphor layer at five different positions across each of the PE insert moulded devices.

The cause of the phosphor layer thickness variation is once again probably due to the presence of particles within the phosphor layer and inconsistencies in the layer application.

Overall, the PE insert moulding method produces parts with the most consistent layer thicknesses so far.

11.1.2.5 PTFE Insert Moulded

The PTFE insert moulded samples cut well on the saw; an encapsulation layer was not required as the water spray caused minimal damage (if any) to the PEDOT:PSS. As with the PE insert moulded devices, no voids were observed in the samples, a cross section of a PTFE insert moulded device is shown in Figure 11-35.

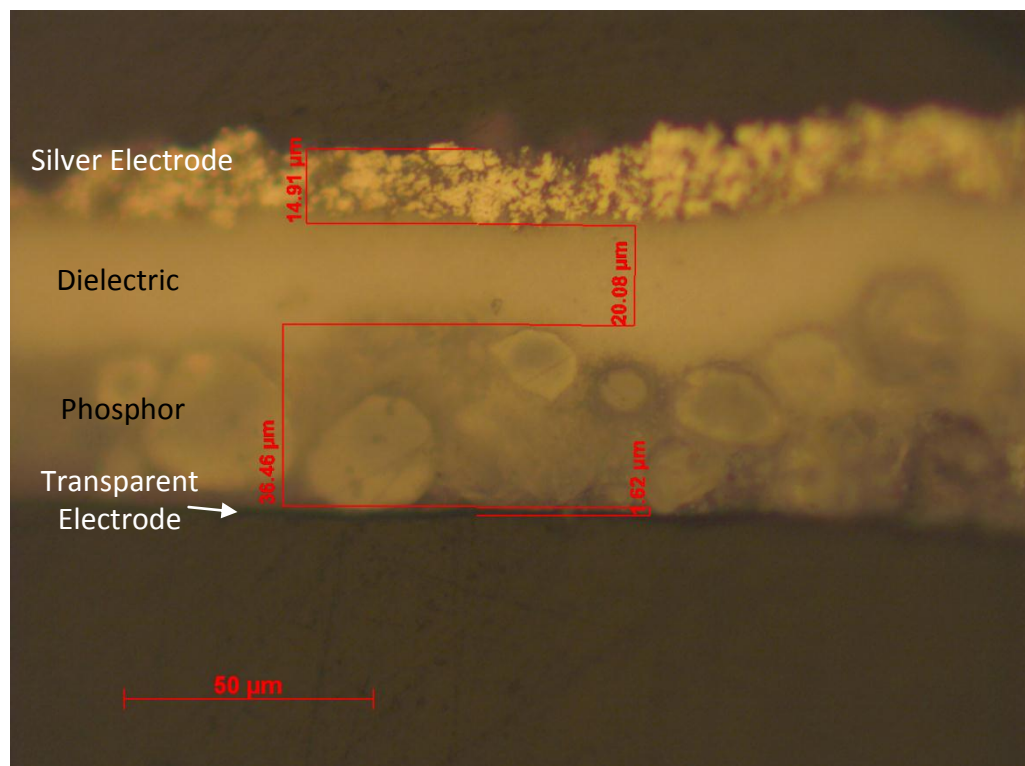


Figure 11-35: A cross section of a PTFE insert moulded EL device.

The thickest layer of the PTFE insert moulded devices was the phosphor, and the thinnest was the PEDOT:PSS. The transparent electrode layer is just a few microns thick so even though the SD is less than one micron this calculates to a large RSD percentage (see Table 11-21).

Table 11-21: The average, SD and RSD values for each layer of each of the PTFE insert moulded samples.

Sample	Layer Thickness Data (µm)											
	PEDOT:PSS			Phosphor			Dielectric			Silver		
	av	SD	RSD (%)	av	SD	RSD (%)	av	SD	RSD (%)	av	SD	RSD (%)
A	2.10	0.99	47.04	28.82	8.43	29.25	27.34	13.63	49.86	14.21	3.99	28.08
B	2.39	0.75	31.41	44.97	4.59	10.20	19.61	7.06	36.02	12.05	2.48	20.56
C	1.90	0.55	29.07	19.25	3.72	19.31	16.40	3.10	18.90	11.06	2.38	21.47
D	1.48	0.23	15.83	42.87	2.26	5.28	19.84	5.81	29.29	10.81	0.79	7.28
E	1.93	0.29	15.07	26.16	0.73	2.77	28.01	5.05	18.03	9.81	2.26	23.01
GROUP	1.96	0.65	33.20	32.41	11.21	34.60	22.24	6.02	27.06	11.59	2.81	24.24

Figure 11-36 shows the average layer thickness of the group and both the PEDOT:PSS and silver layers are fairly consistent across the group. There is a little more variation across the dielectric layers and a large difference in the phosphor layer thicknesses.

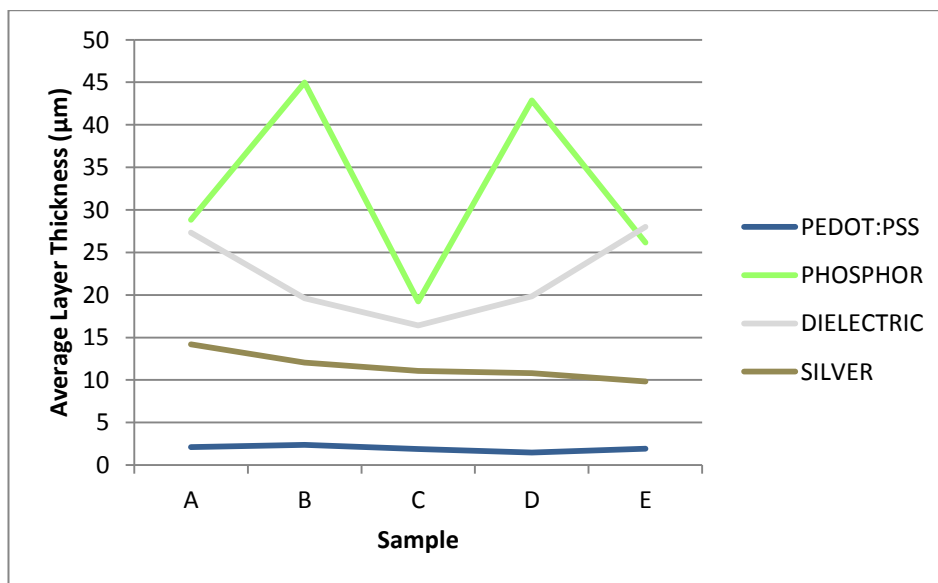


Figure 11-36: The average layer thicknesses of the PTFE insert moulded group.

As already mentioned, the PEDOT:PSS layers have large RSDs; this could be because of the RSD calculation, the thin layer is also difficult to identify and measure on screen so this would increase the variation in the layer thickness measurements.

The individual phosphor and dielectric layer thicknesses are shown in Figure 11-37 and Figure 11-38 and although there is variation between layers, these graphs generally show a fairly even thickness across each layer.

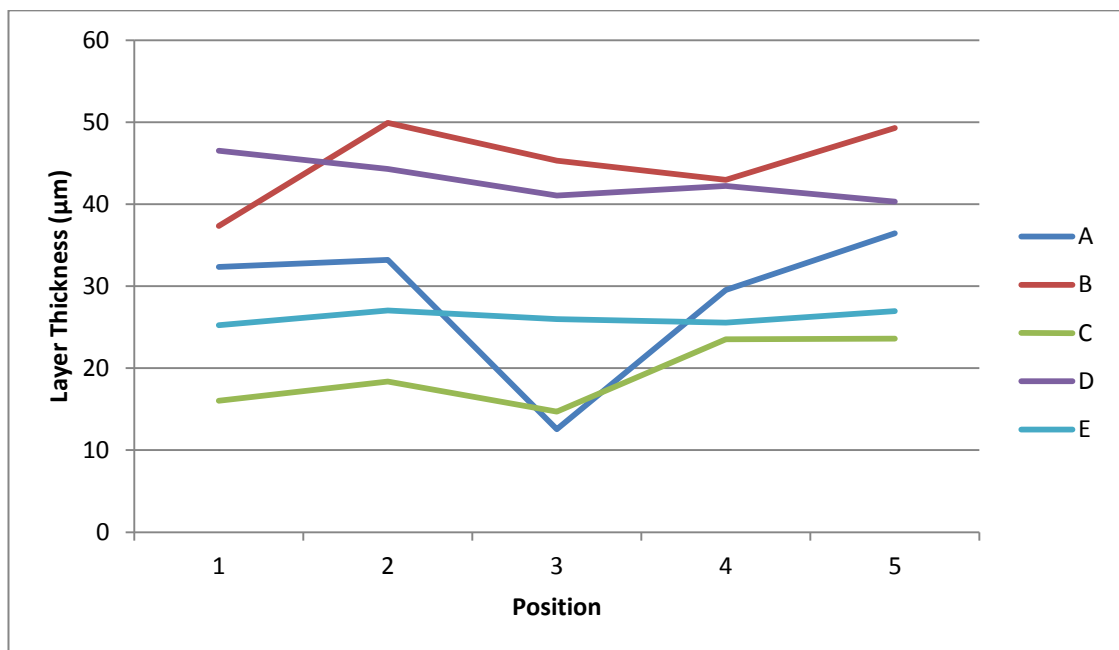


Figure 11-37: Phosphor layer thickness measurements for each of the PTFE insert moulded devices.

On each graph there are a couple of inconsistent points which highlight how the variation in the phosphor layer can affect the thickness of the subsequent dielectric material. One example is device B, on Figure 11-37 in position 3 the phosphor layer is thin and this corresponds to a thick dielectric layer on Figure 11-38. When sprayed over the phosphor layer, the dielectric material has filled any indentations,

resulting in thicker dielectric areas. The silver layers each have a moderate amount of variation across them.

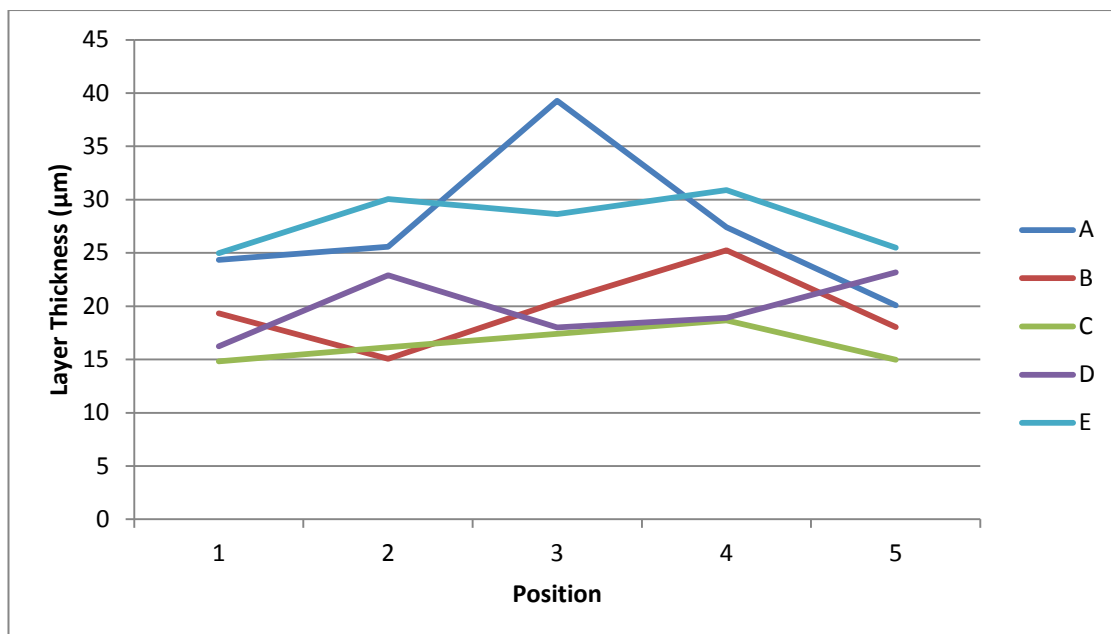


Figure 11-38: Dielectric layer thickness measurements for each of the PTFE insert moulded devices.

Overall, the PTFE insert moulded devices had an even thickness within each layer and little to moderate variation between layers.

11.1.2.6 *In-Mould Layer Application*

The PEDOT:PSS layer washed away when the first in-mould sample was cut using the saw; further samples required acrylic encapsulation. As with the PE insert moulded devices, the PP often peeled off from the encapsulation and EL layers, possibly contributing to the uneven silver surface. The layer structure was not as even as with other processing methods; a cross section of one of the better samples is shown in Figure 11-39. Even on the least disrupted layers, the thickness

measurements are not very accurate because the layer boundaries are not particularly discrete.

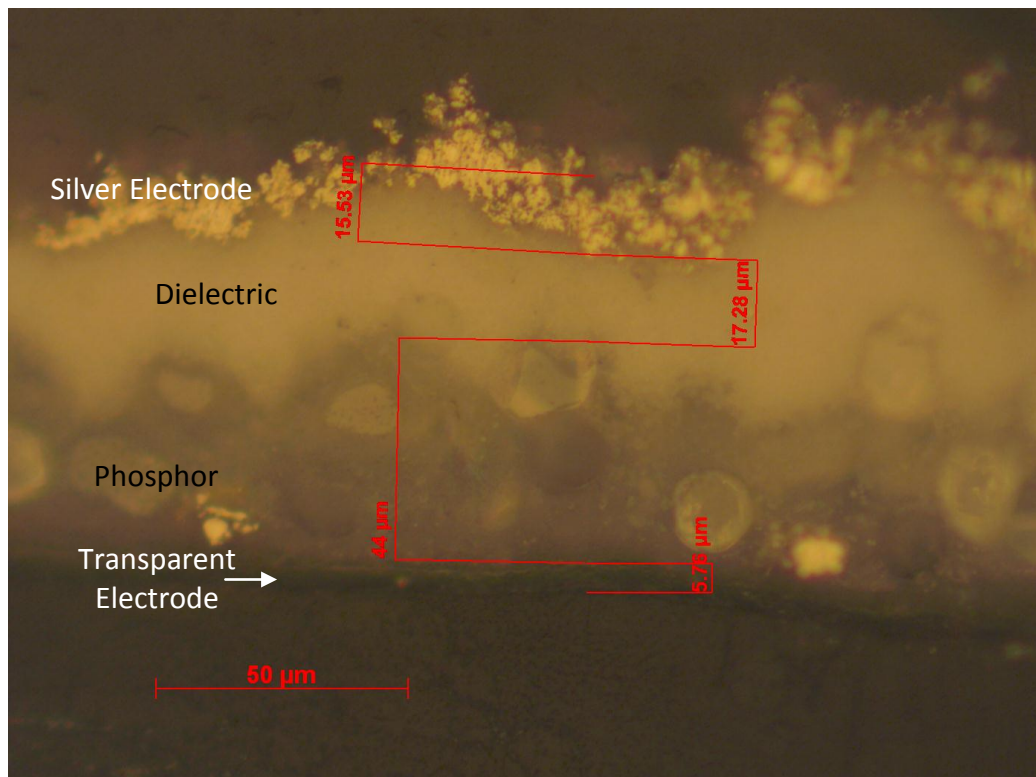


Figure 11-39: A cross section of an in-mould EL device.

When observing and measuring the thicknesses of layers of devices made using the in-mould application, there were some problems which led to missing data:

- There were no measurements taken for sample A because it was damaged during sectioning and mounting,
- Sample C only has no silver layer thickness measurement because the silver was not visible (see Figure 11-40), and
- Sample D had a very disrupted layer structure and all four layer materials could only be measurements in one location.

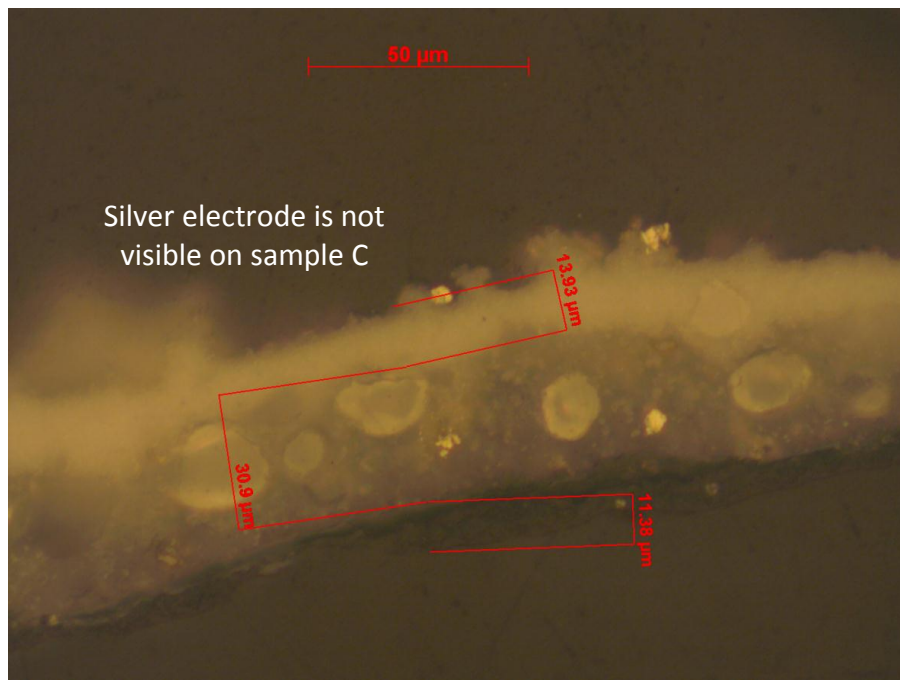
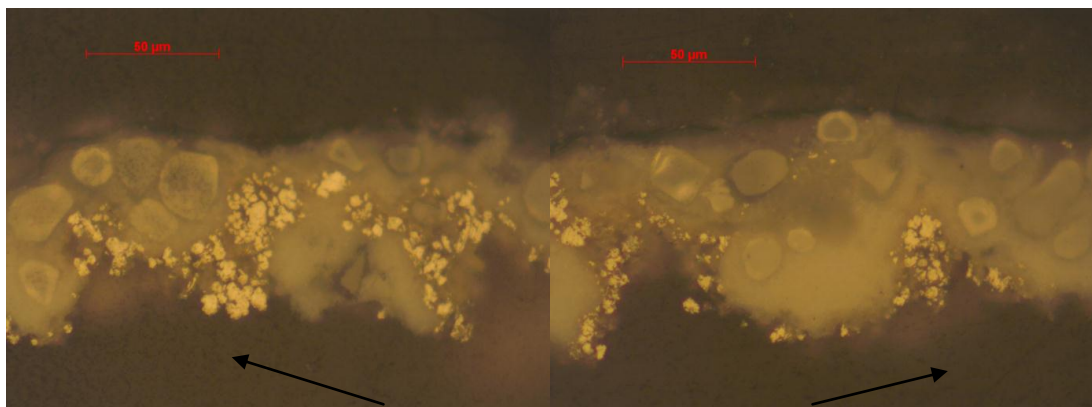


Figure 11-40: Sample C of the in-mould devices; the silver layer was not visible.

Two examples of the layer disruption caused by injection are shown in Figure 11-41; layers formed a wave-like pattern and adjacent materials intermingled. This is caused by the injected polymer displacing the layer materials but these effects can be reduced by changing injection moulding parameters.



Typical disruption pattern caused by injection moulding

Figure 11-41: The disruption to the layer structure caused by the injection of the polymer.

The analysis of layer thickness measurements that were obtained are shown in Table 11-22; it can be seen that the RSD values are approximately the same as those achieved using other processing methods; but the lack of data indicates the unreliability of the process.

Table 11-22: The average, SD and RSD values for each layer of each of the in-mould samples.

Sample	Layer Thickness Data (μm)											
	PEDOT:PSS			Phosphor			Dielectric			Silver		
	av	SD	RSD (%)	av	SD	RSD (%)	av	SD	RSD (%)	av	SD	RSD (%)
A	-	-	-	-	-	-	-	-	-	-	-	-
B	6.07	1.46	24.05	32.59	2.26	6.93	19.54	4.24	21.69	16.67	3.92	23.49
C	8.15	2.45	30.02	32.22	3.49	10.82	16.02	3.74	23.33	-	-	-
D	3.10	N/A	N/A	36.58	N/A	N/A	13.03	N/A	N/A	12.57	N/A	N/A
E	5.85	0.58	9.90	32.66	17.13	52.45	23.56	6.26	26.58	16.79	8.38	49.88
GROUP	6.47	2.03	31.45	32.75	9.16	27.98	19.29	5.59	28.99	16.35	5.98	36.58

From the layer thicknesses that could be measured, Figure 11-42 shows that the equivalent layers on different samples were fairly consistent, with a comparable variation to other methods.

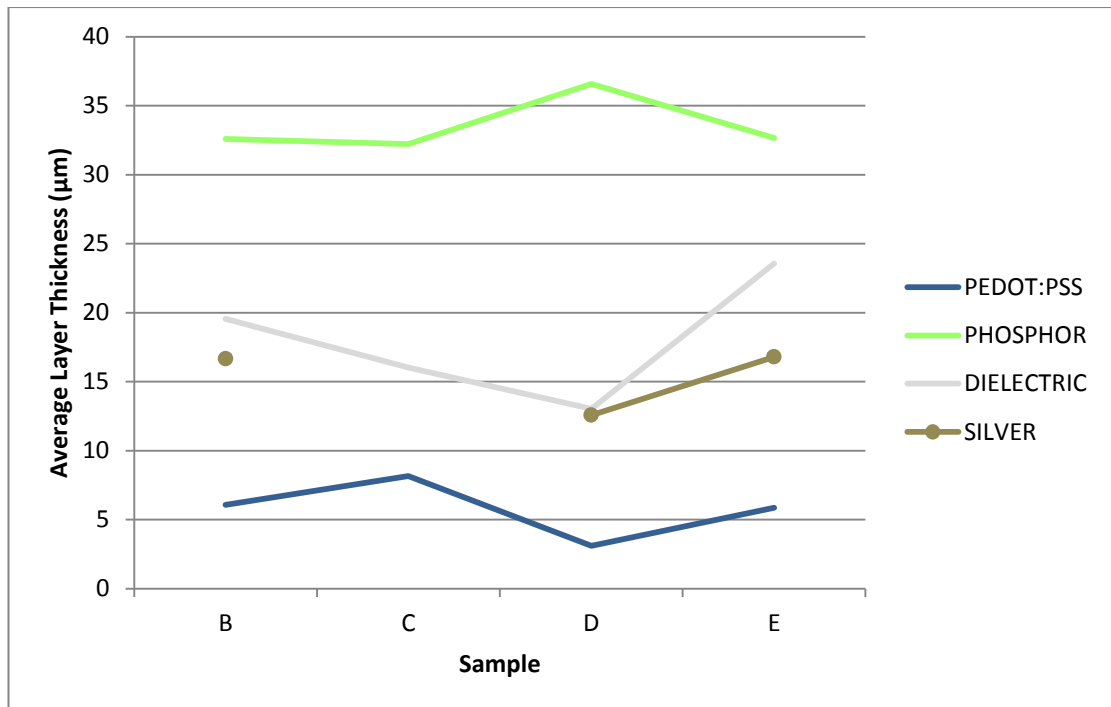


Figure 11-42: The average layer thicknesses of the in-mould group.

However, there is quite a large variation in thickness across each layer; the dielectric layer thicknesses are shown in Figure 11-43 and represent the amount of variation shown across all material layers. The variation across each layer could be caused by uneven manual layer application but also due to the effects of injection moulding. The injected polymer forces material sideways, affecting the layer thickness and causing the disruption shown in Figure 11-41.

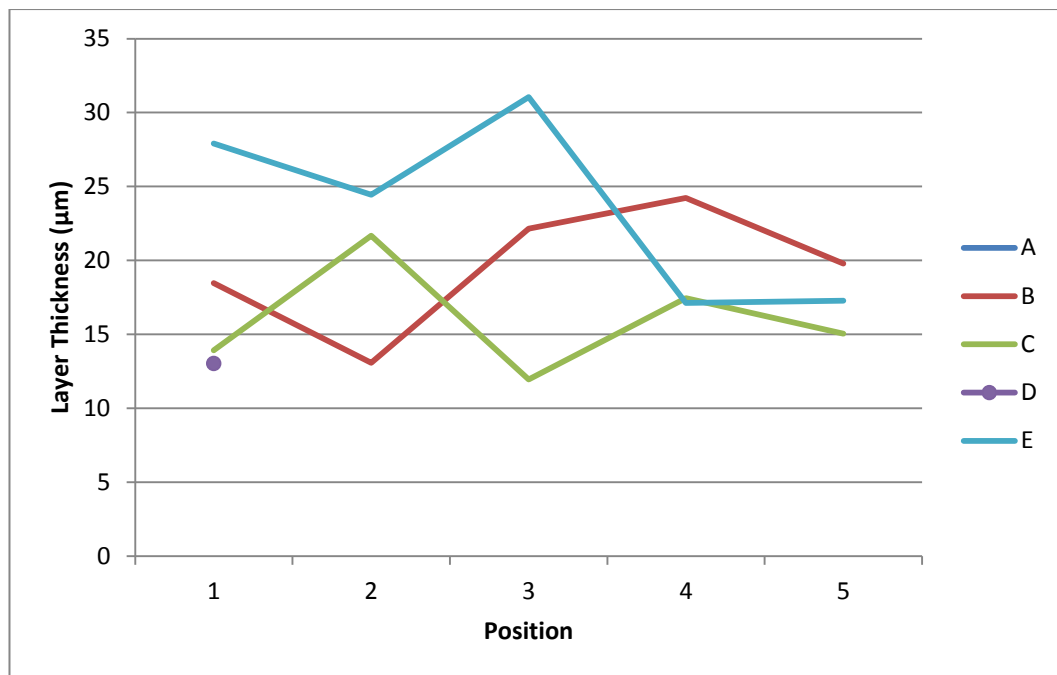


Figure 11-43: The dielectric layer thickness measurements for each of the in-mould devices.

Overall, the in-mould process produces layers with quite a large variation in thickness across them; the average layer thicknesses within the group are quite consistent but the fact that some measurements could not be taken indicates that currently the process is not very repeatable.

11.1.2.7 *Post Mould Layer Application*

When sectioned with the saw, the post mould samples required acrylic encapsulation; this was because the PEDOT:PSS layer flaked away from the remaining part when hit with the lubricating spray from the saw. An example of a sectioned piece of post mould device is shown in Figure 11-44; this shows that the thin phosphor layer has more dispersed phosphor particles than other devices, which could contribute to the low illuminance levels.

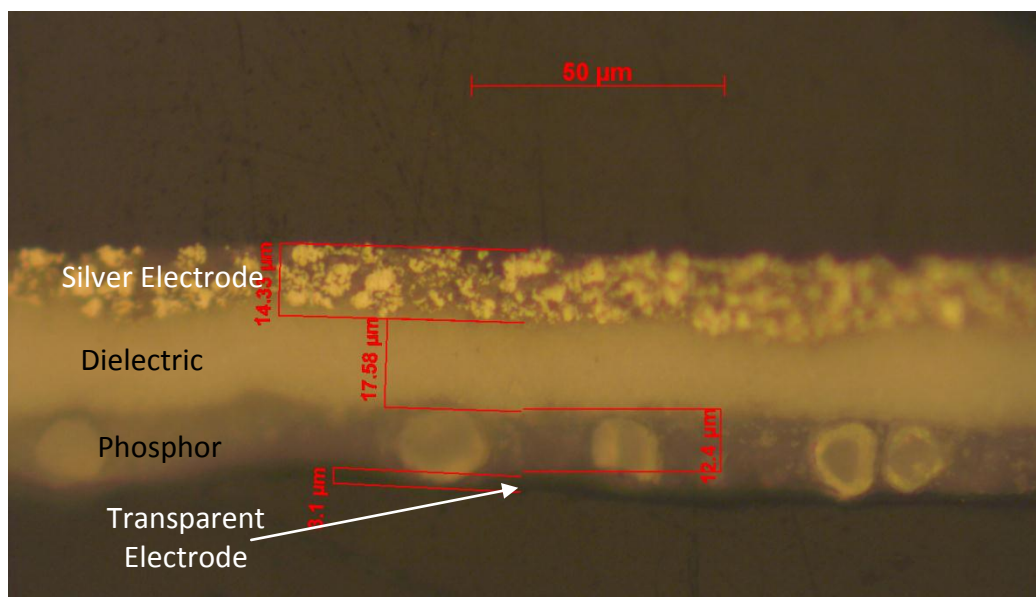


Figure 11-44: A cross section of a post mould EL device.

The analysis of the layer thickness measurements for all of the post mould devices is shown in Table 11-23; although a few individual layer RSD values are low but generally the RSDs are quite large indicating large variations between devices and across layers.

Table 11-23: The average, SD and RSD values for each layer of each of the post mould samples.

Sample	Layer Thickness Data (µm)											
	PEDOT:PSS			Phosphor			Dielectric			Silver		
	av	SD	RSD (%)	av	SD	RSD (%)	av	SD	RSD (%)	av	SD	RSD (%)
A	3.87	0.61	15.84	7.09	2.36	33.35	12.67	4.78	37.77	8.83	1.25	14.13
B	2.92	0.50	16.98	9.74	3.90	40.07	9.96	0.91	9.19	17.97	1.77	9.88
C	3.46	0.34	9.86	16.98	4.41	25.99	17.32	1.51	8.74	13.55	2.03	15.01
D	2.13	0.40	18.96	13.97	4.77	34.14	14.25	1.90	13.30	14.72	4.30	29.22
E	5.29	1.62	30.62	15.89	8.18	51.49	15.71	2.72	17.31	14.58	1.09	7.47
GROUP	3.54	1.32	37.36	12.73	6.03	47.32	13.98	3.59	25.65	13.93	3.72	26.69

The average layer thicknesses plotted on the graph shown in Figure 11-45, confirm the large variation between equivalent layers in different devices.

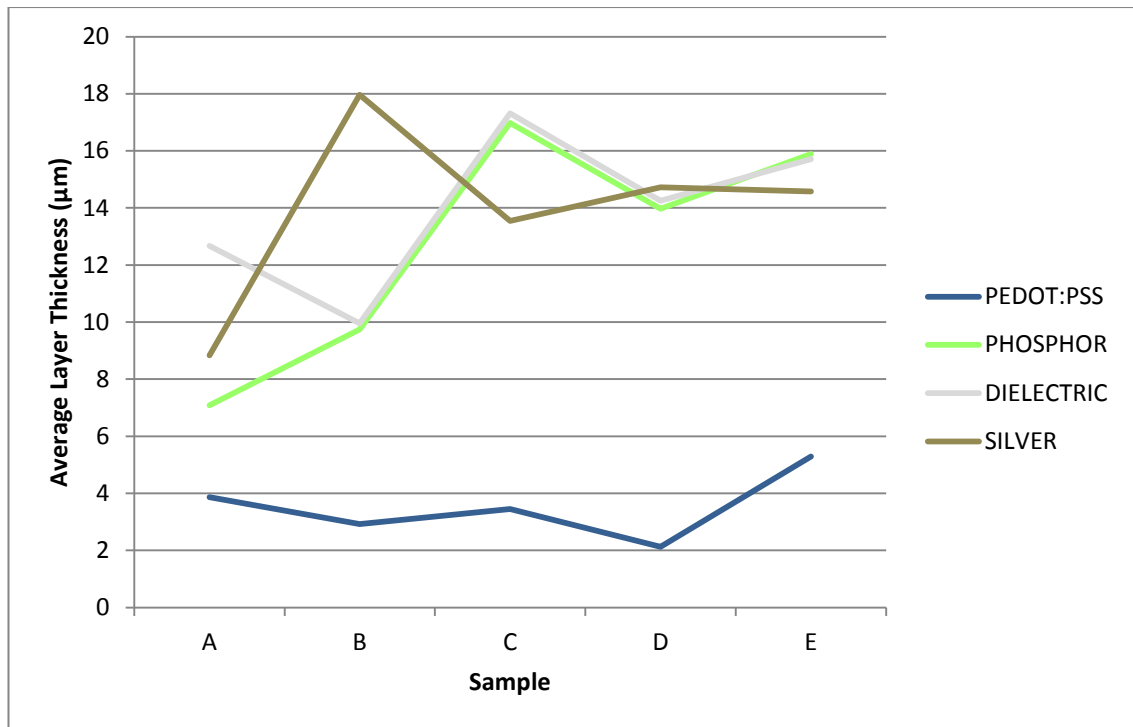


Figure 11-45: The average layer thicknesses of the post mould group.

The thickness across each layer is also inconsistent and the phosphor material is a good example of this (see Figure 11-46). Since these layer materials were applied after moulding, the injection moulding process could not have any effect on the layer thickness variation so the differences must only be due to uneven material application and, in the case of phosphor, the size of the particles of material.

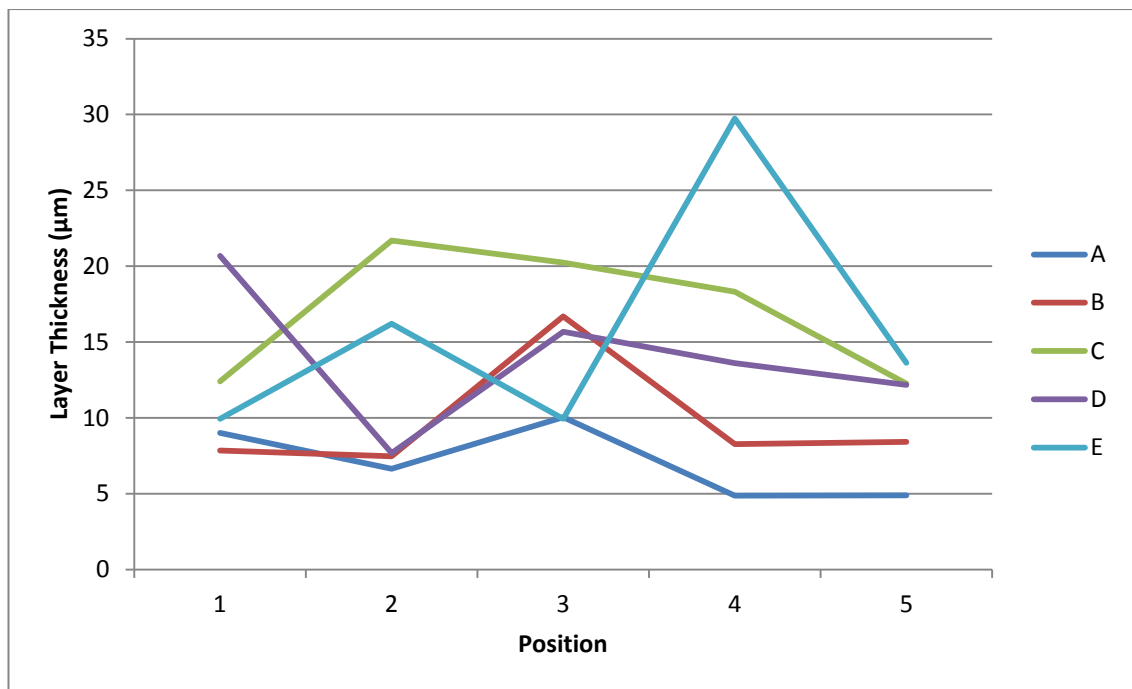


Figure 11-46: The phosphor layer thicknesses for each of the post mould devices.

Overall, when devices are made using this method there is a lot of variation in the thickness of individual layers and are large variation in the layer thicknesses of different samples.

11.1.2.8 Layer Thickness Comparison

When comparing the thickness of layers produced by each processing method it is important to examine both the averages and the variation of the thicknesses applied. When comparing the different devices, the bought device will act as a benchmark; it has already been determined that this is the brightest of the EL lamps tested and so it will be assumed that it has the optimal layer thicknesses. It is acknowledged that this is not the only factor affecting the brightness of the light emitted but this is the only aspect that was compared in this investigation.

Figure 11-47 shows the average layer thicknesses applied using each of the processing techniques; and it appears that the in-house methods that produced devices with the most similar layer thicknesses to the bought device are: the basic airbrush method, the PTFE insert moulding and the in-mould layer application. Despite the in-mould method producing similar average layer thicknesses it has already been shown that the method is not yet able to reliably produce an intact multi-layer structure. Neither the basic airbrush nor PTFE insert methods completely replicate the dimensions of the bought device (ideally the phosphor and dielectric layer thicknesses would be reversed) but this graph shows that the novel application methods developed in this project do have the ability to produce EL devices with a layer architecture very similar to ones produced commercially.

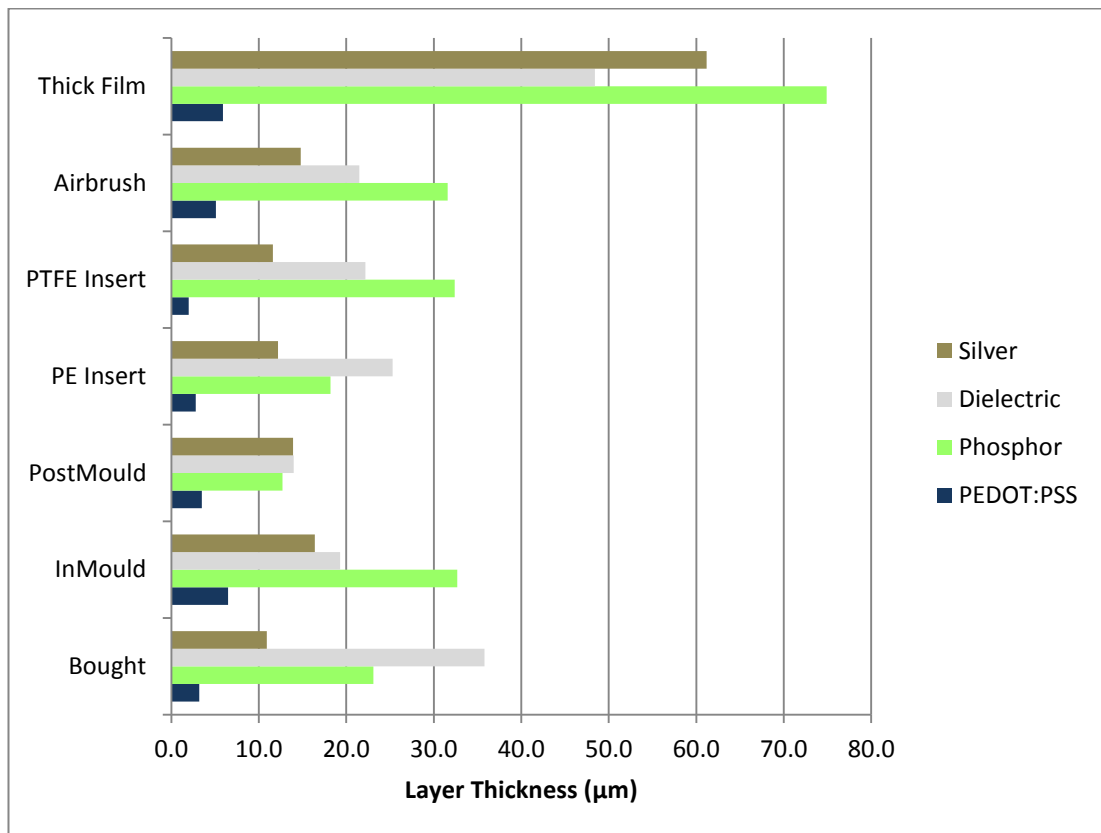


Figure 11-47: The average thicknesses of each layer material produced using each processing technique.

As already mentioned, the combined thickness of the phosphor and dielectric layers is equal to the distance between the electrodes and has an effect the amount of light emitted by the device so this quantity has also been compared (in Figure 11-48).

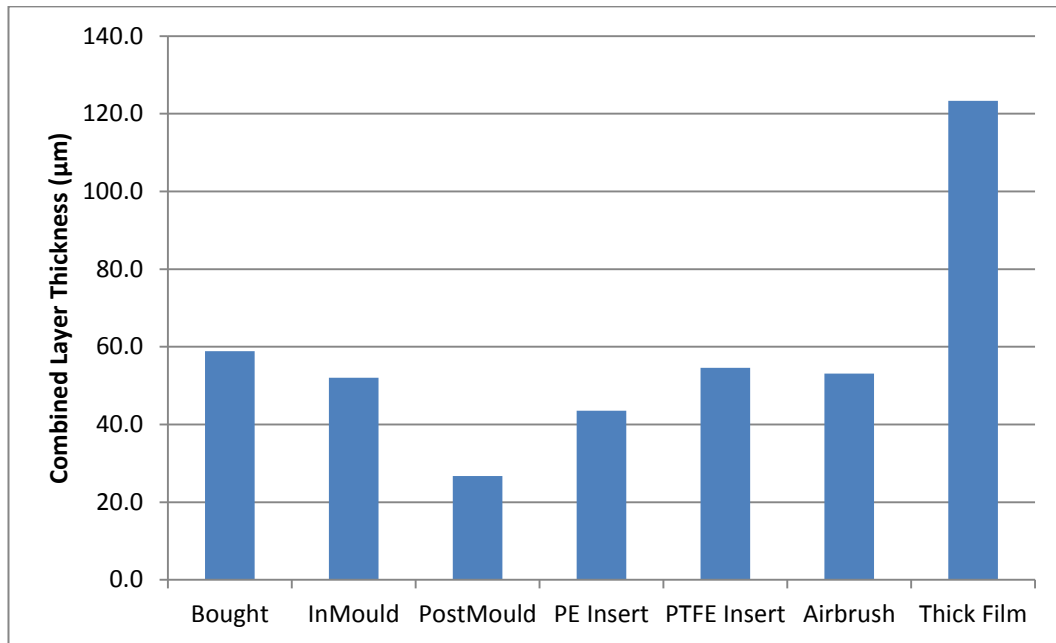


Figure 11-48: The combined phosphor and dielectric layer thicknesses produced by each processing technique.

Once again the PTFE insert moulding and the basic airbrush techniques produce devices with the closest dimensions to the bought device. The fact that these two methods also emitted light of the closest brightness to the bought devices supports the argument that links the layer thicknesses to illuminance.

It is also important for the process to reliably and repeatedly produce parts of a certain standard so the RSDs have also been compared. Table 11-24 shows, for each processing method, the group RSDs and the average individual device RSDs; the group RSD will indicate the repeatability of the process to make comparable parts,

and the average device RSDs will quantify how even the layers within the parts made.

Table 11-24: The group RSD values and average individual RSD values for each material and each processing technique.

Type	Variation within each groups layer thickness measurements								All layers Av. Group RSD (%)
	PEDOT:PSS		Phosphor		Dielectric		Silver		
	Av. Device RSD (%)	Group RSD (%)	Av. Device RSD (%)	Group RSD (%)	Av. Device RSD (%)	Group RSD (%)	Av. Device RSD (%)	Group RSD (%)	
Bought	20.4	N/A	45.4	N/A	25.0	N/A	6.4	N/A	N/A
In-Mould	21.3	31.5	23.4	28.0	23.9	29.0	36.7	36.6	31.3
Post Mould	18.5	37.4	37.0	47.3	17.3	25.7	15.1	26.7	34.3
PE Insert	18.1	17.9	23.5	24.5	10.7	14.9	21.3	31.3	22.2
PTFE Insert	27.7	33.2	13.4	34.6	30.4	27.1	20.1	24.2	29.8
Airbrush	20.4	27.7	29.3	32.7	16.0	28.8	21.3	23.8	28.3
Thick Film	18.4	26.9	28.7	39.2	19.8	27.7	10.7	15.8	27.4

For each layer material the application method providing the best/lowest (**GREEN**) and worst/highest (**RED**) individual and group RSD value have been identified and counted. Using this method it can be seen that when considering the layer structure and consistency, the PE insert moulding method is the most reliable, producing devices with the lowest variation and the post mould and in-mould techniques are quite unreliable, producing devices with a high degree of variation.

The variation that is present both within and in between airbrush applied layers is predominantly due to difference in the layer application. The airbrush is operated by hand and therefore may not be sprayed evenly over the whole surface area; the

coverage is also judged by eye and as such is another source of variation. The rate of material flow from the airbrush would also vary whilst spraying a single layer and different devices. Different materials behave differently and therefore would flow differently; for example the phosphor contained particles of material which could affect flow rate. Changes during dilution and mixing is also likely to cause variation to the different batches; slightly different levels of dilution, evaporation of the solvent, and varying degrees of mixing would all contribute to the differences. The phosphor and silver mixtures also separated upon standing which would affect the flow rate. All of these issues are contributing factors to the variation identified in these airbrush application methods.

As well as gaining quantitative layer thickness data using a microscope; the actual preparation of the samples also gave information about the quality of the layers and adhesion. When sectioning the samples on the saw, the water (and lubricating fluid) sprayed onto the parts and observations were made about the integrity of the EL layers, particularly about the PEDOT:PSS layer as this was often the top layer when cutting. However when making comparisons it is important to note that there are some critical differences between devices:

- On the devices constructed on PC plaques (both the thick film and basic airbrush), the PEDOT:PSS layer was protected by the PC,
- On the moulded devices the PEDOT:PSS was the outermost, unprotected layer and was applied and cured before other layers, and

- On the post mould devices, the PEDOT:PSS layer was the outermost, unprotected layer and was the last layer to be applied and was therefore applied to an already uneven surface.

The observations and the comparisons made earlier have been used to evaluate the quality of the multi-layer structure produced by each method and summary is shown in Table 11-25.

Table 11-25: A qualitative comparison of the whole multi-layer structure applied using each processing method.

Production Method	Layer Quality Considerations				
	Similarity to Bought Device Dimensions	Quality of PEDOT:PSS Layer	Layer Uniformity (across a single part)	Layer Consistency (across a group of parts)	Overall Layer Structure
Thick Film on PC	Much larger layer thicknesses; some layers were twice the thickness	Fully cured and good adhesion	Fairly consistent layer thickness across the part	Moderate variation across the group	Thick even structure, with distinct layers. Large voids present in the phosphor layer
Airbrush on PC	Similar layer thicknesses	Fully cured and good adhesion	Moderate variation in layer thickness	Moderate variation across the group	Fairly even structure, Large voids present in the phosphor layer
Post Mould	Thinner layer thicknesses	Cured but poor adhesion to the phosphor,	Fairly large thickness variation in each layer	Large variation between devices.	Distinct thin layer structure. Some small

		it flaked off during cutting			voids present within layer structure
PE Insert	Thinner layer thicknesses	Flaky, cured but poorly adhered to phosphor. PE easily peels away from PEDOT:PSS.	Good layer consistency	Low variation across the group	Even layer structure. No voids present
PTFE Insert	Similar layer thicknesses	Fully cured, good adhesion, high gloss, smooth finish	Moderate layer consistency	Low to moderate variation across the groups	Good layer structure. No voids present
In-Mould	Similar layer thicknesses	Dull finish, uncured, washed off during cutting	Large thickness variation across the layers	Fairly consistent average layer thicknesses where measurements were possible.	Very poor layer structure; high level of disruption caused by injection. Layer interface not always discrete.

Overall, the insert moulding techniques (both PTFE and PE) reliably produce devices with a similar layer structure to that of the bought device.

11.1.3 Comparing Layer Thickness with Illuminance

This analysis section combines the data gathered from both the illuminance and layer thickness characterisation. The combined thickness of the phosphor and dielectric layer is equal to the distance between the two electrodes and as such will

have an effect on the illuminance. The illuminance was compared to the combined thickness of the phosphor and dielectric layers in order to see if there is a relationship between them and/or an optimal value could be determined. The comparison is shown in Figure 11-49; each point represents a device for which both values were obtained and the key indicates the group they belong to and how they were made.

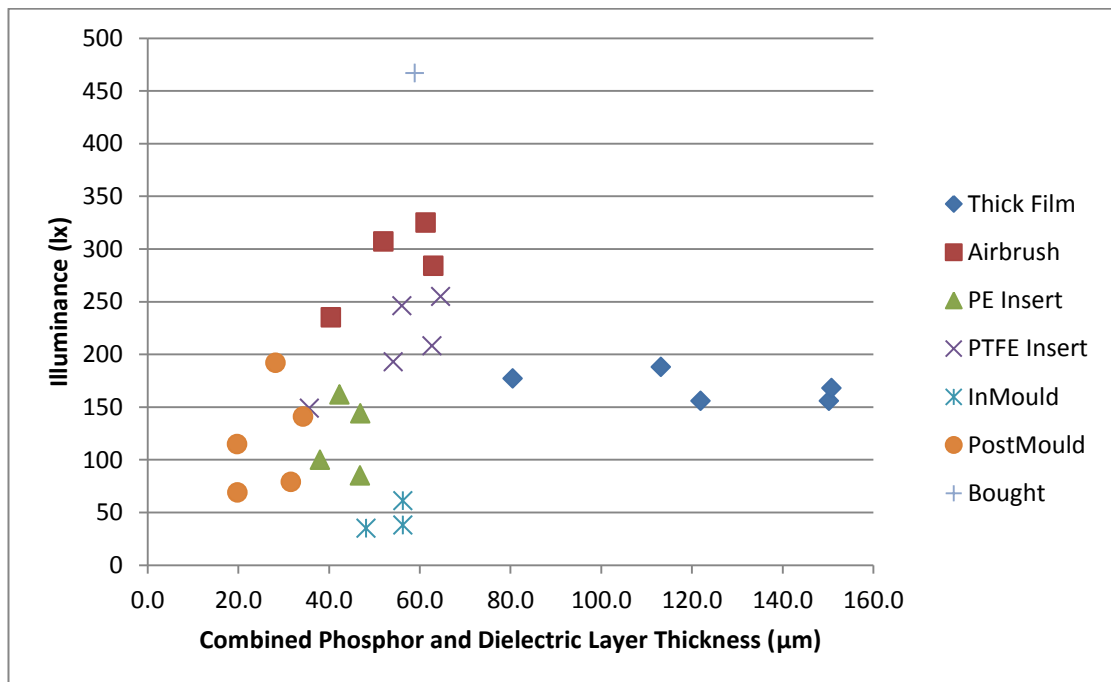


Figure 11-49: A comparison of the illuminance and combined phosphor and dielectric layer thicknesses for each device tested.

With the exception of the bought device and the in-mould group, most of the points fall into a curve where the illuminance rises and falls as the combined layer thickness increases. The graph shows that the devices that emit the brightest light have a combined phosphor and dielectric layer thickness of around 60 microns. The further the combined layer thickness is away from this value, the dimmer the devices are. This is a good indication that the optimal distance between the

electrodes (the combined phosphor and dielectric layer thickness), that would produce the brightest devices is around 60 microns.

The bought device has this optimal dimension within its structure but is much brighter than the devices made during this project; this shows that it is not only layer thickness that affects the illuminance of a device. Other factors such as the conductance of the electrodes, the type of phosphor and the quality of the layer interface will also impact on the brightness of the light emitted and this is something that could be studied further.

The in-mould layer devices also had an optimal combined layer thickness but this group were the dimmest of all the lamps made; this also shows that it is not just the thickness but the integrity of the layers and structure are both important in producing bright devices.

In summary, the methods developed in this project (specifically the basic airbrush and PTFE insert moulding techniques) have the capability to produce devices with the optimal dimensions to produce a bright EL device.

11.1.4 Error Analysis

Each of the manufacturing processes used in this project had different errors associated with it and these can be categorised as material, human, layer application, moulding and structure errors. Table 11-26 shows a consideration of each category and quantifies an estimation of the total error in the layer thickness for each process.

Table 11-26: A consideration of the errors occurring in each processing method.

	Processing Technique											
	Thick Film		Basic Airbrush		PE Insert Moulded		PTFE Insert Moulded		In-mould		Post Mould	
	Contributing Factors	Estimation (%)	Contributing Factor	Estimation (%)	Contributing Factor	Estimation (%)						
Material	Variation between purchased batches, Phosphor particles	5	Variation between purchased batches, Level of dilution, Mixing, Phosphor particles	10	Variation between purchased batches, Level of dilution, Mixing, Phosphor particles	10	Variation between purchased batches, Level of dilution, Mixing, Phosphor particles	10	Variation between purchased batches, Level of dilution, Mixing, Phosphor particles, Level of cure	15	Variation between purchased batches, Level of dilution, Mixing, Phosphor particles	10
Human	Pressure applied during application	5	Spray distance, Spray time, Judgement of coverage	10	Spray distance, Spray time, Judgement of coverage	10	Spray distance, Spray time, Judgement of coverage	10	Spray distance, Spray time, Judgement of coverage	10	Spray distance, Spray time, Judgement of coverage	10
Layer Application	Thickness of masking template, Time in oven	5	Flow of airbrush, Air Pressure, Time in oven	5	Flow of airbrush, Air Pressure, Time in oven	5	Flow of airbrush, Air Pressure, Time in oven	5	Flow of airbrush, Air Pressure, Application time	10	Flow of airbrush, Air Pressure, Time in oven	5
Moulding	N/A	0	N/A	0	Tolerance of moulding parameters	5	Tolerance of moulding parameters	5	Tolerance of moulding parameters, Mould temperature	10	N/A	0
Structure	Voids, Interface contact	10	Voids, Interface contact	10	Interface contact, Layer disruption due to polymer flow	15	Interface contact, Layer disruption due to polymer flow	15	Interface contact, Layer disruption due to polymer flow	15	Interface contact	5
Total (%)	25		35		45		45		60		30	

From Table 11-26 it can be seen that the process which had the greatest error in layer application was the direct in-mould method, this was due to the fact that

there were both more categories to take into consideration and greater error associated with each category. The thick film layer application method had the lowest errors, this was partly because there were no errors associated with the dilution of the materials or the injection moulding process. When these were compared to the layer thickness RSD values for each process (the average of all layer materials) in Table 11-24 on page 274 it could be seen that the errors in layer thickness of unmoulded devices were similar to those in Table 11-26. The thick film method produced layers with an error in thickness of 27 % compared to the 25 % calculated from the different error categories. However the moulded devices produced had layers with lower measured errors than calculated, for example, PTFE insert moulded devices had a layer thickness RSD of 30 % compared to the 45 % calculated in Table 11-26. This suggested that the errors associated with moulding and the subsequent layer disruption caused by it were lower than first predicted.

11.2 Degradation Tests

So far in the analysis, it has been seen that the modified materials applied using an airbrush have the ability to produce brighter EL devices that have an optimised structure when compared to devices made using the unmodified thick film paste materials. However, this is not particularly useful if the airbrushed devices have a much shorter lifetime than those made using the thick film method. Devices made using both methods were tested over 10 weeks to compare the degradation in the light levels they emit.

11.2.1 Thick Film Devices

The illuminance of each of the thick film devices over the course of the ten week test are shown in Figure 11-50; the device kept in damp conditions failed to illuminate after the initial test and the coverlay and PVC encapsulated devices performed much better than the rest of the group. Most of degradation that did occur happened in the first two weeks and the light level plateaued out after that.

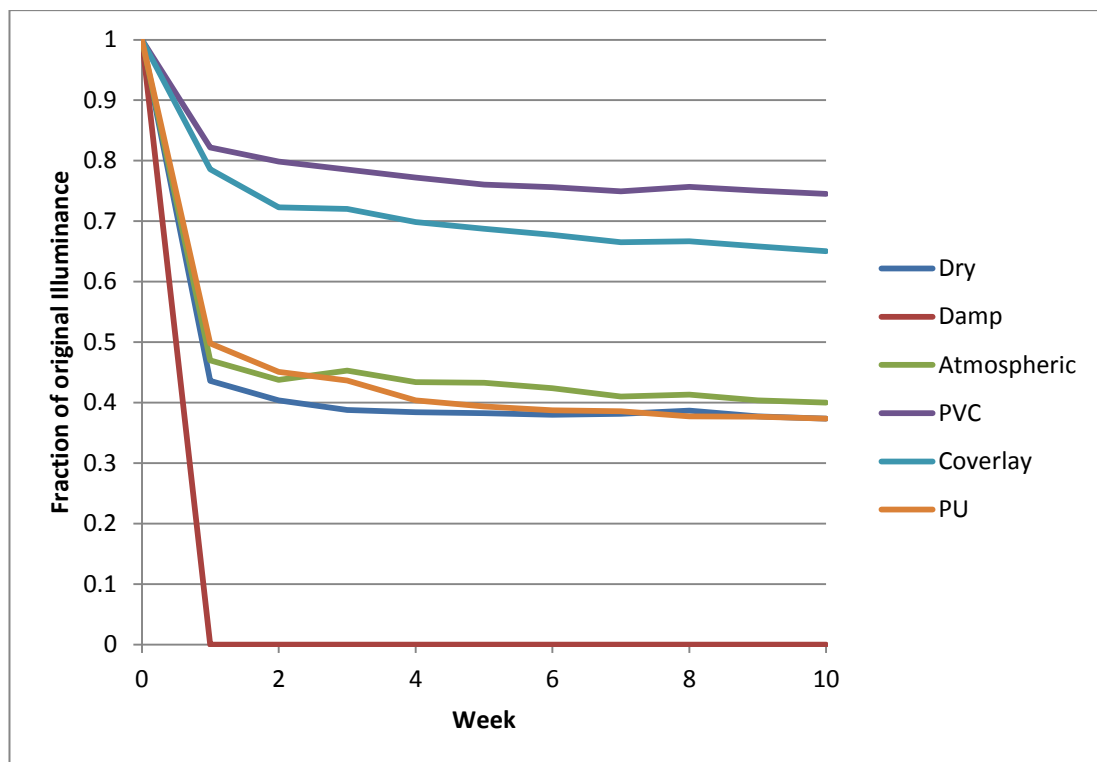


Figure 11-50: The degradation in the level of light emitted by thick film devices kept in different conditions over a ten week period.

The device kept in the 100 %RH, damp conditions completely failed; this is not entirely unexpected as it is well documented that organic EL devices are prone to moisture damage and oxidation & this has been known for some time [157, 158].

The devices kept in dry, atmospheric and PU encapsulated conditions all had similar levels of light degradation over the time of the test. After 10 weeks the dry, atmospheric and PU encapsulated devices respectively emitted 37 %, 40 % and 37 % of their original illuminance. This shows that a commercially bought clear PU spray offers no protection to a thick film device as it degrades at comparatively the same rate as an unprotected device in the same conditions. The level of light emitted from the device kept in “dry” conditions also degraded at the same rate, however there was not a large difference in the humidity of the dry and atmospheric conditions¹¹.

The device encapsulated with the UV curable coverlay maintained an illuminance 65%, ten weeks after it was first tested. This device was expected to perform well in the degradation test as this encapsulation material was designed specifically for that function. One reason why it may not have performed to the highest degree is that when the layer was cured the UV lamp used had no frequency or intensity controls and so the cured layer may not have been in perfect condition.

The encapsulation material that resulted in the least degradation of light emission was the PVC adhesive film; the light level after ten weeks was 75 % of that at the beginning of the test. Although the PVC film was not intended as an EL encapsulation materials, its good barrier properties has meant it has protected the underlying layers well.

¹¹ The “dry” conditions were on average 31.4%RH and the average “atmospheric” conditions were 44.2%RH.

11.2.2 Airbrush Devices

The airbrushed devices were made with the modified layer materials, but also the coverlay was modified in the same way (diluted with an equal amount of MEK) so that it could also be applied with an airbrush. The PU was exactly the same as in the previous degradation test because this was sprayed directly from an aerosol can and the PVC film was exactly the same.

The illuminance of each of the airbrushed devices over the course of the ten week test are shown in Figure 11-51; the first point to make is that these devices generally showed less degradation in illuminance than the thick film devices.

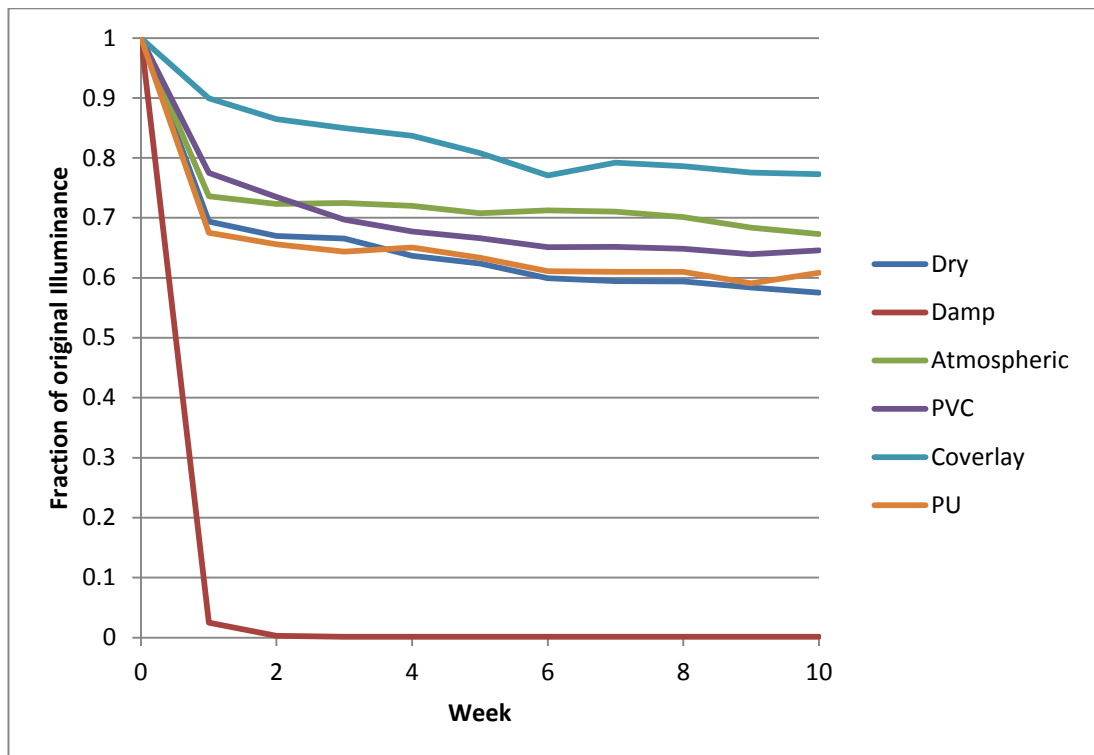


Figure 11-51: The degradation in the level of light emitted by airbrushed devices kept in different conditions over a ten week period.

The degradation of the airbrushed devices appears to happen more gradually than the thick film devices, as shown by the shallower curves shown on Figure 11-51.

Once again the device kept in the damp conditions degraded the most; however this time even until the end of the ten week test a small section of the device emitted a bright light (see Figure 11-52). Even though the light meter measured a low illuminance, the photos in Figure 11-52 show that the device still gave off a bright light but only a small section still illuminated. This could suggest that the modified materials may be more resilient to damp conditions than the unmodified thick film materials.



Figure 11-52: The light emitted by the airbrushed device kept in damp conditions after one week (left) and for two weeks and longer (right).

The device that underwent the least degradation was the one that was coverlay encapsulated; after ten weeks it still emitted light at 77 % the illuminance of when it was first tested.

After ten weeks the devices kept in dry and atmospheric conditions, and PVC and PU encapsulation maintained light levels of 58 %, 67 %, 65 % and 61 % respectively.

11.2.3 Comparisons

By plotting the final relative illuminance of each device, a simple analysis can be made; comparing the degradation of devices made using the modified and unmodified materials. The comparison can be seen in Figure 11-53.

These tests show that in both cases, appropriate encapsulation (either PVC or coverlay), can reduce the amount by which the illuminance of light emitted degrades over 10 weeks.

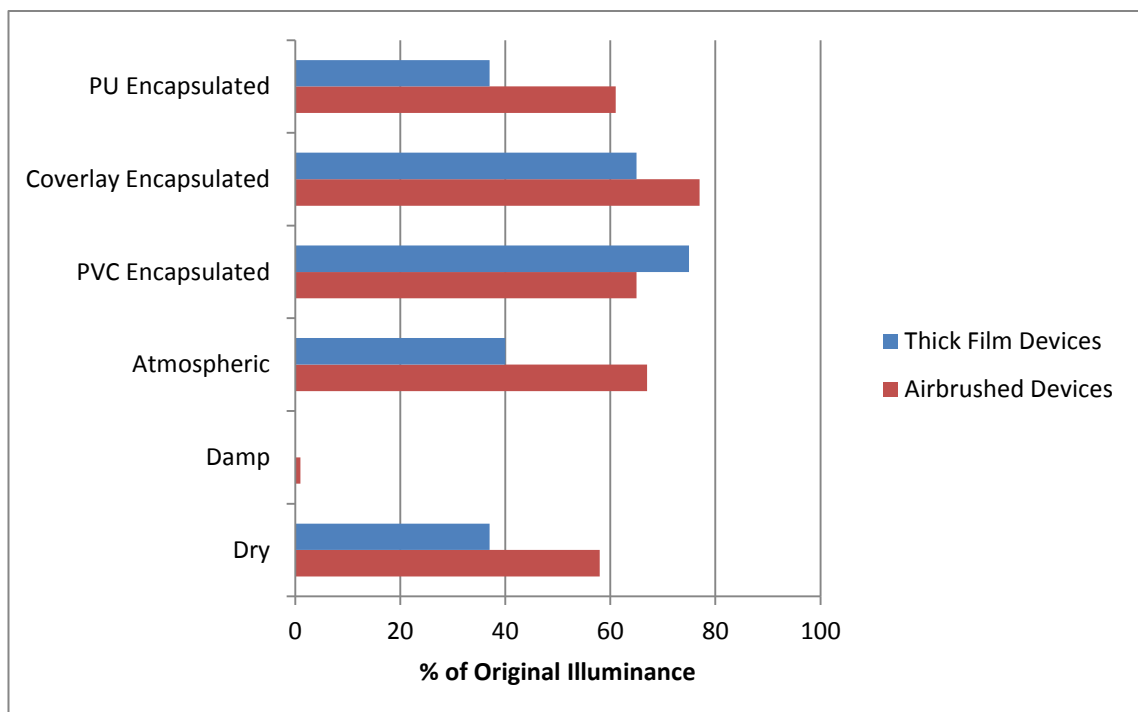


Figure 11-53: The relative illuminance of each device after the ten week degradation test.

With the exception of PVC encapsulation, the airbrushed devices made with modified materials degraded less than the thick film devices. This may suggest that the modified materials may produce more robust devices or that they are more tolerant of extreme humidities but there is simply not enough data to make any

definitive conclusions. The airbrush PVC encapsulated device did degrade more than its thick film counterpart, however more testing would need to be carried out to verify this result. This may simply be an anomaly as only one device for each processing method and storage condition was tested.

One conclusion that can be made is that the MEK dilution and airbrush application method does not seem to negatively impact the lifetime of devices made using the new process.

12 MODELLING A REAL DEVICE

Using the layer thickness data, it was possible to model the thermal profile across the layer structure of a real device. The in-mould layer application method was modelled since this is the only technique where the materials are required to cure in-mould; the insert method cures the layer materials before they are placed in the tool cavity. From section 11.1.2.6, the average layer thicknesses for devices made in-mould are:

- PEDOT:PSS = 6.47 μm ,
- Phosphor = 32.75 μm ,
- Dielectric = 19.29 μm , and
- Silver = 16.35 μm .

The following approximations and assumptions have been made in order to simplify the model:

- A four layer structure of PEDOT:PSS, Phosphor, dielectric and silver, is applied to a mould tool at 65 °C,
- The layer thicknesses (to the nearest micron) are 6 μm , 33 μm , 19 μm , and 16 μm ,
- The layers are injection moulded over with PP thermoplastic at 220 °C,
- The part has dimensions approximately 8 cm x 8 cm x 0.3 cm, including the 74 μm EL multi-layer structure; the EL layers have a surface area of 4 cm x 4 cm.

- The thermal conductivity and specific heat capacity of PP are $0.17 \text{ W.m}^{-1}.\text{K}^{-1}$ and $2.0 \text{ J.g}^{-1}.\text{K}^{-1}$ respectively [159].
- The thermal conductivity of the silver paste was assumed to be $5 \text{ W.m}^{-1}.\text{K}^{-1}$; this is approximately the conductivity of silver thermal compound.
- The thermal conductivity of the PEDOT:PSS was assumed to be $1.7 \text{ W.m}^{-1}.\text{K}^{-1}$ since this is the thermal conductivity of PEDOT:PSS pellets [160].
- The thermal conductivity of the dielectric and phosphor were estimated to be $0.1 \text{ W.m}^{-1}.\text{K}^{-1}$ and $0.15 \text{ W.m}^{-1}.\text{K}^{-1}$ respectively.

A diagram showing the layer thicknesses is shown in Figure 12-1; the colours of the layer materials also correspond to the graph shown in Figure 12-2 to aid the visualisation of the system.

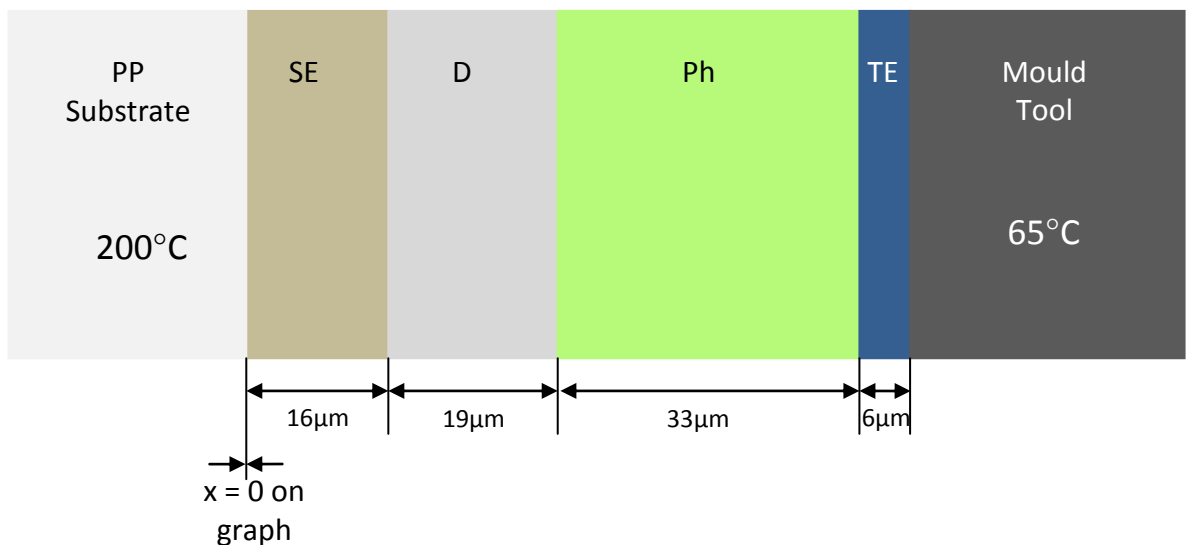


Figure 12-1: A diagram showing the average thicknesses of layers applied in-mould.

The multi-layer model shown in section 6.2 was used and the new layer thicknesses and thermal conductivity values were used. Table 12-1 shows a summary of the data calculated by the model; this shows the layer interface temperatures at particular times after the polymer is injected.

Table 12-1: The layer interface temperatures calculated by the model for specific times after injection.

t (s)	Temperature at Layer Interface (°C)				
	$T_{P(t)}$	$T_{SED(t)}$	$T_{DPh(t)}$	$T_{PhTE(t)}$	$T_{M(t)}$
0	220.00	218.89	153.23	77.20	65.00
1	216.73	215.65	151.37	76.94	65.00
2	213.53	212.47	149.54	76.69	65.00
5	204.32	203.32	144.30	75.96	65.00
10	190.22	189.33	136.28	74.85	65.00
20	166.17	165.44	122.59	72.96	65.00
30	146.73	146.15	111.52	71.43	65.00
45	124.35	123.92	98.78	69.67	65.00
60	108.10	107.79	89.53	68.39	65.00
90	87.72	87.56	77.94	66.79	65.00
120	76.98	76.90	71.82	65.94	65.00
180	68.33	68.31	66.90	65.26	65.00

Figure 12-2 shows the graph created by the model which shows how the temperature profile across the EL layer structure changes during the 60 seconds after injection.

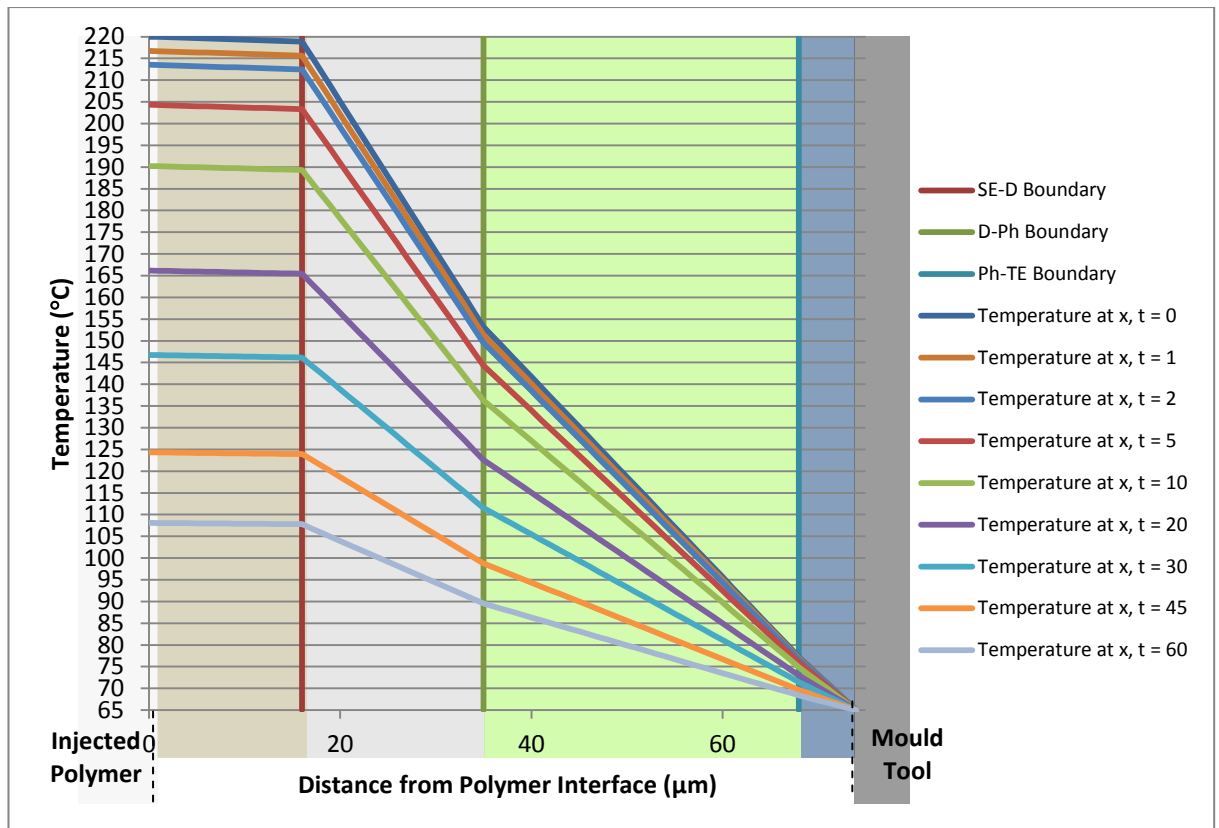


Figure 12-2: The temperature profile across the EL layers at particular times after injection.

Using the model it can be seen that the temperature of the PEDOT:PSS material never exceeds 77.2 °C throughout the moulding cycle. The PEDOT:PSS material used in the in-mould technique is Orgacon and the application sheet supplied with the material indicates that the minimum cure temperature is 80 °C [161]; this means that the cure temperature is never reached so the PEDOT:PSS layer is only dried but not cured. This explains why the PEDOT:PSS material washed off during sectioning; until the material has cross-linked, it is still soluble in water.

However, the model would benefit from more accurate thermal conductivity data. Since thermal conductivity information could not be obtained from the supplier, the thermal conductivity of the dielectric was assumed to be low; this was because the

dielectric was in a polymer matrix which tend to have low values and also because electrical and thermal conductivities are often linked. However, George *et al* state, there are polymer-ceramic thermal sink materials that can have thermal conductivities of $3.7 \text{ W.m}^{-1}.\text{K}^{-1}$ [162] depending on the amount of ceramic in them; this differs greatly from the $0.17 \text{ W.m}^{-1}.\text{K}^{-1}$ estimation used in this model and as such could have a large impact on the findings.

13 DISCUSSION

Following the detailed analysis of each device and process method, the aim of this section is to take a wider look at the developments made during this project and discuss the implications of this work.

13.1 Methods for Injection Moulding 3D Organic EL Devices

The objective of this project was to produce an injection moulded plastic part, incorporating electroluminescent layer materials over a 3D contour; this has been achieved by directly applying layer materials in-mould, and by introducing layer materials into the mould on pre-prepared inserts (using two different insert materials). These are completely novel processes that have never been carried out and published before. The research question specifies integrating the layer application into the injection moulding process; this is clearly achieved by the in-mould method but insert moulding is also a commonly used injection moulding technique so this is also considered as being integrated into the process. Although working parts have been made using all three methods, there has been varying degrees of success; Table 13-1 compares different aspects of each method (both process considerations and the reliability of the parts made using each process) in order to determine the method that currently best suits the injection moulding process. The scores have been judged by the author and are based on:

- Score 0 to 5 in most categories. 0=Very Poor, 1=Poor, 2=Adequate, 3=Good, 4=Very Good, 5=Excellent,
- Score 0 to -3 in “cons” category. 0=No Problems, -1=Easily Overcome, -2=Challenging, -3=Very Problematic.

Table 13-1: An evaluation of the success of each injection moulding process, in its current state of development.

		PE Insert Moulding		PTFE Insert Moulding		Direct In-Mould Application	
		Comment	Score	Comment	Score	Comment	Score
Process Considerations	Type & quality of PEDOT:PSS dilution	ITO-R; dilutes well with MEK and applied well to PE.	4	ITO-R; dilutes well with MEK, can be difficult to get an even coverage on the PTFE.	3	Orgacon™; dilutes with MEK very well and sprays well.	5
	Processing Time	Slow layer drying time due to low oven temperature but is carried out separately to the moulding process.	3	Fast drying times and layer application is carried out separately to moulding.	4	Very slow process time; each layer must dry in-mould and a heated mould lengthens the cooling time during the cycle.	0
	Processing Temperature	Oven at 80 °C; Cures PEDOT:PSS slowly and causes PE to expand and wrinkle.	2	Oven at 130 °C; Fully cures PEDOT:PSS quickly and is well below the limit of PTFE.	5	Mould at 65-75 °C; this is not high enough to cure the PEDOT:PSS, and there is also not enough energy transferred from the injected PP to initiate cure.	0
	Geometric Limitations	Shallow curves can be moulded easily. Cracks occur in layers when moulded over a 1 mm radius edge, not all areas illuminate.	2	Layers can even mould over a 1 mm radius edge; cracks due occur over the edge but all intact areas illuminate.	3	Shallow curves can be moulded easily. The force of injection caused severe layer disruption over a 1mm radius edge.	2

Product Considerations	Surface Finish	Good; encapsulating PE gives a good finish but air bubbles can occur and PEDOT:PSS is not adhered to the clear PE.	3	Very good; smooth, high gloss surface.	5	Poor; the layer forming mould release results in a dull surface finish	1
	Layer Quality	PEDOT:PSS layer is flaky and poorly adhered to the phosphor layer. Other layers fully dried.	2	Fully cured PEDOT:PSS layer that does not separate from the phosphor. Other layers fully dried.	5	Uncured PEDOT:PSS that rubs off on contact. Other layers remain intact.	1
	Illumination Reliability	Reasonable; failure to illuminate can occur but this may be due to separation from the copper external connection points.	3	Very reliable; all samples worked, even at high voltages and emitted a bright light.	5	Poor reliability; some samples failed to illuminate, some only illuminated over a fraction of the surface and all failed at high voltages.	1
	Layer Thickness	Good; very even layers across samples and between different samples in a batch. Less than optimal thickness.	4	Good; even layers across samples and between different samples in a batch. Optimal thickness.	4	Poor; large variation in each layer and disruption caused by injection. Optimal thickness.	1
Other Considerations	Pros	Layers fully encapsulated by the PE, can be processed using a standard injection moulding machine.	4	Processed using a standard injection moulding machine.	3	Parts made in-mould with no additional process stages, or carrier film required.	3

	Cons	Problems associated with connecting encapsulated electrodes to an electrical supply, insert production adds a process stage.	-2	Added expense of PTFE carrier film. No encapsulation layer, insert production adds a process stage.	-1	Lots of further developmental work needed to improve the process, auxiliary equipment required on the injection moulding machine.	-3
Total Score			25		36		11

Table 13-1 brings together the all of the findings from this project and it can be seen that, in the current stage of development, the best method for producing 3D injection moulded plastic parts with electroluminescent capabilities is to mould over a PTFE film pre-coated with the EL layer materials. The PTFE insert is then removed following ejection, leaving the EL layers embedded into the surface of the plastic part. The PTFE insert moulding method produces reliable, brightly illuminating parts with a good surface finish; this method can also produce illuminating surfaces over more acute curves than the other two methods. The PE insert moulding technique could also be viable but would need more development. However, the in-mould method has the significant benefit of complete part production in one manufacturing process. The in-mould process has considerable problems that would need to be overcome, including: poor surface finish, structure disrupted during injection and lighting reliability.

13.2 Solutions to Current Problems

The MEK modified materials can be successfully applied using the airbrush, but there is a moderate amount of variation in the applied layer thicknesses. This could

be reduced by standardising the dilution, mixing and spraying of materials and by measuring the viscosities of the mixtures. In this project the dilution was initially done by volume, but residual waste meant that not all material was transferred to the airbrush container thus causing variation in dilution and so was then carried out by trial and error. If the dilution was done by weight and mixed directly in the airbrush container the mixture would be more consistent. The mixing could be standardised by using magnetic mixing or motorised agitating devices. Material application could be made more repeatable by measuring the spraying time and by using a sample of ideal layer thickness as a standard to compare material coverage when spraying.

Although the PTFE insert moulding technique has been judged to be currently the most suitable method for injection moulding EL devices, this method produces parts with the delicate PEDOT:PSS layer as the outermost surface (a top emission structure). The degradation tests show that appropriate layer encapsulation can reduce light degradation and extend the life of part; although this work was carried out on devices with a bottom emission layer structure, opposite to the insert moulded parts. A logical step to improve the PTFE insert moulding technique would be to incorporate a clear encapsulating material into the layer structure applied to the film. The use of buffer layers could also be investigated as a means of reducing the chemical degradation at electrode interfaces.

With the PE insert moulding process, although the idea of an encapsulating insert material is a good one the PE is not a suitable selection; although this bonded with the PP injected substrate it did not adhere to the EL materials. The use of PET as an

insert film should be further investigated because this is a material that PEDOT:PSS readily adheres to. A thin film should be used (~0.05 mm) in order to avoid the creasing that occurred during the scoping experiments; and a PET injection substrate should be used so that the film bonds with it and seals the device. However the encapsulation means there would still be the issues associated with gaining electrical contact with the sealed electrode layers.

A number of different solutions could be used to improve the in-mould layer application technique; currently poor surface quality, inconsistencies in layers, disruption to the structure and incomplete PEDOT:PSS cure all contribute to the unreliability of the process. The dull surface finish caused by the mould release could be prevented by using a PTFE coated mould tool. The disruption to the layer structure could be dramatically reduced by investigating different injection positions and process parameters. The utilisation of rapid tool heating and cooling methods would speed up the process and ensure that the PEDOT:PSS is fully cured during the injection moulding cycle. This process could also further be taken forward by applying an encapsulating layer in-mould; similar adhesion and release problems would need to be overcome as in this project and a method of allowing contact with electrode layers would need to be considered.

All three of the new methods could also be used with different emitting layer materials (that emit different colour of light), and undergo further process development to apply a number of different coloured areas and/or patterns in one part.

Although a thermal model of the multi-layer system has been created with real layer thickness data, approximations of thermal conductivity were used; in order to improve the calculations made by the model real thermal conductivity data is required. A method of measuring thermal conductivity of polymeric materials has been found; it is done by characterising a section of extruded polymer (of particular dimensions) in a modulated differential scanning calorimeter [163]. This could be used as a basis for developing a methodology for measuring the thermal conductivity of the materials used in this process. Additional thermal characterisation of PEDOT:PSS (using both a DSC and DMTA) would also be useful to determine the accurate cure onset temperature, and cure energy. Along with the model, this information could be used to determine the optimal tool heating and cooling regime.

13.3 The Wider Impact of this Research

It has already been shown that this project has developed three different options for producing electroluminescent parts using the injection moulding process; a transfer insert moulding technique (currently using PTFE film), an encapsulating insert moulding technique (currently using PE but PET is a suggested alternative) and by direct in-mould layer application. With the additional developments suggested in the previous section all of these techniques could become viable options for mass producing electroluminescent plastic parts.

These techniques could be beneficial in three ways; removing the need for multiple components in an illuminating part, combining the functions of two separate devices and providing additional functionality to simple objects.

Lighting units that currently comprise of a housing, bulb, holder, connections and lens cover could just be manufactured as a single illuminating plastic panel that can be easily ejected and replaced when necessary. Using this technology as an alternative to traditional lighting could contribute to weight and space saving in cars and result in having the ability to put lighting into previously difficult areas.

The ability to illuminate different objects also opens up many possibilities to make everyday tasks easier or safer. Panels within glove boxes and cupboards could light up making it easier to find things in dark areas and road safety could be improved by make many plastic items more visible; traffic cones, barriers, temporary roadwork signs and even workmen can be made more visible to other road users.

The ability of objects to illuminate could also be beneficial to people with visual impairments, particularly in aiding the location of objects; entire phone casings could illuminate when they ring and electrical sockets/switches could have an illuminated strip incorporated into the plastic panel.

The techniques developed in this project could also be combined with other research, widening the opportunities offer by this process. Different printing technologies such as gravure and inkjet could be used to make inserts; gravure printing offers the opportunity to produce large scale, patterned illuminating inserts and inkjet printing could produce inserts with more precise material application with the scope to produce insert moulded parts with printed circuits embedded into them.

Another way in which this novel process could enhance the function of plastic parts is to injection mould other multi-layer devices; some current areas of research that may suit this technique are energy generation and storage. Organic photovoltaic's (OPVs) and Organic Radical Batteries (ORBs) [164] are examples of multi-layer systems that have a similar structure to that of the electroluminescent lamp used in this project; they all consist of electrode layers separated by one or more layers including the relevant "*smart*" material. The similarities in the materials and structure suggest that it is feasible that this novel technique could be adapted to apply PV and battery layer materials during manufacture which would further increase the functionality options of injection moulded plastic parts.

Injection moulded parts could capture the Sun's energy, store energy or illuminate... or all three. It may be possible to have a single plastic panel that can generate electricity during daytime, store the energy and then illuminate at night; road signs, bus or train shelters, street light panels (as opposed to tall street lamps) and buildings with no mains electricity are all situations where such a panel could be utilised. This idea could also benefit communities in developing countries that have no access to mains electricity by offering the opportunity to have lighting and a means of generating electricity for other small appliances.

In summary, the new techniques developed in this project could be the basis for future technologies that have a considerable impact by increasing types of everyday objects that can generate, use and store electricity.

14 CONCLUSIONS

The following conclusions can be drawn from the work carried out throughout this project; the original research question was:

“Can electroluminescent technology be integrated into the injection moulding process to produce 3D illuminating plastic parts?”

The answer to this question is that the injection moulding process can be used to manufacture plastic with multi-layer EL materials embedded over a 3D contoured surface. Figure 14-1 shows 3D electroluminescent parts made using three different injection moulding methods; two types of insert moulding and direct in-mould layer application.



Figure 14-1: 3D electroluminescent injection moulded parts shown from different angles; PTFE insert moulded (left), PE insert moulded (middle) and in-mould layer application (right).

The new processes developed in this project are completely novel; multi-layer electroluminescent devices have never been incorporated into injection moulded parts before, by either insert moulding or in-mould layer application.

All of the original specific objectives have also been met; the solution to each one follows:

- **To determine the optimum electroluminescent structure for an in-mould process; this is the minimum number of layers that will reliably form a working EL lamp.**

The optimal structure of an injection moulded EL lamp that is operated at 300 V and 400 Hz is a four layer structure; a PEDOT:PSS transparent electrode (with silver busbar), followed by a phosphor layer, a dielectric layer and finally a silver rear electrode. The combined phosphor and dielectric layer should ideally be 60 μm .

- **To develop a method of integrating the application of electroluminescent layer materials to the injection moulding process.**

The application of the multi-layer electroluminescent structure was incorporated into the injection moulding process by utilising an airbrush layer application method to apply diluted EL materials; this was done by applying layer materials directly into the mould cavity and injection moulding over a pre-prepared insert film. The insert can either be a transfer film (removed after moulding) or an encapsulating film that becomes part of the final part.

- **To produce 3D injection moulded plastic parts with electroluminescent capabilities.**

The in-mould technique and both insert moulding methods successfully produced injection moulded parts with a working EL device moulded over a 3D contour, see Figure 14-1.

- **To describe any geometric limitations observed in the new process.**

The in-mould and PE insert moulded techniques were unable to successfully mould EL layers over a curve with a radius of 1 mm. The PTFE insert moulding method could mould over a 1 mm radius curve but there was some damage/cracking to the layer materials.

- **To model the temperature conditions undergone by the layer materials during an injection moulding cycle.**

The multi-layer model developed during this project showed that the in-mould technique, in its current state, does not provide enough heat energy to cure the PEDOT:PSS transparent electrode layer. With a mould tool at 65 °C, the injected polymer at 220 °C and a total multi-layer thickness of 74 µm, the 6 µm electrode layer does not exceed a temperature of 77.2 °C and the cure onset temperature of PEDOT:PSS is 80 °C.

- **To characterise the layer thickness and illuminance of the injection moulded EL devices.**

At 330 V and 400 Hz, the PE insert moulded devices light up with an average illuminance of 132.6 ± 29.1 lx. The average thicknesses of the layers are: PEDOT:PSS is 2.78 ± 0.50 µm, phosphor is 18.25 ± 4.48 µm, dielectric is 25.27 ± 3.76 µm and silver is 12.20 ± 3.82 µm.

At 330 V and 400 Hz, the PTFE insert moulded devices light up with an average illuminance of 210.2 ± 39.2 lx. The average thicknesses of the layers are: PEDOT:PSS is 1.96 ± 0.65 µm, phosphor is 32.41 ± 11.21 µm, dielectric is 22.24 ± 6.02 µm and silver is 11.59 ± 2.81 µm.

At 330 V and 400 Hz, the in-mould devices light up with an average illuminance of 44.7 ± 14.2 lx. The average thickness of the layers is: PEDOT:PSS is 6.47 ± 2.03 μm , phosphor is 32.75 ± 9.16 μm , dielectric is 19.29 ± 5.59 μm and silver is 16.35 ± 5.98 μm .

- **To compare the layer thicknesses and illuminance of devices made using the new injection moulding process with a bought device and a thick film device made using the EL materials in a paste form.**

At 330V and 400Hz, the PE insert moulded devices emit light 28.5% the brightness of a bought device and 78.7 % the average brightness of the thick film devices. The combined phosphor and dielectric layer thickness of the PE insert moulded device was 73.9 % the thickness of the equivalent layers in the bought device and 35.3 % of those in the thick film devices.

At 330 V and 400 Hz, the PTFE insert moulded devices emit light 45.0 % the brightness of a bought device and 124.3 % the average brightness of the thick film devices. The combined phosphor and dielectric layer thickness of the PTFE insert moulded devices was 92.7 % the thickness of the equivalent layer in the bought device and 44.3 % of those in the thick film devices.

At 330 V and 400 Hz, the in-mould devices emit light 9.64 % the brightness of a bought device and 26.6 % the average brightness of the thick film devices. The combined phosphor and dielectric layer thickness of the in-mould devices was 88.3 % the thickness of the equivalent layer in the bought device and 42.2 % of those in the thick film devices.

- **To monitor the degradation of the intensity of light emitted by devices made by the new process with modified materials over a 10 week period. Different conditions and encapsulation options will be considered.**

After 10 weeks, the airbrushed device kept in atmospheric conditions maintained 67.3 % of its original illuminance. The device encapsulated with the UV cured coverlay had the smallest decrease in illuminance; after 10 weeks it had maintained 77.3 % of its original illuminance.

- **To compare the degradation of the devices made with modified materials to equivalent devices made with materials used as intended.**

After 10 weeks, the thick film device kept in atmospheric conditions maintained 40.0 % of its original illuminance. The device with the smallest decrease in illuminance was PVC encapsulated, followed by the UV cured coverlay; after 10 weeks they had maintained 74.5 % and 65.5 % of their original illuminance. So under atmospheric conditions, the thick film device lost 27.3 more percentage points of its illuminance than the airbrushed device.

15 FURTHER WORK

Although this project has made a significant step forward by showing that 3D plastic parts with EL capabilities can be made by injection moulding, there are many ways in which this work can be taken further and extended along different developmental pathways. This chapter describes how this research can be continued, how it can act as a basis for additional projects and techniques to make the process more commercially viable.

15.1 Extension work related to this project

Injection moulded EL devices can be made using inserts and by applying materials directly in-mould, with PTFE insert moulding producing the most consistent and reliable parts. As already mention in the discussion, a number of different improvements could be made to the current processes and could take this project further; a summary follows:

- Further work for the PTFE insert moulding technique:
 - Incorporation of an additional clear layer
- Further work for the encapsulating insert moulding technique:
 - The use of a PET insert film along with a PET injected substrate
- Further work for the in-mould technique:
 - Injection moulding process parameters
 - Tool design (e.g. injection point)
 - Rapid tool heating and cooling
- Further work for the model:

- Thermal conductivity measurements using MDSC
- PEDOT:PSS cure data using DSC and DMTA
- Calculation of optimal tool heating regime
- General further work
 - Standardising airbrush layer application
 - The use of different and multiple colour phosphors
 - Applying different multi-layer devices such as OLEDs, batteries and PV

Along with these improvements, there are some more extensive investigations that can be undertaken.

Although some simple geometric limitations have been identified in this project (the discontinuation of layer materials when moulded over a curve of radius of 1mm), there needs to be a more detailed investigation into these. Mould tools including profile edges with a large range of radius of curvatures would need to be utilised in order to accurately determine the sharpest edge that the EL layers can be successfully applied and moulded over. More complex shapes could also be investigated to include different corner and cut-out options to give an idea of any shape restrictions of the process.

For the 300 V, 400 Hz power supply used in this project, the optimal combined phosphor and dielectric layer thickness was 60 μm but this may not be true for different power supplies. The optimal thickness of layer materials could be determined in relation to both the power supply available and the geometry of the

plastic part. The geometry of the tool may require a particular thickness of material in order to maintain the continuation of the layer over a shape during moulding.

This project has already established that these devices can be operated using batteries and an inverter; further work could be done in this area looking specifically at the possibility of the use of different layer materials, thicknesses and an even simpler structure. Different batteries and inverters produce different alternating currents and as such may have different optimal layer thicknesses to the ones determined in this project. Early in this project it was determined that a dielectric layer was required since devices without one failed at high voltages; a battery and inverter operates devices at lower voltages so it is possible that the dielectric layer may not be necessary. Additional research could also consider incorporating battery/inverter holders into the part design. The addition of battery connectors after moulding would also need to be considered with regards to the positioning of electrode layers and connection to them.

Towards the end of this project, a company was found working in the area of inkjet printing EL materials; they had developed a printing substrate suitable to use with a readily available inkjet printer and worked with a phosphor company to combine the phosphor and dielectric into one layer [165-167]. This would be of particular interest to this project as the removal of a layer from the structure would shorten production time.

The research could also be continued by investigating the rate of material deposition by the airbrush; this has already been recognised as a cause of variation in layer thickness. The deposition rate is likely to vary for each layer material and if

a particular thickness of layer is required the application time can be calculated and implemented during the production process.

The layer thickness and rate of material deposition data could be combined with the dimensional limitation information to give a more comprehensive guide to the process. For example, the following recommendations could then be given when planning the manufacture of an injection moulded EL part: when an edge/curve is of smaller radius of x mm, a y μm layer thickness is required which can be applied with a z s spraying time.

One final extension to this project is to calculate the cost per unit area of producing electroluminescent injection moulded parts by direct in-mould layer application and using insert moulding. This would provide additional useful information when comparing the two processing methods and could be compared with commercial production costs, to see if it is competitive.

15.2 Developments to make the Process more Commercially Viable

Although this section involves suggestions that would be too costly and complex for university research projects, it has been included to show that the author has considered how existing technology could be used to make the novel process developed in this project more commercially appealing.

The novel process developed in this project works. However, the layer application adds up to 10 minutes onto a single mould cycle and this would not be considered acceptable if the technique was to move beyond research and into mass

production. The following technologies could be used to reduce the amount of time added to each cycle and therefore improve production rates:

- The use of multi-cavity tools; by producing more parts per cycle, the production rate goes up, however, there is the added complexity of having to apply layer materials to numerous cavities simultaneously.
- The use of robotics; controlled, precise, and consistent layer application could be achieved using robotic arms, the process would be considerably faster than the hand operated system used in this project, directly reducing cycle times.
- Using multiple tools rotating through different process stages; each layer application and drying time could take place at different positions in a cycle (injection and ejection would be the last stage). Overall production rates would go up because a number of cycles are carried out simultaneously, staggered in time.

One method also developed in this project (which will incur a minimal increase in cycle time) is insert moulding EL parts; the layer application and drying takes places separately to the injection moulding and therefore does not impact on the machine production rate. The following ideas suggest how the insert production method could be made more commercial by automating the system:

- Robotics could be used to improve and speed up the layer application process, and placing the insert into the empty mould tool,
- More complex layer designs can be applied using inkjet printing,

- Drying a greater number of inserts in larger ovens would reduce the production time per insert,
- A production line could be used where the insert films goes under a series of spray applications and drying ovens; this could be carried out to produce:
 - A continuous roll of EL insert, or
 - Individual inserts on a conveyor belt.

All of these suggestions are existing techniques and technologies, so it is feasible that they could be easily incorporated into the production of injection moulded plastic parts to improve the process now that the initial production methodology has been developed, tested and analysed.

15.3 Further projects

This project has shown that, using an airbrush and compressor, solution based electroluminescent materials can be sprayed onto pre-moulded plastic parts, dried at temperatures achievable with a home oven, and produced illuminating parts. This idea could be taken further to develop a “home spraying system”; a set of aerosol cans containing layer materials that can be applied to already-owned items in order to make them electroluminescent. This “kit” would also need to have an electrode connector kit, linking this idea to the battery operated suggestion in the previous section.

Using the new injection moulding technique, a project which designs modular illuminating parts could be carried out. The outcome would be the production of a set of standard parts that can fit together in any configuration to make different shaped and sized illuminating panels or structures. The challenges to overcome in a

project such as this are: the design of the moulded features to allow easy and secure connection, the continuity of electrode layers over the connection whilst maintaining separation between the two separate electrodes. A power supply (battery & inverter) or power connection (mains adapter) module could be included and the possibility of using different colour or partially illuminating modules to increase the range of achievable shapes and patterns that could be considered.

The aim of this project was to incorporate EL functionality into the body of plastic parts and as such composite materials are produced during the process. As mentioned (briefly) in the literature review, this could negatively impact on the recyclability of those plastic parts. From this, two interesting projects could arise; one related to the recycling of the multi-material part and one about material recovery. Injection moulded EL parts can be ground up, remoulded, characterised and the properties compared with those of virgin and recycled grades of the substrate material in order to see the impact that EL materials have on the quality of the recycled material. In a different project, a study can be carried out into which layer material most requires recovery and different methods of can be investigated and tested. There is also the possibility of attempting to recover more than one material.

16 REFERENCES

- [1] R. Vepa, *Dynamics of smart structures*. Hoboken, NJ: John Wiley, 2010.
- [2] D. J. Leo, *Engineering analysis of smart material systems*. Hoboken, N.J.: John Wiley & Sons, 2007.
- [3] D. M. Addington and D. L. Schodek, *Smart materials and new technologies : for the architecture and design professions*. Amsterdam ; Boston: Architectural Press, 2005.
- [4] M. F. Ashby, P. J. S. G. Ferreira, and D. L. Schodek, *Nanomaterials, nanotechnologies and design : an introduction for engineers and architects*. Amsterdam ; Boston: Butterworth-Heinemann, 2009.
- [5] D. Haranath and V. Shanker, "Electroluminescence," in *Handbook of Electroluminescent Materials*. vol. null, ed: Taylor & Francis, 2004.
- [6] R. J. Mortimer, A. L. Dyer, and J. R. Reynolds, "Electrochromic organic and polymeric materials for display applications," *Displays*, vol. 27, pp. 2-18, 2006.
- [7] P. Bamfield, M. G. Hutchings, and Royal Society of Chemistry (Great Britain). (2010). *Chromic phenomena technological applications of colour chemistry (2nd ed.)*. Available: <http://0-dx.doi.org.pugwash.lib.warwick.ac.uk/10.1039/9781849731034>
- [8] R. Baetens, B. P. Jelle, and A. Gustavsen, "Properties, requirements and possibilities of smart windows for dynamic daylight and solar energy control in buildings: A state-of-the-art review," *Solar Energy Materials and Solar Cells*, vol. 94, pp. 87-105, 2010.
- [9] P. R. Somani and S. Radhakrishnan, "Electrochromic materials and devices: present and future," *Materials Chemistry and Physics*, vol. 77, pp. 117-133, 2003.
- [10] C. G. Granqvist, P. C. Lansåker, N. R. Mlyuka, G. A. Niklasson, and E. Avendaño, "Progress in chromogenics: New results for electrochromic and thermochromic materials and devices," *Solar Energy Materials and Solar Cells*, vol. 93, pp. 2032-2039, 2009.
- [11] C. M. Lampert, "Chromogenic smart materials," *Materials Today*, vol. 7, pp. 28-35, 2004.
- [12] T. Tsujioka and M. Irie, "Electrical functions of photochromic molecules," *Journal of Photochemistry and Photobiology C: Photochemistry Reviews*, vol. 11, pp. 1-14, 2010.
- [13] B. P. Jelle, A. Hynd, A. Gustavsen, D. Arasteh, H. Goudey, and R. Hart, "Fenestration of today and tomorrow: A state-of-the-art review and future research opportunities," *Solar Energy Materials and Solar Cells*, vol. 96, pp. 1-28, 2012.
- [14] J. Ma, X. Ye, and B. Jin, "Structure and application of polarizer film for thin-film-transistor liquid crystal displays," *Displays*, vol. 32, pp. 49-57, 2011.
- [15] L. Tsakalakos. (2010). *Nanotechnology for photovoltaics*. Available: <http://0-marc.crcnetbase.com.pugwash.lib.warwick.ac.uk/isbn/9781420076752>
- [16] V. W. W. Yam. (2010). *WOLEDs and organic photovoltaics recent advances and applications*. Available:

- <http://0-dx.doi.org.pugwash.lib.warwick.ac.uk/10.1007/978-3-642-14935-1>
- [17] P. G. Charalambous, G. G. Maidment, S. A. Kalogirou, and K. Yiakoumetti, "Photovoltaic thermal (PV/T) collectors: A review," *Applied Thermal Engineering*, vol. 27, pp. 275-286, 2007.
- [18] M. A. Hasan and K. Sumathy, "Photovoltaic thermal module concepts and their performance analysis: A review," *Renewable and Sustainable Energy Reviews*, vol. 14, pp. 1845-1859, 2010.
- [19] R. Kumar and M. A. Rosen, "A critical review of photovoltaic–thermal solar collectors for air heating," *Applied Energy*, vol. 88, pp. 3603-3614, 2011.
- [20] C. T.T, "A review on photovoltaic/thermal hybrid solar technology," *Applied Energy*, vol. 87, pp. 365-379, 2010.
- [21] X. Zhang, X. Zhao, S. Smith, J. Xu, and X. Yu, "Review of R&D progress and practical application of the solar photovoltaic/thermal (PV/T) technologies," *Renewable and Sustainable Energy Reviews*, vol. 16, pp. 599-617, 2012.
- [22] J. Minase, T. F. Lu, B. Cazzolato, and S. Grainger, "A review, supported by experimental results, of voltage, charge and capacitor insertion method for driving piezoelectric actuators," *Precision Engineering*, vol. 34, pp. 692-700, 2010.
- [23] S. Mondal, "Recent Developments in Temperature Responsive Shape Memory Polymers," *Mini-Reviews in Organic Chemistry*, vol. 6, pp. 114-119, 2009.
- [24] Q. Meng and J. Hu, "A review of shape memory polymer composites and blends," *Composites Part A: Applied Science and Manufacturing*, vol. 40, pp. 1661-1672, 2009.
- [25] J. Leng, X. Lan, Y. Liu, and S. Du, "Shape-memory polymers and their composites: Stimulus methods and applications," *Progress in Materials Science*, vol. 56, pp. 1077-1135, 2011.
- [26] L. Xue, S. Dai, and Z. Li, "Biodegradable shape-memory block co-polymers for fast self-expandable stents," *Biomaterials*, vol. 31, pp. 8132-8140, 2010.
- [27] H. J. Round, "A Note on Carborundum," *Electrical World*, 1907.
- [28] A. N. Krasnov, "Electroluminescent displays: history and lessons learned," *Displays*, vol. 24, pp. 73-79, 2003.
- [29] P. Kopola, M. Tuomikoski, R. Suhonen, and A. Maaninen, "Gravure printed organic light emitting diodes for lighting applications," *Thin Solid Films*, vol. 517, pp. 5757-5762, 2009.
- [30] R. Meerheim, B. Lussem, and K. Leo, "Efficiency and stability of p-i-n type organic light emitting diodes for display and lighting applications," *Proceedings of the IEEE*, vol. 97, pp. 1606-26, 2009.
- [31] S.-F. Wang, J.-C. Pu, and J. C. Sung, "The characteristics of inorganic electroluminescent devices with an amorphous diamond film as cathode material," *Thin Solid Films*, vol. 517, pp. 1821-1824, 2009.
- [32] G. Sharma, S. D. Han, J. D. Kim, S. P. Khatkar, and Y. Woo Rhee, "Electroluminescent efficiency of alternating current thick film devices using ZnS:Cu,Cl phosphor," *Materials Science and Engineering: B*, vol. 131, pp. 271-276, 2006.

- [33] Z. H. Kafafi and CRC Press. (2005). *Organic electroluminescence*. Available: <http://marc.crcnetbase.com/ISBN/9781420028201> Available: <http://0-marc.crcnetbase.com.pugwash.lib.warwick.ac.uk/ISBN/9781420028201>
- [34] J. Shinar and R. Shinar, "An Overview of Organic Light-Emitting Diodes and their Applications," in *Comprehensive Nanoscience and Technology*, C. Editors in, xA, L. A. David, D. S. Gregory, and P. W. Gary, Eds., ed Amsterdam: Academic Press, 2011, pp. 73-107.
- [35] Z. R. Li, H. Meng, and CRC Press. (2007). *Organic light-emitting materials and devices*. Available: <http://marc.crcnetbase.com/ISBN/9781420017069> Available: <http://0-marc.crcnetbase.com.pugwash.lib.warwick.ac.uk/ISBN/9781420017069>
- [36] M. de Kok, W. Sarfert, and R. Paetzold, "Tuning the colour of white polymer light emitting diodes," *Thin Solid Films*, vol. 518, pp. 5265-5271, 2010.
- [37] A. Leni, "Electroluminescent polymers," *Progress in Polymer Science*, vol. 28, pp. 875-962, 2003.
- [38] R. J. H. Young, P. S. A. Evans, G. I. Hay, D. J. Southee, and D. J. Harrison, "Electroluminescent light sources via soft lithography," *Circuit World*, vol. 34, pp. 9-12, 2008.
- [39] K. Müllen and U. Scherf, *Organic light emitting devices : synthesis, properties, and applications*. Weinheim: Wiley-VCH, 2006.
- [40] M.-C. Choi, Y. Kim, and C.-S. Ha, "Polymers for flexible displays: From material selection to device applications," *Progress in Polymer Science*, vol. 33, pp. 581-630, 2008.
- [41] A. R. Duggal, C. M. Heller, J. J. Shiang, L. J., and L. N. Lewis, "Solution-Processed Organic Light Emitting Diodes for Lighting," *Journal of Display Technology*, vol. 3, pp. 184-192, 2007.
- [42] A. R. Duggal, C. M. Heller, J. J. Shiang, L. Jie, and L. N. Lewis, "Solution-processed organic light-emitting diodes for lighting," *Journal of Display Technology*, vol. 3, pp. 184-92, 2007.
- [43] C. Piliago, M. Mazzeo, B. Cortese, R. Cingolani, and G. Gigli, "Organic light emitting diodes with highly conductive micropatterned polymer anodes," *Organic Electronics*, vol. 9, pp. 401-6, 2008.
- [44] M. Aparna and et al., "White organic LEDs and their recent advancements," *Semiconductor Science and Technology*, vol. 21, p. R35, 2006.
- [45] J. Li, T. Sano, Y. Hirayama, and K. Shibata, "White polymer light emitting diodes with multi-layer device structure," *Synthetic Metals*, vol. 159, pp. 36-40, 2009.
- [46] Z. Lü, Z. Deng, J. Zheng, D. Xu, Z. Chen, E. Zhou, *et al.*, "Organic light-emitting diodes with 2-(4-biphenyl)-5(4-tert-butyl-phenyl)-1,3,4-oxadiazole layer inserted between hole-injecting and hole-transporting layers," *Vacuum*, vol. 84, pp. 1287-1290, 2010.
- [47] J.-H. Jou, S.-M. Shen, C.-R. Lin, Y.-S. Wang, Y.-C. Chou, S.-Z. Chen, *et al.*, "Efficient very-high color rendering index organic light-emitting diode," *Organic Electronics*, vol. 12, pp. 865-868, 2011.
- [48] D. Zhu, H. Ye, J. Gao, and X. Liu, "Modeling and numerical study of electrical characteristics of polymer light-emitting diodes containing an insulating buffer layer," *Thin Solid Films*, vol. 515, pp. 7264-7268, 2007.

- [49] P.-C. Kao, J.-H. Lin, J.-Y. Wang, C.-H. Yang, and S.-H. Chen, "Improved electron injection into Alq3 based OLEDs using a thin lithium carbonate buffer layer," *Synthetic Metals*, vol. 160, pp. 1749-1753, 2010.
- [50] L. Tsung-Hsun, J. C. A. Huang, G. L. Pakhomov, G. Tzung-Fang, W. Ten-Chin, H. Yi-Shun, *et al.*, "Organic-oxide cathode buffer layer in fabricating high-performance polymer light-emitting diodes," *Advanced Functional Materials*, vol. 18, pp. 3036-42, 2008.
- [51] M. Eritt, C. May, K. Leo, M. Toerker, and C. Radehaus, "OLED manufacturing for large area lighting applications," *Thin Solid Films*, vol. 518, pp. 3042-3045, 2010.
- [52] X. Zhang, Z. Wu, B. Jiao, D. Wang, D. Wang, X. Hou, *et al.*, "Solution-processed white organic light-emitting diodes with mixed-host structures," *Journal of Luminescence*, vol. 132, pp. 697-701, 2012.
- [53] T. H. Park, Y. W. Park, J. H. Choi, H. J. Choi, J.-W. Jeong, E. H. Song, *et al.*, "Contact printing of the emitting layer for high performance multilayered phosphorescent organic light-emitting diodes," *Organic Electronics*, vol. 12, pp. 1063-1067, 2011.
- [54] C. W. Joo, S. O. Jeon, K. S. Yook, and J. Y. Lee, "Improved device performances in polymer light-emitting diodes using a stamp transfer printing process," *Organic Electronics*, vol. 10, pp. 372-375, 2009.
- [55] G.-J. A. H. Wetzelaer, D. Hartmann, S. G. Santamaría, M. Pérez-Morales, A. S. Portillo, M. Lenes, *et al.*, "Combined thermal evaporated and solution processed organic light emitting diodes," *Organic Electronics*, vol. 12, pp. 1644-1648, 2011.
- [56] S. Schols and SpringerLink (Online service). (2011). *Device architecture and materials for organic light-emitting devices targeting high current densities and control of the triplet concentration*. Available: <http://0-dx.doi.org.pugwash.lib.warwick.ac.uk/10.1007/978-94-007-1608-7>
- [57] B.-J. De Gans, P. C. Duineveld, and U. S. Schubert, "Inkjet printing of polymers: State of the art and future developments," *Advanced Materials*, vol. 16, pp. 203-213, 2004.
- [58] R. Satoh, S. Naka, M. Shibata, H. Okada, H. Onnagawa, and T. Miyabayashi, "White organic electroluminescent devices fabricated using ink-jet printing method," *Japanese Journal of Applied Physics, Part 1 (Regular Papers, Short Notes & Review Papers)*, vol. 43, pp. 7395-8, 2004.
- [59] D.-Y. Chung, J. Huang, D. D. C. Bradley, and A. J. Campbell, "High performance, flexible polymer light-emitting diodes (PLEDs) with gravure contact printed hole injection and light emitting layers," *Organic Electronics*, vol. 11, pp. 1088-1095, 2010.
- [60] F. C. Krebs, J. Fyenbo, and M. Jorgensen, "Product integration of compact roll-to-roll processed polymer solar cell modules: methods and manufacture using flexographic printing, slot-die coating and rotary screen printing," *Journal of Materials Chemistry*, vol. 20, pp. 8994-9001, 2010.
- [61] K. S. Subrahmanyam, P. Kumar, A. Nag, and C. N. R. Rao, "Blue light emitting graphene-based materials and their use in generating white light," *Solid State Communications*, vol. 150, pp. 1774-1777, 2010.

- [62] Y. Yunchan, P. Jongwoon, and P. Byoungchoo, "Solution-Processed Flexible ITO-Free Organic Light-Emitting Diodes Using Patterned Polymeric Anodes," *Journal of Display Technology*, vol. 6, pp. 252-6, 2010.
- [63] A. Takakuwa, M. Misaki, Y. Yoshida, and K. Yase, "Micropatterning of emitting layers by microcontact printing and application to organic light-emitting diodes," *Thin Solid Films*, vol. 518, pp. 555-558, 2009.
- [64] L. Taik-Min, C. Hyun-Cheol, N. Jae-Ho, and K. Dong-Soo, "EL display printed on curved surface," in *2009 IEEE 22nd International Conference on Micro Electro Mechanical Systems. MEMS 2009, 25-29 Jan. 2009*, Piscataway, NJ, USA, 2009, pp. 943-6.
- [65] J. Jin, J. J. Lee, B.-S. Bae, S. J. Park, S. Yoo, and K. Jung, "Silica nanoparticle-embedded sol-gel organic/inorganic hybrid nanocomposite for transparent OLED encapsulation," *Organic Electronics*, vol. 13, pp. 53-57, 2012.
- [66] S. Cros, R. de Bettignies, S. Berson, S. Bailly, P. Maise, N. Lemaitre, *et al.*, "Definition of encapsulation barrier requirements: A method applied to organic solar cells," *Solar Energy Materials and Solar Cells*, vol. 95, Supplement 1, pp. S65-S69, 2011.
- [67] J.-S. Park, H. Chae, H. K. Chung, and S. I. Lee, "Thin film encapsulation for flexible AM-OLED: A review," *Semiconductor Science and Technology*, vol. 26, 2011.
- [68] Z. A.I, "Enhancement of light extraction from light emitting diodes," *Physics Reports*, vol. 498, pp. 189-241, 2011.
- [69] K. Saxena, V. K. Jain, and D. S. Mehta, "A review on the light extraction techniques in organic electroluminescent devices," *Optical Materials*, vol. 32, pp. 221-233, 2009.
- [70] Z. Lü, Z. Deng, J. Zheng, Y. Yin, Y. Chen, and Y. Wang, "Organic light-emitting diodes with nanostructured fullerene ultrathin layers," *Physica B: Condensed Matter*, vol. 405, pp. 335-339, 2010.
- [71] A. R. Inigo, J. M. Underwood, and S. R. P. Silva, "Carbon nanotube modified electrodes for enhanced brightness in organic light emitting devices," *Carbon*, vol. 49, pp. 4211-4217, 2011.
- [72] H.-S. Koo, M. Chen, H.-W. Yu, S.-K. Kwon, Y.-K. Lee, and J. Jang, "Electroluminescent characteristics of organic light-emitting diodes with doped carbon nanotubes," *Diamond and Related Materials*, vol. 16, pp. 1162-1166.
- [73] T. Chiba, Y.-J. Pu, R. Miyazaki, K.-i. Nakayama, H. Sasabe, and J. Kido, "Ultra-high efficiency by multiple emission from stacked organic light-emitting devices," *Organic Electronics*, vol. 12, pp. 710-715, 2011.
- [74] W. Michaeli, *Plastics processing: an introduction*. Munich: Hanser Publishers, 1995.
- [75] V. Goodship, Arburg (Firm), and Rapra Technology Limited., *Practical guide to injection moulding*. Shawbury: Rapra Technology, 2004.
- [76] R. J. Crawford, *Plastics engineering*, 3rd ed. Oxford: Butterworth-Heinemann, 1998.
- [77] H.-G. Elias, *An introduction to plastics*, 2nd, completely rev. ed. [Weinheim]: Wiley-VCH, 2003.

- [78] N. J. Mills, *Plastics : microstructure and engineering applications*, 3rd ed. Oxford; Burlington, MA: Elsevier Butterworth-Heinemann, 2005.
- [79] V. Goodship, *Introduction to plastics recycling*, 2nd ed. Shawbury, UK: Smithers Rapra, 2007.
- [80] V. Goodship, *The Instant Expert: Plastics, Processing and Properties*. Bristol: Plastics Information Direct, 2010.
- [81] D. M. Bryce, *Plastic injection molding : manufacturing process fundamentals*. Dearborn, Mich.: Society of Manufacturing Engineers, 1996.
- [82] A. N. Wilkinson and A. J. Ryan, *Polymer processing and structure development*. Dordrecht ; London: Kluwer Academic Publishers, 1998.
- [83] J. M. G. Cowie, *Polymers : chemistry and physics of modern materials*, 2nd ed. Glasgow ; London: Blackie, 1991.
- [84] W. Michaeli, *Training in plastics technology : a text- and workbook*, 2nd ed. Cincinnati, OH: Hanser Gardner Publications, 2000.
- [85] P. C. Painter and M. M. Coleman, *Essentials of polymer science and engineering*. Lancaster, Pa: DEStech Publications, Inc., 2009.
- [86] J. A. Brydson, *Plastics materials*, 7th ed. Oxford: Butterworth-Heinemann, 1999.
- [87] H. F. Mark, *Encyclopedia of polymer science and technology*, Concise 3rd ed. Hoboken, N.J.: Wiley-Interscience, 2007.
- [88] R. J. Hernandez, S. E. M. Selke, and J. D. Culter, *Plastics packaging: properties, processing, applications, and regulations*. Munich [Germany]; Cincinnati, Ohio
c2000.: Hanser Publishers : [Distributed by] Hanser Gardener Publishers.
- [89] A. B. Strong, *Plastics : materials and processing*, 3rd ed. Upper Saddle River, NJ: Pearson Prentice Hall, 2006.
- [90] M. Chanda, S. K. Roy, and CRC Press. (2007). *Plastics technology handbook (4th ed.)*. Available: <http://marc.crcnetbase.com/ISBN/9781420006360>
Available: <http://0-marc.crcnetbase.com.pugwash.lib.warwick.ac.uk/ISBN/9781420006360>
- [91] R. W. Dyson, *Specialty polymers*, 2nd ed. London: Blackie Academic and Professional, 1998.
- [92] L. Dai, "Conducting Polymers," in *Intelligent Macromolecules for Smart Devices From Material Synthesis to Device Applications*, ed London: Springer-Verlag, 2004, pp. 41-80.
- [93] S. A. Bashir. (2001, Conducting Polymers and the Evolving Electronics Technology. *EEE Links* 7(2). Available: <https://nepp.nasa.gov/docuploads/4D1C9F67-F567-4E16-8BC92D3B88761016/SyedRevision2.pdf>
- [94] W. R. Salaneck, R. H. Friend, and J. L. Brédas, "Electronic structure of conjugated polymers: consequences of electron–lattice coupling," *Physics Reports*, vol. 319, pp. 231-251, 1999.
- [95] T. Grasser, G. Meller, and M. Baldo. (2010). *Organic electronics*. Available: <http://0-dx.doi.org.pugwash.lib.warwick.ac.uk/10.1007/978-3-642-04538-7>
- [96] F. So. (2010). *Organic electronics materials, processing, devices and applications*. Available:

- <http://0-marc.crcnetbase.com.pugwash.lib.warwick.ac.uk/isbn/9781420072914>
- [97] E. Vitoratos, S. Sakkopoulos, E. Dalas, N. Paliatsas, D. Karageorgopoulos, F. Petraki, *et al.*, "Thermal degradation mechanisms of PEDOT:PSS," *Organic Electronics*, vol. 10, pp. 61-66, 2009.
- [98] E. Andreas, "The spectral sensitivity of PEDOT:PSS films," *Solar Energy Materials and Solar Cells*, vol. 95, pp. 1333-1338, 2011.
- [99] H.-E. Yin, C.-F. Lee, and W.-Y. Chiu, "Preparation of thermally curable conductive films PEDOT:P(SS-NMA) and their performances on weather stability and water resistance," *Polymer*, vol. 52, pp. 5065-5074, 2011.
- [100] M. Jakubowska, M. Słoma, and A. Młodziak, "Printed transparent electrodes containing carbon nanotubes for elastic circuits applications with enhanced electrical durability under severe conditions," *Materials Science and Engineering: B*, vol. 176, pp. 358-362, 2011.
- [101] J. Park, A. Lee, Y. Yim, and E. Han, "Electrical and thermal properties of PEDOT:PSS films doped with carbon nanotubes," *Synthetic Metals*, vol. 161, pp. 523-527, 2011.
- [102] T. Kuilla, S. Bhadra, D. Yao, N. H. Kim, S. Bose, and J. H. Lee, "Recent advances in graphene based polymer composites," *Progress in Polymer Science*, vol. 35, pp. 1350-1375, 2010.
- [103] T. T. Tung, T. Y. Kim, J. P. Shim, W. S. Yang, H. Kim, and K. S. Suh, "Poly(ionic liquid)-stabilized graphene sheets and their hybrid with poly(3,4-ethylenedioxythiophene)," *Organic Electronics*, vol. 12, pp. 2215-2224, 2011.
- [104] Y. Hyun Kim, C. Sachse, M. Hermenau, K. Fehse, M. Riede, L. Müller-Meskamp, *et al.*, "Improved efficiency and lifetime in small molecule organic solar cells with optimized conductive polymer electrodes," *Applied Physics Letters*, vol. 99, 2011.
- [105] M. Kim, Y. S. Lee, Y. C. Kim, M. S. Choi, and J. Y. Lee, "Flexible organic light-emitting diode with a conductive polymer electrode," *Synthetic Metals*, vol. 161, pp. 2318-2322.
- [106] O. P. Dimitriev, D. A. Grinko, Y. V. Noskov, N. A. Ogurtsov, and A. A. Pud, "PEDOT:PSS films—Effect of organic solvent additives and annealing on the film conductivity," *Synthetic Metals*, vol. 159, pp. 2237-2239, 2009.
- [107] Y. Kim, J. Lee, H. Kang, G. Kim, N. Kim, and K. Lee, "Controlled electro-spray deposition of highly conductive PEDOT:PSS films," *Solar Energy Materials and Solar Cells*.
- [108] M. J. Kim, D. W. Shin, J.-Y. Kim, S. H. Park, I. t. Han, and J. B. Yoo, "The production of a flexible electroluminescent device on polyethylene terephthalate films using transparent conducting carbon nanotube electrode," *Carbon*, vol. 47, pp. 3461-3465, 2009.
- [109] Y. H. Kim, L. Müller-Meskamp, A. A. Zakhidov, C. Sachse, J. Meiss, J. Bikova, *et al.*, "Semi-transparent small molecule organic solar cells with laminated free-standing carbon nanotube top electrodes," *Solar Energy Materials and Solar Cells*, vol. 96, pp. 244-250, 2012.
- [110] B.-T. Liu, C.-H. Hsu, and W.-H. Wang, "A comparative study on preparation of conductive and transparent carbon nanotube thin films," *Journal of the Taiwan Institute of Chemical Engineers*.

- [111] K. Byung-Jae, M. A. Mastro, J. Hite, C. R. Eddy, Jr., and K. Jihyun, "Transparent conductive graphene electrode in GaN-based ultra-violet light emitting diodes," *Optics Express*, vol. 18, pp. 23030-4, 2010.
- [112] Y.-Y. Choi, S. J. Kang, H.-K. Kim, W. M. Choi, and S.-I. Na, "Multilayer graphene films as transparent electrodes for organic photovoltaic devices," *Solar Energy Materials and Solar Cells*, vol. 96, pp. 281-285, 2012.
- [113] Y. Xu and I. M. Hutchings, "Cold spray deposition of thermoplastic powder," *Surface and Coatings Technology*, vol. 201, pp. 3044-3050, 2006.
- [114] W. Guilong, Z. Guoqun, L. Huiping, and G. Yanjin, "Analysis of thermal cycling efficiency and optimal design of heating/cooling systems for rapid heat cycle injection molding process," *Materials & Design*, vol. 31, pp. 3426-3441, 2010.
- [115] P. Keun and L. Sang-Ik, "Localized mold heating with the aid of selective induction for injection molding of high aspect ratio micro-features," *Journal of Micromechanics and Microengineering*, vol. 20, p. 035002 (11 pp.), 2010.
- [116] C. Shia-Chung, J. Wen-Ren, C. Yaw-Jen, C. Jen-An, and C. Jin-Chuan, "Rapid mold temperature variation for assisting the micro injection of high aspect ratio micro-feature parts using induction heating technology," *Journal of Micromechanics and Microengineering*, vol. 16, pp. 1783-91, 2006.
- [117] D. E. Dimla, M. Camilotto, and F. Miani, "Design and optimisation of conformal cooling channels in injection moulding tools," *Journal of Materials Processing Technology*, vol. 164-165, pp. 1294-1300, 2005.
- [118] S.-C. Chen, R.-D. Chien, S.-H. Lin, M.-C. Lin, and J.-A. Chang, "Feasibility evaluation of gas-assisted heating for mold surface temperature control during injection molding process," *International Communications in Heat and Mass Transfer*, vol. 36, pp. 806-812, 2009.
- [119] *RocTool: Innovative Molding Technologies*, RocTool S. A., France, Viewed: 16th December 2011, Available: <http://www.roctool.com/plasticInjection.php>.
- [120] M.-C. Jeng, S.-C. Chen, P. S. Minh, J.-A. Chang, and C.-s. Chung, "Rapid mold temperature control in injection molding by using steam heating," *International Communications in Heat and Mass Transfer*, vol. 37, pp. 1295-1304, 2010.
- [121] G. Wang, G. Zhao, H. Li, and Y. Guan, "Multi-objective optimization design of the heating/cooling channels of the steam-heating rapid thermal response mold using particle swarm optimization," *International Journal of Thermal Sciences*, vol. 50, pp. 790-802, 2011.
- [122] S. C. Chen, Y. W. Lin, R. D. Chien, and H. M. Li, "Variable Mold Temperature to Improve Surface Quality of Microcellular Injection Molded Parts Using Induction Heating Technology," *Advances in Polymer Technology*, vol. 27, pp. 224-232, Win 2008.
- [123] P.-C. Chang and S.-J. Hwang, "Simulation of infrared rapid surface heating for injection molding," *International Journal of Heat and Mass Transfer*, vol. 49, pp. 3846-3854, 2006.
- [124] M.-C. Yu, W.-B. Young, and P.-M. Hsu, "Micro-injection molding with the infrared assisted mold heating system," *Materials Science and Engineering: A*, vol. 460-461, pp. 288-295, 2007.

- [125] B. H. Kim, Y. Donggang, and C. Shia-Chung, "Rapid thermal cycling of injection molds: an overview on technical approaches and applications," *Advances in Polymer Technology*, vol. 27, pp. 233-55, 2008.
- [126] G. A. Giles and D. R. Bain, *Technology of plastics packaging for the consumer market*. Sheffield, England. Boca Raton, FL: Sheffield Academic Press; CRC Press, 2001.
- [127] V. Goodship and J. C. Love, "Multi-Material Injection Moulding," Rapra Technology Limited 2002.
- [128] S.-C. Chen, S.-T. Huang, M.-C. Lin, and R.-D. Chien, "Study on the thermoforming of PC films used for in-mold decoration," *International Communications in Heat and Mass Transfer*, vol. 35, pp. 967-973, 2008.
- [129] V. Goodship, C. Lobjoit, I. Dargue, and G. F. Smith, "In-Mould Painting by Spraying Thermoset Powder Coating into a Closed Mould, Followed by Standard Thermoplastic Injection Moulding," *Progress in Rubber, Plastics and Recycling Technology*, vol. 22, p. 14, 2006.
- [130] V. Goodship, N. Cook, I. Dargue, C. Lobjoit, K. Makenji, and G. F. Smith, "In mould painting using thermoset powder coating and thermoplastic substrate in closed tool injection moulding," *Plastics Rubber and Composites*, vol. 36, pp. 34-41, Feb 2007.
- [131] N. J. Teh, S. Prosser, P. P. Conway, P. J. Palmer, and A. Kioul, "Embedding of electronics within thermoplastic polymers using injection moulding technique," in *Electronics Manufacturing Technology Symposium, 2000. Twenty-Sixth IEEE/CPMT International*, 2000, pp. 10-18.
- [132] D. A. Hutt, N. J. Teh, F. Sarvar, D. C. Whalley, P. J. Palmer, P. Anderson, *et al.*, "Overmoulding of electronics for end of life recovery," in *Polytronic 2005: 5th International Conference on Polymers and Adhesives in Microelectronics and Photonics, October 23, 2005 - October 26, 2005*, Warsaw, Poland, 2005, p. 133.
- [133] H. Abhyankar, D. P. Webb, and D. A. Hutt, "Effect of insert temperature on integrity of a thermoplastic circuit board," in *12th Electronics Packaging Technology Conference, EPTC 2010, December 8, 2010 - December 10, 2010*, Singapore, Singapore, 2010, pp. 505-510.
- [134] F. Sarvar, N. J. Teh, D. C. Whalley, D. A. Hutt, and P. J. Palmer, "Thermo-mechanical modelling of polymer encapsulated electronics," in *ITherm 2004 - Ninth Intersociety Conference on Thermal and Thermomechanical Phenomena in Electronic Systems, June 1, 2004 - June 4, 2004*, Las Vegas, NV, United states, 2004, pp. 465-472.
- [135] F. Awaja, M. Gilbert, G. Kelly, B. Fox, and P. J. Pigram, "Adhesion of polymers," *Progress in Polymer Science*, vol. 34, pp. 948-968, 2009.
- [136] A. Islam, H. N. Hansen, and M. Bondo, "Experimental investigation of the factors influencing the polymer-polymer bond strength during two-component injection moulding," *International Journal of Advanced Manufacturing Technology*, vol. 50, pp. 101-111, 2010.
- [137] G. Fourche, "An Overview of the Basic Aspects of Polymer Adhesion. Part 1: Fundamentals," *Polymer Engineering and Science*, vol. 35, pp. 957-967, 1995.

- [138] P. J. Cole, R. F. Cook, and C. W. Macosko, "Adhesion between immiscible polymers correlated with interfacial entanglements," *Macromolecules*, vol. 36, pp. 2808-2815, 2003.
- [139] T. Fukuda, H. Asaki, T. Asano, K. Takagi, Z. Honda, N. Kamata, *et al.*, "Surface morphology of fluorene thin film fabricated by electrospray deposition technique using two organic solvents: Application for organic light-emitting diodes," *Thin Solid Films*, vol. 520, pp. 600-605, 2011.
- [140] C. K. Chan, L. J. Richter, B. Dinardo, C. Jaye, B. R. Conrad, H. W. Ro, *et al.*, "High performance airbrushed organic thin film transistors," *Applied Physics Letters*, vol. 96, 2010.
- [141] A. Abdellah, B. Fabel, P. Lugli, and G. Scarpa, "Spray deposition of organic semiconducting thin-films: Towards the fabrication of arbitrary shaped organic electronic devices," *Organic Electronics*, vol. 11, pp. 1031-1038, 2010.
- [142] M. Aleksandrova, "Spray Deposition of Multilayer Polymer Structures for Optoelectronic Applications," *e-Journal of Surface Science and Nanotechnology*, vol. 7, pp. 859-62, 2009.
- [143] Y. Aoki, M. Shakutsui, and K. Fujita, "Stacking layered structure of polymer light emitting diodes prepared by evaporative spray deposition using ultradilute solution for improving carrier balance," *Thin Solid Films*, vol. 518, pp. 493-496, 2009.
- [144] R. Green, A. Morfa, A. J. Ferguson, N. Kopidakis, G. Rumbles, and S. E. Shaheen, "Performance of bulk heterojunction photovoltaic devices prepared by airbrush spray deposition," *Applied Physics Letters*, vol. 92, 2008.
- [145] *Moldflow*, Autodesk Inc, USA, Viewed: 17th December 2011, Available: <http://usa.autodesk.com/moldflow/>.
- [146] A. Dawson, M. Rides, C. R. G. Allen, and J. M. Urquhart, "Polymer-mould interface heat transfer coefficient measurements for polymer processing," *Polymer Testing*, vol. 27, pp. 555-565, 2008.
- [147] J. Z. Liang and J. N. Ness, "The calculation of cooling time in injection moulding," in *Proceedings of the International Conference on Manufacturing Automation, 10-12 Aug. 1992*, Hong Kong, Hong Kong, 1992, pp. 830-5.
- [148] Anon, "Processing Guide Printing of Electroluminescent Lamps based on Clevios S V3", H C Starck, 2009.
- [149] *BEGINNING AIRBRUSHING TIPS - VOLUME II "SPRAYING, DRYING & MASKING"*, Golden Artist Colors Inc, New York, Viewed: 20th January 2012, Available: <http://www.goldenpaints.com/technicaldata/airtip2.php>.
- [150] H.-W. Lin, C.-P. Chang, W.-H. Hwu, and M.-D. Ger, "The rheological behaviors of screen-printing pastes," *Journal of Materials Processing Technology*, vol. 197, pp. 284-291, 2008.
- [151] *ACMOS release agents for the synthetic resin industry*, ACMOS, Germany, Viewed: 20th January 2012, Available: <http://www.acmos.com/en/kunstharz.html>.
- [152] *Electralux ELX10; Technical datasheet*, Electra Polymers Ltd, UK, 2007, Viewed: 10th January 2012, Available: <http://www.electrapolymers.com/Resources/default.asp?seclD=18#anc193>.

- [153] British Standards Online, "*ISO 2409 Paints and Varnishes - cross cut test*," ed. London: BSI, 2007.
- [154] Oxford Dictionaries Online, *Luminance definition*, Viewed: 6th January 2012. Available: <http://oxforddictionaries.com/definition/luminance?q=luminance>
- [155] *IVL Test Platform*, S.E.A. Datentechnik GmbH, Germany, Viewed: 6th January 2012, Available: <http://www.sea-gmbh.com/en/products/test-systems/ivl-tester/>.
- [156] Oxford Dictionaries Online, *Illuminance definition*, Viewed: 22nd August 2011. Available: <http://oxforddictionaries.com/definition/illumination?q=illumination>
- [157] J. R. Sheats and D. B. Roitman, "Failure modes in polymer-based light-emitting diodes," *Synthetic Metals*, vol. 95, pp. 79-85, 1998.
- [158] M. K. Fung, Z. Q. Gao, C. S. Lee, and S. T. Lee, "Inhibition of dark spots growth in organic electroluminescent devices," *Chemical Physics Letters*, vol. 333, pp. 432-436, 2001.
- [159] T. A. Osswald and G. Menges, *Materials Science of Polymers for Engineering*. Munich: Hanser, 1995.
- [160] F.-X. Jiang, J.-K. Xu, B.-Y. Lu, Y. Xie, R.-J. Huang, and L.-F. Li, "Thermoelectric performance of poly(3,4-ethylenedioxythiophene): poly(styrenesulfonate)," *Chinese Physics Letters*, vol. 25, pp. 2202-5, 2008.
- [161] Anon, "Orgacon Application Sheet," AGFA, 2009.
- [162] S. George, P. S. Anjana, M. T. Sebastian, J. Krupka, S. Uma, and J. Philip, "Dielectric, mechanical, and thermal properties of low-permittivity polymer-ceramic composites for microelectronic applications," *International Journal of Applied Ceramic Technology*, vol. 7, pp. 461-474, 2010.
- [163] S. M. Marcus and R. L. Blaine, "Thermal conductivity of polymers, glasses and ceramics by modulated DSC," *Thermochimica Acta*, vol. 243, pp. 231-239, 1994.
- [164] D. Foley, 2005, *NEC Develops New Ultra-Thin, Flexible, Rechargeable Battery Boasting Super-Fast Charging Capability*. NEC Corporation, Japan, Viewed: 20th January 2012 Available: <http://www.nec.co.jp/press/en/0512/0701.html>
- [165] *PEL Nano P60 Electronic Grade Paper*, Printed Electronics Ltd, UK, 2011, Viewed: 20th January 2012, Available: <http://www.printedelectronics.co.uk/Information%20Sheet%20for%20PEL%20Nano%20P60.pdf>,.
- [166] Dimatix Fujifilm Materials Printing System and Cartridge, Fujifilm, California, 2008, Viewed: 20th January 2012, Available: http://www.dimatix.com/files/printer_Brochure.pdf.
- [167] *LED Phosphors*, Phosphor Technology Ltd, UK, Viewed: 20th January 2012, Available: <http://www.phosphor-technology.com/products/led.htm>.